Functional and biochemical analysis of non-proteasomal ubiquitin and SUMO signalling

Dissertation

submitted for the degree of

Doctor of Natural Sciences (Dr. rer. nat.)

Department of Biology

Johannes Gutenberg University Mainz

Vera Tröster

born 15.02.1992 in Reutlingen

Mainz, August 2022

Dean: Prof. Dr Eckhard Thines

Examiner:

1^{st} examiner: [redacted]

2^{nd} examiner: [redacted]

Date of the oral exam: 21.11.2022

Declaration

I, Vera Tröster, hereby declare that the work presented in this thesis is my own.
I confirm that any information or data that have been derived from other sources, either literally or analogously, are referred to and correctly cited in the thesis and that I have not used any sources or aids other than those specified. Finally, I declare that this work was not yet part of a study or examination in the same or a similar version.

Place, date, Vera Tröster

Zusammenfassung

Posttranslationale Modifikationen (PTM) beschreiben die kovalente und meist enzymatische Modifikation von Proteinen nach ihrer Translation. Sie sind vielseitige zelluläre Werkzeuge zur Erweiterung der Funktionalität von Proteinen durch Modulation ihrer Eigenschaften, Faltung, Stabilität, Wechselwirkung und Lokalisierung. Die Modifikation durch das Protein Ubiquitin ist eine der einflussreichsten und am besten untersuchten PTM, da sie eine wichtige Rolle in fast allen zellulären Prozessen spielt und an der Entstehung verschiedener Krankheiten beteiligt ist. Sie ist bekannt für ihre Rolle beim proteasomalen Abbau, hat aber auch wesentliche nicht-proteolytische Funktionen bei der Signalübertragung, dem Transport, der Lokalisierung und der Wechselwirkung von Proteinen.

Im ersten Teil meiner Doktorarbeit habe ich nach Ubiquitinierungssubstraten von Pib1 gesucht. Pib1 ist ein E3-Enzym der RING-Typ-Familie, das zusammen mit dem heterodimeren E2 Ubc13/Mms2 im endozytotischen System aktiv ist. Insgesamt stehen meine Ergebnisse mit den früheren Erkenntnissen aus unserem Labor und von Anderen im Einklang, dass Pib1 spezifisch in der K63-verknüpften Polyubiquitinierung von Proteinen an endosomalen und vakuolären Membranen wirkt und Proteine für ihren vakuolären Abbau markiert. Allerdings konnte ich in meiner Arbeit keine direkten Substrate für Pib1 identifizieren. Die drei Hauptgründe dafür waren: die Redundanz zwischen den ubiquitinierenden Enzymen im MVB-Weg, die sich noch über die beschriebene für Rsp5, Pib1 und Tul1 hinaus erstrecken könnte. Zweitens ist Pib1 ein E3, das eine bestehende Ubiquitin-Einheit durch K63-Verknüpfung erweitert, aber keine *de-novo*-Ubiquitinierung auf einem Substrat initiiert. Schließlich die schwierige Isolierung von Pib1 wegen seines geringen Vorkommens und der schlechten Löslichkeit.

Im zweiten Teil meiner Doktorarbeit habe ich die potentielle Ubiquitin-Bindung von Spc25 untersucht. Das Spc24/Spc25-Heterodimer ist Teil des Ndc80-Komplexes im zentralen Kinetochor. In früheren Arbeiten aus dem Labor wurde eine bisher unbekannten Ubiquitin-bindenden Domäne in Spc25 identifiziert. Die Kenntnis der genauen Interaktionsstelle zwischen Spc25 und Ubiquitin könnte verwendet werden, um die physiologische Relevanz dieser Interaktion einschließlich der Ubiquitin-Substrate und ubiquitinierenden Enzyme zu analysieren. Jedoch war die Wechselwirkung zwischen der verwendeten Ubiquitin-Variante, welche so entwickelt wurde, dass sie eine stärkere

Bindungsaffinität zu Spc25 als Wildtyp-Ubiquitin aufweist, und Spc25 noch zu schwach, um eine exakte Bindungsstelle in Interaktions-Assays oder durch NMR zu bestimmen.

Eine weitere wichtige PTM ist die Sumoylierung. Die Modifikation durch SUMO ist an vielen zellulären Prozessen beteiligt, wie z. B. Proteintransport, Proteinabbau, Transkription, Chromatinorganisation, Signaltransduktion, Zellzyklusregulation und DNA-Schadensreaktion. Im letzten Teil meiner Doktorarbeit habe ich Werkzeuge (DARPins) zur Untersuchung und Manipulation der Sumoylierung in lebenden Bäckerhefe-Kulturen charakterisiert. DARPins sind genetisch entwickelte Antikörper-imitierende Proteine, die durch „*in-vitro*-Display“ Techniken selektiert werden können. Sie ermöglichen die Analyse und Manipulation von Sumoylierung in der Zelle. Sechs DARPins, die aufgrund ihrer Affinität zum Hefe-SUMO-Protein Smt3 selektiert wurden, wurden auf ihren Einfluss auf die SUMO-Konjugation, Dekonjugation und Bindung *in vitro* analysiert. Kinetische Messungen und kristallographische Strukturen ergänzten diese Studien. Die DARPins wurden auch auf ihre Verwendbarkeit und Vielseitigkeit als *in-vivo*-Sensoren oder Inhibitoren von SUMO-abhängigen Prozessen getestet. Insgesamt konnte ich zeigen, dass die verschiedenen DARPins eine Reihe von Affinitäten abdecken und sich in ihrem Einfluss auf die SUMO-abhängigen Prozesse unterscheiden. Daher könnten die verschiedenen DARPins als Sensoren, Inhibitoren oder Affinitätsreagenzien verwendet werden, um die Sumoylierung in lebenden Hefezellen weiter zu untersuchen.

Abstract

Post-translational modifications (PTM) describe the covalent and mostly enzymatic modification of proteins after their translation. They are versatile cellular tools for expanding the functionality of proteins by modulating their properties, folding, stabilities, interactions and localizations. Modification by the small protein ubiquitin is one of the most powerful and well-studied PTM because ubiquitination is an important player in nearly all cellular processes and is involved in the development of various diseases. It is well known for its role in proteasomal degradation but also has considerable non-proteolytic functions in signalling, trafficking, localization, and interaction of proteins.

In the first part of my thesis, I aimed for finding ubiquitination substrates of Pib1. Pib1 is a poorly characterized E3 enzyme of the RING-type family, which acts together with the heterodimeric E2 Ubc13/Mms2 in the endocytic system. Overall, my results align with the previous findings from our lab and others, that Pib1 is specifically acting in K63-linked polyubiquitination of proteins at endosomal and vacuolar membranes, marking proteins for their vacuolar degradation. However, I was not able to identify any direct substrates of Pib1 in my work. The three main reasons for that were: the redundancy between the ubiquitinating enzymes in the MVB pathway, which might even extend over the described ones for Rsp5, Pib1 and Tul1. Secondly, Pib1 is an E3 that extends an existing ubiquitin moiety by K63-linkage but does not initiate *de novo* ubiquitination on a substrate. Finally, the difficult isolation of Pib1, because of its low abundance and bad solubility.

In the second part of my thesis, I was investigating the ubiquitin-binding ability of Spc25. The Spc24/Spc25 heterodimer is part of the Ndc80 complex in the central kinetochore. In previous work from our lab, the essential kinetochore component Spc25 has been identified as harbouring a so-far unknown ubiquitin-binding domain. The knowledge of the exact interaction site between Spc25 and ubiquitin could be used to analyse the physiological relevance of this interaction including the substrates, and ubiquitinating enzymes. However, the interaction between the used ubiquitin variant, which was raised to have a stronger binding affinity to Spc25 than wild-type ubiquitin, and Spc25 was still too weak to determine an exact binding interface in interaction assays or by NMR.

Another important PTM is sumoylation. Modification by SUMO is involved in many cellular processes, such as protein trafficking, protein degradation, transcription, chromatin organization, nuclear transport, signal transduction, cell cycle regulation, DNA repair, and the DNA damage response. In the final part of my thesis, I was characterizing tools (DARPins) to investigate and manipulate sumoylation in living yeast. DARPins are genetically engineered antibody-mimicking proteins, which can be selected by *in vitro* display techniques. They allow for monitoring and manipulation of targets inside the cell. A set of six DARPins selected for their affinity to the yeast SUMO protein, Smt3, was analysed for the influence on SUMO conjugation, deconjugation and binding *in vitro*. Kinetic measurements and crystallographic approaches complemented these studies. The binders were also analysed for their usefulness and versatility as *in vivo* sensors or inhibitors of SUMO-related processes. Overall, I could show that these DARPins cover a range of affinities and vary in their influence on SUMO-related processes. Therefore, the DARPins might be used as sensors, inhibitors or affinity reagents to further investigate sumoylation in living yeast cells.

Acknowledgements

[redacted]

[redacted]

[redacted]

Contents

List of Figures

List of Tables

Abbreviations

aa	Amino acid
AID	Auxin-inducible degron
Amp	Ampicillin
AQUA	Absolute quantification MS
AR	Ankyrin repeat
ATG	Autophagy-related
ATP	Adenosine triphosphate
B_{max}	Maximal polarisation
bp	Base pair
BSA	Bovine serum albumin
Cdc	Cell division cycle protein
CF	Core-facility
COP	Coat protein complex
CSP	Chemical shift pertubation
CTD	C-terminal domain
C-terminus	Carboxy-terminus
Da	Dalton
DAPI	4',6-Diamidino-2-phenylindole
DARPin	Designed ankyrin repeat protein
ddH_2O	Millipore purified water
DeSI1	Desumoylating isopeptidase 1
DIC	Differential interference contrast
DMSO	Dimethyl sulfoxide
DNA	Deoxyribonucleic acid
dox	Doxycycline
dsDNA	Double strand DNA
DTT	Dithiothreitol
DUB	Deubiquitinating enzyme
E.coli	*Escherichia coli*
E1	Ubiquitin/SUMO activating enzyme
E2	Ubiquitin/SUMO conjugating enzyme
E3	Ubiquitin/SUMO ligase
ELISA	Enzyme-linked immunosorbent assay

ER	Endoplasmatic reticulum
ERK	Extracellular signal-regulated kinase
FAT10	Human leukocyte antigen-F adjacent transcript 10
FL	Full-length
FP-Assay	Fluorescence polarisation assay
FRET	Fluorescence resonance energy transfer
FT	Flow-through
FYVE	Fab1-YOTB-Vac1-EEA1
g	Acceleration of gravity
G2/M	Transition from G2-phase to mitosis
GABP	Guanine-adenine-binding protein
GF	Gel filtration
GFP	Green fluorescent protein
glob	Globular domain
GSH	Glutathione
GST	Glutathione S-transferase
HA	Hemagglutinin
HECT	Homologous to E6-AP carboxyl terminus
HEPES	4-(2-hydroxyethyl)-1-Piperazineethanesulfonic acid
Her2	Epidermal growth factor receptor 2
His	Polyhistidine
HP30	His-tagged PCNA
HR	Homologous recombination
HT	Hering testis
HU	Hydroxyurea
IP	Immunoprecipitation
IPTG	Isopropyl-β-D-thiogalactopyranosid
ISG15	Interferon-stimulated gene 15
JAMM	JAB1/MPN/Mov34 metalloenzyme
K_D	Equilibrium dissociation constant
Kan	Kanamycin
KMN	KNL-1/Mis12 complex/Ndc80 complex
LB	Lysogeny broth (also Luria-Bertani)
Lys, K	Lysine
M	Molar
MAPK	Mitogen-activated protein kinase
MBP	Maltose-binding protein
MIU	Motif interacting with ubiquitin
MJD	Machado-Josephin domain protease
Mms	Methyl methanesulphonate- sensitivity protein
MMS	Methyl methanesulfonate

MS	Mass-spectrometry
MVB	Multivesicular bodies
Ndc	Nuclear division cycle protein
NEB	New England Biolabs
NEDD8	Neural precursor cell expressed developmentally down-regulated 8
NES	Nuclear export sequence
NF-H2O	Nuclease free water
NF-κB	Nuclear factor κ-lightchain-enhancer of activated B-cells
NLS	Nuclear localisation sequence
NMR	Nuclear magnetic resonance
NPC	Nuclear pore complex
NTA	Nitrilotriacetic acid
N-terminus	Amino-terminus
o.n.	Over night
OD	Optical density at 600 nm
OTU	Ovarian tumour domain-containing protease
PBS	Phosphate buffered saline
PCNA	Proliferating cell nuclear antigen
PCR	Polymerase chain reaction
PD	Pull-down
PDB	Protein data bank
PEG	Polyethylene glycol
PI3P	Phosphatidylinositol(3)-phosphate
PIAS	Protein inhibitor of activated STAT
Pib1	PhosphatidylInositol(3)-phosphate binding protein 1
PIP-box	PCNA interaction protein box
PLA	Proximity Ligation Assay
PML	Promyelocytic leukemia
PP_i	Inorganic pyrophosphate
PROTAC	Proteolysis targeting chimaera
PSM	Prospore membrane
PTM	Post-translational modification
RBR	RING-betweenRING-RING
RING	Really interesting new gene
RNA	Ribonucleic acid
RPA	Replication protein A
rpm	Rounds per minute
RT	Room temperature
S. cerevisiae, sc	*Saccharomyces cerevisiae*
SAC	Spindle assembly checkpoint
SC	Synthetic complete

SD	Standard deviations
SDS-PAGE	Sodium dodecyl sulfate polyacrylamide gel electrophoresis
SEC	Size exclusion chromatography
SENP	Sentrin-specific protease
SGD	Saccharomyces genome database
Sgs1	Slow growth suppressor 1
SILAC	Stable isotope labelling with amino acids in cell culture
SIM	SUMO interaction motif
Siz	SAP and Miz-finger domain-containing protein
Smc5/6	Structural maintenance of chromosomes complex
SMT3	Suppressor of Mif Two 3
SNARE	Soluble N-ethylmaleimide-sensitive-factor attachment receptor
SPB	Spindle pole body
Spc	Spindle pole component
SPR	Surface plasmon resonance
Srs2	Suppressor of Rad Six 2
ssDNA	Single-stranded DNA
STUbL	SUMO-targeted ubiquitin ligase
SUBE	SUMO-binding entities
SUMO	Small ubiquitin-like modifier
TAP	Tandem affinity purification
TBE	Tris/borate/EDTA buffer
TCA	Trichloroacetic acid
TetR	Tetracycline-inducible repressor
TLS	Translesion synthesis
TMD	Transmembrane domain
Tris	Tris(hydroxymethyl)aminomethane
ts	Temperature-sensitive
Ub	Ubiquitin
Ub*	Ubiquitin variant
UBA	Ubiquitin activating enzyme
UBAN	Ubiquitin-binding in ABIN and NEMO
UBC	Ubiquitin conjugating enzyme
UBD	Ubiquitin-binding domain
Ubl	Ubiquitin-like protein
UBZ	Ubiquitin-binding zinc finger
UCH	Ubiquitin C-terminal hydrolase
UIM	Ubiquitin-interacting motif
UPS	Ubiquitin-proteasome system
USP	Ubiquitin-specific processing protease
USPL1	Ubiquitin-specific-protease-like 1

UV	Ultra-violet
v/v	Volume by volume
VdW	Van der Waals
VEGF	Vascular endothelial growth factor
w/v	Weight by volume
WB	Western blot
WT	Wild-type
Y2H	Yeast two hybrid screen
YP	Yeast peptone

1 Introduction

1.1 Ubiquitination

Post-translational modifications (PTM) describe the covalent and mostly enzymatic modification of proteins after their translation. Besides modifications like specific cleavage of precursor proteins, or the formation of disulfide bonds, also attachment of small chemical groups such as phosphorylation, acetylation, and methylation are observed. Moreover, the addition of more complex molecules like glycosylation and lipidation, or modification by small proteins like ubiquitin (Ub) or Small ubiquitin-like modifier (SUMO) to a protein are counted as PTM. They are versatile cellular tools as they are able to expand the functionality of proteins by modulating their properties, foldings, stabilities, interactions and localizations. Therefore PTM are involved in nearly all cellular processes, including deoxyribonucleic acid (DNA) replication and repair, proliferation, or signal transduction.[1]
Modification by the small protein ubiquitin is one of the most powerful and well-studied PTM, because it is an important player in nearly all cellular processes and it is involved in the development of various diseases.[2–7] It is well known for its function in proteasomal degradation, but also has considerable non-proteolytic functions in signalling, trafficking, localization, and interaction of proteins. Ubiquitin was first discovered in 1975 by Gideon Goldstein.[8,9] It is highly conserved and is expressed in all eukaryotic cells, where it is covalently attached to lysine (Lys, K) residues of substrate proteins.[9–11]

1.1.1 The structure of ubiquitin

Ubiquitin is a small globular protein made of a single polypeptide chain of 76 amino acid (aa) residues (fig. 6a).[12,13] The amino acid sequence of ubiquitin is highly conserved between different species, for example, the yeast and the human ubiquitin sequence are 96 % conserved.[14] As the presented work is mainly conducted using proteins from *Saccharomyces cerevisiae*, I will focus on describing the ubiquitin system in budding yeast. *S. cerevisiae* expresses ubiquitin from four different loci as linear head-to-tail poly-Ub precursor proteins consisting of five ubiquitin moieties or fusions with ribosomal proteins, which are matured into single ubiquitins by cleavage and refolding.[15,16]

Ubiquitin has a very characteristic globular fold made of a five-stranded mixed β-sheet, a short 310-helix and an α-helix forming a tight, hydrophobic β-grasp fold with a flexible, solvent-exposed C-terminal tail containing the Leu-Arg-Gly-Gly motif that can form peptide and isopeptide bonds (fig. 1a).[12,13,16] It exhibits important hydrophobic patches on its surface, which are recognised by ubiquitin interacting proteins. The most important one is the Isoleucine-44 patch (Leu8, Ile44, Val70 and His68), which is recognized by the proteasome and most ubiquitin-binding domains (UBD) containing proteins. Further hydrophobic patches are, for example, the Isleucine-36 patch (Ile36, Leu71 and Leu73) and the Phenylalanine-4 patch (Gln2, Phe4 and Thr14). Ubiquitin is highly stable against cleavage by proteases, and pH and temperature changes. This is caused by its constrained and inaccessible Amino (N)-terminus and a compact fold formed by a high number of hydrogen bonds.[17–19] Several small proteins, called ubiquitin-like proteins (Ubl), have been identified. They fold similarly to ubiquitin, into the so-called β-grasp. Examples are NEDD8 (neural precursor cell expressed developmentally down-regulated 8), SUMO (Small ubiquitin-like modifier), ATG8 (Autophagy-related protein 8), ISG15 (Interferon-stimulated gene 15), and FAT10 (Human leukocyte antigen-F adjacent transcript 10).[17,20]

1.1.2 The ubiquitin code

Ubiquitination can induce or maintain many different signalling pathways in the cell. This versatility results from the fact that a substrate can be modified by a single ubiquitin residue on a single lysine (monoubiquitination), by a single ubiquitin residue on several lysines (multi-monoubiquitination), by forming a ubiquitin chain through the same ubiquitin lysine residue in each moiety (homotypic polyubiquitination), and by forming mixed (different linkages between succeeding ubiquitin moieties), branched (one ubiquitin is ubiquitinated at several lysine residues), or modified (by SUMO, NEDD8, phosphorylation or acetylation) chains (heterotypic polyubiquitination). Repeated conjugation to ubiquitin itself thus results in the formation of a polyubiquitin chain (fig. 1b).[6,9,12]

Polymeric ubiquitin chains achieve structural diversity of isopeptide linkages, as ubiquitin is containing seven lysine residues (K6, K11, K27, K29, K33, K48, and K63) and the α-amino group on the N-terminal methionine 1 (M1 or linear chain), all of which can be ubiquitinated themselves. In addition, free ubiquitin chains or substrates modified with several chains of different topologies were observed in cells.[3,9,21–23] This diversity of possible substrate modifications by ubiquitin and its ability to store and transmit information is called the ubiquitin code.

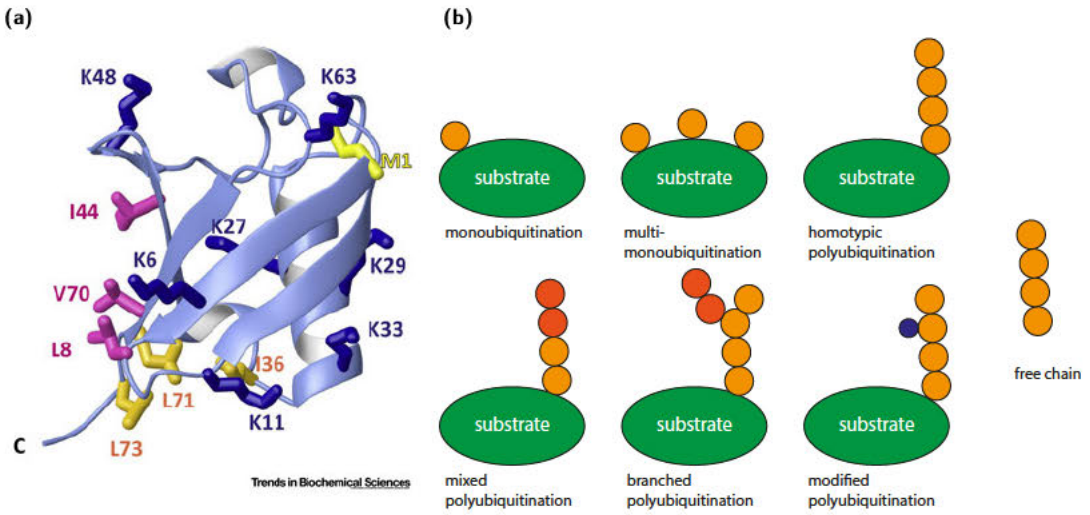

Figure 1: (a) Structure of ubiquitin monomer. Ubiquitin has a compact globular structure consisting of a mixed β-sheet, a short 310-helix and a α-helix. The C-terminus sticks out of the fold, making it accessible to enzymes involved in the formation of both isopeptide and peptide bonds. The main interaction site of ubiquitin is the hydrophobic Isoleucine-44-patch centred on Leu8, Ile44, and Val70 (purple). A second hydrophobic patch lies around Isoleucine-36 (Ile36, Leu71, Leu73, orange). The seven acceptor lysine residues (blue) and the N-terminal Met1 (yellow) are used for ubiquitin chain formation (adapted from Alfano *et al* (2016)).[16] **(b) Topology of ubiquitin chains.** Substrates can be monoubiquitinated (orange circle), multi-monoubiquitinated or polyubiquitinated. Depending on the ubiquitinated lysine residue (or N-terminus) within ubiquitin, different chain types can be generated, such as homogenous, mixed, or branched ubiquitin chains. Ubiquitin can also be further modified by other PTMs resulting in modified chains. Furthermore, if ubiquitin is only attached to itself unanchored ubiquitin chains can arise.

1.1.3 The ubiquitination cascade

Ubiquitin is conjugated with its carboxy (C)-terminal glycine (Gly76) to the ϵ-amino group of a lysine residue within a substrate. This covalent attachment is mediated by the cooperative action of a cascade of three enzyme classes, the so-called writers (fig. 2). First, the C-terminal carboxyl group of Ub is activated by the Ub activating enzyme (E1), requiring adenosine triphosphate (ATP) hydrolysis to adenylate the carboxyl group of Gly76 of ubiquitin, which is subsequently forming an high-energy thioester bond with the catalytic cysteine (Cys, C) residue of the E1 by a nucleophilic attack. Secondly, Ub is transferred to the catalytic cysteine residue of a Ub conjugating enzyme (E2) by transthioesterification. Finally, a Ub ligase (E3) selectively recognizes both the E2 and the substrate and helps to catalyse Ub transfer to the lysine residue of the target protein through the formation of a covalent isopeptide bond. Conjugation to a serine, threonine or cysteine residue or to the N-terminus of a target protein has also been reported.[9,24,25]

The products of ubiquitination are recognized by so-called readers, which typically contain substrate- and ubiquitin-binding sites.[7,26,27] Ubiquitination is a dynamic process, therefore specialized erasers (Deubiquitinating enzymes (DUBs)) can cleave off Ub moieties from target proteins.[9,28] The budding yeast genome encodes one E1, 11 E2s and

60–100 E3s.[29,30] The classes of enzymes involved in writing, reading and erasing the ubiquitin code will be described in the following sections.

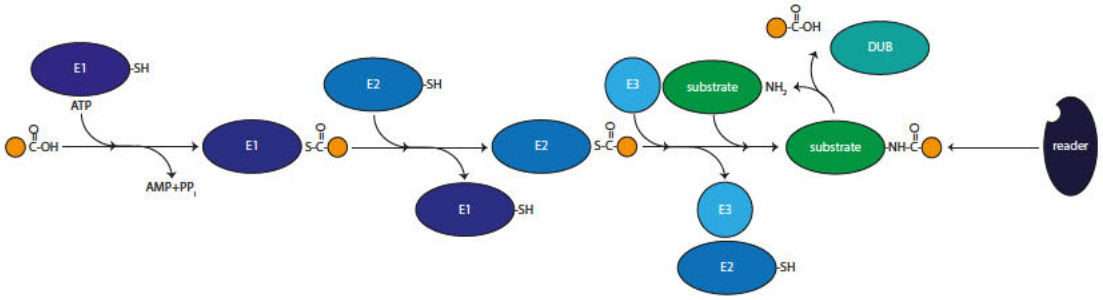

Figure 2: The ubiquitin conjugation cascade. Ubiquitin (orange circle) is covalently attached to a substrate by an enzymatic cascade that involves the activating enzyme (E1), the conjugation enzyme (E2), and a ligase (E3). These enzymes are the so-called writers of the ubiquitin code. Free ubiquitin is activated in an ATP-dependent manner resulting in the formation of a thioester linkage between the active site cysteine of an E1 and the carboxyl terminus of ubiquitin. Ubiquitin is then transferred to an E2 and finally covalently attached to an acceptor lysine in a specific substrate. This process can be facilitated by the action of E3s. For HECT domain E3s, ubiquitin is transferred to the active-site cysteine of the E3 followed by transfer to the substrate. For RING E3s, ubiquitin is directly transferred from the E2 to the substrate. Repeated cycles of ubiquitin conjugation to itself lead to the formation of ubiquitin chains. This process is reversible by the action of deubiquitinating enzymes (DUBs) that are known as erasers, and can cleave a ubiquitin moiety from a substrate. Readers recognize the posttranslationally modified proteins and can bind to them.

1.1.3.1 Ubiquitin activating enzymes (E1s)

The Ubiquitin activating enzyme 1 (*UBA1*) encoding gene of *S. cerevisiae* encodes the essential single E1 protein.[31] A temperature-sensitive *UBA1* mutant (*uba1-206*) shows rapid depletion of ubiquitin conjugates at the non-permissive temperature.[32] The Uba1 enzyme is monomeric with a size of 114 kDa. E1 enzymes from different species have a highly conserved structure and enzymatic activity. They interact with ubiquitin through the Isoleucine-44 patch of ubiquitin and the hydrophobic surface of the active adenylation domain, the four-helix bundle and additional residues of the E1. The affinity of the free E1 to the E2 is quite low, however, it increases drastically after ubiquitin and ATP binding, with binding constants (K_D) in the subnanomolar to nanomolar range. A fully loaded E1 molecule carries two activated ubiquitin molecules: one as a ubiquitin adenylate and the other as a thioester.[33–35]

1.1.3.2 Ubiquitin conjugating enzymes (E2s)

In the second step of the ubiquitination cascade, the ubiquitin moiety is transferred from the E1 to the active cysteine residue in the E2, forming a thioester bond. This essential cysteine lies in a 150-residue core domain conserved between all E2s.[36] Some E2s harbour N- or C-terminal extensions, which can mediate interaction with a substrate or

an E3. These interactions stabilize the ubiquitin-loaded E2s in a closed conformation, which enables a nucleophilic attack between the thioester and the lysine residue in the substrate. As described above for the E1, E2s also contact the hydrophobic Isoleucine-44 patch of Ub with their α2-helix.[37]

Yeast has a total of 13 Ubiquitin conjugating enzyme (*UBC*) encoding genes, 11 of which code for enzymes that are specific for ubiquitin. The other two genes encode for the E2 for SUMO (*UBC9*) and for NEDD8/Rub1 (*UBC12*).[38,39] Among the *UBC* genes only *UBC1*, *UBC3/CDC34* and *UBC9* are essential.[40] Ubiquitin conjugating enzymes interact with the E1 and E3s to ensure a unidirectional transfer of ubiquitin to the substrate. Thereby, usually the E3 and the E1 binding site on the E2 overlap, to guarantee that one ubiquitination cycle finishes before the next one starts.[41]

One E2 can act together with different E3s to ubiquitinate varying substrates. For example, Ubc2/Rad6 can work with the E3 Ubr1 in the process of N-end rule proteolysis.[42] Alternatively, it can cooperate with the E3 Rad18 to ubiquitinate proliferating cell nuclear antigen (PCNA) in the DNA damage tolerance pathway.[43,44] Furthermore, substrates can either be ubiquitinated by a single E2 or several E2s act redundantly on them. Some E2s may also operate sequentially to achieve first monoubiquitination (class I E2) and then elongation to polyubiquitin chains (class II E2) in two distinct conjugation events. For example, Ubc2/Rad6 catalyses monoubiquitination of PCNA, while chain elongation is performed by Ubc13/Mms2.[44,45] In contrast Cell division cycle protein 34 (Cdc34)/Ubc3, can initiate and elongate K48-linked chains.[46]

1.1.3.3 Ubiquitin ligases (E3s)

E3s catalyse the ubiquitin transfer from the E2 active site cysteine to a substrate lysine residue (or N-terminus), by binding the ubiquitin-loaded E2 and the substrate, connecting both and increasing the ubiquitination rate.[47,48] E3s thereby are often responsible for substrate specificity. E3 enzymes can be classified into three main categories: the really interesting new gene (RING) family, which has 47 members in *S. cerevisiae* (more than 600 in human), the homologous to E6-AP carboxyl terminus (HECT) family including five members ($\sim$28 in human), and the RING-betweenRING-RING (RBR) family with two members (14 members in human).[9,12,49,50]

RING E3s help in the direct transfer of a ubiquitin moiety from the charged E2-Ub-thioester to the acceptor lysine in the substrate, as they do not have an active site cysteine. RING domains coordinate two structural Zn^{2+} ions. They can be made of a single subunit where substrate binding and E2 interaction occur in one molecule, or of several subunits where substrate binding occurs in a second specialized subunit of the E3.[47,48,51] Structurally related to RING E3s are the U-box proteins that work with a similar mechanism, but lack the metal ions, and instead harbour a hydrophobic core.[47,52]

The ∼350-amino-acid-long HECT domain is composed of two characteristic parts. The N-lobe, which mediates the contact to the E2 and the C-lobe containing the active site cysteine. Through a transthioesterification reaction, ubiquitin is passed on from the active site cysteine of the E2 to the active site cysteine of the E3, before it is further transferred to a lysine residue of a substrate, forming an isopeptide bond.[48,53–55]
Like the name proposes RBR family E3s contain two RING fingers connected by a cysteine-rich region called the in-between-RING domain. One RING domain binds the E2 and stimulates the transfer of ubiquitin to the RING-like domain that contains an active site cysteine, from where it is then attached to the substrate.[56]
When E2s interact with E3s of the RING-type or no E3, they are able to determine the chain topology, however, when they interact with HECT type or RBR type E3s, the chain topology is dictated by the ubiquitin ligase.[46,49,57]

1.1.4 Erasers of the ubiquitin code

Ubiquitination is a dynamic process with ubiquitin chains being shortened or erased by specific proteases, called deubiquitinating enzymes or deubiquitinases. There are 20 known DUBs in budding yeast (∼100 in human cells).[58] DUBs can either be classified as metalloprotease or cysteine proteases according to the type of active site they harbour. Cysteine proteases catalyse the cleavage of the isopeptide bond between a lysine residue and G76 of ubiquitin or a peptide bond between M1 and G76 of a linear polyubiquitin chains, by a catalytic triad of aspartate, histidine and cysteine, while metalloproteases contain water molecules and a Zn^{2+} ion conjugated by two histidines in their active site, to perform the cleavage. The cysteine proteases are further separated into the ubiquitin-specific processing proteases (USP/UBP), the ovarian tumour domain-containing proteases (OTU), the Machado-Josephin domain proteases (MJD) DUBs and the ubiquitin C-terminal hydrolases (UCHs). Metalloproteases are of the class JAB1/MPN/Mov34 metalloenzymes (JAMM). A variety of DUBs with different activities, localisation and specificity for certain linkages or substrates exist. The most important functions of DUBs are the recovery of ubiquitin moieties from substrates targeted for proteasomal degradation (Rpn11 and Ubp6 in yeast) and the cleavage of the ubiquitin precursor in the maturation process of newly translated ubiquitin. DUBs are involved in many disease-associated pathways, which makes them interesting therapeutic targets.[29,59–63]

1.1.5 Readers of the ubiquitin code

Importantly, after writing the ubiquitin code, it has to be recognised and the signal has to be transduced and translated into a cellular response. This is done by non-covalent interactors (so-called ubiquitin receptors or readers) harbouring specific ubiquitin-binding domains. To date, a still increasing number of about 20 different types of UBDs have been described. Examples of these are the ubiquitin-interacting motif (UIM), the ubiquitin-binding zinc finger (UBZ), the motif interacting with ubiquitin (MIU) and the ubiquitin-binding in ABIN and NEMO (UBAN) domain.[64–66] Individual UBDs are small (20–150 amino acids) and have a low affinity to ubiquitin (10–500 µM). Therefore, often several UBDs of the same or different classes occur in one protein to enhance the binding affinity and selectivity.[67,68] Ubiquitin receptors can specifically recognize monoubiquitin or the different polyubiquitin chains, allowing UBD-containing proteins to be involved in a wide variety of functions. While most UBDs interact with the hydrophobic Isoleucine-44 patch on the surface of ubiquitin, their specific recognition of chain topology is commonly determined by the fact that UBDs bind either to the linker region itself or they recognize the positioning of individual ubiquitin moieties in the chain. This is enabled by the structure and position of several UBDs in a protein. Moreover, UBD-containing proteins additionally often interact with the ubiquitination target itself, thereby further enhancing substrate specificity and affinity.[68,69]

1.1.6 Functions of the ubiquitin code

Originally, ubiquitination was regarded as a degradation signal, however, today we know that ubiquitination is involved in many cellular processes, for example, cell proliferation, DNA repair, transcriptional regulation, viral infection, immune response, apoptosis, angiogenesis, and metastasis.[9,70–72]

Monoubiquitination plays a role for example in endocytosis and intracellular vesicle transport, nuclear import and export, chromatin structure, DNA repair and autophagy.[7,73,74] The fate of the polyubiquitinated substrates is mainly determined by the ability of ubiquitin code readers to discriminate between polyubiquitin chains of different geometries. Therefore, polyubiquitin chains can target proteins for degradation by the 26S proteasome or vacuole or activate a variety of non-proteolytic pathways like inflammatory signalling, protein trafficking or different parts of the DNA damage response.[3,7,23,75–79]

In more detail: the most abundant K48- and K11-linked chains are known for their signalling role in proteasomal degradation. K11-linkages are also involved in the DNA damage response.[9,80] K6-linked polyubiquitin chains play for example a role in mi-

tophagy and DNA repair and K63-linked chains are among other functions, important for intracellular trafficking and DNA damage repair.[3,12,76,81–85] K27, K29 and K33 linkages are only found very rarely in cells and their function is poorly described. They have been linked to DNA damage response, proteasomal degradation and post-Golgi trafficking, respectively.[3,86–88] Linear chains have not been observed in yeast, but were shown in higher eukaryotes to play a role in immune signalling and cell death.[89]
Mixed ubiquitin chains are mostly known for the role of K63-/ M1-ubiquitin mixed ubiquitin chains in nuclear factor κ-lightchain-enhancer of activated B-cells (NF-κB) signalling.[9,12,90] The function of branched ubiquitin chains is not fully understood, however for example K11-/K48-branched chains are a signal for proteasomal degradation.[83,91] Finally, modified ubiquitin chains are important in processes such as mitophagy regulation, controlling ubiquitin chain formation, regulation of heat shock and proteasome inhibition. Unanchored, free ubiquitin chains are described to have second messenger-like functions and a role in the immune system.[3,12]

1.1.6.1 Proteolytic functions of ubiquitin

To remove unfolded, misfolded or damaged proteins that would interfere with the normal biochemical pathways in cells, two major degradation systems are used. On one hand, the ubiquitin-proteasome system (UPS) degrades short-lived, misfolded and damaged proteins, and on the other hand, the autophagy-lysosome pathway, which is responsible for the removal of larger structures or membrane proteins.[29,76] As the first functional significance of ubiquitin chains, K48-linked chains were shown to target modified proteins to the UPS for their degradation.[9,19,75,92–94] These K48 linkages induced protein degradation was shown to be essential in *S. cerevisiae*.[95] Additionally, chain modifications with K11- and K29-linkages share similar functions in proteasomal degradation or contribute to different types of targeted protein destruction.[9,96] Different signals in the cell are used to mark proteins with ubiquitin for degradation by the 26S proteasome (for example the PEST sequence, N-degrons, or the cycline destruction boxes).[97] At least a diubiquitin needs to be formed on the substrate as a signal for proteasomal targeting.[98]
Another chain type with a proteolytic function is K63-linked polyubiquitin. It is involved in vacuolar targeting of proteins.[76,99] Thereby it has been shown as an internalization signal at the plasma membrane, as a sorting signal for multivesicular bodies (MVB) targeting and as a signal in the autophagy system.[76,100–102] The role of K63-ubiquitin linkages in the endocytic system will be important in further parts of this thesis, therefore it is discussed in more detail in the following section.

1.1.6.2 Pib1 as an E3 in the endocytic system; an example for a proteolytic function of ubiquitination

In contrast to K48-linked ubiquitin chains, the K63-linkage type cannot be connected to a single process in the cell. Rather, it seems to be involved in the regulation of numerous pathways ranging from the DNA damage response to inflammatory signalling. Importantly, it also contributes to endocytosis, intracellular membrane trafficking and lysosomal targeting.[76,103–105] The main E3 that ubiquitinates substrates with a K63 chain at the cell membrane is Rsp5, leading to the endocytosis of yeast plasma membrane proteins.[7,106,107] Ubiquitination is also important after internalisation in later steps of the endocytic pathway to control the sorting of substrates.[108–110]

The endocytic pathway mainly transports plasma membrane proteins to the vacuole for their degradation. The proteins are ubiquitinated at the plasma membrane. This triggers their internalisation and the formation of endocytic vesicles. First, the proteins transit through the early endosome, then the late endosome, next these are internalized into the MVB. At this step, the transporters can be recycled to the plasma membrane or are degraded in the vacuole (fig. 3a). Proteins can also directly traffic from the Golgi to the endosomal system, without being delivered to the plasma membrane first (fig. 3a). Through acidification and changes in the enzyme composition, the endocytic compartments differ from each other.[111]

PhosphatidylInositol(3)-phosphate binding protein 1 (Pib1) is a 286 amino acid protein. It harbours an N-terminal Fab1-YOTB-Vac1-EEA1 (FYVE) domain and a C-terminal RING finger (fig. 3b). Its FYVE domain has a high affinity for phosphatidylinositol(3)-phosphate (PI3P). This leads to its localisation to endosomal and vacuolar membranes.[112,113] Pib1 is a poorly characterized E3 enzyme of the RING-type family, which acts together with the heterodimeric E2 Ubc13/Mms2 (Ubiquitin conjugating protein 13/Methyl methanesulphonate-sensitivity protein 2) complex in *S. cerevisiae* to form K63-linked ubiquitin chains on substrates. The interaction between Pib1 and the E2 Ubc13/Mms2 is highly specific.[99]
Specifically, Pib1 was suggested to be involved in ubiquitin-dependent targeting of plasma membrane transporter and endosomal membrane proteins for vacuolar degradation via the multi-vesicular body pathway (fig. 3a). Nikko *et al.* (2009) used the trafficking of the metal ion transporter Smf1 into the vacuole as an example to investigate the role of Pib1 in facilitated ubiquitination. They suggest ubiquitination by Pib1 occurs mainly at the step of endosomes, as Pib1 is found in endosomal membranes rather than at the cell surface.[114] Here, the function of Pib1 seems to be partially redundant with the role of an Rsp5 adaptor protein, called Bsd2, in delivering plasma membrane proteins to the vacuole.[114]

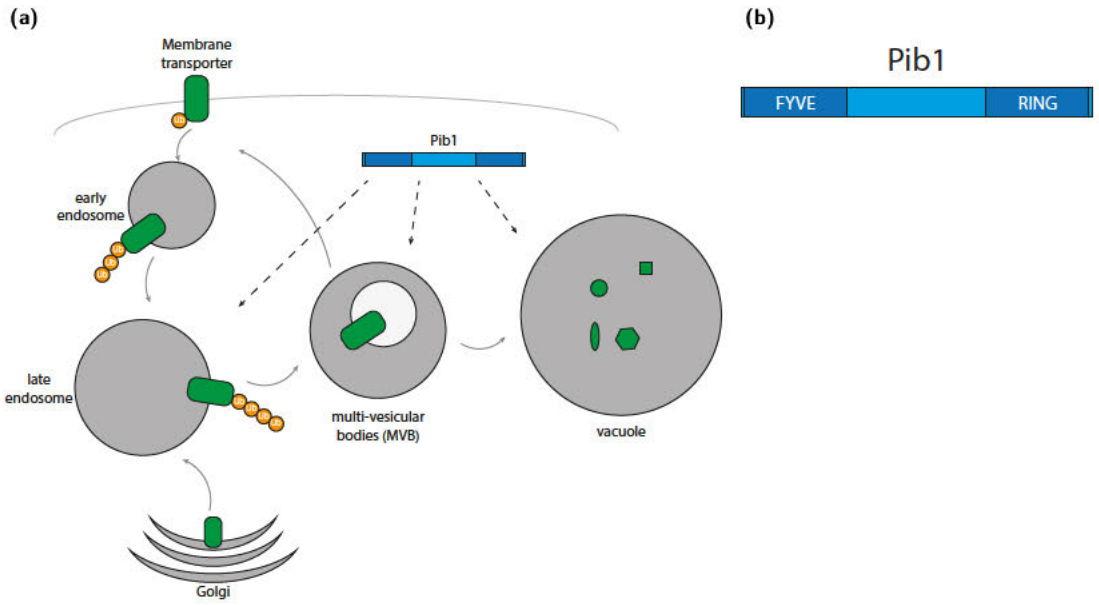

Figure 3: (a) The endocytic pathway transports ubiquitinated plasma membrane proteins to the vacuole for their degradation. Upon ubiquitination of membrane proteins endocytic vesicles form through internalisation. These traffic through the early endosome and late endosome into the MVB. At this step the transporters can be recycled back to the plasma membrane or are degraded in the vacuole. Proteins can also travel directly from the Golgi to the endosomes. The exact step, at which Pib1 ubiquitinates its substrate is not clear so far (dotted lines). **(b) Domain structure of Pib1.** Pib1 harbours an N-terminal FYVE domain and a C-terminal RING finger (figures adapted from Christian Renz).

Moreover, Pib1 was predicted to act partly redundantly with another E3 called Tul1, which is a subunit of the Defective for SREBP Cleavage protein (DSC) ubiquitin ligase complex.[115] Tul1 is an integral membrane protein, that has been implicated in the MVB pathway as well as Golgi protein quality control.[116] Xu *et al.* (2017) showed that deletion of both *PIB1* and *TUL1* inhibited the recycling of an example substrate, and genetic fusion of a non-specific deubiquitinating enzyme to Pib1 or Tul1 interfered with substrate ubiquitination and trafficking.[117]

The redundant action of different E3 enzymes in the MVB pathway is described to be necessary, for more specific ubiquitin modifications, for adding modification at different stages in the pathway or to enhance the length of ubiquitin chains or their number on a substrate. Moreover, different ubiquitin ligases likely recognize distinct features of cargo proteins and thereby provide surveillance of their degradation.[114,118] More recently, the redundancy of multiple E3 enzymes in the MVB pathway was further analysed by Yang *et al.* (2020) They showed a redundancy of Pib1 with Tul1 and with Rsp5 for ubiquitination of some targets for vacuolar degradation by localisation and degradation studies. In addition, they found Ypl162c, a putative vacuolar membrane transporter, as a substrate, for which ubiquitination by all three enzymes was needed for complete degradation and that the protein levels of Pib1 were modestly increased after natural starvation of *S. cerevisiae*.[119]

Additionally to its role in endocytosis, Pib1 is suggested to be involved in the shut-

down of gluconeogenesis and glucose repression when glucose is available. Vengayil *et al.* (2019) showed that Rds2, a major gluconeogenic transcription factor, is rapidly ubiquitinated and degraded by the proteasome upon glucose addition in a Pib1-dependent manner.[120]

Snc1 is a Vesicle-Soluble N-ethylmaleimide-sensitive-factor Attachment Receptor (v-SNARE) involved in the fusion of exocytic vesicles to the plasma membrane and it is subsequently endocytosed back to the Golgi by coat protein complex I (COPI) vesicle trafficking.[121] Three distinct and parallel recycling pathways mediated by Drs2/Rcy1/ COPI, Snx4/Atg20, and the retromer complex are involved in this process.[122,123] Snc1 was found to be subject to K63-linked ubiquitination. A COPI vesicle coat recognizes K63-linked polyubiquitin and this interaction is necessary for recycling of Snc1. Moreover, Xu *et al.* (2017) suggested that Pib1 and Tul1 could be the respective E3s for Snc1 ubiquitination, as DUB fusions of these proteins reduced Snc1 ubiquitination and a double deletion strain of both displayed a recycling defect of green fluorescent protein (GFP) -tagged Snc1.[117]

1.1.6.3 Nonproteolytic functions of ubiquitin

Besides its well-known role in the degradation of proteins, ubiquitination is involved in numerous cellular pathways being mostly signalled through monoubiquitination and linkages other than K48. Their functions range from regulation of interactions of a substrate, changes in its localisation, to modulation of its activity. Processes involving non-proteolytic ubiquitin chains are, for example, cell, proliferation, DNA repair, transcriptional regulation, nuclear import and export, chromatin structure, viral infection, inflammatory signalling, protein trafficking, immune response, apoptosis, angiogenesis, and metastasis.[3,7,9,23,70–72,75–79] To serve as signals in this wide variety of pathways one ubiquitin chain type is not restricted to a single function, but often the combination of localisation, timing, readers and the mixture of linkages determines the outcome of a signalling event.
For the purpose of this thesis, the function of ubiquitination of proliferating cell nuclear antigen (PCNA) in DNA damage response and the ubiquitination of the kinetochore proteins around the Nuclear division cycle protein 80 (Ndc80) complex will be discussed in more detail below.

1.1.6.4 PCNA ubiquitination as an example for a non-proteolytic function of ubiquitin conjugation

A non-degradative ubiquitin function is the regulation of DNA damage bypass by ubiquitination of the trimeric PCNA. PCNA is the replication sliding clamp protein, which in response to replication stress, is modified by monoubiquitination and K63-linked polyubiquitination, at K164. This enables the cell to replicate damaged DNA templates via either of two pathways, translesion synthesis (TLS) or template switching (fig. 4).[44,124–127] Under normal conditions PCNA functions as a processivity factor for replicative DNA polymerases. However, if the replication fork encounters a site of DNA damage or replicative stress, helicase and polymerase activity can partially uncouple. This results in single-stranded DNA (ssDNA) that is subsequently covered with replication protein A (RPA). This RPA signal recruits the E2/E3 complex, Rad6/Rad18, via direct interaction of Rad18 with the RPA complex on chromatin. Rad18's activity towards PCNA is also enhanced by damage-independent sumoylation of PCNA (see section 1.2.5.1). Monoubiquitination of PCNA by the E2/E3 pair Rad6/Rad18 promotes the recruitment of mutagenic, damage tolerant polymerases activating TLS.[23,126,128–130] Monoubiquitination on PCNA can be extended to a K63-linked chain by the action of Ubc13-Mms2 in combination with the E3 Rad5. This leads to a process similar to homologous recombination (HR), in which the undamaged sister chromatid is used as a replication template to complete the replication of the damaged part in a largely error-free pathway, called template switching.[44,131,132] Ubiquitination on PCNA is removed by the specialised DUBs, Ubp10 and Ubp12.[133,134]

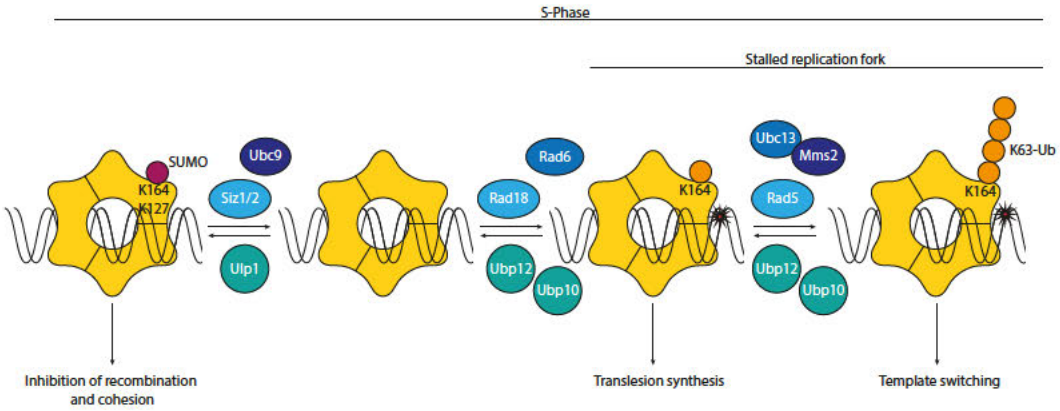

Figure 4: Posttranslational modification of PCNA by ubiquitin and SUMO. During S-phase budding yeast PCNA (yellow ring) is loaded onto DNA by the Rfc1–5 complex. In unperturbed replication, PCNA is modified by SUMO (purple circle) at K164 and to a lesser extent on K127. SUMOylation at K164 leads to the recruitment of the helicase Srs2, which prevents unwanted homologous recombination at the replication fork. PCNA is ubiquitinated (orange circle) at K164, in response to DNA damage (red star) and stalled replication. Monoubiquitination recruits TLS polymerases and promotes translesion synthesis. Polyubiquitination of K164 facilitates the mainly error-free template switching pathway. The corresponding E2/E3 pairs for sumoylation, mono- and polyubiquitination are indicated. The signal is terminated by the action of DUBs/ULPs.

1.1.6.5 Ubiquitination of the kinetochore proteins around the Ndc80 complex as a second example for a non-proteolytic function of ubiquitination

Kinetochores are multi-protein complexes, which connect chromosomes to the plus end of microtubules for correct separation during mitosis and meiosis. Budding yeast has a point centromere, in which only one microtubule is connected to ~125 base pairs (bp) of DNA in a complex of over 60 proteins.[135,136] In higher eukaryotes, the centromere is much bigger (called a regional centromere) and it connects to more than one microtubule.[137]

The kinetochore complex in *S. cerevisiae* can be subdivided into the inner, central and outer kinetochore (fig. 5a). The inner kinetochore connects to the centromeres of the chromosomes, while the outer kinetochore binds the microtubule plus ends. The central kinetochore links these two parts to each other, but also shows microtubule-binding ability.[138,139] Proteins of the central kinetochore are Spc105 (Spindle Pole Component 105) and the Nuclear division cycle protein 80 (Ndc80) complex (composed of Ndc80, Nuf2, Spc24, and Spc25), and the MIND complex (composed of Mtw1, Nnf1, Nsl1, and Dsn1) and COMA complex (composed of Ctf19, Okp1, Mcm21 and Ame1). Spc105 and the NDC80 complex mediate contact to the microtubule, The MIND and COMA complexes contact proteins of the inner kinetochore.[140–142]

The Spc24/Spc25 heterodimer is part of the Ndc80 complex in the central kinetochore. It binds the Ndc80/Nuf2 heterodimer, which connects it to the distal site of the microtubules and the Dam1 complex (composed of Duo1, Dam1, Dad1 and Ask1).[139,143] The Spc24/25 globular domains (glob) make contact with the Spc105 and MIND complex, forming together the KNL-1/Mis12 complex/Ndc80 complex (KMN) network (fig. 5a).[141] The globular domains of the Ndc80 complex point in opposite directions. The connection of the two heterodimers, Spc24/25 and Ndc80/Nuf2, is formed by the coiled-coiled domains present in all four proteins. They lie in the N-terminus of the Spc24/25 complex and the Carboxy (C)-terminus of the Ndc80/Nuf2 complex (fig. 5b).[144]

The *S. cerevisiae* Spc25 protein can be subdivided into three regions (fig. 5c): the N-terminal coiled-coiled region, the C-terminal globular domain and the flexible linker located in between these parts. The coiled-coiled region from amino acid 1–106 consists mostly of α-helices and forms the connection to the Nuf/Ndc80 dimer. From amino acid 133 to 221 the globular domain links Spc25 to other central kinetochore proteins like Spc105.[145] The human Spc25 has an high conservation in its secondary structure, while the amino acid sequence differs from the yeast protein (12 % identity and 23 % similarity). Structural data shows that in both organisms the globular domain consists of two α-helices, which flank an anti-parallel β-sheet.[145,146] Temperature-sensitive budding yeast variants of *spc24/spc25* show segregation defects and spindle checkpoint failure. Their deletion is lethal.[143]

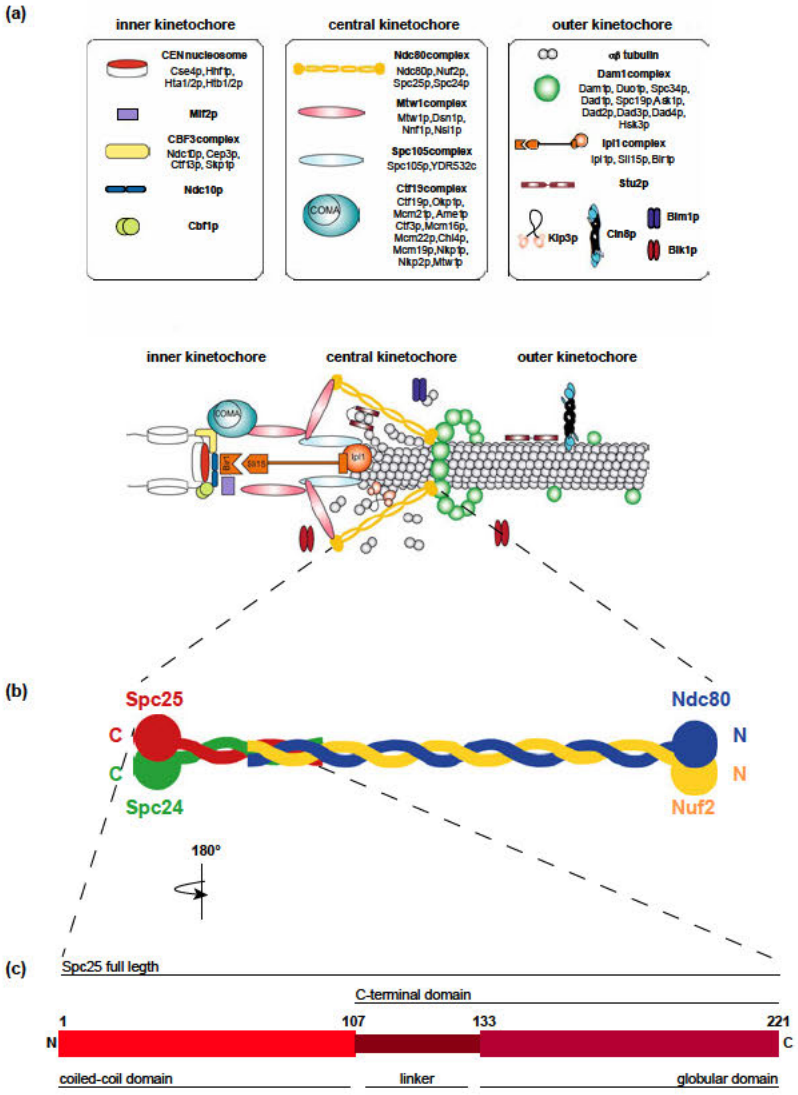

Figure 5: (a) Schematic model of the budding yeast kinetochore protein complexes around Spc25. (adapted from Westermann *et al* (2007)).[147] **(b) Structural model of the budding yeast Ndc80 complex.** (adapted from Hanna Windecker). **(c) Scheme of Spc25 domain structure.** The purified proteins used in this work are the full-length protein (FL), the C-terminal domain (CTD) and the globular domain (glob). The model is rotated by 180° compared to the view in (b).

In previous work from the [redacted] lab, the essential kinetochore component Spc25 has been identified as harbouring a so-far unknown ubiquitin-binding domain. Additionally, ubiquitination of kinetochore proteins was found, such as on Spc105, Mcm21, Mad1, Nsl1, Mad2, Mps1, Ame1, Okp1, Mcm21, Mtw1, Nuf2 and Dsn1, but the type of ubiquitination was not analysed. No ubiquitination could be detected on Ndc80, Spc24 and Spc25.[148,149] This raises the possibility for a proteasome-independent function of ubiquitin at kinetochores.
A role for ubiquitination at kinetochores would not be surprising as other post-translational modifications like phosphorylation and sumoylation are commonly used for chromosome segregation regulation. For example, phosphorylation by Aurora B kinase Ipl1 has been found on several kinetochore proteins (e.g. Dam1, Spc34, Ask1, Ndc80, Ipl1, and Sli15).[140] These phosphorylation events are proposed to have inhibitory functions for the microtubule attachment.[141,150] Another example of phosphorylation is found on Dsn1, where it promotes the interaction between outer and inner kinetochore proteins.[151] The action of Ipl1 is antagonized by Protein phosphatase I.[152] Additionally, several kinetochore proteins, such as Ndc10, Bir1 and Ndc80, were shown to be sumoylated. For example, sumoylation of Ndc10 was suggested to be required for its localisation to the mitotic spindle.[153]

1.1.7 Tools to study ubiquitination

Various methods have been used *in vitro* and *in vivo* to elucidate the different functions of ubiquitin. Technologies to explore the ubiquitination landscape are, for example, ubiquitin mutants, chain-specific antibodies, engineered UBDs, and DUBs, or quantitative proteomics.
Ubiquitin antibodies are available in a huge variety and they can be employed for many different *in vitro* techniques like western blotting, enzyme-linked immunosorbent assay (ELISA) or immunoprecipitation (IP). Also linkage-specific antibodies for the detection of K48-, K63-, K11- and linear chains are available.[154,155]
Moreover, specific DUBs for nearly all linkage types are used for the determination of linkages of polyubiquitin chains *in vitro*.[90,156]
Furthermore, UBDs have been extensively used as a tool for investigating ubiquitination, because of their often exclusive way of binding to the Isoleucine-44 patch and the possibility of combining several equal or different UBDs to reach linkage selectivity and different binding affinities.[69] They are useful for example for the purification of polyubiquitin conjugates from native cell extracts, for immunoprecipitation, or to stabilize specific chains through protection from DUBs *in vivo*.[157,158]
In combination with ubiquitin tools that enrich certain linkage types and trypsin digestion, mass-spectrometric (MS)-based techniques were of greatest value to our un-

derstanding of the ubiquitin code. For example, the quantitative techniques stable isotope labelling with amino acids in cell culture (SILAC) or labelled ubiquitin standards (AQUA) are employed to identify ubiquitinated substrates in a 'bottom-up' approach.[159]

Expressions of fusion proteins between ubiquitin and selected substrates have also led to the exploration of the function of ubiquitination *in vivo*. Insights into the importance of different chain linkage types on substrates can be gained using an enzyme-based strategy of *in vivo* ubiquitin linkage reprogramming with substrate-selective, tailor-made E3s.[23,160,161]

For *in vivo* targeted degradation of selected substrates by K48-ubiquitination, different techniques were developed. One example is the proteolysis targeting chimaera (PROTAC) technique, where a specifically adapted (to a selected E3/target pair) small molecule, simultaneously binds an E3 and a target protein, directing polyubiquitination to the lysine residues of the targets.[162] Another example is the auxin-dependent degradation pathway from plants that was adapted to polyubiquitinate an auxin-inducible degron (AID)-tagged substrate in cells upon addition of auxin.[163]

Widely used are also ubiquitin lysine mutants to assess the role of different linkages in specific pathways *in vitro* and *in vivo*. *In vivo*, ubiquitin-replacement strategies with ubiquitin mutants can reveal relevant information if no alternative pathways are present.[96,164,165]

Also ubiquitin variants with a higher affinity to a specific target protein have been used to inhibit, activate and modulate ubiquitin-binding proteins, thereby elucidating their function and the pathway they are involved in. A more detailed description of ubiquitin variants will be done in the following subsection.

1.1.7.1 Ubiquitin variants: using *in vitro* selection to explore the ubiquitination system

The interactions between ubiquitin and ubiquitin binding proteins are generally weak, because the determined equilibrium dissociation constants (K_Ds) lie above 2 µM.[68] Therefore, the [redacted] laboratory (University of Toronto) has generated genetic libraries, using ubiquitin as a scaffold, from which they can select ubiquitin variants (Ub*) with a higher affinity to a specific target protein. Originally, the library was described to generate highly specific and potent inhibitors of ubiquitin-specific proteases.[166] Since then, several additional ubiquitin variants for various ubiquitin interacting target proteins have been identified with the above-described strategy. Among these targets are for example dual-USPs, RING/ U-box or HECT ligases (E3s), multi-subunit E3s, ubiquitin-conjugating enzymes (E2s), small ubiquitin-interacting motifs, ubiquitin adaptor proteins, transcription factors, and receptor extracellular domains.[167–176]

To capture the ubiquitin variants that show higher affinity to their target protein than wild-type (*WT*)-ubiquitin, phage display assays are conducted. The original two libraries were based on the analysis of available USP-ubiquitin structures. Approximately 30 residues in three regions of ubiquitin are targeted by site-directed mutagenesis with varying combinations of degenerate oligonucleotides.[166] More recently, not only monoubiquitin, but also ubiquitin dimers were used as templates.[167,177] Even the generation of inhibitory, high-affinity hSUMO2 variants that bind the back-side SUMO binding site of Ubc9 has been described.[178]
For the selection of variants from the library, the binding partner is immobilised on a solid phase. Each single ubiquitin variant from the library is genetically fused to a phage coat protein so that the phages present them on their surface. The phages are added to the immobilised protein and allowed to bind. Unbound phages are washed away and the attached ones are eluted. The obtained ubiquitin DNA is amplified by infection of bacterial hosts with the eluted phages, and then again added to the immobilised protein for the second round of selection. This cycle is repeated five times, before the DNA of the best binding ubiquitin variants (verified by phage ELISA) is retained from the phages and sequenced.[168]

Interaction of ubiquitin variants to their binding protein can lead to their inhibition, activation or modulation. These very diverse influences might be caused by the need for low-affinity interactions of the target protein with other proteins for its proper function, which is disrupted by higher-affinity interaction resulting from the ubiquitin variants.[166]
Cohen *et al.* (2017) have analysed different ubiquitin variants using computational methods. They found that most variants contain amino acid mutations from polar to hydrophobic residues. In addition, the variants contain mostly larger amino acids, at positions that differ from *WT*-ubiquitin. These were commonly mutations to Arg and aromatic amino acids, replacing Gly of *WT*-ubiquitin. These changes result in a better surface complementarity between ubiquitin and the binding partner. Additionally, van der Waals energy and hydrogen bond patterns were improved in the interaction interface.[179]

Ubiquitin variants mostly interact with the active site of an enzyme or a known ubiquitin interaction site, but some are also found that bind to a surface distinct from the expected site. These are often interaction sites that have not previously been described.[175] Ubiquitin variants are active *in vitro* and in cells. Therefore, they can be used to identify uncharacterised ubiquitin-binding sites, for structural analysis of interaction sites, and as inhibitors in research (e.g. for functional analysis of weak interactions and to study the biological function of ubiquitin binding proteins) and clinics (e.g. for use in small molecule displacement screens and therapeutic target validation).[166,168]

1.2 Introduction to the SUMO system

Another important PTM is sumoylation. Sumoylation is essential for the viability of most eukaryotic cells. While there is only one SUMO isoform in budding yeast (called Smt3 (Suppressor of Mif Two 3)), four different SUMO isoforms (SUMO1–4) can be found in human. SUMO1 shares about 48 % sequence identity with SUMO2, while SUMO2 and SUMO3 are highly similar with 95 % sequence identity (fig. 6a). Despite their very similar three-dimensional structure, SUMO shares only ∼18 % sequence identity with ubiquitin (fig. 6b).[180,181]
Sumoylation can have a variety of consequences, depending on the target, the localisation and other factors, influencing on intra- or intermolecular interaction.[182,183] Sumoylation can lead to conformational changes in the substrate, changed interactions, and it can compete with or promote other post-translational modifications such as ubiquitination and acetylation.[183–188] Modification by SUMO is involved in many cellular processes, such as protein trafficking, protein degradation, transcription, chromatin organization, nuclear transport, signal transduction, cell cycle regulation, DNA repair, and the DNA damage response.[189,190] Additionally, sumoylation was shown to play a role in cancer and neurodegenerative diseases.[191–193] Its ability to change the function and activity of a protein has made it a useful target for drug development. So far, small molecules and protein aptamers are considered possible drugs to target sumoylation in disease.[194,195] In the following sections the sumoylation system of *S. cerevisiae* is described in further detail.

1.2.1 The structure of SUMO

SUMO is a 98 amino acid large protein and shares a common three-dimensional β-grasp fold with other members of the ubiquitin-like modifier family (fig. 6b). It possesses a C-terminal Gly-Gly-motif for the formation of an isopeptide bond with a lysine residue in a substrate.[196] Its 20 amino acid long N-terminus is highly flexible and extended compared to other ubiquitin-like modifiers. SUMO is translated as a longer precursor and needs to be cleaved by SUMO specific proteases to become active. Substrates of SUMO can be modified with only one copy of SUMO per attachment site (monosumoylation), or can have attachments of mono-SUMO at several sites (multi-monosumoylation).[197] SUMO can also form polymeric chains on its substrates. These are linked via the lysine residues in the N-terminal tail of SUMO (K11, K15, K19).[181,198]

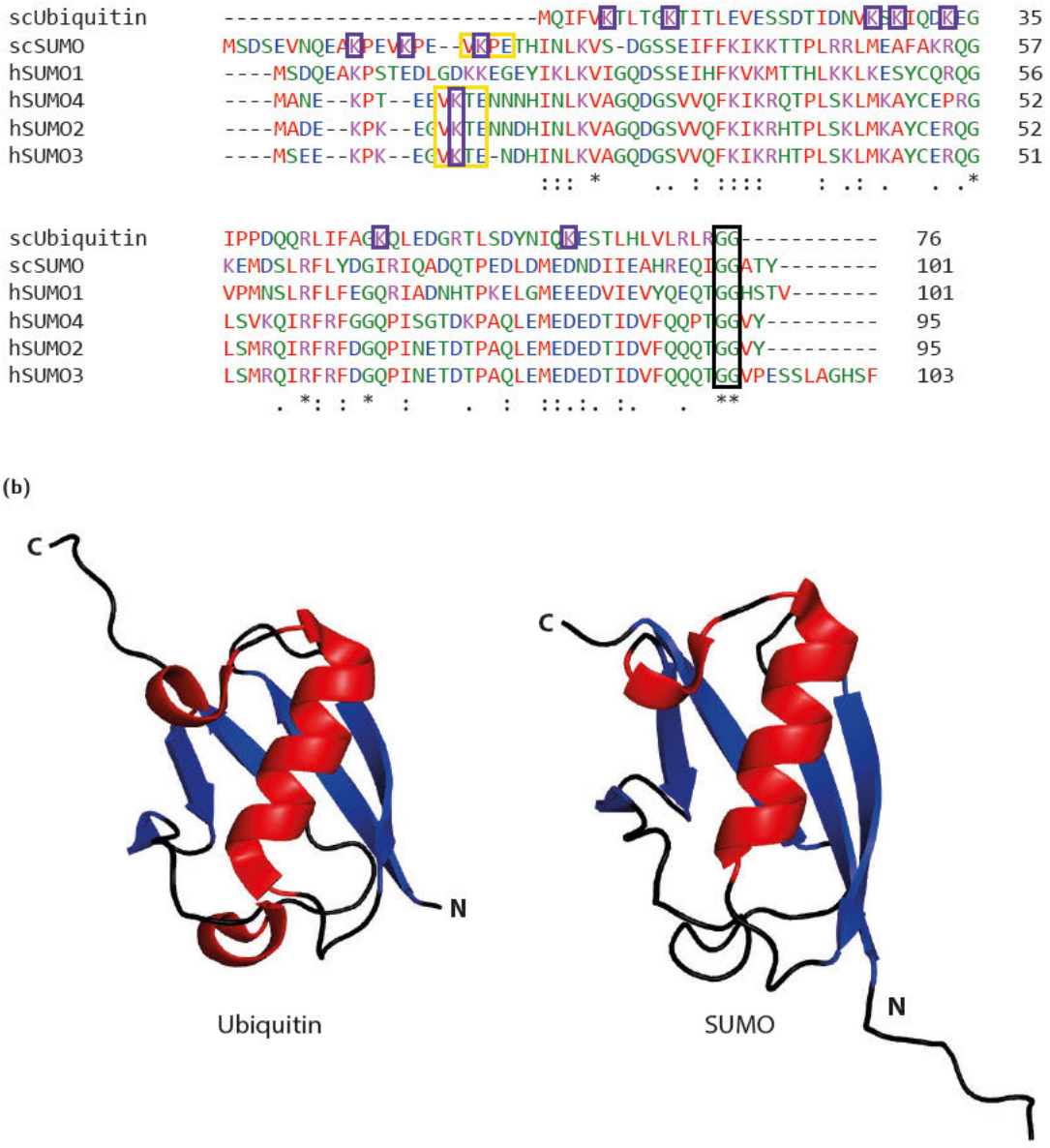

Figure 6: (a) Protein sequence alignment of the *S. cerevisiae* (sc) ubiquitin and *S. cerevisiae* SUMO and human (h) SUMO1–4 proteins. The consensus motif for sumoylation is indicated by a yellow box. SUMO or ubiquitin acceptor lysines (K) are marked by a purple box. The C-terminal di-glycine motif is boxed in black. Alignment was performed using Clustal Omega (https://www.ebi.ac.uk/Tools/msa/clustalo/). An asterisk (*) indicates positions which have a single, fully conserved residue. A colon (:) indicates conservation between groups of strongly similar properties. A period (.) indicates conservation between groups of weakly similar properties. The alignment is coloured according to the chemical properties of the amino acids, small/ hydrophobic/aromatic residues are coloured red, acidic residues are coloured blue, basic residues are coloured magenta, and polar residues (hydroxyl/ sulfhydryl/ amine/ G) are coloured green. **(b) Ribbon diagram of structurally related yeast SUMO (right) and ubiquitin (left).** Structural elements of both proteins are shown, highlighting the similarity of the three-dimensional structures of both. α-helices are coloured in red, β-sheets are coloured in green and β-turns and loops are coloured in black. The image was created using PyMOL (https://pymol.org). Structures are commonly available from the protein data bank (pdb) (ubiquitin: 6NYA, SUMO: 2EKE). Part of the unstructured N-terminus of SUMO is cut from the image.

1.2.2 The sumoylation cascade

Similar to the conjugation of ubiquitin, SUMO has to undergo a cascade of different steps (precursor cleavage, activation by an E1 enzyme, and transfer and conjugation by an E2 (and E3) enzyme (fig. 7), before it is attached to a lysine residue in its target. In the first step of the conjugation, cascade SUMO is activated in an ATP-dependent manner by the heterodimeric E1 enzyme (Aos1/Uba2 in *S. cerevisiae* and Sae1/Sae2 in human). The resulting thioester bond between the active site cysteine of the E1 enzyme and the C-terminus of SUMO is then transferred to the active site cysteine of the E2 enzyme (Ubc9 in *S. cerevisiae* and human). Finally, SUMO is conjugated to a lysine residue in its substrate protein. *In vitro* this final step can happen in most cases without an E3 enzyme being present (E3s in yeast: Siz1, Siz2, Mms21 and Zip3 and ∼10 E3s in human). *In vivo* sumoylation of most targets requires an E3.[182,183,199–203]

Sumoylation is a reversible process and modification by SUMO can be removed by the activity of SUMO-specific proteases, called Ubiquitin-Like specific Proteases (ULPs) (Ulp1/2 in *S. cerevisiae* and SENP1–3, SENP5–7, DESI1–2, and USPL1 in human). Moreover, SUMO is expressed in the cell as a precursor protein, which is cleaved by SUMO-specific proteases (Ulp1 in *S. cerevisiae* and (mainly) SENP1/2/5 in human). Ulp1 and Ulp2 have different subcellular localizations and are responsible for desumoylating different proteins.[204–206] The specific localisation and recruitment of the factors of the (de-)sumoylation machinery allows highly process-specific SUMO signals.[203,206–208]

In *S. cerevisiae* many of the genes encoding SUMO pathway proteins are essential, including *SMT3*, *UBA2*, *AOS1*, *UBC9*, and *ULP1*.[181]

Proteins that recognize SUMO-modified substrates often contain SUMO interaction motives (SIM). These consist of two to four hydrophobic amino acids embedded in a β-strand and followed or preceded by a negatively charged amino acid. They can recognize different surfaces of the SUMO molecule. The most common SIMs (class I) make contact with a hydrophobic patch between α-helix 1 and β-sheet 2 of SUMO.[208–210]

1.2.2.1 The SUMO E1 (Uba2/Aos1)

AOS1 and *UBA2* are essential genes.[38] Their protein products form a hetero-dimer that shares sequence similarity to the N- and C-terminal domains of the ubiquitin-activating enzyme.[38,211]

Like for ubiquitin, the E1 Aos1/Uba2 binds ATP, magnesium and SUMO to catalyse the formation of a high-energy thioester bond between the E1s catalytic cysteine and SUMO under the release of adenosine monophosphate. Secondly, the E1 catalyses a trans-thioesterification reaction to Ubc9 to form an E2/SUMO thioester. A second

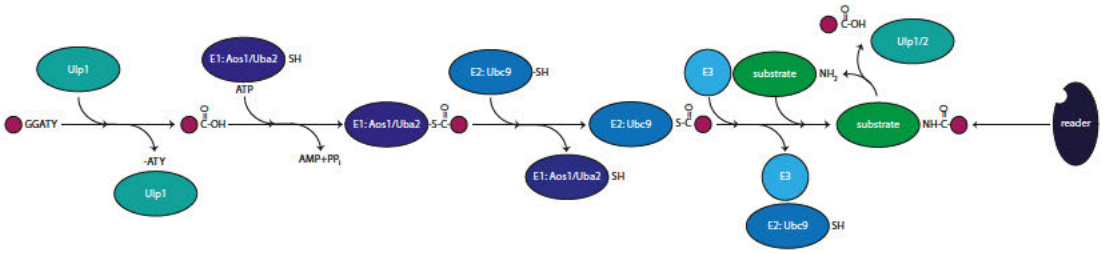

Figure 7: (a) Reversible sumoylation cascade. SUMO (purple cycle) is translated as a longer, inactive, precursor (-GGATY). It is cleaved to reveal a C-terminal di-glycine motif (GG) by the SUMO protease Ulp1. The mature SUMO is activated by the heterodimeric E1 enzyme Aos1/Uba2 in an ATP-dependent manner, forming an energy-rich thioester bond. SUMO is then transferred to the E2 enzyme Ubc9 (conjugating enzyme), again forming a thioester with the active site cysteine. Next, it is covalently attached to specific lysines within a target protein. That step can be supported by one of several SUMO E3s (ligases, Siz1, Siz2, Mms21 and Zip3). Ubc9 can sumoylate SUMO itself, leading to the formation of poly-SUMO chains. Readers of the SUMO code recognize the posttranslationally modified proteins and can bind to them. They usually contain a SUMO interaction motif (SIM). SUMO can be deconjugated from proteins by the SUMO-specific proteases Ulp1 or Ulp2 (eraser). GGATY = glycine-glycine-alanine-threonine-tyrosine, PPi = inorganic pyrophosphate.

SUMO molecule can be adenylated while the E1 carries out the thioester formation between SUMO and the E2.[4,212]

1.2.2.2 The SUMO E2 (Ubc9)

Like the E1, *UBC9* is an essential gene. Ubc9 receives SUMO from the E1 through a transthioesterification reaction. Following this step, it can transfer SUMO to a lysine residue through the formation of a thioester bond. Sumoylation often occurs at the so-called SUMO consensus motif Ψ-Lys-X-Asp/Glu (Ψ is a hydrophobic residue, lysine is the target lysine, to which SUMO is attached, and X is any amino acid) or a similar/reverse motif, which can be directly recognized by Ubc9. In addition, SUMO can also be conjugated to non-consensus sites.[4,203,208,213–216] The formation of SUMO chains is catalysed by the common action of several Ubc9 molecules via their ability to bind a second SUMO molecule on their backside.[4,217–220] E3s bind to other surfaces of the substrate and the E2 to enhance specificity and efficiency.[208,221,222]

1.2.2.3 SUMO E3 enzymes

There are four E3s in *S. cerevisiae*: Siz1, Siz2, Mms21 and Zip3. In human cells, several E3s are known (e.g. Pias1-4, RanBP2, ZNF451-3 and MMS21).
Single mutants of the Protein inhibitor of activated STAT (PIAS)/SAP and Miz-finger domain-containing protein (Siz) E3 family members *siz1* and *siz2* grow well without obvious phenotypes.[181,223,224] The *siz1/siz2* double mutant is also viable, but it is cold-

sensitive, shows delays in the cell cycle at transition from G2-phase to mitosis (G_2/M), and has very low levels of SUMO conjugates.[181,225,226] The methyl methanesulphonate-sensitivity protein 21 (Mms21 or Nse2) is a subunit of the Structural Maintenance of Chromosomes complex (Smc5/6 complex) and is required for DNA replication and repair and for efficient sister chromatid cohesion. Mutants are viable, but sensitive to Methyl methanesulfonate (MMS), show increased spontaneous mutation and mitotic recombination. Inactivating all three mitotic SUMO E3 enzymes results in lethality. Thus, Siz1 and Siz2 and Mms21 can act redundantly on some substrates.[227–229]
The meiosis-specific Zip3 protein (ZIPping up meiotic chromosomes 9, also known as Cst9) is required for synaptonemal complex formation. It is not essential, and deletion leads to reduced sporulation.[40,230,231]
All yeast E3s contain an SP-RING domain and a SIM (or SIM-like) domain. The SP-RING domain is a hybrid between a RING and a U-box domain. It coordinates only one Zn^{2+}. The other is replaced by a loop that is held together by side-chain interactions. Like other RING-type E3s, SUMO E3 enzymes are considered to increase the rate of SUMO conjugation to substrates by facilitating their interaction with the SUMO-loaded E2.[4,232]

1.2.3 SUMO deconjugation

There are two SUMO deconjugating enzymes (SUMO proteases) described in *S. cerevisiae*, Ulp1 and Ulp2. In human cells six SUMO specific proteases (SENP1, -2, -3, -5, -6 and -7) have been found. All eight are members of the sentrin-specific proteases (SENPs) family. They are cysteine protease with a conserved, ∼200-amino acid long, catalytic region (ULP domain).[204–206,233,234] Recent studies have identified three new SUMO proteases in humans, desumoylating isopeptidase 1 (DeSI1), DeSI2 and ubiquitin-specific protease-like 1 (USPL1), which share little sequence similarity with the SENP protease class.[206,235,236]
Besides deconjugation of SUMO from substrates, SUMO proteases can also trim SUMO chains and they are needed for the maturation of newly synthesized SUMO. *ULP1* in yeast is essential as it is responsible for the SUMO precursor cleavage. *ULP2* mutants are viable, but exhibit poor growth, sensitivity to a variety of stress conditions, and they have defects in chromosome segregation.[181,205,237,238] SUMO proteases have varying preferences for chain lengths and show specific localizations within the cell. These two factors largely determine their substrate specificity. Ulp1 is located mostly at the inner surface of the nuclear pore complex (NPC), but it is also transported to the cytoplasm. Ulp1 processes a broad range of substrates and is involved, for example, in the desumoylation of Septins during cell division or of the spindle-orientation protein Kar9 during cell cycle progression.
Ulp2 can be found in the nucleus and has a strong preference for the cleavage of SUMO

chains, but can also cleave isopeptide linkages between a substrate and SUMO. Its main substrate is sumoylated Top2 during centromere cohesion and cell division after DNA damage.[126,181,205,206,239–243]

1.2.4 Readers of sumoylation

Analogous, to ubiquitin-binding domains, SUMO-binding proteins contain a so-called SUMO-Interacting Motif, with which they non-covalently interact with SUMO. Most SIM motifs consist of an essential hydrophobic core of three to four amino acids in the [IVL]-X-[IVL]-[IVL] (X is any amino acid) consensus sequence or a reverse consensus motif. This core is often flanked by several negatively charged amino acids or amino acids that can be phosphorylated (at serine or threonine). The hydrophobic core adopts a β-strand structure that complements the hydrophobic surface of SUMO. The interaction between a SIM and SUMO can occur in a parallel or an anti-parallel orientation with respect to the sense of the β2-strand of SUMO. SIMs are found in Uba2, in all known SUMO E3s, in SUMO-Targeted Ubiquitin Ligases (STUbLs), and in some SUMO substrates and most SUMO readers.[4,244–248]
As expected for dynamic protein-protein interactions, the SUMO-SIM interaction is relatively weak. SIMs typically interact with SUMO with affinities in the micromolar range.[4,209,246,249–252] However, interaction strength can vary towards different SUMO isoforms, in response to PTMs (especially phosphorylation and acetylation) of the SIM or adjacent amino acids, depending on the orientation of the binding, or in the presence of additional binding sited that interact with the target protein rather than the SIM motif.[4,187,250,253,254] Some proteins even contain multiple SIM motifs, which often enhance their affinity to SUMO chains, by simultaneous interaction with several SUMO molecules.[4,255–258]

In addition to SIMs, two other types of SUMO-binding domains have been identified in mammalian cells. The ZZ zinc finger domain of HERC2 interacts with SUMO in a zinc-dependent manner.[4,259] And the MYM-type zinc finger that interacts with SUMO1.[4,260]

1.2.4.1 SUMO-Targeted Ubiquitin Ligases (STUbLs)

STUbLs are ubiquitin E3s that harbour one or more SIM domains and thereby recognize SUMO moieties. This leads to the ubiquitination of sumoylated target proteins or of SUMO itself, resulting in mixed SUMO-Ub chains. The mixed chains often lead to proteasomal degradation of the substrate. Four STUbLs have been described in yeast,

Uls1, Irc20, Rad18 and the Slx5/Slx8 complex.[261] As an example, the function of yeast Rad18 protein is further discussed in section 1.1.6.4.[262]
The best characterized STUbLs in humans are RNF4 and RNF111/Arkadia. The human RNF4 E3 will be important later in this thesis. RNF4 harbours a RING domain and four SIM motifs. It can recognize single SUMO moieties, but has a higher preference for chains of at least two SUMO2 residues.[256,263] Upon binding to a SUMO chain it transfers ubiquitin to the distal SUMO of the bound chain. RNF4 can synthesize K11, K48, and K63-linked ubiquitin chains *in vitro*.[264,265] One of the best-characterized targets of RNF4 are Promyelocytic leukemia (PML) nuclear bodies,[263,266,267] additional roles have been described in the (dis-) assembly of DNA repair complexes.[265]

1.2.5 Functions of sumoylation

Most identified SUMO substrates are found in the nucleus, where sumoylation is regulating processes like transcription, replication, DNA repair and protein transport.[66,268] The most prominent non-nuclear sumoylation target in *S. cerevisiae* are the Septins during bud formation.[223] The function of sumoylation is nearly impossible to predict, however it often leads to the degradation of a protein, a change in its localisation or activity, or to the recruitment of further factors. In the following section sumoylation of two nuclear targets, namely PCNA and RPA during DNA replication, and repair and the sumoylation of Septins will be discussed.

1.2.5.1 Sumoylation of PCNA

As described in section 1.2.4.1 several substrates exist that are modified by sumoylation and ubiquitination at the same time. One example is PCNA. Its ubiquitination and the resulting cellular functions in DNA repair are described in section 1.1.6.4.
In *S. cerevisiae*, PCNA has been shown to be sumoylated during DNA replication in a DNA damage independent way (fig. 4). This modification recruits the anti-recombinogenic helicase, Suppressor of Rad Six 2 (Srs2), to prevent unwanted HR at replication forks during S-Phase.[44,126,187,269,270] Sumoylation occurs at K164 of PCNA, and to a lower extent also at K127. Sumoylation of PCNA only happens when it is loaded onto DNA. The E3 Siz1 is needed for sumoylation at K164, while modification of K127 requires Siz2 *in vivo*.[103,271]
Srs2 harbours a PCNA interaction protein box (PIP-box) like motif and a SIM motif in its C-terminus, both of which are involved in the recognition of PCNA.[103,269,272] Unscheduled HR is prevented in the presence of Srs2 by the disruption of Rad51 filament formation.[103,187,269,273,274]

Although they both target the same site on PCNA, sumoylation and ubiquitination do not seem to compete. In contrast, SUMO on PCNA can be recognised by the ubiquitin ligase Rad18 through its SIM. Interaction enhances Rad18 depended ubiquitination of PCNA upon encounter of replication-stalling DNA lesions, leading to a preselection in DNA damage repair pathway choice away from HR towards a Rad6 dependent pathway.[130,198] Sumoylation of PCNA also increases, but is not essential for, its interaction with the alternative clamp loader complex, Elg1-RFC2–5. It is proposed to unload PCNA after replication.[103,275–277]
To a lower extent than in yeast, SUMO conjugation to PCNA is also found, in mammalian cells and *Xenopus laevis* egg extract, but its function is still unclear.[278–280]

1.2.5.2 Sumoylation of RPA

Replication factor A (RPA) is a heterotrimeric single-strand DNA binding complex (consisting of RFA1/RFA2/RFA3) involved in DNA replication, repair, and recombination, telomere protection and other processes that involve single-strand DNA. It protects single-strand DNA against degradation by nucleases and serves as a platform for protein recruitment.[129,281–284] At the sites of DNA double-strand breaks in *S. cerevisiae*, the 5' DNA strand is resected to produce a long 3' single-strand DNA overhang. After the end-resection, the single-strand DNA is covered with RPA. When RPA is bound to DNA it can be sumoylated at the junction between single-strand DNA and double-strand DNA with the help of the E3 Siz2. Sumoylation of RPA predominantly occurs on two lysines of its largest subunits Rfa1 (K170 and K427). The SUMO-RPA signal is amplified by successive rounds of sumoylation, during which the SUMO-modified RPA complexes readily exchange with unmodified RPA at the junction.[285–288]
Sumoylation of RPA contributes to DNA repair, through the possibly SIM-SUMO-dependent recruitment and Siz2-dependent sumoylation of proteins involved in recombinational repair (e.g. Rad52 and Rad59).[208,286,288] Sumoylation of RPA leads to its increased interaction with Slow Growth Suppressor 1 (Sgs1), which contains four SIMs.[208,287,289] Sgs1 is a helicase with roles in checkpoint regulation, and its recruitment to DNA through RPA interaction enhances the DNA damage checkpoint kinase activation.[208,287,288]
Also in mammalian cells, RPA1 is described to be modified with SUMO in response to replication-mediated or radiation-induced double-strand breaks to promote the HR repair pathway.[103,290]

1.2.5.3 Sumoylation of Septins

Septins were discovered in 1971 by L.H. Hartwell.[291] They are present in all eukaryotes, except for plants.[292] Septin mutants show abnormal morphology at the bud neck, especially misdirected growth. Septins are required for correct nuclear positioning and timing of the cell cycle. They act as a scaffold to recruit proteins to the bud neck, and as a barrier to control diffusion between mother and daughter cell. Moreover, they promote membrane curvature and have been described to play a role in endocytosis and endoplasmic reticulum (ER) composition.[293,294]
Budding yeast has five mitotic Septin proteins: Cell division cylcle proteins 3/10/11/12 (Cdc3/10/11/12) and Shs1. *CDC3* and *CDC12* are essential. Deletion of *CDC10* and *CDC11* causes severe phenotypes, while in *SHS1* mutants only mild phenotypes with respect to Septin structure formation during cell division are observed.[295–297]
During mitosis, Septins assemble into a hetero-octamer, consisting of two times Cdc3/10/12 capped on both sides by either Shs1 or Cdc11 (fig. 8a). In the early G_1-phase Septins assemble at the future bud site in a patch. Shortly before the bud emerges, the Septin patch changes into a ring structure and filaments are formed at the plasma membrane. After the bud has emerged, an hourglass-like or collar-like shape is established. This stays until mitosis starts. Before cytokinesis, the hourglass splits into two rings, between which the actin-myosin contractile ring assemblies and cell separation occurs (fig. 8b). After cell division, the old Septin ring disassembles. Some of the Septins are degraded, and others are recycled. Septin assembly and transition from the ring to the collar structure is mediated by acetylation and phosphorylation. Splitting of the hourglass is initiated by a switch in the orientation of the Septins and accompanied by their phosphorylation and their sumoylation on the mother cell site.[298–300]
Septins are the most abundant SUMO target in budding yeast. Their sumoylation occurs shortly before anaphase and disappears during cytokinesis. The E3 enzyme Siz1 is needed for Septin sumoylation. Cdc3 has four sumoylation sites, Cdc11 has one sumoylation site and Shs1 has two sumoylation sites.[223,301] In yeast cells expressing sumoylation defective Septins, rings from previous cell cycles stay at the bud site without getting disassembled. However, no growth defect is visible in these strains. Yet, the lysine residues mutated in this study to gain the sumoylation of defective Septins might also be a target for modification by other PTMs.[223]

During meiosis, expression of Cdc3 and Cdc10 is upregulated, while the expression of Cdc11, Cdc12 and Shs1 stays the same as during mitosis. Two additional Septins (Spr3 and Spr28) become expressed.[303–305] Prospore membranes (PSM) of *S. cerevisiae* form the plasma membrane of spores. During meiosis II PSMs form round caps and then extend to tube-like shapes. Septin filaments first localize to microtubules during meiosis I, before forming structures parallel along the PSM during meiosis II. They are

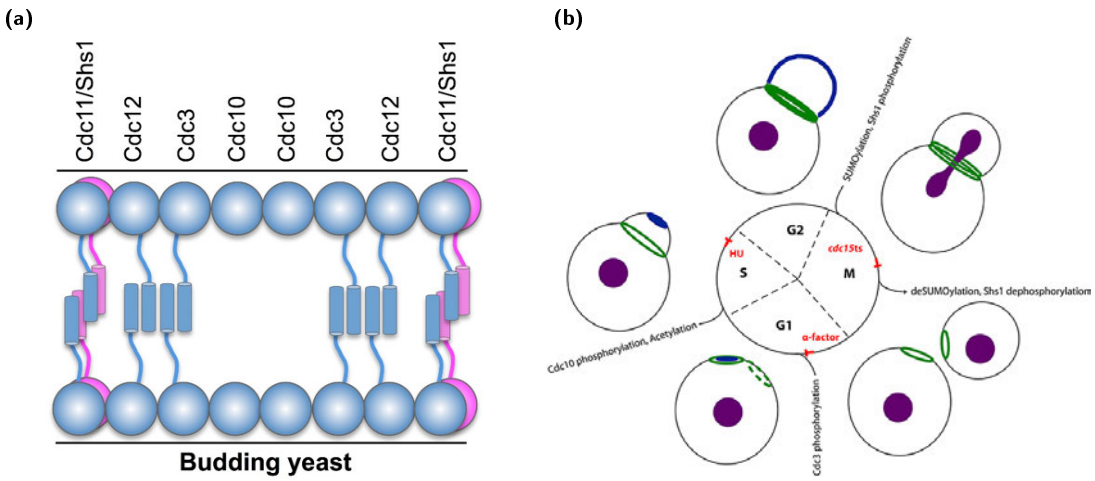

Figure 8: (a) Budding yeast Septins. Hetero-octamer of the five different Septins Cdc3/10/11/12 and Shs1 formed during mitosis. (Adapted from the Finnigan lab webpage: https://www.k-state.edu/bmb/department/directory/Finnigan/lab.)[302] **(b) Cell cycle-dependent localisation and modification of Septins in *S. cerevisiae*.** During early G_1-Phase, Septins assemble as a patch at the future bud site. This patch is then converted into a ring. After the bud has formed, an hourglass-like shape is established. Before cytokinesis the hourglass splits into two rings, between which cell separation occurs (Adapted from Glomb *et al* (2016)).[300]

required for PSM extension and as a scaffold for the recruitment of proteins to the PSM. Loss of both or one meiotic Septin impairs spore formation and changes the structural integrity of the spore.[305–308]

1.2.6 Tools to study sumoylation

There are various tools available to study and manipulate the sumoylation landscape of a cell.

Early genetic analysis of SUMO conjugation cascade components in *S. cerevisiae* showed that mutants arrest as large budded cells in metaphase and have defects in the degradation of securin, Pds1, and mitotic cyclins, indicating that sumoylation is important for metaphase to anaphase transition.[309–312] Lysine mutants of SUMO have also been studied to understand the functions of SUMO chains. This has resulted in the findings that SUMO chains are not essential for yeast survival, but regulate normal chromatin structure and are needed for viability under stress conditions. Chains that are formed through the conjugation of different lysines of SUMOs N-terminus appear to be functionally equivalent.[181,312,313]

Using genetic manipulation of yeast, It was also demonstrated that human SUMO1, but not SUMO2/3, can complement the loss of SUMO in yeast. However, possibly due to the low chain formation ability of SUMO1, yeast expressing SUMO1 instead of yeast SUMO protein are sensitive to various stress conditions, a phenotype similar to

the one in strains lacking the major SUMO E3 enzyme, Siz1.[223,312,314] A comprehensive study of the effect of SUMO mutant expression in *S. cerevisiae* was performed by Newman *et al.* (2017). They analysed a library of >250 mutant strains with single or multiple amino acid substitutions of surface and core residues of SUMO. This was done using plate-based assays to identify residues critical for the response to different stress treatments and for the viability of yeast under normal and stress conditions.[312]

Most commonly used for the detection of SUMO or sumoylated species are antibodies. They can be employed for many different *in vitro* techniques like western blotting, ELISA or IP. There are antibodies available specific to yeast SUMO, and other species. Antibodies against human SUMO can also be specific to the different SUMO isoforms such as SUMO1 and SUMO2/3. However, SUMO2 and SUMO3 can not be differentiated by antibodies.[315] Immunoprecipitation of sumoylated species with SUMO antibodies is often combined with the detection of a selected protein of interest using protein-specific antibodies or mass spectrometry.
Another widely used technique to isolate sumoylated species is the expression of His-tagged SUMO followed by denaturing nickel chromatography to isolate the sumoylated species and their detection and identification by western blot. The denaturing conditions ensure the removal of most unspecific contaminants or non-covalent SUMO interactors and in the inactivation of SUMO proteases.[125,316] Alternatively, hemagglutinin (HA), FLAG, and Myc tagged or biotinylated versions of SUMO have been used to immunoprecipitated SUMO conjugates.[216,317–320]
Several approaches to use SIM-motif-containing protein domains or SIM-peptides for the isolation of endogenous sumoylated proteins are also described.[321,322] One example is the use of so-called SUMO-binding entities (SUBEs), consisting of tandem repeats of SIMs from RNF4 (SIM2 and SIM3). They recognize proteins with SUMO chains with an increased affinity compared to monosumoylated proteins. SUBE binding can be further combined with biotin labelling, marking the SUMO surrounding proteins with a biotin molecule that can be isolated and the proteins can be subsequently identified.[322]

Not only tools to identify sumoylation sites in proteins, but also many techniques that help to identify interactors of SUMO, often containing a SIM domain, have been developed in the past years. SUMO-ID is a technology that uses split SUMO protein complementation and proximal protein labelling with biotin to find interactors of sumoylated proteins. This is usually combined with affinity-purification coupled to mass spectrometry methods to identify the labelled proteins.[320,323]

The Proximity Ligation Assay (PLA) was also adapted to localize sumoylated protein using primary antibodies directed against GFP and SUMO-2/-3 and secondary antibodies labelled with oligonucleotides.[324] Another tool for the identification of transient SUMO-SIM interaction is introducing a photo-inducible crosslinker moiety into SUMO,

within or close to the SIM interaction site. Irradiation of cells expressing this SUMO probe results in covalent bond formation between SUMO and its binding partners.[325]

Like for ubiquitin, identification of isolated proteins is often done using mass spectrometric approaches, like SILAC or AQUA. However, the sumoylation-specific remnant that is left after trypsin digestion is larger than the di-Gly that is found on ubiquitinated substrates. This makes it complicated to identify these sumoylation remnants. Several strategies have been used to overcome this problem. For example, the introduction of artificial trypsin cleavage sites into SUMO to generate short, easily identifiable, SUMO-derived peptides.[324,326–328] Mass spectrometric analysis have led to the identification of more than 40 700 sumoylation sites within 6 700 SUMO substrates.[329]

Additionally, bioinformatic tools to predict sumoylation sites have been developed. Examples are SUMOplot (http://www.abgent.com/tools/sumoplot), PhosphoSitePlus (http://www.phosphosite.org/) and SUMOsp (http://sumosp.biocuckoo.org/).[319]

SUMO interactors or sumoylation sites predicted by *in silico* or high-throughput methods can be validated using purified proteins of the sumoylation cascade for *in vitro* sumoylation reactions or interaction studies.[125,330,331]
Fluorescence resonance energy transfer (FRET) has been used to detect and characterize enzyme kinetics of SUMO conjugation and deconjugation.[316,332–334]

Another approach to study sumoylation is the inhibition of SUMO conjugation, deconjugation or SIM interaction. A tool to inhibit the interaction of SUMO with SIM-containing proteins *in vitro* and in cells are Affimers. These are synthetic binding proteins that interfere with either SUMO1-mediated interactions or interactions mediated by either SUMO2/-3 or both, enabling the specific analysis of SUMO-induced protein-protein interactions.[195]
Sumoylation cascade inhibitors have not only been developed for use in research, but also for medical use, especially for the treatment of cancers. Several natural and synthetic compounds have been reported to inhibit different steps of SUMO (de-)conjugation. Specifically, they target the SUMO E1 or E2, or SENP1 or -2. TAK-981 is the only sumoylation inhibitor that is currently undergoing clinical Phase1/2 trials. These studies are conducted in adult patients with advanced or metastatic solid tumours or relapsed/refractory hematologic malignancies. It is a selective SUMO E1 inhibitor that binds to the nucleotide-binding pocket of SAE1 forming an adduct with SUMO.[335–337]

One part of this thesis (section 3.3) focuses on finding tools to study sumoylation *in vivo* with/-out inhibiting effects on the sumoylation cascade. The technology used for this will be described in the following sections.

1.2.6.1 DARPins: using *in vitro* selection to explore the sumoylation system

For most cell biological and biochemical approaches as well as pharmaceutical applications and drug development, antibodies are the most commonly used binding reagents. However, their complex structure and elaborate production process have led to the exploration of alternative engineering methods that avoid animal immunisation and the development of new and simpler binding reagents, which can either be immunoglobin derivates (e.g. nanobodies) or based on different protein scaffolds (e.g. Designed Ankyrin Repeat Proteins (DARPins)).[338] The importance of these tools is highlighted by how the 2018 Nobel prize for Chemistry was awarded; namely for the development of the phage display technology for the selection of peptides and antibodies.

DARPins are an example for non-immunoglobulin-binding proteins. Their structure is based on natural occurring elongated solenoid proteins, called ankyrin repeat proteins.[339,340] Ankyrin repeat proteins can be found in all kingdoms of life, where they mediate various protein-protein interactions.[341,342] For example in *Homo sapiens*, 145 genes encode ~400 ankyrin repeat (AR) domains.[339,343,344] An example of a naturally occurring AR protein is IκBα, which inhibits the DNA binding of NF-κB with a K_i of 3.1 nM.[339,345]

One AR domain usually consists of four to six tightly packed repeats, each made of 33 amino acid residues. At the structural level, each repeat forms a β-turn followed by two antiparallel α-helices and a loop connecting it to the next repeat. The single repeats in one domain form a right-handed solenoid structure. This structure leads to a large solvent-accessible surface and a hydrophobic core.[339–341,344,346–348] In nature, different AR-containing proteins have adapted to bind to virtually any target protein through changes in their variable residues. This adaptability is further supported by their modularity, allowing not only the exchange of single surface residues but also the insertion and deletions of repeats during evolution.[348,349]

The modular architecture of ankyrin repeat proteins allowed the construction of DARPins through a consensus design approach.[339,342,349,350] DARPins consist of two to three internal, randomized repeats flanked by N- and C-terminal capping repeats (N- and C-Caps) forming an elongated AR domain (fig. 9a).[339,351] Originally, the N- and C-Caps of DARPins were taken from the human guanine-adenine-binding protein (GABPβ1, all cysteines were replaced to prevent dimerization and oxidation), but have been adapted over time for higher stability and to introduce randomized residues in the caps.[339,344,349,352,353] Each repeat consists of fixed amino acids, which form the framework of the protein and six variable amino acids (positions 2, 3, 5, 13, 14 and 33) that lie on a groove-like surface and can make contact to other proteins (fig. 9b).[339,344,354] The randomized interacting residues are located in the loop, β-turn and the first α-helix. The positions of these variable residues were chosen based on studies of the interaction locations of natural AR proteins.[339,349]

(a)

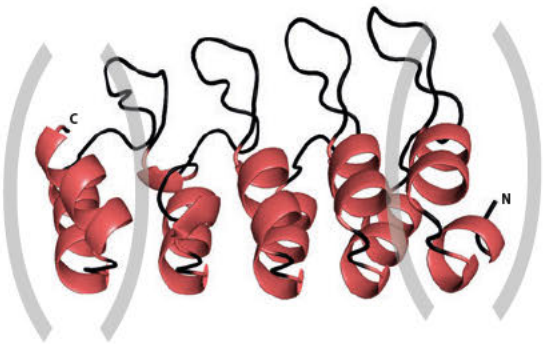

(b)

```
                 α-helix1        α-helix2                β-turn    α-helix1    α-helix2
general          GSDLGKKLLEAARAGQDDEVRILMANGADVNAxDxxGxTPLHLAAxxGHLEIVEVLLKzG    60

E3.5             GSDLGKKLLEAARAGQDDEVRILMANGADVNATDNDGYTPLHLAASNGHLEIVEVLLKNG    60
A10              GSDLGKKLLEAARAGQDDEVRILMANGADVNAEDLRGFTPLHLAANSGHLEIVEVLLKTG    60
C10              GSDLGKKLLEAARAGQDDEVRILMANGADVNAQ----------------------------    33
F10              GSDLGKKLLEAANNGQDDEVRILMANGADVNAQ----------------------------    33
E11              GSDLGKKLLEAATHGQLDEVRILMANGADVNAV----------------------------    33
G11              GSDLGKKLLEAARAGQDDEVRILMANGADVNASDSDGATPLHLAAHQGHLEIVEVLLKTG    60
B12              GSDLCKKLLEAARAGQDDEVRILMANGADVNAVDQWGLTPLHLAAHQGHLEIVEVLLKTG    60
                 **** *******  ** ***************
                 N-capping module ->            repeat module 1 ->

                       β-turn    α-helix1    α-helix2                β-turn    α-helix1    α-helix2
general          ADVNAxDxxGxTPLHLAAxxGHLEIVEVLLKzGADVNAxDxxGxTPLHLAAx-xGHLEIV  119

E3.5             ADVNASDLTGITPLHLAAATGHLEIVEVLLKHGADVNAYDNDGHTPLHLAAK-YGHLEIV  119
A10              ADVNAQDNYGWTPLHLAAVIGHLEIVEVLLKHGADVNAKDNFGSTPLHLAAR-LGHLEIV  119
C10              ------DTQGRTPLHLAAQRGHLEIVEVLLKAGADVNAHDQYGWTPLHLAAHANGHLEIV  87
F10              ------DWAGWTPLHLATTIGHLEIVEVLLKTGADVNASDQYGTTPLHLAAR-LGHLEIV  86
E11              ------DNTGMTPLHLAAYEGHLEIVEVLLKHGADVNALDVHGWTPLHLAAQ-EGHLEIV  86
G11              ADVNATDNEGHTPLHLAAEHGHLEIVEVLLKAGADVNAHDQYGWTPLHLAAHANGHLEIV  120
B12              ADVNATDNEGHTPLHLAAEHGHLEIVEVLLKAGADVNAHDQYGWTPLHLAAHANGHLEIV  120
                       *  * ******:  *********** ****** *  * *******:  ******
                       repeat module 2 ->                repeat module 3 ->

                                β-turn    α-helix1    α-helix2
general          EVLLKzGADVNAQDxxGxTAFDISIxxGNEDLAEILQKLN---   159

E3.5             EVLLKHGADVNAQDKFGKTAFDISIDNGNEDLAEILQ---KLN   159
A10              EVLLKHGADVNAQDKWGETPFDLAIDNGNEDIAEVLQKAAKLN   162
C10              EVLLKHGADVNAQDWIGVTPFDLAVDDGNEDIAEVLQKAAKLN   130
F10              EVLLKHGADVNAQDKWGETPFDLAIDIGNEDIAEVLQKAAKLN   129
E11              EVLLKHGADVNAQDHAGDTPFDLAAMYGNEDIAEVLQKAAKLN   129
G11              EVLLKHGADVNAQDWIGVTPFDLAVDDGNEDIAEVLQKAAKLN   163
B12              EVLLKHGADVNAQDWIGVTPFDLAADDGNEDIAEVLQKAAKLN   163
                 **************  * * **::   ****:**:**   ***
                                C-capping module ->
```

Figure 9: (a) Structure of an exemplary DARPin (A10). Structural elements of an exemplary DARPin (A10) are shown. α-helices are coloured in red and β-turns and loops are coloured in black. The N-capping module and the C-capping module are bracketed. The image was created using PyMOL (https://pymol.org). **(b) Alignment of DARPins from this thesis.** Sequences of ankyrin repeat (AR) modules of a general DARPin (black) and the DARPins used in this thesis are aligned. DARPin E3.5 is not raised against yeast SUMO. The secondary structure elements are indicated above the sequences. The N-terminal capping AR and the C-terminal capping AR are separated from the variable repeats by black lines. The DARPins consist of 2–3 variable repeats. The six randomized residues are marked by a red x in the general sequence, the residue marked with a z is a randomized framework residue, which can be an asparagine, histidine, or tyrosine.[344,351] The alignment was performed using Clustal Omega (https://www.ebi.ac.uk/Tools/msa/clustalo/). An asterisk (*) indicates positions which have a single, fully conserved residue. A colon (:) indicates conservation between groups of strongly similar properties. A period (.) indicates conservation between groups of weakly similar properties. The alignment is coloured according to the chemical properties of the amino acids, small/ hydrophobic/aromatic residues are coloured red, acidic residues are coloured blue, basic residues are coloured magenta, and polar residues (hydroxyl/ sulfhydryl/ amine/ G) are coloured green.

In the DARPin libraries, which are used as the starting point for *in vitro* selection, the amino acids responsible for interaction are randomized. Library members are not allowed to contain glycine, proline (both structurally unfavourable) or cysteine (which forms disulfide bonds).[339,349] The theoretical diversities of the DARPin libraries are 5.2×10^{15} or 3.8×10^{23} for two-repeat or three-repeat DARPins, respectively.[344,354] The first DARPin to be crystallized was the unspecific DARPin E3.5. It shows a very regular and ordered AR domain fold, and the structure is highly homologous to mouse GABPβ1 (69.7 % sequence identity).[349,355] In the first selection experiment that was carried out, four to five selection rounds were performed to generate specific binders with high affinities for the *Escherichia coli* (*E.coli*) maltose-binding protein (MBP) and two eukaryotic mitogen-activated protein kinases (MAPKs), resulting in DARPins with low nanomolar affinities for their targets. The association rates of the gained DARPins are in the typical range for protein-protein interactions (10^5–10^6 $M^{-1}s^{-1}$)[351,356] and the dissociation rates are between 10^{-2} to 2×10^{-3} s^{-1} (all determined by surface plasmon resonance (SPR)).[351] Interestingly, the selected DARPins contain numerous aromatic residues, especially tyrosines, which can mediate dual interactions via H-bonds and hydrophobic contacts.[351]

Application of DARPins

Antibody production needs a relatively elaborate expression process with low expression yields and the reproducibility between batches is low, as they are commonly gained through immunization of animals. Antibodies consist of four polypeptide chains and can have more than four chains when produced recombinantly, making them prone to aggregation. Antibodies are also depend on disulfide bonds for stability.[357,358]

DARPins do not require animal immunisation but can be produced by *in vitro* selection processes. DARPins generally express very well in *E.coli* as soluble monomers, which makes their production process much less elaborate and highly reproducible. The typical yield from *E.coli* expression is ~1 g/L in a simple shake-flask expression or 15 g/L in high-cell-density fermentation.[349,357,359,360]

DARPins are made up of a single polypeptide chain. Therefore, they show high thermodynamic and denaturing stability and can be expressed and used in high concentrations without aggregation. Their stability increases with length.[349] They are very small and do not require disulfide bonds for proper folding. Hence, they can be expressed and applied in the reducing intracellular environment under physiological conditions.[339,351] Their value for intracellular applications is further supported by the high affinity (routinely in the nanomolar to the picomolar range) and excellent specificity that DARPins display towards their targets.[360–362]

Apart from being useful for intercellular application, DARPins have been used to enable and improve crystallisation of their target proteins, as they facilitate crystal formation and can lock proteins in specific conformations, which otherwise could not be captured

by crystallisation.[344,363–366] In addition and similar to antibodies, DARPins can be used to capture molecules on protein chips for interaction analysis or for affinity purification. Moreover, DARPins can be used to detect or block their targets in specific conformations or in different post-translational modification stages. Taken together these properties make them a useful tool to study biological processes in real space and time.[360,367–369]
An example of conformation-specific DARPins are those selected specifically for either binding to Extracellular signal-regulated kinase (ERK) or its phosphorylated form p-ERK. They recognize the conformational change that the kinase undergoes upon activation by phosphorylation. When coupled to a fluorescence dye they have been shown to be useful for the visualisation of activated ERK in mouse embryo fibroblasts.[344,370]

Additionally to their usefulness for the scientific community, the Zurich-based company Molecular Partners AG have developed DARPins for clinical use.[371]
The first DARPin that became clinically validated is called abicipar pegol. This pharmaceutical contains a DARPin that binds specifically to the human vascular endothelial growth factor (VEGF-A).[344,357,361] It is used for the treatment of diabetic macular edema and age-related macular degeneration.[344,372] Randomized phase 3 clinical trials showed that patients treated with abicipar pegol maintain vision gains with more than 50 per cent fewer injections versus an approved product from a different producer. However, patients also display a higher level of intraocular inflammation compared to the approved product, which led to the retrieval of abicipar pegol from the admission procedure for further research to be done.[373]

One of the most exciting recent developments is ensovibep, a multi-specific anti-SARS-CoV-2 DARPin.[371,374] It has entered clinical trials in November 2020 and is currently in phase 2/3. The first results from a Phase 2 global clinical study showed an approximately 80 per cent reduction of the combined risk of hospitalization, emergency room visits, or death of an ambulatory treated patient in an early stage of acute COVID-19 infection compared to the placebo group.[374]
Ensovibep combines five DARPin domains on a single polypeptide chain. Two domains bind human serum albumin for serum half-life extension of the drug. The other three domains associate with different epitopes of the receptor-binding domain of the SARS-CoV-2 spike protein.[375,376] Binding of the DARPins inhibits ACE2 interaction of the virus by locking the spike protein in an open conformation. A multivalent binding mode was chosen to limit possible viral escape.[375] The success of this strategy was shown in December 2021 as ensovibep could inhibit all, by then occurring, SARS-CoV-2 variants, including Omicron, and it can prevent the development of escape mutations comparably to a cocktail of monoclonal antibodies.[377]

In addition to the two DARPins-based drugs described above, Molecular Partners is also developing DARPin-based anti-cancer drugs (immuno-oncology) that are currently in preclinical or Phase I trials. They are designed to activate immune cells specifically in the tumour, but not in the rest of the body, leading to an activation of the body's own defence against the cancerous cells.[371] Moreover, different DARPins and DARPin complexes selected against Epidermal growth factor receptor 2 (Her2), a cell surface receptor overexpressed in several cancer tissues, have been characterized in *in vitro* experiments, and nude mouse xenografts for their affinity and tumour accumulation.[362,378]

Selection of DARPins

DARPins can be selected from synthetic DNA libraries by *in vitro* techniques like ribosome display, phage display, or yeast display, with ribosome display being the most commonly used method. It was first developed by Mattheakis *et al.* (1994, 1996) for the selection of small peptides[354,379,380]. And shortly afterwards advanced for the *in vitro* evolution of proteins.[381]

For ribosome-display-based selection, the library DNA or PCR products coding for the DARPins are ligated into a ribosome display vector. The vector contains a strong promotor, a ribosome binding site and a spacer sequence. After a PCR from the promoter to the middle of the spacer, the construct codes for a start codon, but no stop codon. The DARPin DNA is *in vitro* transcribed and the mRNA translated *in vitro* by isolated ribosomes. Because of the lack of a stop codon the mRNA and the freshly transcribed DARPins are not released from the ribosome, forming a ternary complex. The nascent proteins are still covalently attached to the tRNA within the ribosome, with the spacer in the tunnel of the ribosome, and the DARPin readily folded on the outside. These ternary complexes are then exposed to a target protein that is immobilised on a solid surface, for example via biotinylation and streptavidin binding. DARPins that interact with the target are enriched, while unbound ribosome complexes are washed away. Next, bound ternary complexes are destabilized via EDTA addition. The ribonucleic acid (RNA) encoding for potential target-specific DARPins from the complexes is reverse transcribed and PCR amplified. For introducing diversity, this can be an error-prone mutagenesis PCR. The DNA from this PCR can then undergo the next round of selection or can be cloned into a vector for expression of the DARPins in *E.coli* and verification of the interaction by ELISA. To recover binders with good affinity, typically 3–5 rounds of selection are performed.[354,382]

To enhance the specificity of the received DARPins, for example, to a specific isoform of a protein or to a conformational state, a selection round can be performed, where the the non-desired target is added as a competitor during binding, such that all members of the library that do not discriminate between the desired target and an unspecific target can be washed out after binding to the non-immobilized competitor.[354]

To isolate DARPins with even higher affinities, an off-rate selection can be performed: an excess of the non-biotinylated target is added after the binding reaction between

the ternary complex and the immobilized target has already been equilibrated. This ensures that fast dissociating binders are washed out as they are occupied by the non-immobilized targets, while high-affinity binders with a slow off-rate are retained on the immobilized target and not washed away.[382]

In ribosome display, the analysed library size can be up to 10^{12}–10^{14} DARPins per selection process as there is no laborious transformation step needed in the protocol that is limiting the library size.[354,382]

2 Materials and Methods

2.1 Materials

2.1.1 Oligonucleotides

DNA oligonucleotides for the experiments of this study were purchased either from Sigma-Aldrich or Integrated DNA Technologies (IDT).

Table 2: List of oligonucleotides strains used in this study.

ID	Name	Sequence 5'–3'	Use	Created by
291	PIB1-I227A-r	GAGTGCCCGGCGTGTTTT GAGAATATG	mutagenesis	[redacted]
292	PIB1-I227A-f	CTCAAAACACGCCGGGCA CTCCTTAAT	mutagenesis	[redacted]
312	RFA1-tag-f	TCTCATATGTTACATAGAT TAAATAGTACTTGATTATT TGATACAATCGATGAATTC GAGCTCG	PCR tagging	[redacted]
409	POL30-promoter-r	ATTAGAATTCCTTAACTGC TGAAGAAAAGC	sequencing/ colony PCR	[redacted]
623	TUL1-ko-r	AATTCAGGCAAAAAAGGA AAGTCCTACAGCAAAAGA GGCAAAAGTACAGTCGTA CGCTGCAGGTCGAC	PCR knock-out	[redacted]
624	TUL1-ko-f	GATCTTGAATACAAATACA GTATATAGTTCTTAGGATC AAGAGATGCTATATCGATG AATTCGAGCTCG	PCR knock-out	[redacted]
625	TUL1-ko-test-f	GCTTAGTGTTCATAATTCT TCACTC	sequencing/ colony PCR	[redacted]
905	POL30-N-term-f	CTCTTGAAAAGGGATGCTT CTTC	sequencing/ colony PCR	[redacted]
1205	Spc25-133-r	CGCGGATCCCGAACGATGC CGCAGAGGTCGCA	restriction cloning	[redacted]
1329	SMT3-(stop-after-GG)-f	ATCGGATCCTTAACCACCA ATCTGTT	restriction cloning	[redacted]
1644	TetR-domain-r	GATCACCAAGGTGCAGAGC	sequencing/ colony PCR	[redacted]

1793	SMT3-BamHI-set2-r	CCTGGGATCCAAAATGTCG GACTCAGAAGTC	restriction cloning	[redacted]
1881	spc25(107-221)-L109A-f	GCAGCAGCGAGTCGGCCTC GCGCGGGATCCCCGG GAATTCGG	mutagenesis	[redacted]
1893	GFP-tag-test-f	CCTTCTGGCATGGCAGAC TTG	sequencing/ colony PCR	[redacted]
2056	hygromycin-B-f	CAGCCATCGGTCCAGACG	sequencing/ colony PCR	[redacted]
2227	POL30-670-f	TATCAGAAAGGGAGGAGC CC	sequencing/ colony PCR	[redacted]
2259	CYC1-TT-primer-r	GCGTGAATGTAAGCGTGA C	sequencing/ colony PCR	[redacted]
2346	T7P-seq-primer-f	TAATACGACTCACTATAGG G	sequencing/ colony PCR	[redacted]
2378	spADH-promoter-r	GTTTTTGCTTTGCCGATG TT	sequencing/ colony PCR	[redacted]
2580	Lys1-5'-tagging-r	ATACCATAAGATAACAACG AAAACGCTTTATTTTTCAC ACAACCGCAAAACGTACGC TGCAGGTCGAC	PCR tagging	[redacted]
2581	Lys1-3'-tagging-f	TAAACTTGTAAATGTCAGC GTAACGATAATGTATATACT TTAAATGTAAAATCGATGA ATTCGAGCTCG	PCR tagging	[redacted]
2705	Pib1-BamHI-f	GCAAGGATCCATGGTTATT AAAGAGGACTG	restriction cloning	[redacted]
2707	Pib1-EcoRI-r	GCAAGAATTCTTAAAATAC GGCATCATGGAAAG	restriction cloning	[redacted]
2757	yeGFP-SalI-NotI-r	AAATATGGCGGCCGCGGT CGACTTATTTGTACAATTC ATCCAT	restriction cloning	[redacted]
2763	Cyc1-TATA-f	TATACTTCTATAGACACGC	sequencing/ colony PCR	[redacted]
2866	mCherry-test-r	CTTGGTCACCTTCAGCTTG	sequencing/ colony PCR	[redacted]
2964	LacZa-f	GATTGTACTGAGAGTGCAC	sequencing/ colony PCR	[redacted]
3018	GFP-cloning-BamHI-with-ATG-r	GGATGGATCCATGTCTAAA GGTGAAGAATTATTCACTG GTGTTGT	restriction cloning	[redacted]
3019	SPC42-tag-f	CACAGAACGCTTTAAGAAT GCGCCATACTCCTTAACTG CTTTTTAAATCAATCGATG AATTCGAGCTCG	PCR tagging	[redacted]
3020	SPC42-tag-r	CTGAAAATAATATGTCAGA AACATTCGCAACTCCCACT CCCAATAATCGACGTACGC TGCAGGTCGAC	PCR tagging	[redacted]

3021	KRE28-tag-f	CTTTTTTTTTGGCTAGTAAT ATTACATACATCTTTATCTA GATAATTAATATCGATGAAT TCGAGCTCG	PCR tagging	[redacted]
3022	KRE28-tag-r	TGCAAATCTTTGAGGTAAT GGATGACATTATAAGCGAG CTAACAAACGAACGTACGC TGCAGGTCGAC	PCR tagging	[redacted]
3046	KRE28-276-bp-5'-of-stop-f	CTCAAAGGGTCAAAGACGA C	sequencing/ colony PCR	[redacted]
3047	SPC42-218-bp-5'-of-stop-f	AGCTGCAAAGCATGATGGA C	sequencing/ colony PCR	[redacted]
3958	Ub-*WT*-CGS-Insertion-f	CAAAGATGACGATGACAAA TGTGGAAGTATGCAGATT TTCGTGAAAACCC	mutagenesis	this study
3959	Ub-*WT*-CGS-Insertion-r	GGGTTTTCACGAAAATCTG CATACTTCCACATTTGTCA TCGTCATCTTTG	mutagenesis	this study
3960	I44A-Mutation-f	GCAAACGGGTCTCGTGACC TTACGCTTTTTCTTGG	mutagenesis	this study
3961	I44A-Mutation-r	CCAGCTGCTTGCCAGCAAA GGCCAGTCTCTGCTGATCA GGAGG	mutagenesis	this study
4072	Spc25-glob-NcoI	GGCCATGGGTAACGATGCC GCAGAGGTCGC	restriction cloning	this study
4073	CGS-FLAG-A12-f	GTACAAAAAAGCAGGCTCC ACCCTGCGGAAGGATTACA AAGATGACGATGA	mutagenesis	this study
4074	CGS-FLAG-A12-r	TCATCGTCATCTTTGTAATC CTTCCGCAGGGTGGAGC CTGCTTTTTTGTAC	mutagenesis	this study
4121	BamHI-yomRuby2-f	GCATGGATCCATGGTGTCC AAAGGAGAGGAG	restriction cloning	[redacted]
4261	RFA1-mRuby2-3'-tagging-f	GAAGCCGACTATCTTGCCG ATGAGTTATCCAAGGCTTT GTTAGCTGGTGACGGTGCT GGTTTA	PCR tagging	[redacted]
4279	Rfa1-test-3'-f	ACACAGCTTGAATTACAGG GCTGAAG	sequencing/ colony PCR	[redacted]
4331	HindIII-TAP-f	GAAAAACAAACTGTAACGG ATCCAAGCTTATGGCAGGC CTTGCGCAAC	restriction cloning	this study
4332	TAP-KpnI-r	GGTCGACGGTATCGATAAG CTTGGTACCATCGTCATCA TCAAGTGC	restriction cloning	this study
4338	Ubi-linker-NotI-f	AATAATGCGGCCGCAGGCG GATCTGGTCAGATTTTCGT CAAGACTTTGACC	restriction cloning	this study
4339	Ubi-XbaI-r	CTTCTTTCTAGATTAACCA CCTCTTAGCCTTAGCACAA GATGTAAGG	restriction cloning	this study

4340	Ubi-deltaGG-XbaI-r	CTTCTTTCTAGATTATCTTA GCCTTAGCACAAGATGTAA GGTGGACTCC	restriction cloning	this study
4347	Pib1-EcoRI-r	GGAATTCGGTAAAATACGG CATCATGGAAAGGAC	restriction cloning	this study
4376	mRuby2-test-r	CGACACCCCCATCTTCGTA TCT	sequencing/ colony PCR	[redacted]
4487	Ubait-vector-r	AATAATTCTTCACCTTTAGA CATAAGCTTAATATTCCCTA TAGTGAGTCGTATTACAG	Gibson assembly	this study
4488	Ubait-vector-f	GTATGGATGAATTGTACAA AGAGCTCGGATCCATGGTT ATTAAAGAGG	Gibson assembly	this study
4489	yeGFP-r	ATAACCATGGATCCGAGCT CTTTGTACAATTCATCCAT ACCATGGGTAATACCAG	Gibson assembly	this study
4490	yeGFP-f	TAGGGAATATTAAGCTTAT GTCTAAAGGTGAAGAATTA TTCACTGGTGTTG	Gibson assembly	this study
4496	Sec4-tagging-f	CATCAATAGTGGGAGCGGA AACAGTTCTAAATCAAATT GCTGTCGTACGCTGCAGG TCGAC	PCR tagging	this study
4497	Sec4-tagging-r	CCAGTTCACGATTAATTCT CAAAGAAGCAAAAATCTTC TTTTCTTCATCGATGAATT CGAGCTCG	PCR tagging	this study
4500	Sec4-tagging-CTR-f	GCACAGCTACTGTTGGTT GG	sequencing/ colony PCR	this study
4501	Ypt1-tagging-f	CCTGAAGGGACAGAGTTT AACCAACACCGGTGGGGG CTGCTGTCGTACGCTGCA GGTCGAC	PCR tagging	this study
4502	Ypt1-tagging-r	GTTATTATATTATATGGGT CTGCAAGGTAGAGGCGCG CTTGTTCATCGATGAATTC GAGCTCG	PCR tagging	this study
4503	Ypt1-tagging-ctr-f	GCTATTGGTAGGTAACAA GTGTG	sequencing/ colony PCR	this study
4504	Vti1-tagging-f	GTCCTTATATTATTGATTT TGCTAGTTTTGTTCTCAA AGTTTAAACGTACGCTGC AGGTCGAC	PCR tagging	this study
4505	Vti-tagging-r	GTTCTTTAGATTCTAGAGG TTTTTTATTGAATTTGTTT TCCCACCTCATCGATGAAT TCGAGCTCG	PCR tagging	this study
4506	Vti-tagging-ctr-f	CTTACAGAAATCGGGAGA TAGAC	sequencing/ colony PCR	this study

4507	Gos1-tagging-f	GCCACGATAACCACCCTTT GTATACTGTTTTTGTTTTT CACATGGCGTACGCTGCAG GTCGAC	PCR tagging	this study
4508	Gos1-tagging-r	GATTCTTGTTATGTTTTTA CATACGTTGTTTAATAAAA GTCGTTATTCATCGATGAA TTCGAGCTCG	PCR tagging	this study
4509	Gos1-tagging-ctr-f	CTGCGATTCTAACCCGGC	sequencing/ colony PCR	this study
4510	Pep12-tagging-f	GTGCTTCTCGTAATGCTT CTTTTTATTTTTCTCATT ATGAAATTGCGTACGCTG CAGGTCGAC	PCR tagging	this study
4511	Pep12-tagging-r	GTATATATTATGTATATGA TATTTGACGACGTGTGTT GGTTTGGTTCATCGATGA ATTCGAGCTCG	PCR tagging	this study
4512	Pep12-tagging-ctr-f	GCGGCAGTTTACCCAAGT AATG	sequencing/ colony PCR	this study
4513	Snc1-tagging-f	GCTTGTTGTAATCATCGT CCCCATTGCTGTTCACTT TAGTCGACGTACGCTGCA GGTCGAC	PCR tagging	this study
4514	Snc1-tagging-r	CTACATATGGAAGCTCCC TATATATATAGCATTGCGA GTGAACTTTCATCGATGA ATTCGAGCTCG	PCR tagging	this study
4515	Snc1-tagging-ctr-f	CCATTGATTGCAGGGTAA CAGAC	sequencing/ colony PCR	this study
4516	Sec3-tagging-f	CGAAGAACGATATCATAA GTGCGTTCGAGGAATACA AGAATGCCCGTACGCTGC AGGTCGAC	PCR tagging	this study
4517	Sec3-tagging-r	CTTAATTAGTCTAAATATG TAATATGAAGCGACAATGC AGAGGTTACTCATCGATGA ATTCGAGCTCG	PCR tagging	this study
4518	Sec3-tagging-ctr-f	GGATGGTATATTTGATACG TCATTGC	sequencing/ colony PCR	this study
4519	Vps21-tagging-f	GAACGCTGCTAATGATGGG ACCAGCGCAAACAGTGCTT GCAGTTGTCGTACGCTGCA GGTCGAC	PCR tagging	this study
4520	Vps21-tagging-r	CAATTTGCCCAGACTTTTT TTTTATATATATTTATTTTC CCCTCTTCATCGATGAATT CGAGCTCG	PCR tagging	this study
4521	Vps21-tagging-ctr-f	GTTAAGTTTGAAATATGGG AC	sequencing/ colony PCR	this study

4612	Snc1-NdeI-f	GCAACATATGTCGTCATCTA CTCCCTTTG	restriction cloning	this study
4613	Snc1-1-93-XhoI-r	GCAACTCGAGCTTCATTTT TAGATCCTTGTACCAC	restriction cloning	this study
4614	Snc1-full-XhoI-r	GCAACTCGAGTCGACTAAA GTGAACAGCAATGG	restriction cloning	this study
4635	Snc1-8KR-1-93-XhoI-r	GCAACTCGAGCCTCATCCT TAGATCCCTGTAC	restriction cloning	this study
4658	SalI-Ypt1-f	GCAAGTCGACGCAAATAGC GAGTACGATTACCTGTTC	restriction cloning	this study
4659	Ypt1-NotI-r	GCAAGCGGCCGCGCAATCA ACAGCAGCCCCCACC	restriction cloning	this study
4660	Vti1-SalI-f	GCAAGTCGACGCAAGTTCC CTATTAATATCATACGAATC TGAC	restriction cloning	this study
4661	Vti1-NotI-r	GCAAGCGGCCGCGCAATTA TTTAAACTTTGAGAACAAA ACTAGCAAAATC	restriction cloning	this study
4662	Vps21-SalI-f	GCAAGTCGACGCAAACACA TCAGTCACTTCCATAAAG	restriction cloning	this study
4663	Vps21-NotI-r	GCAAGCGGCCGCGCAACTA ACAACTGCAAGCACTGTTT G	restriction cloning	this study
4664	Sec4-SalI-f	GCAAGTCGACGCATCAGGC TTGAGAACTGTTTCTG	restriction cloning	this study
4665	Sec4-NotI-r	GCAAGCGGCCGCGCAATC AACAGCAATTTGATTTAGA ACTGTTTCC	restriction cloning	this study
4666	Sec3-SalI-f	GCAAGTCGACGCAAGGTC CTCGAAGTCTCCTTTTAAA AG	restriction cloning	this study
4667	Sec3-NotI-r	GCAAGCGGCCGCGCAATT AGGCATTCTTGTATTCCTC GAACG	restriction cloning	this study
4668	Pep12-SalI-f	GCAAGTCGACGCATCGGA AGACGAATTTTTTGGTGG	restriction cloning	this study
4669	Pep12-NotI-r	GCAAGCGGCCGCGCAATT ACAATTTCATAATGAGAAA AATAAAAAGAAGCATTACG	restriction cloning	this study
4673	Cdc48-tag-S3-f	CAGGTGCTGCATTTGGTT CTAATGCGGAGGAAGATG ATGATTTGTATAGTCGTAC GCTGCAGGTCGAC	PCR tagging	[redacted]
4675	Cdc48-tag-S2-r	AGAAATGACTTGAATTTA CGATTTAAAATAAAAATA TACCTGGCATATAAATCG ATGAATTCGAGCTCG	PCR tagging	[redacted]
4676	Cdc48-test-f	AATTAATTTATGTTCCATT GCCAGA	sequencing/ colony PCR	[redacted]

4701	Gos1-NotI-r	GCAAGCGGCCGCGCAATT ACCATGTGAAAAACAAAA ACAGTATACAAAGGG	restriction cloning	this study
4702	Gos1-EcoRI-f	GCAAGAATTCGCAAGCTC ACAACCGTCTTTCGTCAC	restriction cloning	this study
4740	Pep12-L271D-f	CGAGCAGATGGAGGGTGT ATGACTTGATTGTGCTTC TCGTAAT	mutagenesis	this study
4741	Pep12-L271D-r	ATTACGAGAAGCACAATC AAGTCATACACCCTCCAT CTGCTCG	mutagenesis	this study
4742	Doa4-ko-test-f	CTGGTCCTATCGTATTTAG TCATATC	sequencing/ colony PCR	this study
4743	Doa4-ko-f	AGTGTGCACGCTTCCAAA GTTTTTTTTACTATTTGAT ACATGCTTAAGTTTCGTAC GCTGCAGGTCGAC	PCR knock-out	this study
4744	Doa4-ko-r	CGGGAAAAAAAGTGTATA GACAACGGTTTTCAGTTA TTTATTCAAATGAAATCGA TGAATTCGAGCTCG	PCR knock-out	this study
4810	Pep12-L271D-BsiWI-f	GCAACGTACGAGCAGATG GAGGGTGTATGACTTGAT TGTGCTTCTCGT	restriction cloning	this study
4844	Ubc9-K157R-f	GCTTCAAGCTCGACAGTA TTCTCGAGGGTACCACCA CCATCATCAC	mutagenesis	this study
4845	Ubc9-K157R-r	GTGATGATGGTGGTGGTA CCCTCGAGAATACTGTCG AGCTTGAAGC	mutagenesis	this study
4851	SMT3-20-98-NdeI-r	GCAACATATGCCTGAGAC TCACATCAATTTAAAGG	restriction cloning	this study
4995	BglII-2NLS-Smt3Darpins-f	GCAAAGATCTGCAAATGC CCAAGAAAAAGCGTAAGG TCCCCAAGAAAAAGCGTA AGGTCATGGGATCCGACC TGGGTAAGAAAC	restriction cloning	this study
4996	KpnI-Smt3Darpin-FLAG-r	GCAAGGTACCGCACTTGT CGTCGTCATCCTTGTAG	restriction cloning	this study
4997	BglII-Darpin-f	GCAAAGATCTGCAAATGGG ATCCGACCTGGGTAAGAAA C	restriction cloning	this study
5110	Smt3-R47A-f	GACCACTCCTTTAAGAGCA CTGATGGAAGCGTTCGC	mutagenesis	this study
5111	Smt3-R47A-r	GCGAACGCTTCCATCAGTG CTCTTAAAGGAGTGGTC	mutagenesis	this study
5117	Darpin(Flag)-GFP-overlap-r	CCTGCTCCGGATCCGGTAC CCTTAAGCTTGTCGTCGTC ATCCTTGTAGTC	overlap PCR	this study
5402	Shs1-test-f	CAGAAACCGTTCCATATGT C	sequencing/ colony PCR	this study

5403	Shs1-tagging-S3-f	AATGACACGTATACTGATT TAGCCTCTATTGCATCGGG TAGAGATCGTACGCTGCAG GTCGAC	PCR tagging	this study
5404	Shs1-tagging-S2-r	TTTATTTATTTATTTGCTCA GCTTTGGATTTTGTACAGA TACAACATCGATGAATTCG AGCTCG	PCR tagging	this study
5432	BamHI-mCherry-f	CGCGGATCCTTAATTAACA TGGTGAGCAAGGGCGAGG	restriction cloning	[redacted]
5451	NotI-r	ATAGTTTAGCGGCCGC	restriction cloning	this study
5604	BglII-2xNES-EcoRI-DARPins-f	GATCAGATCTGTCATGCTG CCTCCCCTGGAGCGCCTGA CCCTGCTGCCTCCCCTGGA GCGCCTGACCCTGGATCGA ATTCGGATCGGATCCGACC TGGGT	restriction cloning	this study
5605	BglII-FLAG-r	GATCCAGATCTGATCTTGT CGTCGTCATCCTTG	restriction cloning	this study
5606	pYm16-His6-Stop-mut-r	GCCTTAATTAACCCGGTTA GCTATGGTGATGGTGATGG TGTCCTCCGCTAGAAGCGT AA	mutagenesis	this study
5607	pYm16-His6-Stop-mut-f	CCAGATTACGCTTCTAGCG GAGGACACCATCACCATCA CCATAGCTAACCGGGTTAA TTAAGGC	mutagenesis	this study
5830	mCherry-test-f	CCAACTTCCCCTCCG	sequencing/ colony PCR	this study
5831	mCherry-SacI-f	CGATGAGCTCGATCATGGT GAGCAAGGGCGAGGAGG	restriction cloning	this study
5832	mCherry-XbaI-r	GATCTCTAGAGATCCTTTG TACAGCTCGTCCATGCCGC	restriction cloning	this study
5852	NdeI-3His-f	GGAATTCCATATGTCGTAC TACCATCACCATC	restriction cloning	this study
5853	NdeI-mVenus-r	GGAATTCCATATGACGGAT CCCTTTGTACAGCTCG	restriction cloning	this study
5889	BamHI-mCherrry-noStop-r	GCGCGGATCCGCGTTTGTA CAGCTCGTCCATGCCG	restriction cloning	this study
5924	SacI-ADH1-terminator-r	GATCGAGCTCGATCGCGGA TCTGCCGGTAG	restriction cloning	this study
5925	NotI-Spr3-promotor-f	AAGGAAAAAAGCGGCCGCA AAAGGAAAACGATACTAAT CAAGAAGGCATTGC	restriction cloning	this study

2.1.2 Plasmids

Table 3: List of plasmids used in this study.

ID	Name	Selection	Use	Construction	Source
233	pFA-HIS3	Amp	PCR-based knock-out (HIS) in yeast	–	[redacted]
245	pGEX-Ubi	Amp	protein expression in *E.coli*	–	[redacted]
732	YIp128-P30-His-POL30	Amp, LEU	integration/ expression in yeast	–	[redacted]
733	pET-UBA2	Amp	protein expression in *E.coli*	–	[redacted]
734	pET-AOS1	Kan	protein expression in *E.coli*	–	[redacted]
736	pET-UBC9	Amp	protein expression in *E.coli*	–	[redacted]
821	YEp181-CUP-His-Ubi	Amp, LEU	episomal expression in yeast	–	[redacted]
1214	YEp195-CUP-His-Ubi	Amp, URA	episomal expression in yeast	–	[redacted]
1633	pFA6a-natNT2	Amp	PCR-based knock-out (nourseothricin) in yeast	–	[redacted]
1633	pFA6a-natNT2	Amp	PCR-based knock-out (nourseothricin) in yeast	–	[redacted]
1634	pFA6a-hphNT1	Amp	PCR-based knock-out (hygromycin B) in yeast	–	[redacted]
1717	pET28a-Spc25-(107-221)	Kan	protein expression in *E.coli*	–	[redacted]
1720	pET15b-SPC24-(154-213)	Kan	protein expression in *E.coli*	–	[redacted]
2120	pET15b-Spc25-(107-221)	Amp	protein expression in *E.coli*	–	[redacted]
2215	pET28-Spc25-full-length	Kan	protein expression in *E.coli*	–	[redacted]
2216	pET22-Spc24-full-length	Amp	protein expression in *E.coli*	–	[redacted]
2393	TetR-SSN6	Amp, HIS	integration/ expression in yeast	–	[redacted]
2403	pFA6a-link-yomRuby2-Kan	Amp, G418	Ruby2-tagging in yeast	–	[redacted]

2413	pYM26-yeGFP-klTRP1	Amp, TRP	GFP-tagging in yeast	–	
2442	pYM-yeGFP-Nat	Amp, Nat	GFP-tagging in yeast	–	
2622	pYM-mCherry-Nat	Amp, Nat	mCherry-tagging in yeast	–	
2856	pGEX6P1-Spc25(107-221)	Amp	protein expression in *E.coli*	–	
2857	pGEX6P1-Spc24-(154-213)	Amp	protein expression in *E.coli*	–	
2877	pGEX-6P1-SPC25-CTD-L109A–L112A–V121A	Amp	protein expression in *E.coli*	–	
3264	pGEX-GST-Spc25-glob	Amp	protein expression in *E.coli*	Amplification of Spc25glob from p1716 with oHU1205/1881. Insert and p2889 cut with SalI and BamHI and ligated	this study
3265	pGEX-GST-FLAG-UbvarA12	Amp	protein expression in *E.coli*	Gateway cloning from p3272 into p1794.	this study
3266	pGEX-GST-FLAG-UbvarA13	Amp	protein expression in *E.coli*	Gateway cloning from p3273 into p1794.	this study
3267	pGEX-GST-FLAG-UbvarA15	Amp	protein expression in *E.coli*	Gateway cloning from p3274 into p1794.	this study
3268	pGEX-GST-FLAG-UbvarB16	Amp	protein expression in *E.coli*	Gateway cloning from p3275 into p1794.	this study
3269	pGEX-GST-FLAG-UbvarC11	Amp	protein expression in *E.coli*	Gateway cloning from p3276 into p1794.	this study
3270	pGEX-GST-FLAG-wtUb	Amp	protein expression in *E.coli*	Gateway cloning from p3277 into p1794.	this study
3271	pGEX-GST-wtUb	Amp	protein expression in *E.coli*	Gateway cloning from p3278 into p1794.	this study
3348	pGEX-GST-FLAG-CGS-UbvarI44A	Amp	protein expression in *E.coli*	Mutagenesis PCR with oHU3960/3961 on 3309.	this study
3373	pET28a-His-Spc25glob	Kan	protein expression in *E.coli*	Amplification of Spc25glob from p1716 with oHU1205/1880. Insert and p1679 cut with SalI and BamHI and ligated.	this study

3423	pET15b-Spc25glob	Amp	protein expression in *E.coli*	Amplification of Spc25-(133-221) from p3264 with oHU1664/4072. Insert and p839 cut with NcoI and BamHI and ligated.	this study
3424	pGEX-GST-CGS-FLAG-UbvarA12	Amp	protein expression in *E.coli*	Mutagenesis PCR with oHU4075/4076 on p3265.	this study
3482	pYES2-TAP-Pib1-ubi	Amp	centromeric expression in yeast	Amplification of Pib1 from p2577 with oHU2705/4347. Inserts and p3480 cut using BamHI and EcoRI and ligated.	this study
3483	pYES2-TAP-Pib1-ubi-deltaGG	Amp	centromeric expression in yeast	Amplification of Pib1 from p2577 with oHU2705/4347. Inserts and p3481 cut using BamHI and EcoRI and ligated.	this study
3484	pYES2-TAP-Pib1	Amp	centromeric expression in yeast	Amplification of Pib1 from p2577 with oHU2705/2707. Inserts and p3479 cut using BamHI and EcoRI and ligated.	this study
3485	pYES2-TAP-Pib1-I227A-ubi	Amp	centromeric expression in yeast	Mutagenesis PCR with oHU291/292 on p3482.	this study
3490	pFA6a-mRuby2-NAT	Amp, Nat	Ruby2-tagging in yeast	–	[redacted]
3590	pYES2-GFP-Pib1-ubi	Amp	centromeric expression in yeast	Amplification of GFP from p3057 with oHU4489/4490 and of vector p3482 with oHU4488/4487 followed by Gibson assembly.	this study
3591	pYES2-GFP-Pib1-ubi-deltaGG	Amp	centromeric expression in yeast	Amplification of GFP from p3057 with oHU4489/4490 and of vector p3483 with oHU4488/4487 followed by Gibson assembly.	this study
3645	YEp195-Gal-antiSmt3DARPin-A10	Amp, URA	episomal expression in yeast	–	[redacted]

3646	YEp195-Gal-antiSmt3DARPin-C10	Amp, URA	episomal expression in yeast	–	[redacted]
3647	YEp195-Gal-antiSmt3DARPin-E10	Amp, URA	episomal expression in yeast	–	[redacted]
3648	YEp195-Gal-antiSmt3DARPin-F10	Amp, URA	episomal expression in yeast	–	[redacted]
3649	YEp195-Gal-antiSmt3DARPin-E11	Amp, URA	episomal expression in yeast	–	[redacted]
3650	YEp195-Gal-antiSmt3DARPin-G11	Amp, URA	episomal expression in yeast	–	[redacted]
3651	YEp195-Gal-antiSmt3DARPin-B12	Amp, URA	episomal expression in yeast	–	[redacted]
3670	pET-His-AVI-SMT3	Amp	protein expression in *E.coli*	–	[redacted]
3673	pQIq-MRS-His6-GCCG-antiSMT3-DARPin-A10	Amp	protein expression in *E.coli*	–	[redacted]
3674	pQIq-MRS-His6-GCCG-antiSMT3-DARPin-C10	Amp	protein expression in *E.coli*	–	[redacted]
3675	pQIq-MRS-His6-GCCG-antiSMT3-DARPin-E10	Amp	protein expression in *E.coli*	–	[redacted]
3676	pQIq-MRS-His6-GCCG-antiSMT3-DARPin-F10	Amp	protein expression in *E.coli*	–	[redacted]
3677	pQIq-MRS-His6-GCCG-antiSMT3-DARPin-E11	Amp	protein expression in *E.coli*	–	[redacted]
3678	pQIq-MRS-His6-GCCG-antiSMT3-DARPin-G11	Amp	protein expression in *E.coli*	–	[redacted]
3679	pQIq-MRS-His6-GCCG-antiSMT3-DARPin-B12	Amp	protein expression in *E.coli*	–	[redacted]

3751	pET30-Snc1-His	Kan	protein expression in *E.coli*	Amplification of Snc1 from p3748 with oHU4612/4614. Inserts and p1985 cut with NdeI and XhoI and ligated.	this study
3752	pET30-Snc1-1-93-His	Kan	protein expression in *E.coli*	Amplification of Snc1 from p3748 with oHU4612/4613. Inserts and p1985 cut with NdeI and XhoI and ligated.	this study
3753	pET30-Snc1-K8R-His	Kan	protein expression in *E.coli*	Amplification of Snc1 from p3749 with oHU4612/4614. Inserts and p1985 cut with NdeI and XhoI and ligated.	this study
3754	pET30-Snc1-K8R-1-93-His	Kan	protein expression in *E.coli*	Amplification of Snc1 from p3749 with oHU4612/4635. Inserts and p1985 cut with NdeI and XhoI and ligated.	this study
3762	pLou3-Rnf4-*WT*	Amp	protein expression in *E.coli*	–	[redacted]
3841	pRS416-2HA	Amp, URA	centromeric expression in yeast	Snc1 cut out from p3748 with BamHI and vector religated.	this study
3842	pRS416-2HA-Gos1	Amp, URA	centromeric expression in yeast	Amplification of Gos1 from yeast genomic DNA with oHU4702/4701. Inserts and p3841 cut with SalI and NotI and ligated.	this study
3843	pRS416-2HA-Pep12	Amp, URA	centromeric expression in yeast	Amplification of Pep12 from yeast genomic DNA with oHU4668/4669. Inserts and p3841 cut with SalI and NotI and ligated.	this study
3844	pRS416-2HA-Sec3	Amp, URA	centromeric expression in yeast	Amplification of Sec3 from yeast genomic DNA with oHU4666/4667. Inserts and p3841 cut with SalI and NotI and ligated.	this study

3845	pRS416-2HA-Sec4	Amp, URA	centromeric expression in yeast	Amplification of Sec4 from yeast genomic DNA with oHU4665/4664. Inserts and p3841 cut with SalI and NotI and ligated.	this study
3846	pRS416-2HA-Vps21	Amp, URA	centromeric expression in yeast	Amplification of Vps21 from yeast genomic DNA with oHU4662/4663. Inserts and p3841 cut with SalI and NotI and ligated.	this study
3847	pRS416-2HA-Vti1	Amp, URA	centromeric expression in yeast	Amplification of Vti1 from yeast genomic DNA with oHU4661/4660. Inserts and p3841 cut with SalI and NotI and ligated.	this study
3848	pRS416-2HA-Ypt1	Amp, URA	centromeric expression in yeast	Amplification of Ypt1 from yeast genomic DNA with oHU4659/4658. Inserts and p3841 cut with SalI and NotI and ligated.	this study
3893	pRS416-2HA-Pep12-L271D	Amp, URA	centromeric expression in yeast	Amplification of Pep12 from p3843 with mutagenic oHU4810/4669. Insert and p3843 cut with NotI and BsiWI and ligated.	this study
3940	pET-Ubc9-K153R-K157R	Amp	protein expression in *E.coli*	Mutagenesis PCR with oHU4844/4845 on p1059.	this study
3942	pET3a-SMT3-20-98-untagged	Amp	protein expression in *E.coli*	Amplification of SMT3 FL from p735 with oHU1329/4851. Insert and p684 cut with BamHI and Nde1 and ligated.	this study

4479	YIp211-TetO7-DarpinF10-Flag-GFP	URA, Amp	integration/ expression in yeast	Amplification of F10 from p3528 with oHU4996/4997. Amplification of GFP from p2729 with oHU 2746 and 2757. Inserts and p2590 cut with BglII, KpnI and NotI and ligated.	this study
4480	YIp211-TetO7-DarpinA10-Flag-GFP	URA, Amp	integration/ expression in yeast	Amplification of A10 from p3523 with oHU5117/4997. Insert cut with BglII and p4479 cut with BamHI and ligated.	this study
4481	YIp211-TetO7-DarpinC10-Flag-GFP	URA, Amp	integration/ expression in yeast	Amplification of C10 from p3525 with oHU5117/4997. Insert cut with BglII and p4479 cut with BamHI and ligated.	this study
4482	YIp211-TetO7-DarpinE11-Flag-GFP	URA, Amp	integration/ expression in yeast	Amplification of E11 from p3535 with oHU5117/4997. Insert cut with BglII and p4479 cut with BamHI and ligated.	this study
4483	YIp211-TetO7-DarpinG11-Flag-GFP	URA, Amp	integration/ expression in yeast	Amplification of G11 from p3537 with oHU5117/4997. Insert cut with BglII and p4479 cut with BamHI and ligated.	this study
4484	YIp211-TetO7-DarpinB12-Flag-GFP	URA, Amp	integration/ expression in yeast	Amplification of B12 from p3540 with oHU5117/4997. Insert cut with BglII and p4479 cut with BamHI and ligated.	this study
4485	YIp211-TetO7-DarpinE3-5-Flag-GFP	URA, Amp	integration/ expression in yeast	Amplification of E3.5 from p3522 with oHU5117/4997. Insert cut with BglII and p4479 cut with BamHI and ligated.	this study
4486	YIp211-TetO7-GFP	URA, Amp	integration/ expression in yeast	Amplification of GFP from p2790 with oHU3018/2757. Insert and p2590 cut with BamHI and NotI and ligated.	this study

4495	pET21a-His-AVI-SMT3-R47A	Amp	protein expression in *E.coli*	Mutagenesis PCR with oHU5110/5111 on p3670.	this study
4502	pET21a-His-AVI-SMT3-E34A-E50A-E59A	Amp	protein expression in *E.coli*	Mutagenesis PCR with oHU5108/5109 on p4500.	this study
4513	pBirA-Amp	Amp	protein expression in *E.coli*	–	[redacted]
4514	pBirA-Kan	Kan	protein expression in *E.coli*	–	[redacted]
4631	YIp204-TetR-ssn6	Amp, TRP	integration/ expression in yeast	TetR cut out from p2393 with SalI and EcoRI and ligated into p67.	this study
4648	pET30-His-AVI-SMT3-8M	Kan	protein expression in *E.coli*	Amplification of gBlock (IDT) with oHU1793/5451. Insert and p4012 cut with BamHI and NotI and ligated.	this study
4730	pET-His-AVI-SMT3-F36H-R47K-E59P	Amp	protein expression in *E.coli*	Mutagenesis PCR with oHU5410/5415 on p3670.	this study
4731	pET-His-AVI-SMT3-I35D-F36D-F37D	Kan	protein expression in *E.coli*	Amplification of gBlock (IDT) with oHU1793/5451. Insert and p4012 cut with BamHI and NotI and ligated.	this study
4876	pET30a-His-TEV-ECFP-GAPtail1(RanGAP1)	Kan	protein expression in *E.coli*	–	[redacted]
4914	pET30-His-AVI-Smt3-H23Y-N25K-F36H-I39V-K41M-R46K-R47K-A51S-K54Q-K58V-E59P	Kan	protein expression in *E.coli*	Amplification of gBlock (IDT) with oHU1793/5451. Insert and p4012 cut with BamHI and NotI and ligated.	this study
4925	pYM16-3HA-6His-Stop	Amp, Hygro	3HA-6His-tagging in yeast	Mutagenesis PCR with oHU5606/5607 on p3280.	this study
4965	YIp211-TetON-2xNES-DARPIN-E3.5-Flag-GFP	Amp, URA	integration/ expression in yeast	Amplification of DARPin from p3522 with oHU5604/5605. Insert cut with BglII and p4486 cut with BamHI and ligated.	this study

4966	YIp211-TetON-2xNES-DARPIN-F10-Flag-GFP	Amp, URA	integration/ expression in yeast	Amplification of DARPin from p3528 with oHU5604/5605. Insert cut with BglII and p4486 cut with BamHI and ligated.	this study
4967	YIp211-TetON-2xNES-DARPIN-E11-Flag-GFP	Amp, URA	integration/ expression in yeast	Amplification of DARPin from p3535 with oHU5604/5605. Insert cut with BglII and p4486 cut with BamHI and ligated.	this study
4968	YIp211-TetON-2xNLS-DARPin-E11-Flag-GFP	Amp, URA	integration/ expression in yeast	Amplification of DARPin from p3535 with oHU5605/4995. Insert cut with BglII and p4486 cut with BamHI and ligated.	this study
4969	YIp211-TetON-2xNLS-DARPin-F10-Flag-GFP	Amp, URA	integration/ expression in yeast	Amplification of DARPin from p3528 with oHU5605/4995. Insert cut with BglII and p4486 cut with BamHI and ligated.	this study
4970	YIp211-TetON-2xNLS-DARPin-E3.5-Flag-GFP	Amp, URA	integration/ expression in yeast	Amplification of DARPin from p3522 with oHU5605/4995. Insert cut with BglII and p4486 cut with BamHI and ligated.	this study
5057	pET30-His-AVI-Smt3-H23Y-N25K-I39V-A51S	Kan	protein expression in *E.coli*	Amplification of gBlock (IDT) with oHU1793/5451. Insert and p4012 cut with BamHI and NotI and ligated.	this study
5058	pET30-His-AVI-Smt3-H23Y-N25K-I39V-A51S-F36H-R47K	Kan	protein expression in *E.coli*	Amplification of gBlock (IDT) with oHU1793/5451. Insert and p4012 cut with BamHI and NotI and ligated.	this study
5059	pET30-His-AVI-Smt3-T22A-I35S-F37S-K38E-K40E-T43A-L48S-R55E-N86A	Kan	protein expression in *E.coli*	Amplification of gBlock (IDT) with oHU1793/5451. Insert and p4012 cut with BamHI and NotI and ligated.	this study

5097	YIp128-pPol30-mRuby2-Pol30	Amp, LEU	integration/ expression in yeast	–	[redacted]
5103	yIp128-TetON-2xNES-DARPin-E3.5-Flag-GFP	Amp, LEU	integration/ expression in yeast	Amplification of DARPin from p4965 with oHU2757/5604. Insert cut with BglII/NotI and p2998 cut with BamHI /NotI and ligated.	this study
5104	yIp128-TetON-2xNES-DARPin-F10-Flag-GFP	Amp, LEU	integration/ expression in yeast	Amplification of DARPin from p4966 with oHU2757/5604. Insert cut with BglII/NotI and p2998 cut with BamHI /NotI and ligated.	this study
5105	yIp128-TetON-2xNES-DARPin-E11-Flag-GFP	Amp, LEU	integration/ expression in yeast	Amplification of DARPin from p4967 with oHU2757/5604. Insert cut with BglII/NotI and p2998 cut with BamHI /NotI and ligated.	this study
5119	yIp128-TetON-DARPin-E11-Flag-GFP	Amp, LEU	integration/ expression in yeast	Amplification of DARPin from p4479 with oHU2757/4997. Insert cut with BglII/NotI and p2998 cut with BamHI /NotI and ligated.	this study
5120	yIp128-TetON-DARPin-F10-Flag-GFP	Amp, LEU	integration/ expression in yeast	Amplification of DARPin from p4482 with oHU2757/4997. Insert cut with BglII/NotI and p2998 cut with BamHI /NotI and ligated.	this study
5121	yIp128-TetON-DARPin-E3.5-Flag-GFP	Amp, LEU	integration/ expression in yeast	Amplification of DARPin from p4485 with oHU2757/4997. Insert cut with BglII/NotI and p2998 cut with BamHI /NotI and ligated.	this study
5209	pYM-mCherry	Amp, G418	mCherry-tagging in yeast	Amplification of mCherry from p2622 with oHU5831/5832. Insert and p4397 cut with SacI and XbaI and ligated.	this study

5210	pET-His-TEV-YFP-Smt3-3R	Amp	protein expression in *E.coli*	Amplification of His-TEV-YFP from p4871 with oHU5852/5853. Insert and p1640 cut with NdeI and ligated.	this study
5237	YEp195-CUP1-mCherry-His-SMT3	Amp, URA	episomal expression in yeast	Amplification of mCherry from p5209 with oHU5889/5432. Insert and p1251 cut with BamHI-HF and ligated.	this study
5280	pRS315-Spr3-mCherry-Leu	Amp, LEU	centromeric expression in yeast	Amplification of mCherry tagged Spr3 from sc5315 with oHU5925/5924. Insert and p833 cut with NotI and SacI and ligated.	this study

2.1.3 Bacterial strains

Table 4: List of *E coli* strains used in this study.

ID	Name	Genotype	Use	Source
3	Bl21 (DE3)	B F– dcm ompT hsdS(rB – mB –) gal λ(DE3)	Expression	Novagen
5	BL21 Codonplus (DE3) RIL- (Codon +)	B F– ompT hsdSB(rB-mB-) dcm+ Tetr gal l(DE3) endA Hte [argU ileY leuW Camr]	Expression	Stratagene
21	Rosetta 2 (DE3)	F- ompT hsdSB(rB- mB-) gal dcm (DE3) pRARE2 (CamR)	Expression	Novagen
25	Rosetta 2 (DE3) pLysS	F- ompT hsdSB(rB- mB-) gal dcm (DE3) pLysSRARE2 (CamR)	Expression	Novagen
14	Top Ten	F– mcrA Δ(mrr-hsdRMS-mcrBC) φ80lacZΔM15 ΔlacX74 recA1 araD139 Δ(ara-leu)7697 galU galK λ– rpsL(StrR) endA1 nupG	Cloning	Invitrogen

2.1.4 Yeast strains

Table 5: List of *S cerevisiae* strains used in this study.

ID	Name	Mating Type	Chromosomal Genotype	Background	Source
3	DF5	a	his3Δ200, leu2-3,2-112, lys2-801, trp1-1(am), ura3-52	DF5	[redacted]
584	ubc9ts	alpha	ubc9ts	DF5	[redacted]
592	rsp5-2	a	rsp5-2 bar1::HIS3		[redacted]
790	BY4741	a	leu2Δ0, met15Δ0, ura3Δ0, his3Δ0	BY4741 Euroscarf	[redacted]
791	ubc13	a	leu2Δ0, met15Δ0, ura3Δ0, his3Δ0, ubc13::kanMX4	BY4741	[redacted]
801	BY4742	alpha	leu2Δ0, lys2Δ0, ura3Δ0, his3Δ0	BY4742 Euroscarf	[redacted]
1347	HP30 bar1	a	his3Δ200, lys2-801, trp1-1(am), ura3-52, pol30::hisG, leu2-3,2-112::YIp128-P30-His6-POL30-LEU2, bar1::HISMX6	DF5	[redacted]
1560	HP30 (K127/164R)	a	his3Δ200, lys2-801, trp1-1(am), ura3-52, pol30::URA3, leu2-3,2-112::YIp128-P30-His6-pol30(K127/164R)-LEU2	DF5	[redacted]
2210	siz1 siz2	alpha	his3Δ200, leu2-3,2-112, lys2-801, trp1-1(am), ura3-52, siz1Δ::KanMX6, siz2Δ::HIS3MX6	DF5	[redacted]
2639	DSN1-6HA	a	his3Δ200, leu2-3,2-112, lys2-801, ura3-52, trp1-1(am)::DSN1-6HA-klTRP1	DF5	[redacted]
2905	ubc13 bsd2	unknown	leu2Δ0, [met15Δ0], [lys2Δ0], ura3Δ0, his3Δ0, bsd2::kanMX, ubc13::KanMX	BY	[redacted]
3202	YAL6b	a	his3Δ1, leu2Δ0, ura3Δ0, (met15Δ0, lys2Δ0 not scored), arg4Δ (YHR018c)::kanMX4, lys1Δ, (YIR034c)::KanMX4		[redacted]
4282	tul1	a	his3Δ1, leu2Δ0, met15Δ0, ura3Δ0 tul1::hphNT1	BY4741	this study
4283	pib1 tul1	a	leu2Δ0, met15Δ0, ura3Δ0, his3Δ0, pib1::KanMX, tul1::hphNT1	BY4741	this study
4288	GFP-Sec4	a	his3Δ1, leu2Δ0, met15Δ0, ura3Δ0, lys+, can1Δ::GAL1pr-SceI::STE2pr-SpHIS5, lyp1Δ::STE3pr-LEU2; XXXpr-sfGFP-XXX	BY4741	[redacted]

4289	GFP-Ypt1	a	his3Δ1, leu2Δ0, met15Δ0, ura3Δ0, lys+, can1Δ::GAL1pr-SceI::STE2pr-SpHIS5, lyp1Δ::STE3pr-LEU2; XXXpr-sfGFP-XXX	BY4741	
4290	GFP-Vps21	a	his3Δ1, leu2Δ0, met15Δ0, ura3Δ0, lys+, can1Δ::GAL1pr-SceI::STE2pr-SpHIS5, lyp1Δ::STE3pr-LEU2; XXXpr-sfGFP-XXX	BY4741	
4291	GFP-Pep12	a	his3Δ1, leu2Δ0, met15Δ0, ura3Δ0, lys+, can1Δ::GAL1pr-SceI::STE2pr-SpHIS5, lyp1Δ::STE3pr-LEU2; XXXpr-sfGFP-XXX"	BY4741	
4292	Vps21-GFP	alpha	his3Δ1, leu2Δ0, lys2Δ0, ura3Δ0, Vps21-GFP::natNT2	BY4742	this study
4293	Pep12-GFP	alpha	his3Δ1, leu2Δ0, lys2Δ0, ura3Δ0, Pep12-GFP::natNT2	BY4742	this study
4294	Vti1-GFP	alpha	his3Δ1, leu2Δ0, lys2Δ0, ura3Δ0, Vti1-GFP::natNT2	BY4742	this study
4295	Snc1-GFP	alpha	his3Δ1, leu2Δ0, lys2Δ0, ura3Δ0, Snc1-GFP::natNT2	BY4742	this study
4296	Gos1-GFP	alpha	his3Δ1, leu2Δ0, lys2Δ0, ura3Δ0, Gos1-GFP::natNT2	BY4742	this study
4297	Sec3-GFP	alpha	his3Δ1, leu2Δ0, lys2Δ0, ura3Δ0, Sec3-GFP::natNT2	BY4742	this study
4298	Sec4-GFP	alpha	his3Δ1, leu2Δ0, lys2Δ0, ura3Δ0, Sec4-GFP::natNT2	BY4742	this study
4474	doa4	a	his3Δ1, leu2Δ0, met15Δ0, ura3Δ0, doa4::natNT2	BY4741	this study
4475	pib1 doa4	a	his3Δ1, leu2Δ0, met15Δ0, ura3Δ0, doa4::natNT2	BY4741	this study
4476	tul1 doa4	a	his3Δ1, leu2Δ0, met15Δ0, ura3Δ0, doa4::natNT2	BY4741	this study
4477	pib1 tul1 doa4	a	his3Δ1, leu2Δ0, met15Δ0, ura3Δ0, doa4::natNT2	BY4741	this study
4480	lys1 a	a	his3-Δ200, leu2-3,2-112, lys2-801, trp1-1(am), ura3-52, lys1::natNT2	DF5	this study
4889	DF5 HP30 bar1 TetON-A10-Flag-GFP	a	his3-Δ200, lys2-801, trp1-1(am), pol30::hisG, leu2-3,2-112::YIp128-P30-His6-POL30-LEU2, bar1::HISMX6, URA::yIp211-TetO7-A10-Flag-GFP-URA	DF5	this study
4890	DF5 HP30 bar1 TetON-C10-Flag-GFP	a	his3-Δ200, lys2-801, trp1-1(am), pol30::hisG,leu2-3,2-112::YIp128-P30-His6-POL30-LEU2, bar1::HISMX6, URA::yIp211-TetO7-C10-Flag-GFP-URA	DF5	this study

4891	DF5 HP30 bar1 TetON-F10-Flag-GFP	a	his3-Δ200, lys2-801, trp1-1(am), pol30::hisG,leu2-3,2-112::YIp128-P30-His6-POL30-LEU2, bar1::HISMX6, URA::yIp211-TetO7-F10-Flag-GFP-URA	DF5	this study
4892	DF5 HP30 bar1 TetON-E11-Flag-GFP	a	his3-Δ200, lys2-801, trp1-1(am), pol30::hisG, leu2-3,2-112::YIp128-P30-His6-POL30-LEU2, bar1::HISMX6, URA::yIp211-TetO7-E11-Flag-GFP-URA	DF5	this study
4893	DF5 HP30 bar1 TetON-G11-Flag-GFP	a	his3-Δ200, lys2-801, trp1-1(am), pol30::hisG, leu2-3,2-112::YIp128-P30-His6-POL30-LEU2, bar1::HISMX6, URA::yIp211-TetO7-G11-Flag-GFP-URA	DF5	this study
4894	DF5 HP30 bar1 TetON-B12-Flag-GFP	a	his3-Δ200, lys2-801, trp1-1(am), pol30::hisG, leu2-3,2-112::YIp128-P30-His6-POL30-LEU2, bar1::HISMX6, URA::yIp211-TetO7-B12-Flag-GFP-URA	DF5	this study
4895	DF5 HP30 bar1 TetON-E3.5-Flag-GFP	a	his3-Δ200, lys2-801, trp1-1(am), pol30::hisG, leu2-3,2-112::YIp128-P30-His6-POL30-LEU2, bar1::HISMX6, URA::yIp211-TetO7-E3.5-Flag-GFP-URA	DF5	this study
4896	DF5 HP30 bar1 TetON-GFP	a	his3-Δ200, lys2-801, trp1-1(am), pol30::hisG, leu2-3,2-112::YIp128-P30-His6-POL30-LEU2, bar1::HISMX6, URA::yIp211-TetO7-GFP-URA	DF5	this study
4984	DF5 HP30 bar1 TetR	a	his3-Δ200, lys2-801, trp1-1(am)::TetR, pol30::hisG, leu2-3,2-112::YIp128-P30-His6-POL30-LEU2, bar1::HISMX6, ura3-52	DF5	this study
4985	DF5 HP30 bar1 TetR-SSN6 TetON-A10-Flag-GFP	a	his3-Δ200, lys2-801, trp1-1(am):: YIp204-TetR-ssn6-TRP, pol30::hisG, leu2-3,2-112::YIp128-P30-His6-POL30-LEU2, bar1::HISMX6, URA::yIp211-TetO7-A10-Flag-GFP-URA	DF5	this study
4986	DF5 HP30 bar1 TetR-SSN6 TetON-C10-Flag-GFP	a	his3-Δ200, lys2-801, trp1-1(am):: YIp204-TetR-ssn6-TRP, pol30::hisG, leu2-3,2-112::YIp128-P30-His6-POL30-LEU2 bar1::HISMX6, URA::yIp211-TetO7-C10-Flag-GFP-URA	DF5	this study

4987	DF5 HP30 bar1 TetR-SSN6 TetON-F10-Flag-GFP	a	his3-Δ200, lys2-801, trp1-1(am)::YIp204-TetR-ssn6-TRP, pol30::hisG, leu2-3,2-112::YIp128-P30-His6-POL30-LEU2, bar1::HISMX6, URA::yIp211-TetO7-F10-Flag-GFP-URA	DF5	this study
4988	DF5 HP30 bar1 TetR-SSN6 TetON-E11-Flag-GFP	a	his3-Δ200, lys2-801, trp1-1(am)::YIp204-TetR-ssn6-TRP, pol30::hisG, leu2-3,2-112::YIp128-P30-His6-POL30-LEU2, bar1::HISMX6, URA::yIp211-TetO7-E11-Flag-GFP-URA	DF5	this study
4989	DF5 HP30 bar1 TetR-SSN6 TetON-G11-Flag-GFP	a	his3-Δ200, lys2-801, trp1-1(am)::YIp204-TetR-ssn6-TRP, pol30::hisG, leu2-3,2-112::YIp128-P30-His6-POL30-LEU2, bar1::HISMX6, URA::yIp211-TetO7-G11-Flag-GFP-URA	DF5	this study
4990	DF5 HP30 bar1 TetR-SSN6 TetON-B12-Flag-GFP	a	his3-Δ200, lys2-801, trp1-1(am)::YIp204-TetR-ssn6-TRP, pol30::hisG, leu2-3,2-112::YIp128-P30-His6-POL30-LEU2, bar1::HISMX6, URA::yIp211-TetO7-B12-Flag-GFP-URA	DF5	this study
4991	DF5 HP30 bar1 TetR-SSN6 TetON-E3.5-Flag-GFP	a	his3-Δ200, lys2-801, trp1-1(am)::YIp204-TetR-ssn6-TRP, pol30::hisG, leu2-3,2-112::YIp128-P30-His6-POL30-LEU2, bar1::HISMX6, URA::yIp211-TetO7-E3.5-Flag-GFP-URA	DF5	this study
5001	pib1	a	his3Δ1, leu2Δ0, met15Δ0, ura3Δ0, pib1::his3MX	BY4741	[redacted]
5002	DF5 HP30 bar1 TetR-SSN6 TetON-GFP	a	his3-Δ200, lys2-801, trp1-1(am)::YIp204-TetR-ssn6-TRP, pol30::hisG, leu2-3,2-112::YIp128-P30-His6-POL30-LEU2, bar1::HISMX6, URA::yIp211-TetO7-GFP-URA	DF5	this study
5034	DF5 HP30 bar1 TetR-SSN6 Shs1-mCherry	a	his3-Δ200, lys2-801, trp1-1(am)::TetR-ssn6-TRP, pol30::hisG, leu2-3,2-112::YIp128-P30-His6-POL30-LEU2, bar1::HISMX6, ura3-52, Shs1-mCherry-natNT2	DF5	this study
5035	DF5 HP30 bar1 TetR-SSN6 TetON-GFP Shs1-mCherry	a	his3-Δ200, lys2-801, trp1-1(am)::YIp204-TetR-ssn6-TRP, pol30::hisG, leu2-3,2-112::YIp128-P30-His6-POL30-LEU2, bar1::HISMX6, URA::yIp211-TetO7-GFP-URA, Shs1-mCherry-natNT2	DF5	this study

5036	DF5 HP30 bar1 TetR-SSN6 TetON-E3.5-Flag-GFP Shs1-mCherry	a	his3-Δ200, lys2-801, trp1-1(am)::YIp204-TetR-ssn6-TRP, pol30::hisG, leu2-3,2-112::YIp128-P30-His6-POL30-LEU2, bar1::HISMX6, URA::yIp211-TetO7-E3.5-Flag-GFP-URA, Shs1-mCherry-natNT2	DF5	this study
5037	DF5 HP30 bar1 TetR-SSN6 TetON-A10-Flag-GFP Shs1-mCherry	a	his3-Δ200, lys2-801, trp1-1(am)::YIp204-TetR-ssn6-TRP, pol30::hisG, leu2-3,2-112::YIp128-P30-His6-POL30-LEU2, bar1::HISMX6, URA::yIp211-TetO7-A10-Flag-GFP-URA, Shs1-mCherry-natNT2	DF5	this study
5038	DF5 HP30 bar1 TetR-SSN6 TetON-C10-Flag-GFP Shs1-mCherry	a	his3-Δ200, lys2-801, trp1-1(am)::YIp204-TetR-ssn6-TRP, pol30::hisG, leu2-3,2-112::YIp128-P30-His6-POL30-LEU2, bar1::HISMX6, URA::yIp211-TetO7-C10-Flag-GFP-URA, Shs1-mCherry-natNT2	DF5	this study
5039	DF5 HP30 bar1 TetR-SSN6 TetON-F10-Flag-GFP Shs1-mCherry	a	his3-Δ200, lys2-801, trp1-1(am)::YIp204-TetR-ssn6-TRP, pol30::hisG, leu2-3,2-112::YIp128-P30-His6-POL30-LEU2, bar1::HISMX6, URA::yIp211-TetO7-F10-Flag-GFP-URA, Shs1-mCherry-natNT2	DF5	this study
5040	DF5 HP30 bar1 TetR-SSN6 TetON-E11-Flag-GFP Shs1-mCherry	a	his3-Δ200, lys2-801, trp1-1(am)::YIp204-TetR-ssn6-TRP, pol30::hisG, leu2-3,2-112::YIp128-P30-His6-POL30-LEU2, bar1::HISMX6, URA::yIp211-TetO7-E11-Flag-GFP-URA, Shs1-mCherry-natNT2	DF5	this study
5041	DF5 HP30 bar1 TetR-SSN6 TetON-G11-Flag-GFP Shs1-mCherry	a	his3-Δ200, lys2-801, trp1-1(am)::YIp204-TetR-ssn6-TRP, pol30::hisG, leu2-3,2-112::YIp128-P30-His6-POL30-LEU2, bar1::HISMX6, URA::yIp211-TetO7-G11-Flag-GFP-URA, Shs1-mCherry-natNT2	DF5	this study
5042	DF5 HP30 bar1 TetR-SSN6 TetON-B12-Flag-GFP Shs1-mCherry	a	his3-Δ200, lys2-801, trp1-1(am)::YIp204-TetR-ssn6-TRP, pol30::hisG, leu2-3,2-112::YIp128-P30-His6-POL30-LEU2, bar1::HISMX6, URA::yIp211-TetO7-B12-Flag-GFP-URA, Shs1-mCherry-natNT2	DF5	this study

5144	DF5 TetR-SSN6	a	his3-Δ200::TetR-SSN6-His, leu2-3,2-112, lys2-801, trp1-1(am), ura3-52	DF5	this study
5173	DF5 siz1 siz2 TetR-SSN6	alpha	leu2-3,2-112, lys2-801, trp1-1(am), ura3-52, siz1Δ::KanMX6, siz2Δ::HIS3 MX6, trp1-1::TetR-SSN6-TRP	DF5	this study
5174	DF5 siz1 siz2 TetR-SSN6 YIp211-TetON-E3.5-Flag-GFP	alpha	leu2-3,2-112, lys2-801, trp1-1(am), siz1Δ::KanMX6, siz2Δ::HIS3 MX6, trp1-1::TetR-SSN6-TRP, ura3-52::TetO7-DarpinE3.5-Flag-GFP-URA	DF5	this study
5175	DF5 siz1 siz2 TetR-SSN6 YIp211-TetON-E11-Flag-GFP	alpha	leu2-3,2-112, lys2-801, trp1-1(am), siz1Δ::KanMX6, siz2Δ::HIS3 MX6, trp1-1::TetR-SSN6-TRP, ura3-52::TetO7-DarpinE11-Flag-GFP-URA	DF5	this study
5176	DF5 siz1 siz2 TetR-SSN6 YIp211-TetON-F10-Flag-GFP	alpha	leu2-3,2-112, lys2-801, trp1-1(am), siz1Δ::KanMX6, siz2Δ::HIS3 MX6, trp1-1::TetR-SSN6-TRP, ura3-52::TetO7-DarpinF10-Flag-GFP-URA	DF5	this study
5235	DF5 TetR-SSN6 Shs1-mCherry	a	his3-Δ200::TetR-SSN6-HIS, leu2-3,2-112, lys2-801, trp1-1(am), ura3-52, Shs1-mCherr-natNT2	DF5	this study
5236	DF5 TetR-SSN6 Shs1-mCherry TetON-2xNES-E3.5-Flag-GFP	a	his3-Δ200::TetR-SSN6-HIS, leu2-3,2-112, lys2-801, trp1-1(am), ura3-52::TetON-2xNES-DARPIN-E3.5-Flag-GFP-URA, Shs1-mCherry-natNT2	DF5	this study
5237	DF5 TetR-SSN6 Shs1-mCherry TetON-2xNES-F10-Flag-GFP	a	his3-Δ200::TetR-SSN6-HIS, leu2-3,2-112, lys2-801, trp1-1(am), ura3-52::TetON-2xNES-DARPIN-F10-Flag-GFP-URA, Shs1-mCherry-natNT2	DF5	this study
5238	DF5 TetR-SSN6 Shs1-mCherry TetON-2xNES-E11-Flag-GFP	a	his3-Δ200::TetR-SSN6-HIS, leu2-3,2-112, lys2-801, trp1-1(am), ura3-52::TetON-2xNES-DARPIN-E11-Flag-GFP-URA, Shs1-mCherry-natNT2	DF5	this study
5239	DF5 TetR-SSN6 Shs1-3HA-6His	a	his3-Δ200::TetR-SSN6-HIS, leu2-3,2-112, lys2-801, trp1-1(am), ura3-52, Shs1-3HA-6His-hphNT1	DF5	this study

5240	DF5 TetR-SSN6 Shs1-3HA-6His TetON-2xNES-E3.5-Flag-GFP	a	his3-Δ200::TetR-SSN6-HIS, leu2-3,2-112, lys2-801, trp1-1(am), ura3-52::TetON-2xNES-DARPIN-E3.5-Flag-GFP-URA, Shs1-3HA-6His-hphNT1	DF5	this study
5241	DF5 TetR-SSN6 Shs1-3HA-6His TetON-2xNES-F10-Flag-GFP	a	his3-Δ200::TetR-SSN6-HIS, leu2-3,2-112, lys2-801, trp1-1(am), ura3-52::TetON-2xNES-DARPIN-F10-Flag-GFP-URA, Shs1-3HA-6His-hphNT1	DF5	this study
5242	DF5 TetR-SSN6 Shs1-3HA-6His TetON-2xNES-E11-Flag-GFP	a	his3-Δ200::TetR-SSN6-HIS, leu2-3,2-112, lys2-801, trp1-1(am), ura3-52::TetON-2xNES-DARPIN-E11-Flag-GFP-URA, Shs1-3HA-6His-hphNT1	DF5	this study
5320	SK1 Spr3-mCherry TetR-SSN6 diploid	a/alpha	hom3-10, his1-7, ade2, leu2, can1, his1-1 trp2::TetR-SSN6-TRP, Spr3-mCherry-hphNT1	SK1	this study
5321	SK1 Spr3-mCherry TetR-SSN6 TetON-NES-E3.5-Flag-GFP diploid	a/alpha	hom3-10, his1-7, ade2, leu2::TetO7-NES-E3.5-GFP-LEU, can1, his1-1 trp2::TetR-SSN6-TRP, Spr3-mCherry-hphNT1	SK1	this study
5322	SK1 Spr3-mCherry TetR-SSN6 TetON-NES-F10-Flag-GFP diploid	a/alpha	hom3-10, his1-7, ade2, leu2::TetO7-NES-F10-GFP-LEU, can1, his1-1 trp2::TetR-SSN6-TRP, Spr3-mCherry-hphNT1	SK1	this study
5323	SK1 Spr3-mCherry TetR-SSN6 TetON-NES-E11-Flag-GFP diploid	a/alpha	hom3-10, his1-7, ade2, leu2::TetO7-NES-E11-GFP-LEU, can1, his1-1 trp2::TetR-SSN6-TRP, Spr3-mCherry-hphNT1	SK1	this study
5378	SK1 TetR-SSN6 diploid	a/alpha	"ho::LYS2, lys2, ura3, leu2::hisG, his3::TetR-SSN6-HIS, trp1::hisG ho::LYS2, lys2, ura3, leu2::hisG, his3::TetR-SSN6-HIS, trp1::hisG"	SK1	this study
5379	SK1 TetR-SSN6 TetON-NES-E3.5-Flag-GFP diploid	a/alpha	"ho::LYS2, lys2, ura3::TetO7-NES-E3.5-GFP-URA, leu2::hisG, his3::TetR-SSN6-HIS, trp1::hisG ho::LYS2, lys2, ura3::TetO7-NES-E3.5-GFP-URA, leu2::hisG, his3::TetR-SSN6-HIS, trp1::hisG"	SK1	this study

5380	SK1 TetR-SSN6 TetON-NES-F10-Flag-GFP diploid	a/alpha	"ho::LYS2, lys2, ura3::TetO7-NES-F10-GFP-URA, leu2::hisG, his3::TetR-SSN6-HIS, trp1::hisG ho::LYS2, lys2, ura3::TetO7-NES-F10-GFP-URA, leu2::hisG, his3::TetR-SSN6-HIS, trp1::hisG"	SK1	this study
5381	SK1 TetR-SSN6 TetON-NES-E11-Flag-GFP diploid	a/alpha	"ho::LYS2, lys2, ura3::TetO7-NES-E11-GFP-URA, leu2::hisG, his3::TetR-SSN6-HIS, trp1::hisG ho::LYS2, lys2, ura3::TetO7-NES-E11-GFP-URA, leu2::hisG, his3::TetR-SSN6-HIS, trp1::hisG"	SK1	this study
5382	SK1 TetR-SSN6 TetON-E11-Flag-GFP diploid	a/alpha	"ho::LYS2, lys2, ura3::TetO7-E11-GFP-URA, leu2::hisG, his3::TetR-SSN6-HIS, trp1::hisG ho::LYS2, lys2, ura3::TetO7-E11-GFP-URA, leu2::hisG, his3::TetR-SSN6-HIS, trp1::hisG"	SK1	this study
5383	SK1 TetR-SSN6 TetON-F10-Flag-GFP diploid	a/alpha	"ho::LYS2, lys2, ura3::TetO7-F10-GFP-URA, leu2::hisG, his3::TetR-SSN6-HIS, trp1::hisG ho::LYS2, lys2, ura3::TetO7-F10-GFP-URA, leu2::hisG, his3::TetR-SSN6-HIS, trp1::hisG"	SK1	this study
5384	SK1 TetR-SSN6 TetON-E3.5-Flag-GFP diploid	a/alpha	"ho::LYS2, lys2, ura3::TetO7-E3.5-GFP-URA, leu2::hisG, his3::TetR-SSN6-HIS, trp1::hisG ho::LYS2, lys2, ura3::TetO7-E3.5-GFP-URA, leu2::hisG, his3::TetR-SSN6-HIS, trp1::hisG"	SK1	this study
5386	SK1 Shs1-mCherry TetR-SSN6 diploid	a/alpha	"his3-Δ200::TetR-SSN6-HIS, leu2-3,2-112, lys2-801, trp1-1(am), ura3-52, Shs1-mCherry-natNT2 ho::LYS2, lys2, ura3, leu2::hisG, his3::hisG, trp1::hisG"	SK1	this study
5387	DF5 HP30 bar1 TetR-SSN6 TetON-2xNES-E3.5-Flag-GFP	a	his3-Δ200, lys2-801, trp1-1(am)::TetR-SSN6-TRP, pol30::hisG, leu2-3,2-112::YIp128-P30-His6-POL30-LEU, bar1::HISMX6, ura3-52::TetON-2xNES-DARPIN-E3.5-Flag-GFP-URA	DF5	this study
5388	DF5 HP30 bar1 TetR-SSN6 TetON-2xNLS-E3.5-Flag-GFP	a	his3-Δ200, lys2-801, trp1-1(am)::TetR-SSN6-TRP, pol30::hisG, leu2-3,2-112::YIp128-P30-His6-POL30-LEU, bar1::HISMX6, ura3-52::TetON-2xNLS-DARPIN-E3.5-Flag-GFP-URA	DF5	this study

5389	DF5 HP30 bar1 TetR-SSN6 TetON-2xNLS-F10-Flag-GFP	a	his3-Δ200, lys2-801, trp1-1(am)::TetR-SSN6-TRP, pol30::hisG, leu2-3,2-112::YIp128-P30-His6-POL30-LEU, bar1::HISMX6, ura3-52::TetON-2xNLS-DARPIN-F10-Flag-GFP-URA	DF5	this study
5390	DF5 HP30 bar1 TetR-SSN6 TetON-2xNES-F10-Flag-GFP	a	his3-Δ200, lys2-801, trp1-1(am)::TetR-SSN6-TRP, pol30::hisG, leu2-3,2-112::YIp128-P30-His6-POL30-LEU, bar1::HISMX6, ura3-52::TetON-2xNES-DARPIN-F10-Flag-GFP-URA	DF5	this study
5391	DF5 HP30 bar1 TetR-SSN6 TetON-2xNES-E11-Flag-GFP	a	his3-Δ200, lys2-801, trp1-1(am)::TetR-SSN6-TRP, pol30::hisG, leu2-3,2-112::YIp128-P30-His6-POL30-LEU, bar1::HISMX6, ura3-52::TetON-2xNES-DARPIN-E11-Flag-GFP-URA	DF5	this study
5392	DF5 HP30 bar1 TetR-SSN6 TetON-2xNLS-E11-Flag-GFP	a	his3-Δ200, lys2-801, trp1-1(am)::TetR-SSN6-TRP, pol30::hisG, leu2-3,2-112::YIp128-P30-His6-POL30-LEU, bar1::HISMX6, ura3-52::TetON-2xNLS-DARPIN-E11-Flag-GFP-URA	DF5	this study
5399	SK1 Shs1-mCherry TetR-SSN6 TetON-E3.5-Flag-GFP	a/alpha	"his3-Δ200::TetR-SSN6-HIS, leu2-3,2-112, lys2-801, trp1-1(am), ura3-52::E3.5-GFP-URA, Shs1-mCherry-natNT2 ho::LYS2, lys2, ura3, leu2::hisG, his3::hisG, trp1::hisG"	SK1	this study
5400	SK1 Shs1-mCherry TetR-SSN6 TetON-NES-E3.5-Flag-GFP	a/alpha	"his3-Δ200::TetR-SSN6-HIS, leu2-3,2-112, lys2-801, trp1-1(am), ura3-52::NES-E3.5-GFP-URA, Shs1-mCherry-natNT2 ho::LYS2, lys2, ura3, leu2::hisG, his3::hisG, trp1::hisG"	SK1	this study
5402	SK1 Shs1-mCherry TetR-SSN6 TetON-NES-F10-Flag-GFP	a/alpha	"his3-Δ200::TetR-SSN6-HIS, leu2-3,2-112, lys2-801, trp1-1(am), ura3-52::NES-F10-GFP-URA, Shs1-mCherry-natNT2 ho::LYS2, lys2, ura3, leu2::hisG, his3::hisG, trp1::hisG"	SK1	this study

5403	SK1 Shs1-mCherry TetR-SSN6 TetON-NES-E11-Flag-GFP	a/alpha	"his3-Δ200::TetR-SSN6-HIS, leu2-3,2-112, lys2-801, trp1-1(am), ura3-52::NES-E11-GFP-URA, Shs1-mCherry-natNT2 ho::LYS2, lys2, ura3, leu2::hisG, his3::hisG, trp1::hisG"	SK1	this study
5404	DF5 HP30 bar1 TetR-SSN6 Cdc48-mCherry	a	his3-Δ200, lys2-801, trp1-1(am)::TetR-SSN6-TRP, pol30::hisG, leu2-3,2-112::YIp128-P30-His6-POL30-LEU, bar1::HISMX6, ura3-52, Cdc48-mCherry-natNT2	DF5	this study
5405	DF5 HP30 bar1 TetR-SSN6 TetON-E3.5-Flag-GFP Cdc48-mCherry	a	his3-Δ200, lys2-801, trp1-1(am)::TetR-SSN6-TRP, pol30::hisG, leu2-3,2-112::YIp128-P30-His6-POL30-LEU, bar1::HISMX6, ura3-52::yIp211-TetO7-E3.5-Flag-GFP-URA, Cdc48-mCherry-natNT2	DF5	this study
5406	DF5 HP30 bar1 TetR-SSN6 TetON-F10-Flag-GFP Cdc48-mCherry	a	his3-Δ200 lys2-801, trp1-1(am)::TetR-SSN6-TRP, pol30::hisG, leu2-3,2-112::YIp128-P30-His6-POL30-LEU, bar1::HISMX6, ura3-52::yIp211-TetO7-F10-Flag-GFP-URA, Cdc48-mCherry-natNT2	DF5	this study
5407	DF5 HP30 bar1 TetR-SSN6 TetON-E11-Flag-GFP Cdc48-mCherry	a	his3-Δ200, lys2-801, trp1-1(am)::TetR-SSN6-TRP, pol30::hisG, leu2-3,2-112::YIp128-P30-His6-POL30-LEU, bar1::HISMX6, ura3-52::yIp211-TetO7-E11-Flag-GFP-URA, Cdc48-mCherry-natNT2	DF5	this study
5408	DF5 HP30 bar1 TetR-SSN6 Spc42-mCherry	a	his3-Δ200, lys2-801, trp1-1(am)::TetR-SSN6-TRP, pol30::hisG, leu2-3,2-112::YIp128-P30-His6-POL30-LEU, bar1::HISMX6, ura3-52, Spc42-mCherry-natNT2	DF5	this study
5409	DF5 HP30 bar1 TetR-SSN6 TetON-E3.5-Flag-GFP Spc42-mCherry	a	his3-Δ200, lys2-801, trp1-1(am)::TetR-SSN6-TRP, pol30::hisG, leu2-3,2-112::YIp128-P30-His6-POL30-LEU, bar1::HISMX6, ura3-52::yIp211-TetO7-E3.5-Flag-GFP-URA, Spc42-mCherry-natNT2	DF5	this study

5410	DF5 HP30 bar1 TetR-SSN6 TetON-F10-Flag-GFP Spc42-mCherry	a	his3-Δ200, lys2-801, trp1-1(am)::TetR-SSN6-TRP, pol30::hisG, leu2-3,2-112::YIp128-P30-His6-POL30-LEU, bar1::HISMX6, ura3-52::yIp211-TetO7-F10-Flag-GFP-URA, Spc42-mCherry-natNT2	DF5	this study
5411	DF5 HP30 bar1 TetR-SSN6 TetON-E11-Flag-GFP Spc42-mCherry	a	his3-Δ200, lys2-801, trp1-1(am)::TetR-SSN6-TRP, pol30::hisG, leu2-3,2-112::YIp128-P30-His6-POL30-LEU, bar1::HISMX6, ura3-52::yIp211-TetO7-E11-Flag-GFP-URA, Spc42-mCherry-natNT2	DF5	this study
5412	DF5 HP30 bar1 TetR-SSN6 Kre28-mCherry	a	his3-Δ200, lys2-801, trp1-1(am)::TetR-SSN6-TRP, pol30::hisG, leu2-3,2-112::YIp128-P30-His6-POL30-LEU, bar1::HISMX6, ura3-52, Kre28-mCherry-natNT2	DF5	this study
5413	DF5 HP30 bar1 TetR-SSN6 TetON-E3.5-Flag-GFP Kre28-mCherry	a	his3-Δ200, lys2-801, trp1-1(am)::TetR-SSN6-TRP, pol30::hisG, leu2-3,2-112::YIp128-P30-His6-POL30-LEU, bar1::HISMX6, ura3-52::yIp211-TetO7-E3.5-Flag-GFP-URA, Kre28-mCherry-natNT2	DF5	this study
5414	DF5 HP30 bar1 TetR-SSN6 TetON-F10-Flag-GFP Kre28-mCherry	a	his3-Δ200, lys2-801, trp1-1(am)::TetR-SSN6-TRP, pol30::hisG, leu2-3,2-112::YIp128-P30-His6-POL30-LEU, bar1::HISMX6, ura3-52::yIp211-TetO7-F10-Flag-GFP-URA, Kre28-mCherry-natNT2	DF5	this study
5415	DF5 HP30 bar1 TetR-SSN6 TetON-E11-Flag-GFP Kre28-mCherry	a	his3-Δ200, lys2-801, trp1-1(am)::TetR-SSN6-TRP, pol30::hisG, leu2-3,2-112::YIp128-P30-His6-POL30-LEU, bar1::HISMX6, ura3-52::yIp211-TetO7-E11-Flag-GFP-URA, Kre28-mCherry-natNT2	DF5	this study
5433	DF5 TetR-SSN6 TetON-F10-Flag-GFP mRuby2-Pol30	a	his3-Δ200::TetR-SSN6-HIS, leu2-3,2-112::pPol30-mRuby-Pol30-LEU, lys2-801, trp1-1(am), ura3-52::TetO7-F10-GFP-URA	DF5	this study
5434	DF5 TetR-SSN6 TetON-E11-Flag-GFP mRuby2-Pol30	a	his3-Δ200::TetR-SSN6-HIS, leu2-3,2-112::pPol30-mRuby-Pol30-LEU, lys2-801, trp1-1(am), ura3-52::TetO7-E11-GFP-URA	DF5	this study

5435	DF5 TetR-SSN6 TetON-E3.5-Flag-GFP mRuby2-Pol30	a	his3-Δ200::TetR-SSN6-HIS, leu2-3,2-112::pPol30-mRuby-Pol30-LEU, lys2-801, trp1-1(am), ura3-52::TetO7-E3.5-GFP-URA	DF5	this study
5436	DF5 TetR-SSN6 mRuby2-Pol30	a	his3-Δ200::TetR-SSN6-HIS, leu2-3,2-112::pPol30-mRuby-Pol30-LEU, lys2-801, trp1-1(am), ura3-52	DF5	this study
5437	DF5 HP30 bar1 TetR-SSN6 Rfa1-mRuby	a	his3-Δ200, leu2-3,2-112, lys2-801, trp1-1(am)::TetR-SSN6-TRP, pol30::hisG, LEU2::YIp128-P30-His6-POL30-LEU, bar1::HISMX6, ura3-52, Rfa1-mRuby2-NrsR	DF5	this study
5438	DF5 HP30 bar1 TetR-SSN6 TetON-F10-Flag-GFP Rfa1-mRuby	a	his3-Δ200, leu2-3,2-112, lys2-801, trp1-1(am):: TetR-SSN6-TRP, pol30::hisG, LEU2::YIp128-P30-His6-POL30-LEU, bar1::HISMX6, ura3-52::yIp211-TetO7-F10-Flag-GFP-URA, Rfa1-mRuby1-NrsR	DF5	this study
5439	DF5 HP30 bar1 TetR-SSN6 TetON-E11-Flag-GFP Rfa1-mRuby	a	his3-Δ200, leu2-3,2-112, lys2-801, trp1-1(am):: TetR-SSN6-TRP, pol30::hisG, LEU2::YIp128-P30-His6-POL30-LEU, bar1::HISMX6, ura3-52::yIp211-TetO7-E11-Flag-GFP-URA, Rfa1-mRuby-NrsR	DF5	this study
5440	DF5 HP30 bar1 TetR-SSN6 TetON-E3.5-Flag-GFP Rfa1-mRuby	a	his3-Δ200, leu2-3,2-112, lys2-801, trp1-1(am):: TetR-SSN6-TRP, pol30::hisG, LEU2::YIp128-P30-His6-POL30-LEU, bar1::HISMX6, ura3-52::yIp211-TetO7-E3.5-Flag-GFP-URA, Rfa1-mRuby2-NrsR	DF5	this study
–	lys1 Pib1-TAP	a	his3::pib1p-pib1-TAP-his3MX, leu2-3,2-112, lys2-801, trp1-1(am), ura3-52, lys1::NatNT1	DF5	[redacted]
–	lys1 Pib1-GFP	a	his3::pib1p-pib1-GFP-his3MX, leu2-3,2-112, lys2-801, trp1-1(am), ura3-52, lys1::NatNT2	DF5	[redacted]
del3771	bre1	a	leu2D0, met15D0, ura3D0, his3D0, bre1::KanMX	BY4741	Deletion collection
del4425	rad6	a	leu2D0, met15D0, ura3D0, his3D0, rad6::KanMX	BY4741	Deletion collection

2.1.5 Enzymes and proteins

Table 6: List of restriction enzymes, DNA modifying enzymes and commercial proteins used in this study.

Enzyme/Protein	Source
α-factor	Eurogentec Germany
Antarctic phosphatase	New England Biolabs
Benzonase	Sigma-Aldrich
Bovine serum albumin (BSA)	Sigma-Aldrich
DNase I (RNase-Free)	New England Biolabs
FastAP Thermosensitive Alkaline Phosphatase (1 U/µL)	Thermo Fisher Scientific
Herculase II Fusion DNA Polymerase	Agilent
His-Ubi	BioTechne
One Taq	Protein Production Core Facility
Pfu Turbo DNA polymerase	Agilent
Pfu Ultra high fidelity	DNA Polymerase Agilent
Phusion HF DNA Polymerase	New England Biolabs
Precision protease	purified by [redacted]
Proteinase K	Sigma-Aldrich
Q5 DNA polymerase	New England Biolabs
Restriction enzymes	New England Biolabs
RNase A	Sigma-Aldrich
T4 DNA Ligase	Protein Production Core Facility
T4 DNA Ligase	New England Biolabs
Taq DNA polymerase	Protein Production Core Facility
TEV Protease	Protein Production Core Facility
Thrombin cleavage and capture kit	Merck Millipore
Zymolyase 20T	AMS Biotechnology

2.1.6 Antibodies

Table 7: List of antibodies used in this study.

ID	Name	Species/ type	Clone	Source	Dilution	primary/ secondary
24	mCherry	Mouse/ mAb	1C51	Abcam ab125096	Western blot: 5% milk, 1:2000	primary
42	FLAG	Mouse/ mAb	M2	Sigma F1804	Western blot: 5% milk, 1:2000	primary
49	GFP	Mouse/ mAb	7.1 and 13.1	Roche 11814460001	Western blot: 5% milk, 1:5000	primary
56	GST	Mouse/ mAb	B-14	Santa Cruz sc-138	Western blot: 5% milk, 1:5000	primary
70	His	Mouse/ mAb	HIS-1	Sigma H1029	Western blot: 5% milk, 1:2000	primary

139	Pib1	Rabbit/ pAb	–	SA2294	Western blot: 5% milk, 1:500	primary
150	PCNA	Rabbit/ pAb	R37/38 (serum)	[redacted] lab	Western blot: 5% milk, 1:2000	primary
195	RNF4	Goat/ pAb	–	Bio-techne AF7964	Western blot: 5% milk, 1:2000	primary
210	Sumo	Rabbit/ pAb	–	[redacted] lab	Western blot: 5% milk, 1:10000	primary
218	Strep	Mouse/ mAb	GT661	Sigma SAB2702216	Western blot: PBST, 1:2500	primary
229	TAP	Rabbit/ pAb	–	Thermo CAB1001	Western blot: 5% milk, 1:5000	primary
230	TETR	Rabbit/ pAb	–	N/A	Western blot: 5% milk, 1:1000	primary
250	α-Tubulin	Rabbit/ mAb	EPR13799	Abcam ab184970	Western blot: 5% milk, 1:20000, IF: 1:500	primary
260	Ubiquitin	Rabbit/ pAb	–	Dako Z045801-2	Western blot: 5% milk, 1:1000	primary
265	Ubiquitin	Mouse/ mAb	P4D1	CST 3936	Western blot: 5% milk, 1:2000	primary
267	Ubiquitin, Lys63-specific	Rabbit/ mAb	Apu3	Millipore 05-1308	Western blot: 5% milk, 1:1000	primary
311	HA	Mouse/ mAb	F-7	Santa Cruz sc-7392	Western blot: 3% milk, 1:500	primary
329	Protein A	Rabbit/ pAb	–	Sigma P3775	Western blot: 5% milk, 1:5000	primary
343	GFP nanobody Atto 488	Nanobody	–	IMB - PPCF	IF:1:500	primary
353	tRFP	Rabbit/ pAb	–	BioCat AB233	Western blot: 5% milk, 1:2500	primary
55	IRDye 800CW anti-goat IgG	Donkey	–	Licor 926-32214	Western blot: PBST, 1:10000	secondary

91	IRDye 680CW anti-mouse IgG	Donkey	–	Licor 926-68022	Western blot: PBST, 1:10000	secondary
92	IRDye 800CW anti-mouse IgG	Donkey	–	Licor 926-32212	Western blot: PBST, 1:10000	secondary
93	HRP conjugated anti-mouse IgG	Goat/ pAb	–	Pierce 1858413	Western blot: PBST, 1:10000	secondary
154	IRDye 680CW anti-rabbit IgG	Donkey	–	Licor 926-68023	Western blot: PBST, 1:10000	secondary
155	IRDye 800CW anti-rabbit IgG	Goat	–	Licor 926-32211	Western blot: PBST, 1:10000	secondary
156	HRP conjugated anti-rabbit IgG	Goat/ pAb	–	Pierce 31460	Western blot: PBST, 1:10000	secondary
157	Alexa Fluor 594 anti-rabbit IgG	Goat/ pAb	–	Life A-11012	IF: 1:100	secondary
159	HRP conjugated anti-rabbit IgG	Mouse/ mAb	N/A	Jackson IR 211-002-171	Western blot: PBST, 1:10000	secondary

2.1.7 Chemicals and reagents

Unless stated differently, chemicals were purchased from Sigma-Aldrich (Merck) or Thermo Fisher Scientific.

Table 8: List of most important chemicals used in this study.

Reagent	Source
10x Antarctic phosphatase reaction buffer	New England Biolabs
10x Pfu reaction buffer	Agilent
10x Restriction enzymes reaction buffer	New England Biolabs
10x T4 DNA ligase buffer	New England Biolabs
4x NuPAGE LDS buffer	Thermo Fisher Scientific
5x Green GoTaq Reaction Buffer	Promega
5x Herculase reaction buffer	Agilent
Ammonium-^{15}N chloride >98 atoms	Sigma-Aldrich
BODIPY TMR C5-Maleimide, 1 mg	Thermo Fisher Scientific
SIGMAFAST Protease Inhibitor Cocktail Tablets, EDTA-Free	Sigma-Aldrich
Concanavalin A	Sigma-Aldrich
DNA Ladder 1 kb and 100 bp	New England Biolabs
dNTPs	New England Biolabs
Doxycycline hydrochloride	Sigma-Aldrich
FACSFlow, FACSRinse, and FACSClean	BD Biosciences
InstantBlue Ultrafast Protein Stain	Biozol Diagnostica
IPTG, ultrapure,	Generon
Methyl methanesulfonate	Sigma-Aldrich
Nitrocellulose Membrane, Roll, 0.2 µm, 30 cm x 3.5 m	Bio-Rad Laboratories
Nocodazole	Sigma-Aldrich
PageRuler Prestained Protein Ladder	Fisher Scientific
ProLong Diamond Antifade Mountant	Molecular Probes

Table 9: List of most important kits used in this study.

kit	Source
Additive Screen	Hampton Research
Biotin CAPture kit	GE Healthcare
GeneJET Plasmid Miniprep kit	Fisher Scientific
Index Screen	Hampton Research
JCSG+ Screen	Hampton Research
MasterPure Yeast DNA Purification Kit	Biozym
QIAquick Gel Extraction Kit	Qiagen
Thermo Scientific GeneJET PCR Purification Kit	Fisher Scientific
Trans-Blot Turbo RTA Midi Nitrocellulose Transfer Kit	Bio-Rad Laboratories
Trans-Blot Turbo RTA transfer kit nitrocellulose	Bio-Rad Laboratories

2.1.8 Purification materials

Table 10: List of purification reagents used in this study.

Material	Source
Amylose Resin	New England Biolabs
Anti-FLAG M2 Magnetic Beads	Sigma-Aldrich
Column NAP-5	GE Healthcare
Column PD 10	Fisher Scientific
GFP-Trap magnetic agarose beads	Chromotek
Glutathione Sepharose 4 fast flow	GE Healthcare
HiLOAD 16/600 Superdex 200 pg large	GE Healthcare
HiLOAD 16/600 Superdex 75 pg large	GE Healthcare
HisTrap HP, 5 x 5 ml	GE Healthcare
HiTrap Q HP	Fisher Scientific
IgG Sepharose 6 Fast Flow, 10 ml	Fisher Scientific
MONO Q 10/100 GL FORPACKAD small-med	GE Healthcare
MONO Q 5/50 GL FORPACKAD small	GE Healthcare
Ni^{2+}-NTA agarose beads	Qiagen
Streptavidin Agarose Resin	Fisher Scientific
Superdex 200 INCREASE 10/300 GL	Sigma-Aldrich
Superdex 200 10/300 GL	Sigma-Aldrich
Superdex 75 INCREASE 10/300 GL	GE Healthcare
Superdex 75 10/300 GL	GE Healthcare

2.1.9 Media

2.1.9.1 Media for bacterial work

Luria Broth (LB) plates containing kanamycin (Kan, 30 µg /mL) or ampicillin (Amp, 100 µg/mL) and liquid LB-media were purchased from the Core facility (CF) media lab.

Table 11: List of antibiotics used in this study.

antibiotics	stock solution	working concentration
Ampicillin	100 mg/mL in ddH_2O	100 µg/mL
Chloramohenicol	34 mg/mL in EtOH	34 µg/mL
Gentamycin	10 mg /mL in ddH_2O	10 µg /mL
Kanamycin	30 mg/mL in ddH_2O	30 µg/mL
Nourseothricin	100 mg/mL in ddH_2O	100 µg/mL

Labelled M9 media: 0.3 mM $CaCl_2$, 0.4 % weight by volume (w/v) Glucose, 1 mg/mL Ampicillin, 1 g/L $^{15}NH_4Cl$, 1x M9 buffer (0.3 g KH_2PO_4, 0.6 g Na_2HPO_4, 0.5 g NaCl, 0.1 mL 1 M $MgSO_4$ in 500 mL), autoclaved.

2.1.9.2 Media for yeast work

Yeast Peptone (YP) medium, YPD plates, 4 % (w/v) water-agar and 20 % (w/v) glucose were purchased from the CF media lab.

2.5x Synthetic Complete (SC) -media: 4.25 g of yeast nitrogen base (without amino acids and ammonium sulfate), 12.5 g of ammonium sulfate and 5 g of the SC powder (depleted of the amino acids of interest and prepared as described in our lab database) were mixed in 1 L of sterile water, afterwards stirred for 30 min and autoclaved.

1x SC medium: 200 mL of 2.5x SC medium, 250 mL of ddH_2O and 50 mL of 20 % (w/v) glucose, galactose or raffinose were mixed.

SC medium agar: 200 mL of 2.5 SC medium, 250 mL of 4 % volume by volume (v/v) water-agar and 50 mL of 20 % (w/v) glucose were mixed and poured into sterile plates.

20 % (w/v) galactose: 200 g of galactose and warm water up to 1 L were mixed and autoclaved.

20 % (w/v) raffinose: 200 g of raffinose and warm water up to 1 L were mixed and autoclaved.

100 mM $CuSO_4$: 24.97 g of copper sulphate pentahydrate was mixed with water up to 100 mL and filter-sterilised.

2.1.10 Buffer and solutions

The CF media lab prepared the following buffers according to general recipes: 0.5 M EDTA pH 8.0, 5 M NaCl, 5x Phosphate buffered saline (PBS), 10x SDS running buffer, 10x transfer buffer (for wet Western blot), 10x Tris(hydroxymethyl)aminomethane (Tris)-HCl pH 7.5, 10x Tris/borate/EDTA buffer (TBE), 2 M $MgCl_2$, 1 M KCl, and 20x SSC pH 7.0.

2.1.10.1 Buffer for general DNA and protein work

5x Laemmli buffer: 250 mM Tris-HCl pH 6.8, 10 % (w/v) SDS, 0.1 % (w/v) bromophenol blue, 10 % (v/v) glycerol with freshly supplemented 100 mM dithiothreitol (DTT).

6x DNA loading buffer: 50 % (w/v) sucrose, 0.1 % (w/v) bromophenol blue and 0.1 % (w/v) xylene cyanol F in 1x TE.

Blocking solution: 5 % (w/v) skim milk powder in 1x PBS-T.

Blotting buffer (wet transfer): 1x transfer buffer containing 15 % (v/v) methanol.

HU buffer: 8 M hydroxyurea (HU), 5 % (w/v) SDS, 200 mM Tris-HCl pH 6.8, 1 mM EDTA, 0.1 % (w/v) bromophenol blue and 50 mM DTT.

MES SDS running buffer: 50 mM MES hydrate, 50 mM Tris-HCl pH 7.3, 0.1 % (v/v) SDS, 1 mM ETDA.

MOPS SDS running buffer: 50 mM MOPS, 50 mM Tris-HCl pH 7.7, 0.1 % (v/v) SDS, 1 mM ETDA.

PBS-T: 1x PBS, 0.1 % (v/v) Tween 20.

Ponceau S solution: 0.1 % (w/v) Ponceau S in 5 % (v/v) acetic acid.

Stripping buffer: 200 mM Glycine, 0.1 % (v/v) SDS, 1 % (v/v) Tween20 pH 2.2.

2.1.10.2 Buffer for yeast work

BSA/PBS buffer: 0.04 M HK_2PO_4, 0.01 M H_2KPO_4, 0.15 M NaCl, 0.1 % (v/v) Sodiumazide, 1 % (w/v) BSA.

Citrate buffer: 2.94 g of trisodium citrate (50 mM) dissolved in ddH_2O, pH adjusted to 7.0 with 1 N citric acid.

Denaturating buffer A: 6 M guanidine-HCl, 100 mM $NaPO_4$ pH 8, 10 mM Tris-HCl pH 8.

Denaturating buffer C: 8 M urea, 100 mM $NaPO_4$ pH 6.3, 10 mM Tris-HCl pH 6.3.

HT single-strand DNA solution: Herring testes DNA Type XIV (Sigma) was dissolved and vigorously sonicated in TE buffer (10 mg/mL), phenol/chloroform extracted, precipitated with ethanol and resuspended in TE buffer before boiling at 95°C for 5 min. Afterwards, the solution was quickly incubated on ice for 5 min and stored at 4 ℃.

LiT/polyethylene glycol (PEG) buffer: 10 mM Tris-HCl pH 8, 100 mM lithium acetate, 1 mM EDTA pH 8, 40 % (w/v) PEG 3350 in LiT buffer, autoclaved.

NaOH/β-mercaptoethanol solution: 925 mL of 2 M NaOH and 75 mL of β-mercaptoethanol.

Propidium iodide stock solution: 20 µg/mL propidium iodide in 50 mM citrate buffer.

SORB buffer: 10 mM Tris-HCl pH 8, 1 mM EDTA pH 8, 100 mM lithium acetate, 1 M Sorbitol, autoclaved.

Spheroblasting buffer: 0.1 M potassium phosphate buffer pH 7.4, 1.2 M Sorbitol, 0.5 mM $MgCl_2$.

Yeast Presporulation medium: 0.5 % (w/v) Bacto yeast extract, 1 % (w/v) Bacto peptone, 1 % (w/v) potassium acetate, 0.17 % (w/v) Yeast nitrogen base without amino acids and ammonium sulfate, 0.5 % (w/v) ammonium sulfate, 0.05 M potassium hydrogen phthalate. Adjust pH to 5.5 with 10 N KOH and autoclave. Supplement with amino acids according to the auxotrophic requirements of the yeast strain of interest.

Yeast Sporulation medium for SK1 strains: 1 % (w/v) potassium acetate, 0.02 % (w/v) Raffinose adjust the pH to 7 with 10 N KOH and autoclave. Supplement with amino acids according to the auxotrophic requirements of the yeast strain of interest.

Yeast sporulation solution for strain creation: 1 % (w/v) potassium acetate, autoclaved.

2.1.10.3 Buffers for protein purification

Lysis buffer for biotinylated SUMO: 40 mM 4-(2-hydroxyethyl)-1-piperazineethanesulfonic acid (Hepes), pH 7.5, 150 mM NaCl, 20 mM imidazole, 1 mM DTT, SIGMAFAST Protease Inhibitor Cocktail.
Elution buffer for biotinylated SUMO: 40 mM Hepes, pH 7.5, 150 mM NaCl, 500 mM imidazole, 1 mM DTT.
Gel filtration (GF) buffer for biotinylated SUMO: HBS-EP (10 mM Hepes pH 7.4, 150 mM NaCl, 3 mM EDTA, 0.005 % (v/v) P20 (Tween)).

Lysis buffer for DARPins: 40 mM Hepes, pH 7.5, 150 mM NaCl, 20 mM imidazole, 1 mM DTT, SIGMAFAST Protease Inhibitor Cocktail.
Elution buffer for DARPins: 40 mM Hepes, pH 7.5, 150 mM NaCl, 500 mM imidazole, 1 mM DTT.
GF buffer for DARPins: dependent on downstream application (e.g. 1x MAB, FRET assay buffer, RNF4 pull-down (PD) buffer, Ulp1 cleavage buffer, crystallisation buffer).

Lysis buffer for RNF4: 50 mM Tris, 0.5 M NaCl, 10 mM imidazole, 2 mM enzamidine, SIGMAFAST Protease Inhibitor Cocktail, pH 7.5.
Elution buffer for RNF4: 20 mM Tris pH 8, 150 mM NaCl, 500 mM imidiazol, 1 mM EDTA).
GF buffer for RNF4: 20 mM Tris, 150 mM NaCl, 1 mM TCEP, pH 7.5.

Lysis buffer for untagged SUMO: 25 mM Tris–HCl, pH 7.5, 50 mM NaCl, 0.5 mM EDTA, 1 mM DTT, SIGMAFAST Protease Inhibitor Cocktail.
Buffer A for untagged SUMO: 25 mM Tris–HCl, pH 7.5, 0.5 mM DTT, 1 mM EDTA.
GF for untagged SUMO/crystallisation buffer: 40 mM Hepes, pH 7.4, 50 mM NaCl, 1 mM DTT.

Lysis buffer for YFP-H-SUMO-3R: 50 mM Tris-HCl, 50 mM NaCl, 1 mM EDTA, pH 8.0, 1 mM DTT, SIGMAFAST Protease Inhibitor Cocktail.

Wash buffer for YFP-H-SUMO-3R: 50 mM Tris-HCl, 50 mM NaCl, 30 mM imidiazole, pH 8.0, 1 mM DTT.
Elution buffer for YFP-H-SUMO-3R: 50 mM Tris-HCl, 50 mM NaCl, 500 mM imidiazole, pH 8.0, 1 mM DTT.
Storage buffer for YFP-H-SUMO-3R: 20 mM HEPES, 110 mM potassium acetate, 2 mM magnesium acetate, 1 mM EGTA, pH 7.3, 1 mM DTT, SIGMAFAST Protease Inhibitor Cocktail.

Lysis buffer for SUMO E1: 50 mM Na-phosphate pH 8.0, 300 mM NaCl, 10 mM imidazole, SIGMAFAST Protease Inhibitor Cocktail.
Wash buffer for SUMO E1: 50 mM Na-phosphate, pH 8.0, 300 mM NaCl, 20 mM imidazole, 1 mM β-mercaptoethanol, SIGMAFAST Protease Inhibitor Cocktail.
Elution buffer for SUMO E1: 50 mM Na-phosphate, pH 8.0, 300 mM NaCl, 250 mM imidazole, 1 mM β-mercaptoethanol, SIGMAFAST Protease Inhibitor Cocktail.
Gel filtration buffer for SUMO E1: 50 mM Tris-HCl, pH 7.5, 50 mM NaCl, 1 mM DTT, SIGMAFAST Protease Inhibitor Cocktail.
MonoQ buffer for SUMO E1: 50 mM Tris-HCl, pH 7.5, 500 mM NaCl, 1 mM DTT, SIGMAFAST Protease Inhibitor Cocktail.
Storage buffer for SUMO E1: 20 mM HEPES, pH 7.3, 110 mM potassium acetate, 2 mM magnesium acetate, 1 mM EGTA, 1 mM DTT, SIGMAFAST Protease Inhibitor Cocktail.

Lysis buffer for Ubc9: 40 mM Tris–HCl, pH 7.5, 300 mM NaCl, 30 mM imidazole, 1 mM DTT.
Elution buffer for Ubc9: 40 mM Tris–HCl, pH 7.5, 200 mM NaCl, 300 mM imidiazole, 1 mM DTT, SIGMAFAST Protease Inhibitor Cocktail.
GF buffer for Ubc9: 40 mM Tris–HCl, pH 7.5, 200 mM NaCl, 1 mM EDTA, 1 mM DTT, 10 % (v/v) glycerol.

Lysis buffer for Snc1 constructs: 25 mM HEPES-KOH, pH 7.7, 400 mM KCl, 10 % (v/v) glycerol, 2 mM β-mercaptoethanol, SIGMAFAST Protease Inhibitor Cocktail and 4 % (v/v) Triton X100.
TX-100 wash buffer for Snc1: 25 mM HEPES-KOH, pH 7.7, 400 mM KCl, 10 % (v/v) glycerol, 2 mM β-mercaptoethanol, 1 % (v/v) Triton X100.
Octyl glucoside (OG) wash buffer for Snc1: 25 mM HEPES-KOH, pH 7.7, 100 mM KCl, 10 % (v/v) glycerol, 2 mM β-mercaptoethanol, 50 mM imidazole-OAc, pH 7.5, 1 % (w/v) OG.
Elution buffer for Snc1: 50 mM Hepes pH 7.4, 150 mM NaCl, 1 mM DTT, 10 % (v/v) glycerol, 500 mM imidiazole.
Gel filtration buffer for Snc1: 50 mM Hepes pH 7.4, 150 mM NaCl, 1 mM DTT, 10 % (v/v) glycerol.

Lysis buffer for Spc24/25 and Ub variants: 1x PBS, 0.1 % (v/v) Triton X100, 1 mM DTT, SIGMAFAST Protease Inhibitor Cocktail.
Wash buffer for Spc24/25 and Ub variants: 1x PBS, 0.01 % (v/v) Triton X100, 1 mM DTT, SIGMAFAST Protease Inhibitor Cocktail.
Maintenance buffer for Spc24/25 and Ub variants: 50 mM Tris pH 7.5, 100 mM NaCl, 10 % (v/v) glycerol, 1 mM DTT.

2.1.10.4 Buffers for enzymatic assays

10x MAB: 400 mM HEPES, pH 7.4, 80 mM magnesium acetate, 500 mM NaCl.

FRET assay buffer: 400 mM Hepes pH 7.4, 80 mM MgAc, 500 mM NaCl, 1 % (v/v) Tween20.

PD buffer for SUMO from yeast extract: 50 mM HEPES pH7.4, 50 mM NaCl, 1 % (v/v) glycerol, 1 % (v/v) Triton X100.

RNF4 PD buffer: 50 mM HEPES pH 7.4, 50 mM NaCl, 1 % (v/v) glycerol, 1 % (v/v) Triton X100.

Ulp1 cleavage buffer: 50 mM Tris pH 8.0, 250 mM NaCl, 1 mM DTT.

2.1.10.5 Other buffers

MS buffers Pib1-TAP:

- Lysis buffer: 50 mM Tris pH 7.5, 150 mM NaCl, 10 % (v/v) glycerol, 1 mM DTT, 5 mM EDTA, 10 mM NEM, SIGMAFAST Protease Inhibitor Cocktail.
- Extract buffer: 50 mM Tris pH 7.5, 150 mM NaCl, 10 % (v/v) glycerol, 1 mM DTT, 5 mM EDTA, 10 mM NEM, SIGMAFAST Protease Inhibitor Cocktail, 0.5 % Igepal, 0.25 % (v/v) Triton X100.
- Dilution buffer: 50 mM Tris pH 7.5, 150 mM NaCl, 10 % (v/v) glycerol.
- Wash buffer: 50 mM Tris pH 7.5, 300 mM NaCl, 0.5 % (v/v) Triton X100, 0.5 mM EDTA.
- TEV-cleavage buffer: 10 mM Tris pH 8.0, 150 mM NaCl, 1 mM DTT, 1 mM EDTA.
- Elution buffer: 0.1 M Glycine-HCL pH 3.

MS buffer Pib1-GFP:

- Lysis buffer: 50 mM Tris pH 7.5, 150 mM NaCl, 0.5 % (v/v) Triton X100, 1 mM EDTA, 10 mM NEM, SIGMAFAST Protease Inhibitor Cocktail.
- Dilution buffer: 10 mM Tris pH 7.5, 150 mM NaCl, 0.5 mM EDTA, 10 mM NEM, SIGMAFAST Protease Inhibitor Cocktail.
- Denaturing wash buffer: 8 M urea, 1 % (v/v) SDS, 1x PBS.
- SDS-Buffer: 1 % (v/v) SDS, 1x PBS.

MS buffers Ubait:

- Lysis buffer: 50 mM Tris pH 7.5, 150 mM NaCl, 10 % (v/v) glycerol, 1 mM DTT, 5 mM EDTA, 10 mM NEM, SIGMAFAST Protease Inhibitor Cocktail.
- Wash buffer: Lysis buffer, 0.1 % (v/v) Igepal, SIGMAFAST Protease Inhibitor Cocktail.
- Denaturing buffer: 20 mM Tris pH 8, 50 mM NaCl, 5 mM DTT, 1 % (v/v) SDS.

NMR buffer: 50 mM Sodiumphosphate buffer pH 7.0, 100 mM NaCl.

2.1.11 Software

Table 12: Software used in this study.

Software	Use	Source
Adobe products	Assembly of figures	https://www.adobe.com/
Biacore X100 software	Recording and analysis of affinity and kinetic studies	Biacore
CCP4	Macromolecular X-Ray Crystallography analysis	Collaborative Computational Project No. 4
ChromLab	FPLC control	BioRad
Epson Scan perfection V700	Scanner	Epson
FlowJo - V10	Analysis of flow cytometry data	FlowJo, LLC
FusionCapt Advanced	Image acquisition of western blots and agarose gels	Vilber Lourmat
Image Lab	Image acquisition of western blots and agarose gels	Bio-Rad
Image StudioTM	Analysis of western blots	LI-COR
ImageJ - Fiji	Analysis and editing of microscopy images	Schindelin *et al.* (2012) [383]
NanoDrop 1000 3.7.0	DNA and protein concentration measurement	PEQLAB Biotechnologie
PyMol	Analysis and manipulation of crystal structures	Schrödinger, Inc

SnapGene	Designing oligonucleotides, creating plasmid maps, and simulating cloning	Insightful Science
SoftWoRx	Acquisition and deconvolution of microscopy images	GE Healthcare
Spark control Dashboard	Acquisition of fluorescence data and optical density	Tecan Trading AG
TopSpin	Analysis of NMR data	Bruker

2.2 Methods

2.2.1 DNA manipulation and cloning

2.2.1.1 Polymerase Chain Reaction (PCR)

Polymerase Chain Reactions (PCR) were performed in order to amplify genes of interest. This method is based on the activity of heat-stable DNA-Polymerases to synthesize the complementary strand to an offered single-stranded DNA template.[384] All primers were ordered from Sigma or IDT. Their sequences are listed in section 2.1.1. The reaction was performed using the Phusion® High-Fidelity DNA Polymerase (New England Biolabs (NEB)) or a home-made high fidelity polymerase (CF Protein production) according to the manufacturer's protocol. The reaction took place in a Professional TRIO 48 cycler (Biometra). The reaction was composed of 200 µM dNTPs, 10 µL HF or GC buffer (5x), 50 ng template, 1 U DNA Polymerase, 0.5 µM forward primer and 0.5 µM reverse primer. The reaction was filled up to 50 µL with nuclease-free water. The PCR program for all reactions included 5 minutes of initial denaturation (98 °C). Followed by 30 cycles of 10 s denaturation (98 °C), 30 s primer annealing (T_m of primers) and 30 s of extension (72 °C). A final extension was performed for 10 minutes (72 °C). For the clean-up of PCR reactions, the GeneJET PCR Purification Kit (Thermo Fisher Scientific) or the QIAquick Gel Extraction Kit (250) (Qiagen) was used according to the manufacturer's instructions. Elution took place with 50 µL millipore purified water (ddH_2O).

2.2.1.2 Mutagenesis PCR

Using primers containing the mutation of interest, the whole template was amplified to mutate single sites in a plasmid DNA. For the PCR the high fidelity polymerases Pfu Turbo, Pfu Ultra, Herculase (all Agilent) or Q5 polymerase (NEB) were used according

to their respective manufacturer protocol. 3 % (v/v) dimethyl sulfoxide (DMSO) was added in each case. The duration of the elongation step was adjusted to the size of the template and the elongation speed of the respective polymerase. To remove the template DNA, the PCR reaction was subsequently digested with 1 µL of DpnI for 1 h at 37 °C and finally transformed into Top10 competent cells (see section 2.2.2.1).

2.2.1.3 Native agarose gel electrophoresis

DNA fragments or (digested) plasmids were separated using agarose gel electrophoresis. The molecules were separated by size according to their electrophoretic mobility.[385] Separation took place in 1 % (w/v) agarose gels (agarose dissolves in 1x TBE). For detection of DNA 1x SYBR safe DNA stain (Invitrogen) was added to the gels. DNA was mixed 5:1 with 6x DNA loading dye before loading on the solidified gel. To determine the product size 100 bp or 1 kb DNA ladder (NEB) were used according to the manufacturer's instructions. Electrophoresis took place for 30 minutes at a constant voltage (100 V) in Bio-Rads horizontal gel electrophoresis apparatus. Imaging was done at 460 nm either using Chemidoc XRS Imager (Bio-Rad) or Fusion FX7 (Vilber Lourmat S.A) instruments.

2.2.1.4 Determination of DNA concentration

The concentration of DNA samples was determined using the absorbance at 260 nm in the Multiskan GO Mikrotiterplatten-Spektralphotometer (Thermo Scientific) or the NanoDrop 2000 (Thermo Scientific) with the corresponding software, ScanIt RE or NanoDrop 1000 3.7.0. For calculation of the DNA concentration, one assumed that 50 µg/mL pure double-strand DNA gives an absorbance of 1 at 260 nm.

2.2.1.5 Restriction cloning

Restriction cloning was performed, to clone a gene of interest into a plasmid backbone. Digestion of DNA with enzymes that cut double-strand DNA at specific recognition sequences was performed for the introduction of genes of interest into the respective vectors. For digestion of vector and insert DNA $\sim$ 1 µg target DNA was digested with restriction enzymes from NEB (table 6) in a 20 µL reaction according to the manufacturer's protocol for one to four hours.
Dephosphorylation of 5'-ends of the digested vectors was performed in order to prevent self-annealing of the sticky ends. Therefore the digestion reactions were mixed with

1 Unit of Fast alkaline phosphatase (Thermo Scientific). The samples were incubated for 1 hour at 37 ℃. After gel electrophoresis (see section 2.2.1.3) plasmids and inserts were purified using the QIAquick Gel Extraction Kit (Qiagen) according to the manufacturer's instructions.
Ligation of insert DNA with the dephosphorylated vector was performed using T4 DNA ligase (NEB) or homemade T4 DNA Ligase (CF Protein Production) according to the manufacturer's protocol. The composition of the ligation reaction contained 50 ng vector and five times molar excess of the insert. The reactions were incubated at room temperature (RT) for one hour. As a control, a ligation reaction without the insert was used to check for religation of the vector. Finally, the ligation product was transformed into Top10 competent cells (see section 2.2.2.1). The successful ligation was checked by colony PCR (section 2.2.2.3). Single clones were added into 4 mL of LB containing the respective selection antibiotics and grown overnight at 37 ℃ with 200 rpm agitation. The GeneJET Plasmid Miniprep Kit (Thermo Fisher Scientific) was used for the purification of plasmid DNA according to the manufacturer's instructions. Correct ligation was checked by sequencing (section 2.2.1.6). All plasmids constructed in this study can be found in table 3.

2.2.1.6 Sequencing of DNA

The required amount of DNA was mixed with the DNA sequencing primer and sent to GATC (Eurofins) or StarSEQ GmbH, for sequencing. DNA sequences were controlled using the SnapGene software.

2.2.2 Methods for working with *E.coli*

2.2.2.1 Transformation of chemical competent *E.coli* with DNA

All competent *E.coli* strains listed in section 2.1.3 were transformed in the following way. 50 µL competent cells were slowly unfrozen on ice. Then the cells were mixed with 50–200 ng DNA of interest and incubated on ice for 30–60 min. Afterwards, a heat shock at 42 ℃ for 30 s was performed. Next, the cells were recovered on ice for 2–5 minutes. For selection with Ampicillin, cells were directly plated on LB plates containing Ampicillin, while for all other antibiotic resistances 700 µL of LB medium were added and the transformation mixtures were incubated at 37 ℃ for 1 h. Finally, the cells were plated onto LB-plates containing the respective selection antibiotics and cultured overnight at 37 ℃. For better transformation efficiency with some strains, 1 µL

of a 1:10 dilution of β-mercaptoethanol was added 10 min before the DNA was put into the mixture.

2.2.2.2 Preparation of bacterial stock cultures

To freeze bacterial cells carrying the confirmed plasmid DNA, 100 µL of a bacterial overnight culture were mixed with 500 µL sterile 98 % glycerol and quickly transferred to -80 °C.

2.2.2.3 *E.coli* colony PCR

For the determination of transformation of *E.coli* with the correct ligation product, colony PCR was performed. Per reaction 0.75 µL forward primer, 0.75 µL reverse primer, 0.3 µL 10 mM dNTPs, 3 µL 5x green GoTaq buffer (Promega), 0.08 µL Homemade Taq Polymerase (CF Protein Production) and 10.12 µL nuclease free (NF) -H_2O were mixed to a total volume of 15 µL. Per reaction tube one colony was added. As a negative control, a PCR from an empty plasmid was run in parallel. The reaction was initiated by incubation for 2 min at 95 °C, followed by 30 cycles of 30 s at 95 °C, 30 s at 55 °C and 30 s at 72 °C. The final extension was done for 5 min at 72 °C. Products were analysed on an agarose gel as described in section 2.2.1.3.

2.2.3 Methods for working with yeast

2.2.3.1 Growth condition yeast

All media used in this study can be found in section 2.1.9. Yeast strains containing integrated expression constructs were grown in SC-complete media or YPD media. 2 % (w/v) Glucose was used as a carbon source, if not stated differently. Yeast strains containing episomal expression plasmid were grown in SC-media lacking the respective amino acid or containing an antibiotic for selection. All strains were grown at 30 °C at 200 rpm. Temperature-sensitive strains were grown at 25 °C to allow for the expression of the respective gene and switched to 37 °C for repression of the gene of interest.

2.2.3.2 Stocking of yeast strains

All yeast strains used in this study can be found in section 2.1.4. Yeast strains with integrated expression constructs were stored by mixing 1.2 mL of an overnight culture with 300 µL of 98 % glycerol and quickly transferring to -80 °C.

2.2.3.3 Transformation of yeast (episomal/centromeric vectors)

For transformation of yeast with episomal vectors, the respective strain was inoculated into YPD and grown overnight (o.n.) at 30 °C. In the morning the culture was diluted into the needed amount of YPD to OD_{600} 0.2 and then grown to the exponential phase (OD_{600} 0.5–0.7). Next, 1 mL yeast culture per construct was transferred into a 1.5 mL tube and harvested at 8000 rpm for 2 min at RT. The pellet was washed with 500 µL sterile ddH_2O and 200 µL SORB buffer, subsequently. Now, it was resuspended in 50 µL SORB/herring testis (HT)-single-strand DNA (45 µL SORB with 5 µL HT-single-strand DNA, HT-single-strand DNA was heated to 95 °C for 5 min and cooled on ice before usage), and 100 ng plasmid DNA were added. Before incubating the samples for 30 min at RT, 300 µL LiT/PEG buffer were added. After the addition of 38.9 µL DMSO, the cells were heat-shocked for 10 min at 42 °C. Then, they were pelleted at 4000 rpm for 2 min at RT and resuspended in 1000 µL sterile H_2O. 100–150 µL were plated on selective plates and grown for 2–4 days at 30 °C.

2.2.3.4 Transformation of yeast (integrative plasmids, PCR based tagging or knock out)

For transformation of yeast with integrative plasmids, for PCR-based tagging or knock out of specific genes, cell transformation was performed. 0.5–1 µg plasmid were digested for 2 h with a restriction enzyme that cuts in the selection marker to allow for integration into the yeast genome. For PCR-based tagging or knock out the gene of interest or knock-out cassette was amplified by PCR with primers creating a homology to the integration area. Genomic DNA from yeast was gained using MasterPureTM Yeast DNA Purification Kit according to the manufacturer's protocol.
For transformation of yeast with integrative vectors or PCR products for tagging or knockout, the respective strain was inoculated into YPD and grown o.n. at 30 °C. In the morning the culture was diluted into the needed amount of YPD to OD_{600} 0.2 and then grown to the exponential phase (OD_{600} 0.5–0.7). 5 mL yeast culture per construct was transferred into a 15 mL tube and harvested at 3000 rpm for 3 min at RT. The pellet was washed with 5 mL sterile ddH_2O and 2 mL SORB buffer, subsequently. Now,

it was resuspended in 50 µL SORB/HT-single-strand DNA (45 µL SORB with 5 µL HT-single-strand DNA, HT-single-strand DNA was heated to 95 ℃ for 5 min and cooled on ice before usage) and 500–1000 ng plasmid DNA or PCR product were added. Before incubating the samples for 30 min at RT, 6x LiT/PEG buffer were added. After the addition of 1/9 DMSO, the cells were heat shocked for 15 min at 42 ℃ in a water bath. For nutrient selection, the cells were directly plated on SC-plates lacking the respective amino acid. For antibiotic resistance, the pellet was resuspended in 1 mL YPD and incubated for 3 h at 30 ℃ with shaking. Then, cells were pelleted at 4000 rpm for 2 min at RT and resuspended in 100 µL sterile H_2O. Half of the sample was plated on a selective plate and the other half on a YPD plate. Both were grown for 2–4 days at 30 ℃. The yeast on the YPD plate were transferred to a selective plate after 2 days with the help of a cotton cloth and incubated for another 2–3 days at 30 ℃.

2.2.3.5 Yeast colony PCR

For the determination of integration of the right construct into *S. cerevisiae* a colony PCR was performed. Single colonies from the transformation were restreaked onto selective plates and incubated overnight at 30 ℃. From these plates 2–3 colonies were boiled for 15 min at 95 ℃ in 20 mM NaOH. The samples were vortexed for 1 min before insoluble debris was spun down for 1 min at 13000 rpm in RT. 25 µL of the supernatant were transferred into fresh tubes and mixed with 25 µL NF-H_2O.
Per reaction 0.5 µL forward primer, 0.5 µL reverse primer, 0.5 µL 10 mM dNTP, 5 µL 5x green GoTaq buffer (Promega), 0.25 µL Homemade Taq, 2 µL DNA and 16.45 µL NF-H_2O were mixed to a total volume of 25 µL. As a negative control, a PCR on the parental strain was run in parallel. The reaction was performed in a Professional TRIO 48 cycler (Biometra). It was initiated by incubation for 4 min at 95 ℃, followed by 35 cycles of 30 s at 95 ℃, 30 s at 55 ℃ and 1 min at 72 ℃. The final extension was performed for 5 min at 72 ℃. Products were analysed on an agarose gel as described in section 2.2.1.3.

2.2.3.6 Total cell extract from yeast

Yeast cells are lysed as follows, to analyse protein expression: Overnight cultures of the yeast strains of interest were diluted to OD_{600} 0.2 and grown to exponential phase (OD_{600} 0.5–0.7). From these cultures, 1 mL of cells was harvested by centrifugation at 16000 g for 15 min at RT. Cells were resuspended in 1 mL ice cold H_2O. Next, 150 µL ice-cold NaOH/β-mercaptoethanol mix (1.85 M NaOH+ 7.5 % (v/v) β-mercaptoethanol) were added and mixed. The samples were incubated for 15 min on ice, subsequently,

150 µL ice cold 55 % (w/v) trichloroacetic acid (TCA) was added. Samples were mixed and incubated for another 15 min on ice. Now, they were spun at 14000 rpm for 15 min at 4 °C. The supernatant was discarded. To get rid of the remaining liquid, the samples were spun again for 2 min and the leftover supernatant was removed. Pellets were resuspended in 30 µL 2x NuPage buffer. If the suspension turns yellow, 1–2 µL of 1 M Tris-HCl pH 8 were added. Finally, samples were heated for 10 min at 65 °C and analysed by SDS-PAGE (section 2.2.4.1) and Western blot (section 2.2.4.4).

2.2.3.7 Denaturing Ni^{2+}-NTA pull-down

A denaturing Ni^{2+}-Nitrilotriacetic acid (NTA) pull-down (PD) of polyhistidine (His)-tagged substrates was performed, to detect modification on substrates by ubiquitin or SUMO. For that, the strain of interest was transformed with His-ubiquitin or the substrate of interest as a His-tagged version (e.g. His-PCNA (HP30)) as described in section 2.2.3.4. The PD was performed as described in Davies and Ulrich 2012.[386]
In brief, around 10^9 cells of a yeast culture (50 mL of OD_{600} 1) were harvested by centrifugation at 3000 g for 5 min at RT. The pellet was resuspended in 5 mL of ice cold water, then 0.8 mL of NaOH/β-mercaptoethanol (1.85 M NaOH+ 7.5 % (v/v) β-mercaptoethanol) were added and the samples were incubated on ice for 20 min. Next, 0.8 mL of 55 % (w/v) TCA solution were added, followed by another incubation on ice for 20 min. Samples were centrifuged at 8000 g for 20 min at 4 °C and the supernatant was removed. To get rid of residual supernatant another centrifugation for 2 min and the removal of remaining liquid followed. Now, the pellet was resuspended in 1 mL of buffer A and incubated on a shaking platform at 250 rpm at room temperature for 1 h to solubilize the precipitate completely. Next, the samples were spun down at 16,000 g for 10 min at 4 °C and the supernatant was transferred to a fresh tube. A 20 µL aliquot of Ni^{2+}-NTA agarose (40 µL slurry) was equilibrated by washing three times with buffer A containing 0.05 % (v/v) Tween-20. The prepared cell extract was added to the tube containing the Ni^{2+}-NTA agarose beads. Then, 0.05 % (v/v) Tween-20 and 15 mM imidazole solution were added and the samples were incubated overnight at RT on a rotating wheel. On the next day, the Ni^{2+}-NTA agarose beads were spun down at 200 g for 2 min to remove the supernatant. The beads were washed twice with 1 mL of buffer A containing 0.05 % (v/v) Tween-20 and four times with 1 mL of buffer C containing 0.05 % (v/v) Tween-20. After the last wash 30 µL of 2x HU buffer were added and the samples were denatured at 65 °C for 10 min. The samples were analysed by SDS-PAGE (section 2.2.4.1) on a NuPAGE 4–12 % Bis-Tris gradient gel and by wet blotting or Turbo blotting (section 2.2.4.4, section 2.2.4.3). Each sample was loaded twice for separate detection of the substrate of interest and the modification by SUMO or ubiquitin.

For detection of ubiquitinylation of possible Pib1 substrates, the protocol was performed with double the amount of cells. All volumes were doubled accordingly.
For the detection of ubiquitination after oxidative stress treatment, 2.4 mM H_2O_2 were added to an exponentially growing culture for 45 min.
For the detection of PCNA modification, an exponentially growing culture was treated for 90–120 min with 0.03 % (v/v) MMS (for ubiquitination) or 0.3 % (v/v) MMS (for sumoylation).

2.2.3.8 Spotting of yeast cells

A spot assay was performed, to check for the viability of yeast strains and the ability to replicate under different conditions.
An exponentially growing culture was adjusted to OD_{600} 0.16 as a first dilution for the spot assay. From that four 1:5 serial dilutions were made in sterile ddH_2O in a 96 well plate. Using the Replica Plater for 96-Well Plate (Sigma-Aldrich) the dilutions were spotted on the respective plates. If more than eight strains were used, spotting was done manually using 3 µL of yeast culture for each spot. The plates were incubated for 2–4 days at the temperature of interest. Then pictures were taken from plates without lids using Epson Scan Perfection V700 Photo and the software "Epson scan" with the following settings: positive film, 8-bit grayscale, 600 dpi.

Treatments for spot assays:
NaCl: 0 M, 0.1 M, 0.5 M, 1 M, 1.25 M
MMS (v/v) : 0 %, 0.0025 %, 0.005 %, 0.01 %, 0.02 %, 0.03 %, 0,1 %, 0.3 %
H_2O_2: 0 mM, 0.05 mM, 0.1 mM, 0.5 mM, 1 mM
Ultra-violet light (UV) (254 nm): 0, 20, 50, 100 J/m^2
Temperature: 17 ℃, 30 ℃, 37 ℃, 40 ℃

2.2.3.9 Synchronisation of yeast cultures

For synchronizing cells in the G_1 phase an exponentially growing culture was treated for two hours with 10 µg/mL α-factor at 30 ℃.
For synchronizing cells in G_2/M-phase an exponentially growing culture was treated with 15 µg/mL nocodazole (containing 1 % (v/v) DMSO final concentration in culture) for two hours at 30 ℃.

2.2.3.10 Growth curve of yeast cultures

The OD_{600} of a yeast culture is followed, to monitor cell growth over a longer time period. Exponentially growing cultures were diluted into a 96 well plate to OD_{600} 0.025, or 0.0125 in 200 µL SC-complete media containing 2 µg/ mL doxycycline (dox). The cell growth was monitored using the TECAN Spark 20M multimode microplate reader at 30 ℃ for 20 h with a wavelength of 600 nM and bandwidth 3.5 nm. For evaluation, the value from a well containing only media with doxycycline was subtracted from each sample.

2.2.3.11 Cell cycle analysis by flow cytometry

For cell cycle analysis of cells expressing a construct of interest tagged with GFP, the following protocol was used. For cells without GFP expression the formaldehyde fixation step was left out and the procedure was started by permeabilisation with ethanol. From an exponentially growing culture, $1.5*10^7$ cells were taken. For storage at 4 ℃, 1 % (v/v) sodium azide was added. Cells were harvested at 7000 g for 2 min at 4 ℃. They were fixed for 10 min at RT in 2.5 % (v/v) formaldehyde (in 0.1 M potassium phosphate buffer pH 6.4). Subsequently, cells were washed two times in potassium phosphate buffer pH 6.6 (7000 g/5 min/4 ℃) and one time in potassium phosphate buffer pH 7.4. Now, cells were permeabilized in 1 mL 70 % (v/v) ethanol for 10 minutes at RT. Followed by two times washing with 50 mM citrate buffer pH 7. After the last wash, the pellet was resuspended in 1 mL citrate buffer containing 800 µg RNaseA. Samples were incubated for 1 h at 50 ℃. Again samples were washed once with citrate buffer and propidium iodide was added to a final concentration of 32 µg/mL in citrate buffer. Before cell cycle analysis, samples were sonicated (Branson Sonifier, 3 mm tip, output control 1, duty cycle 10 %, 10 s). Finally, they were analysed on the LSRFortessa SORP (BD Biosciences) device equipped with the BD FACSDIVA software. The evaluation was done using the FlowJo v10 software (FlowJo, LLC). The following gating strategy was applied: First I gated for cells (FSC-A to SSC-A), and then for GFP expression (SSC-A to BL488nm530/30-A). GFP positive or negative cells were further gated separately for single cells (YG561nm610/20-A to YG561nm610/20-W) and finally, their DNA content was analysed (YG561nm610/20-A to event count).

2.2.3.12 Live-cell imaging

To monitor living yeast under the microscope 200 µL of culture in the exponential growth phase or synchronized (section 2.2.3.9) were plated into a concanavalin A coated

chambered coverslip with a glass-bottom (Ibidi), washed three times with media, and released into fresh prewarmed SC-medium (30 ℃) containing if needed doxycycline or the stated drug for treatment. Imaging took place at different time points in an environmental control chamber at 30 ℃.
The imaging was done using a wide-field DeltaVision Elite system (GE Healthcare) equipped with a 60x oil immersion objective (NA 1.42), InsightSSITM solid-state illumination, Scientific CMOS camera, SoftWoRxTM software, and a built-in deconvolution algorithm. Z stacks with 21 steps (step size 0.2 mm) were acquired for each image. Fluorescent dyes were imaged with their optimised filters. Differential interference contrast (DIC) was used for whole-cell images. The built-in deconvolution algorithm from SoftWoRxTM was used to reconstruct images. Images of cells were taken at the indicated time points.

2.2.3.13 Fixation and DAPI staining for microscopy

Staining of the DNA with 4',6-diamidino-2-phenylindole (DAPI) was performed, to be able to detect the nucleus in the microscope. DAPI is a fluorescence stain, whose intensity is enriched when it is bound to adenine–thymine-rich regions in double-strand DNA. For fixation and DAPI staining of yeast cells, 1 mL of a logarithmic growing culture was harvested by centrifuging at 8000 g for 1 min. Cells were resuspended in 2.5 % (v/v) formaldehyde in 0.1 M potassium phosphate buffer pH 6.4. Samples were fixed for 10 min at RT, washed two times with potassium phosphate pH 6.6 and one time in potassium phosphate pH 7.4. The cells were resuspended in 500 µL of 70 % (v/v) ethanol and permeabilized for 10 min at RT. Samples were washed once with citrate buffer and resuspended in 20 µL of citrate buffer. 3 µL of cells were mixed with DAPI solution (1:10000 of a 0.1 mg/mL solution) on a slide, covered immediately with a coverslip and imaged as described in section 2.2.3.12.

2.2.3.14 Immunofluorescence

To be able to stain different proteins of interest for microscopy, an exponentially growing yeast culture was mixed with 0.1 volumes of a 37 % (v/v) formaldehyde solution and incubated for 15–20 min at RT. 10 mL were harvested and resuspended in a potassium phosphate buffer pH 6.4 containing 3.7 % formaldehyde and incubated for 15 min at RT. Now, cells were washed three times with 0.1 M potassium phosphate buffer pH 6.4 and one time with spheroblasting buffer. Samples were resuspended in spheroblasting buffer and 1:500 β-mercaptoethanol was added and incubated for 15 min at 30 ℃. Now, 50 µL of a 1 mg/mL Zymolase T100 were added and samples were incubated for 10–20 min at

30 °C. Cells were carefully washed with spheroblasting buffer and resuspended in 200 µL of it. Successful spheroblasting was checked by incubating 10 µL of cells in a 1 % (v/v) SDS solution and observing the drop in OD_{600}. 15 µL of spheroplasts were immobilised on a poly-Lysine (0.1 % (w/v)) coated slide for 15 min. Slides were fixed in ice-cold methanol for 3 min and in ice-cold acetone for 10 s. After drying off the liquid, slides were incubated for 30 min in a wet chamber with BSA solution in PBS. Now, the first antibody in a BSA/PBS solution was added for one hour in the wet chamber. After washing four times with BSA/PBS solution, samples were incubated for one hour in the wet chamber with the secondary antibody. After washing off the excess antibody, DAPI (1:10000 of a 0.1 mg/mL solution) was added for 15 min. After the addition of Prolong Diamant mounting media, samples were sealed with coverslips. Samples were kept at 4 °C in the dark until imaging. Imaging was performed as described in section 2.2.3.12.

2.2.3.15 Autophagy assay

The following assay with GFP-Atg8 as a test substrate was performed, to analyse, if a protein of interest is involved in autophagy. A logarithmic growing yeast culture expressing GFP-Atg8 and harbouring a deletion in the protein of interest was treated with 100 nM Rapamycin for 3 h. Proteins were extracted as described under section 2.2.3.6 and analysed by Western blot section 2.2.4.4 for the presence or absence of GFP-Atg8.

2.2.3.16 Mating of yeast cells

For mating of two haploid strains with opposite mating types, 15 µL overnight cultures were mixed on YPD agar plates and incubated for 5 h at 30 °C. Some cells were transferred in 15 µL sterile water on a small part of a fresh YPD plate. Then, zygotes were picked up using the MSM micromanipulator (Singer) and transferred to YPD plates and incubated for 2–3 days at 30 °C. The resulting colonies were streaked on selective agar plates to ensure proper isolation of diploids.

2.2.3.17 Sporulation of diploid yeast

For creating haploid strains from diploid parental strains, sporulation was performed by growing diploids overnight in liquid YPD media. 500 µL of the overnight culture were washed five times with sterile water and once with the sporulation media (1 % (w/v) KOAc). Cells were resuspended in 2 mL of sporulation media and incubated for 4 days at 25 °C.

For induction of synchronous sporulation of the SK1 yeast strain, 2 mL of liquid SC-complete media were inoculated with 5 colonies. Cultures were incubated for 24–26 h at 30 °C. Approximately 16–18 h before the desired time of meiosis induction, 20 mL of pre-sporulation media were inoculated with the culture to an OD_{600} of 0.01 (1/200 dilution). According to the auxotrophic needs of the strain amino acids and 0.5 µg/mL doxycycline for DARPin induction were added. Cultures were incubated at 200–300 rpm overnight at 30 °C. When the OD_{600} reached 0.9–1.2, the cells were harvested by centrifuging at 3000 g for 3 min at room temperature. The pellet was washed once with one volume of prewarmed (30 °C) sporulation media and resuspended in the same volume of sporulation media as the pre-culture. Again doxycycline and amino acids were supplemented. The sporulation cultures were incubated at 30 °C for 24 h and samples at the time points of interest were collected, including one at t 0 min.

2.2.4 Methods for protein analysis

2.2.4.1 Sodium dodecyl sulfate polyacrylamide gel electrophoresis (SDS-PAGE)

An SDS-PAGE was performed to separate the proteins from a sample, according to their electrophoretic mobility in a gel. Before loading, samples were mixed with NuPAGE LDS loading dye (Invitrogen) or HU buffer containing 100 µM DTT. Samples were boiled at 65 °C for 15 min or 95 °C for 5 min dependent on the type of analysis (65 °C were used for whole-cell extracts from yeast and for membrane proteins, for all other applications 95 °C were applied). They were run on 4–15 % Criterion TGX Stain-Free Protein Gel (Bio-Rad Laboratories) in 1x SDS buffer, a NuPAGE 4–12 % BT gels (Invitrogen) in 1x MOPS or 1x MES buffer or on RunBlue SDS Gel 4–12 % (Expedeon) in 1x RunBlue Rapid SDS buffer. The gels were used in Criterion™ Vertical Electrophoresis, Cell (Bio-Rad), X-Cell SureLock Mini-Cells Samples (Invitrogen) or Mini-PROTEAN system (Bio-Rad). Samples were resolved at a constant voltage of 200 V, 160 V or 150 V, respectively until the loading dye reached the bottom of the gel. For size estimation, the pre-stained PageRuler (Thermo Scientific) was loaded.

2.2.4.2 Protein visualisation in gels

For staining of proteins after SDS-PAGE the gels were incubated for 30–60 minutes in 10 mL InstantBlue (Expedeon) with shaking. Destaining was done by overnight incubation in ddH_2O.

2.2.4.3 Western blot (WB) by wet blotting

The Western blot method (immunoblotting) was used to detect a specific protein after the resolution of a sample using SDS-PAGE.
Therefore, the gel, the membrane and the Whatman papers were equilibrated for 5 to 10 minutes in transfer buffer. A sponge, a Whatman filter paper, the gel, the nitrocellulose membrane (Invitrogen), again a filter paper and finally a sponge were put into a blotting frame. All things need to be properly wetted in transfer buffer and no air bubbles should be present between the layers, to allow a uniform transfer of the proteins. The frame was placed vertically in a Mini Trans-Blot cell (Bio-Rad). The blotting took place at 100 V for 60 min at 4 ℃. Then the membrane was blocked in 5 % (w/v) milk in PBS-T for 30–60 minutes while shaking. The primary antibody solution that recognizes the antigen in the protein of interest was prepared in a dilution according to the manufacturer's recommendation in 5–15 mL 5 % (w/v) milk in PBS-T. The membranes were covered with the primary antibody solution and incubated for 1–2 h at RT or overnight a 4 ℃. After incubation, the membranes were washed three times for 5 min in PBS-T. Then a 1:10000 dilution of secondary antibody conjugated either to HRP or a fluorescence probe in PBS-T was added and incubated for 30 min with shaking at room temperature. Afterwards, the excess antibody was washed off by incubation of the membrane three times 5 min in PBS-T. The membranes were developed using Amersham ECL Select or Prime Western Blotting Detection Reagents (GE Healthcare) following the manufacturer's instructions and imaged on a Chemidoc XRS (Bio-Rad) or Fusion FX (Vilber Lourmat S.A) System or by directly detecting fluorescence using the Odyssey CLx Imaging System (LI-COR). All antibodies used in this study can be found section 2.1.6.

2.2.4.4 Western blot (WB) using the TransBlot Turbo system (BioRad)

For faster blotting of proteins after SDS-PAGE they were blotted onto a nitrocellulose membrane (Bio-Rad) by using the Trans-Blot Turbo System (Bio-Rad) according to the manufacturer's instruction. For that, either the Trans-Blot Turbo RTA Mini Nitrocellulose Transfer Kit (Bio-Rad) or the Trans-Blot Turbo RTA Midi Nitrocellulose Transfer Kit (Bio-Rad) was used. 4–15 % Criterion TGX Stain-Free Protein Gels (26 wells) were run with the pre-installed program for high or mixed molecular weight proteins (Midi gels), NuPAGE 4-12 % BT gels were transferred at 25 V (1.3 A) for 12 min. The membranes were developed as described in section 2.2.4.3.

2.2.4.5 Stripping of nitrocellulose membranes

The signal from the first antibody was removed using highly denaturing conditions, in order to develop a Western blot membrane against a second primary antibody of the same species
The membrane was incubated for 40 minutes in 20 mL stripping buffer at 50 °C. Afterwards, it was washed six times for 5 minutes in PBS-T. After blocking for 30 minutes in 5 % (w/v) milk in PBS-T, the membrane can be developed anew with a different antibody (as described in section 2.2.4.3).

2.2.4.6 Determination of protein concentrations

For determination of the protein concentration a Bradford assay was performed (Bradford Protein Assay kit, BioRad) or the Nanodrop2000 spectrophotometer (ThermoScientific) was used.
For protein concentration determination by Bradford, a standard curve was preprepared using increasing concentrations (0–12 µg) of BSA. The standards were filled up to 800 µL with ddH_2O and 200 µL BioRad kit solution was added. A fraction of the samples, in which the protein concentration should be determined were filled up to 800 µL and mixed with 200 µL BioRad Protein Assay Dye Reagent Concentrate solution. All tubes were incubated for 30 minutes at RT and the absorption at 595 nm wavelength was measured using the Eppendorf Biophotometer or the TECAN Spark 20M multimode microplate reader.
The OD_{280} of purified proteins was measured with a Nanodrop2000 spectrophotometer (Thermo Scientific). Their extinction coefficients (ϵ) were calculated using the ExPASy ProtParam online tool. The concentration of proteins were calculated according to Beer-Lamberts law ($Concentration = \frac{OD_{280}}{pathlength \cdot \epsilon}$) using the provided software NanoDrop 1000 3.7.0.

2.2.5 Protein purification

2.2.5.1 Cleavage of tags by proteases

Proteins harbouring a Thrombin cleavage site between the protein of interest and the tag were cleaved for 4 h at RT in Thrombin cleavage buffer using 10 U of Thrombin per 5 mg protein.

Proteins harbouring a TEV cleavage site were cleaved with 2 µg TEV-Protease per 5 mg protein for 3 h at 16 °C in TEV cleavage buffer.

Proteins harbouring a PreScission 3C cleavage site were cleaved overnight at 4 °C with 100 µg of PreScission for 5 mg protein in the respective buffer.

Proteases were removed by gel filtration.

2.2.5.2 Purification of biotinylated proteins for BIACORE analysis

Biotinylated proteins were expressed in the *E.coli* Rosetta pLysS strain by co-transformation of the plasmid for the expression of the protein of interest with a plasmid for the expression of BirA following a protocol from the Plückthun lab in Zurich. Shortly summarized, a 10 mL overnight culture was grown in LB media supplemented with the appropriate antibiotics at 37 °C. In the morning the overnight culture was diluted to an OD_{600} of 0.1 in LB media with 100 µg/mL of selection antibiotics, and cultures were incubated at 250 rpm at 37 °C until their OD_{600} reaches 0.7–0.8. Then 10 mL of 5 mM biotin solution (50 µM final) were added. The biotin solution was prepared by mixing 12 mg of d-biotin with 10 mL of warm 10 mM bicine buffer (pH 8.3) and filter-sterilizing the solution with a 0.2-micron filter. Protein expression was induced at the same time by the addition of 50 µM Isopropyl-β-D-thiogalactopyranosid (IPTG). The expression took place for 6 h at 30 °C.
After collection of the cells, they were resuspended in 20 mL lysis buffer per 1L culture (section 2.1.10.3). Cells were disrupted by sonication on ice (Branson sonifier 5 mm tip, 2 min, output control: 4–5, duty cycle: 50 %) and SIGMAFAST Protease Inhibitor Cocktail was added. To clarify the lysate centrifugation at 18400 rpm for 30 min at 4 °C was performed. The lysate was incubated with 750 µL of Ni^{2+}-NTA agarose for 120 min on a roller at 4 °C. Next, the beads were washed three times with 30 mL lysis buffer (1000g/2 min/4 °C). The protein of interest was eluted with five times 1 mL elution buffer (section 2.1.10.3) containing 500 mM imidazole (1000g/2 min/4 °C). In each elution step, the samples were incubated in elution buffer for 2 min. The elution fraction were analysed by SDS-PAGE (section 2.2.4.1) and Coomassie staining (section 2.2.4.2). The fractions containing the protein of interest were pooled and concentrated to 0.5 mL. These were loaded onto a gel filtration column (S75 10/300 GL, 0.5 mL/min) in HBS-EP buffer (section 2.1.10.3). Fractions were again analysed by SDS-PAGE (section 2.2.4.1) and Coomassie staining (section 2.2.4.2) and relevant fractions were pooled, concentrated if necessary with Vivaspin concentrators (Thermo Fisher Scientific) and stored at -80 °C.

The degree of biotinylation was analysed by performing a streptavidin shift assay with the purified protein. For that, 0.2 to 5 µg of protein were incubated in 1x SDS loading buffer for 10 minutes at 95 °C. The samples were cooled to room temperature and 1 µL of streptavidin solution (1 mg/mL in PBS) was added. Samples were incubated for 30 min at room temperature and analysed by SDS-PAGE. Biotinylation was quantified by comparing bands of the control (only protein) with streptavidin-containing samples using the Image-J software.

2.2.5.3 Purification of DARPins

His-tagged DARPin constructs were expressed in BL21 DE3 competent *E.coli* cells. Induction was done by the addition of 0.75 mM IPTG. The expression took place for 4 h at 37 °C. Lysis was done by sonification on ice (Branson sonifier 5 mm tip, 2 min, output control: 4–5, duty cycle: 50 %). After clearing the lysate, it was incubated for 3 h with 1 mL of Ni^{2+}-NTA agarose beads slurry per 1 L culture. Elution took place with five times 1 mL elution buffer containing 500 mM imidazole. The final purification was performed by gel filtration (S75 10/300 GL, 0.5 mL/min) in the buffer that was used for downstream application. Proteins were stored at -80 °C.

2.2.5.4 Purification of RNF4

His-MBP-RNF4 (from rat) was purified similar to the procedure described in Plechanovová A, *et al.* (2011).[264]
Expression was performed using *E.coli* Rosetta (DE3) cells at 20 °C overnight after induction with 0.1 mM IPTG at an OD_{600} of 0.6–0.8. Cells were lysed by sonication on ice (Branson sonifier 5 mm tip, 2 min, output control: 4–5, duty cycle: 50 %). After clarifying the lysate, 500 µL Ni^{2+}-NTA beads (per 500 mL culture) were added and incubated for 2 h at 4 °C. Elution was done with five times 750 µL elution buffer by incubation for 4 min in each elution step. RNF4 was further purified by gel filtration chromatography (S75 10/300 GL, 0.5 mL/min) and stored at -80 °C.

2.2.5.5 Purification of untagged SUMO

The SUMO construct for crystallisation (SUMO-aa20–aa98) was purified from BL21 Codon Plus *E.coli* cells. Expression was induced by the addition of 0.2 mM IPTG and took place at 37 °C for 4 h. Lysis was performed by sonification on ice (Branson sonifier 8 mm tip, 2 min, output control: 4–5, duty cycle: 50 %). After filtering the

cleared lysate through a 0.45 µM filter, it was loaded onto an anion exchange column (HiTrap™ Q, 5 mL) equilibrated in buffer A + 40 mM NaCl (lysis buffer). Elution was done with a linear gradient of NaCl (100–700 mM in steps of 20, 40, 60, 100 %). SUMO eluted at ∼ 20 % (v/v) buffer B. The relevant fractions were pooled and the buffer was exchanged to buffer A + 40 mM NaCl. The protein was then applied to a cation exchange column (HiTrap™ SP) equilibrated in buffer A + 40 mM NaCl. SUMO eluted in the flow-through (FT). Finally, a gel filtration step (S75 Increase 10/300 GL, 0.4 mL/min) was performed and the purified protein was stored at -80 ℃.

2.2.5.6 Purification of Ubc9 and Ubc9-K153R

Ubc9 and Ubc9-K153R were purified as described in Parker J.L., Ulrich H.D. (*In Vitro* PCNA Modification Assays, 2012).[130] In short, Ubc9 constructs were expressed in BL21 Codon Plus *E.coli* cells. Expression was induced by the addition of 0.2 mM IPTG and took place at 37 ℃ for 4 h. Cells were lysed by sonification and incubated with 2.5 mL of Ni^{2+}-NTA agarose beads per 1L culture for 60 min at 4 ℃. Elution was done six times with 1.5 mL elution buffer supplemented with 300 mM imidazole. Relevant fractions were further purified by gel filtration (S75 Increase 10/300 GL, 0.4 mL/min) and stored at -80 ℃.

2.2.5.7 Purification of dimeric SUMO E1

Purification of the dimeric SUMO E1 His-Aos1/Uba2 Complex was performed as described by Werner *et al.* (2009).[387] Plasmids for expression of His-Aos1 and Uba2 were transformed simultaneously into *E.coli* strain BL21(DE3). Expression took place in 2 L of LB medium supplemented with 50 µg/mL ampicillin, 30 µg/mL kanamycin, 1 mM $MgCl_2$ and 0.1 % (w/v) glucose and was induce at an OD_{600} of 0.6 by adding 0.1 mM IPTG. Proteins were expressed for 5 h at 25 ℃. Lysis was performed in lysis buffer containing SIGMAFAST Protease Inhibitor Cocktail and 1 mM β-mercaptoethanol, by passing cells for two passages over a high-pressure cell disruption system (1.8 mPa, 2 rounds, 4 ℃). The cleared supernatant was applied to 2 mL Ni^{2+}-NTA agarose beads and incubated for 90 min at 4 ℃. Proteins were eluted with five times 2 mL of elution buffer. Concentrated, protein-containing fractions were subject to gel filtration (S200 Increase 10/300 GL, 0.5mL/min). Next, protein-containing fractions were loaded onto an anion exchange column (Mono Q 10/100 GL) equilibrated in GF buffer and eluted using a linear gradient (20 column volumes) of 50 to 500 mM NaCl in GF buffer. Finally, protein-containing fractions were dialysed (PD 10 column) against storage buffer, flash-frozen in small aliquots in liquid nitrogen and stored at -80 ℃.

2.2.5.8 YFP-SUMO and CFP-GAPtail Purification

FRET substrates were purified according to Stankovic-Valentin *et al.* (2009).[334] In short, expression took place using the *E.coli* Codon Plus strain in 2 L of LB with ampicillin, 1 mM $MgCl_2$, and 0.1 % (w/v) glucose. Protein expression was induced with 0.4 mM IPTG and took place for 5 h at 20 ℃. Cells were lysed by sonication (Branson sonifier 5 mm tip, 2 min, output control: 4–5, duty cycle: 50 %) in lysis buffer. The clear supernatant was added to 5 mL Ni^{2+}-NTA agarose beads for 2 h. Proteins were eluted with four times 4 mL elution buffer with incubation of each fraction for 4 min. The cleanest fractions were loaded onto a preparative gel filtration column and equilibrated with storage buffer (S75 Increase 10/300 GL, 0.5 mL/min). Cleanest fractions were pooled and concentrated down to 1 mg/mL and flash-frozen in small aliquots in liquid nitrogen and stored at -80 ℃.

2.2.5.9 Purification of Spc24/Spc25 constructs

His-Spc24-full-length (-FL)/His-Spc25-FL, His-Spc24-glob/His-Spc25-C-terminal domain (CTD) and His-Spc24-glob/His-Spc25-glob were purified by double transfection of both constructs into BL21 DE3 *E.coli* strain. After induction at OD_{600} 0.5–0.8 with 0.75 mM IPTG, protein expression took place overnight at 20 ℃.
Cells were lysed by sonification (Branson sonifier 5 mm tip, 2 min, output control: 4–5, duty cycle: 50 %) and incubated with 750 µL of Ni^{2+}-NTA agarose per 1 L culture for 2 h at 4 ℃. After washing, elution was done with six times 1 mL elution buffer supplemented with 500 mM imidazole. Relevant fractions were further purified by gel filtration (S75 10/300 GL, 0.6 mL/min or S200 Increase 0.5 mL/min) and stored at -80 ℃.

Spc24/Spc25-Glutathione S-transferases (GST) constructs were purified in the same way as His-tagged constructs. Only that instead of Ni^{2+}-NTA beads, Glutathione (GSH) beads were added and incubation was prolonged to 3 h. Elution took place with five times 1 mL GSH elution buffer.

2.2.5.10 Purification of ubiquitin variants

Expression was performed using BL21 DE3 *E.coli* cells at 37 ℃ for 4 h after induction with 1 mM IPTG at an OD_{600} of 0.6–0.8. Cells were lysed by sonication (Branson sonifier 5 mm tip, 2 min, output control: 4–5, duty cycle: 50 %). To the clarified lysate 750 µL Ni^{2+}-NTA beads were added and samples were incubated for 2 h at 4 ℃. After

5 washes, elution was done with five times 750 µL elution buffer for 4 min in each step. Ubiquitin variants were further purified by gel filtration chromatography (S75 10/300 GL, 0.5 mL/min), aliquoted and stored at -80 °C.

GST-tagged constructs were purified in the same way as His-tagged constructs. Only that instead of Ni^{2+}-NTA beads, GSH beads were added and the incubation was prolonged to 3 h. Elution took place with five times 1 mL GSH elution buffer.

2.2.5.11 Purification of ^{15}N-labelled protein

Cells from an overnight culture of the respective *E.coli* strains carrying the plasmid of interest were harvested and transferred into 30 mL ^{15}N-M9-media. Cells were grown at 37 °C for 14 h and then added into 1 L ^{15}N-M9-media. Expression and purification took place as described in the respective purification section of the protein of interest.

2.2.5.12 Purification of Snc1-His, Snc1-1–93-His, Snc1-K8R-His, Snc1-K8R-1–93-His

Snc1 constructs were purified as described in McNew *et al.* (2000).[388]
The Snc1 constructs were expressed in the BL21 DE3 *E.coli* strain. Protein expression was induced with 0.3 mM IPTG for 4 h at 37 °C. Cells were resuspended in 25 mL lysis buffer. Cells were opened using a high-pressure cell disruption system (1.8 mPa, 2 rounds, 4 °C). Now, 2 mM β-mercaptoethanol, SIGMAFAST Protease Inhibitor Cocktail and 4 % (v/v) Triton X100 were added and samples were incubated for 1 h at 4 °C rotating. After clearing the supernatant, it was incubated with 500 µL Ni^{2+}-NTA agarose beads overnight. The beads were washed two times with TX-100 wash buffer, and three times with OG wash buffer. The protein was eluted with three times 1 mL elution buffer (5 min incubation in each step). Proteins were further purified by gel filtration chromatography (S75 10/300 GL, 0.5 mL/min), aliquoted and stored at -80 °C.

2.2.6 Biochemical assays

2.2.6.1 E1-Thioester formation

In order to analyse the thioester formation between SUMO and the E1 enzyme in the presence of the DARPins the following assay was performed: 5 µM SUMO and 25 µM

DARPin were pre-incubated on ice for 10 min. Then, 500 nM E1 (Aos1/Uba2) and 1 mM ATP were added in 1x MAB. The reaction was incubated at 30 ℃. Samples were taken after 0, 5 min and 15 min. HU buffer without reducing agent was added to stop the reaction. Samples were not boiled, before being analysed by SDS-PAGE (section 2.2.4.1) and Coomassie staining (section 2.2.4.2).
Quantification was done using the Image Studio software. The relative E1 thioester signal was calculated by dividing the thioester signal band by the amount of total E1 (thioester plus free E1). All values were normalized to the value of a sample treated with reducing agent. The mean and standard deviation of three to six independent experiments was calculated.

2.2.6.2 E2 Thioester formation

The following assay was performed, to analyse the thioester formation between SUMO and the E2 enzyme in the presence of the DARPins. 5 µM SUMO-3R, 500 nM E1 (Aos1/Uba2) and 1 mM ATP were pre-incubated in MAB for 15 min at 30 ℃. Then 25 µM DARPin was added and the samples were incubated for 10 min at 30 ℃. 750 nM Ubc9-K153R were added and the reaction was incubated at 30 ℃. Samples were taken after 0, 5 min and 10 min. HU buffer without reducing agent was added to stop the reaction. Samples were not boiled before being analysed by SDS-PAGE (section 2.2.4.1) and Coomassie staining (section 2.2.4.2).

2.2.6.3 Free SUMO chain formation

In order to analyse SUMO chain formation in the presence of the DARPins, the following assay was performed: 1 mM ATP, 50 nM E2 (Ubc9-K153R), 1 µM SUMO, 5 µM DARPin and if needed 50 nM E3 (Siz1) were mixed in 40 µL 1x MAB reaction buffer and incubated for 10 min on ice. The chain formation reaction was then started by the addition of 100 nM E1 (Aos1/UBA2) and transferring the tube to 30 ℃. Samples were taken after 0, 5, 15 and 45 min and the reaction was stopped by the addition of SDS loading dye and boiling at 95 ℃ for 5 min. The reaction products were analysed by SDS-PAGE (section 2.2.4.1) and Western blot (section 2.2.4.4) using an anti-SUMO antibody. For reactions without an E3, the E3 was replaced by water. A control without E1 addition was run in parallel.

2.2.6.4 Sumoylation of PCNA *in vitro*

For *in vitro* sumoylation of PCNA, 1 µM SUMO was pre-incubated with 3 µM DARPin in 1x MAB reaction buffer on ice for 10 min. Now, 2.5 nM nicked plasmid DNA (pBluescript SK+), 30 nM RFC, 1 mM ATP, 50 nM PCNA, 100 nM E1 (SAE1/UBA2), 50 nM E2 (Ubc9-K153R) and 25 nM E3 (Siz1) were added. The reaction was incubated for 1 h at 30 °C and stopped by the addition of loading dye. The reaction products were analysed by SDS-PAGE (section 2.2.4.1) and Western blot (section 2.2.4.4) using an anti-PCNA and an anti-SUMO antibody.

2.2.6.5 Ulp1 cleavage assay

The following assay was performed, to analyse SUMO cleavage in the presence of the DARPins. 4 µM His-Cys-SUMO-eGFP was pre-incubated with a five-fold molar excess of a DARPin for 10 min at 4 °C. Then 50 nM Ulp1 protease were added and the reaction was incubated at 20 °C. Samples were taken after 1, 2 and 5 min. The reaction was stopped by the addition of SDS loading dye and boiling at 95 °C for 5 min. Reaction products were analysed by SDS-PAGE (section 2.2.4.1) and Coomassie staining (section 2.2.4.2).
Quantification was done using the Image Studio software. The activity of cleavage was calculated by dividing the signal from the uncleaved construct by the signal from the cleavaged product. The values were normalized to the value at 0 min and the mean and standard deviation of three experiments was calculated.

2.2.6.6 FRET-based sumoylation assay

A FRET-based sumoylation assay was performed according to Stankovic-Valentin *et al.* (2009), in order to analyse the sumoylation of a purified substrate in the presence of DARPins.[334] A master mix that contains 10 nM E1 enzyme, 10 nM E2 (Ubc9-K153R), 100 nM eCFP-GAPtail, 100 nM YFP-SUMO-3R and 0.2 mg/mL BSA in FRET buffer was prepared. It was distributed to a 364 well plate and preincubated for 10 min at 20 °C with 100 nM DARPin. To start the reaction 1 mM ATP was added to all, but one reaction. Measurement took place for 20 min at 20 °C in the Tecan Spark plate reader using the 430 nM filter for excitation of CFP and 485 nm and 535 nm for recording emission of CFP and YFP respectively. Fluorescence was recorded every 30 s. Analysis was done using the Graphpad Prism software by dividing the YFP by the CFP fluorescence signal, normalizing them to the values at t 0 min and correcting the baseline to the reaction without ATP. Analysed is the mean of three to five experiments.

2.2.7 Analysis of protein-protein interactions

2.2.7.1 Pull-down of ubiquitin and ubiquitin variants with Spc24/25

A pull-down assay was performed, to analyse the interaction between ubiquitin or ubiquitin variants and Spc24/25. 10 µM Spc24/25 constructs were immobilized on 15 µL GSH bead slurry in maintenance buffer containing 0.1 % (v/v) Triton X100. Next, beads were blocked with BSA. After washing, 10 µM of ubiquitin or the ubiquitin variant were added for 1 h at 4 °C. After washing the beads again, bound proteins were eluted by boiling in NuPAGE buffer at 95 °C. Analysis of pulled-out proteins was performed by Western blot to detect ubiquitin or the ubiquitin variants.

2.2.7.2 Pull-down of Spc24/25 constructs by ubiquitin or ubiquitin variants

A pull-down assay was performed, to analyse the interaction between ubiquitin or the ubiquitin variants and Spc24/25. 10 µM ubiquitin variants were immobilized on 25 µL equilibrated anti-FLAG beads or GSH-beads for 1 h at 4 °C in maintenance buffer. Beads were blocked with BSA, before 10 µM Spc24/25 constructs were added and incubated for 2 h at 4 °C. Afterwards, the excess protein was washed off three times with maintenance buffer containing 0.1 % (v/v) Triton X100. Elution was performed by boiling the samples for 5 min at 95 °C. Analysis of the eluted fraction was done by Western blot.

2.2.7.3 Pull-down of RNF4 by SUMO in the presence of DARPins

In order to analyse the interaction between SUMO and the SIM-containing protein RNF4 in the presence of DARPins, the following PD was performed. 15 µL slurry of Streptavidin Agarose beads per sample were equilibrated with 3x 500 µL 1x Pull-down buffer. Then, 100 µL of 2.5 µM SUMO per sample was added and incubated for 60–90 min at 4 °C on a rotation wheel. The samples were washed with 3 x 500 µL PD-buffer, before 500 µL of 1:10 BSA (from 10 mg/mL stock) per sample were added. The samples were incubated for 30 min at 4 °C on the rotation wheel, and again washed three times with 500 µL PD-buffer. Next, 200 µL 50 µM DARPin per sample were added followed by an incubation of 30 min at 4 °C on the rotation wheel. Now, 5 µM RNF4 was added and the samples were incubated for another 60–90 min at 4 °C on the rotation wheel. Again samples were washed three times with 500 µL PD-buffer and bound proteins were eluted by the addition of 15 µL 1x NuPage loading dye and boiling of the samples at 95 °C for 5 min. The whole elution and 5 % input (purified RNF4) were analysed by

SDS-PAGE (section 2.2.4.1) and Western blot (section 2.2.4.4) with anti-RNF4 (goat, 1:1000,on 4 ℃) and anti-His tag (1:5000, mouse) antibodies.
The PD of RNF4 by SUMO was quantified with Image studio using the rectangle shape including the RNF4 band and the degradation products directly below. The band in the empty beads sample was quantified as background. The background band was subtracted from the total signal in the PD and the resulting signal was divided by the signal from the control DARPin E3.5. The mean and standard deviation (SD) from three independent experiments were blotted.

2.2.7.4 Pull-down from yeast extract

The following pull-down was performed, to analyse, if SUMO gets pulled out from yeast cell extract by DARPins. 1 L yeast culture of OD_{600} 1 was harvested at 5000 g for 15 min at RT, washed with 25 mL lysis buffer and finally resuspended in 20–25 mL lysis buffer. Cells were opened using a high-pressure cell disruption system (35000 psi, 3 rounds, 4 ℃). After the addition of SIGMAFAST Protease Inhibitor Cocktail and 10 mM NEM, samples were spun at 300 g for 5 min at 4 ℃. Now, 0.5 % (v/v) Igepal and 0.25 % (v/v) Triton X100 were added to the supernatant. Samples were incubated for 1 h at 4 ℃ rolling, spun down at 20000 g for 30 min at 4 ℃ and the protein concentration was determined as described in section 2.2.4.6. The extract was stored at -80 ℃ until usage.
15 µL equilibrated Ni^{2+}-NTA Agarose beads slurry was pre-incubated with 100 µL of 5 µM DARPin for 60–90 min at 4 ℃ on the rotation wheel. Beads were washed three times with 500 µL PD-buffer and blocked for 30 min at 4 ℃ with 500 µL of 1:10 BSA (from 10 mg/mL stock). After three more washing steps, 10 mg yeast extract were added and incubated for 90 min (or overnight) at 4 ℃. The samples were washed three times and the bound protein fraction was eluted by the addition of 15 µL 1xLDS, and boiling at 95 ℃ for 5 min. Elution, input and FT were analysed by SDS-PAGE (section 2.2.4.1) and Western blot (section 2.2.4.4) using an anti-SUMO antibody (1:10000, rabbit).

2.2.7.5 Affinity and kinetic analysis using surface plasmon resonance

For interaction, affinity and kinetic analysis surface plasmon resonance measurements using the BIACORE X100 (GE Healthcare) were performed.
For interaction and affinity determination 200–500 RU of biotinylated SUMO or SUMO mutants were immobilised on a streptavidin-coated chip using the Biotin capture kit (GE Healthcare). For kinetic analysis 50–100 RU of biotinylated SUMO or SUMO mutants were immobilised on the streptavidin-coated chip. If not indicated differently, binding,

dissociation, and regeneration took place for 120 s and capture was performed for 180 s. The concentrations of the analyte varied, dependent on its interaction strength. Analysis was performed using the Biacore Evaluation Software (GE Healthcare).

2.2.7.6 Protein labelling and fluorescence polarisation assay (FP-assay)

The ubiquitin variant constructs for A12 and A15, coding for a cysteine in front of the protein, were expressed, purified, and labelled with the Bodipy TMR C5 fluorescent dye (Thermo Fisher Scientific). For that, the dye was diluted to 2 mM in DMSO and then further diluted in ddH_2O to 500 µM. Cysteines in the proteins were reduced using 1 mM TCEP. For the maleimide reaction, 200 µM dye were mixed with 50 µM protein and incubated for 2 h at RT in the dark. The reaction was stopped by the addition of 10 mM DTT. Excess dye was removed by running the sample over two NAP5 columns into a buffer containing 50 mM Tris-HCL and 100 mM NaCl. Purity and labelling efficiency was analysed by SDS-PAGE (section 2.2.4.1) and imaging using the Typhoon FLA9500 scanner (GE Healthcare).
Before running the assay, the labelled protein was tested for the smallest possible concentration with which stable tumbling was observed. This was done by analysing a concentration range of the labelled protein in the Tecan Spark fluorescence plate reader using the specific excitation (535 nM) and emission (595 nm) wavelength of the dye and the following settings: gain 60–100, flashes 30, G-factor 1, mirror automatic, settle time 300 s, Z-position 19200.
For the FP-assay, a 1:2 dilution series of Spc24/25-FL was added into a 96-well plate with a start concentration of 250 µM. To check binding, 40 nM of the labelled ubiquitin variant A12 or 64 nM of the ubiquitin variant A15 were added in a total volume of 20 µL, filled up with maintenance buffer (+0.1 % (v/v) Triton X100). The resulting fluorescence was measured using the Tecan Spark fluorescence plate reader and the same settings as above. The binding constant (K_D) was calculated in GraphPad Prism using one site-specific non-linear regression

2.2.8 Crystallisation of DARPin-SUMO complexes

2.2.8.1 Crystallisation of E11-SUMO

The complex of E11 and SUMO was purified by incubating equal amounts of DARPin and SUMO for 30 min on ice and subsequently running a size exclusion column (S75, 0.5 mL/min) in crystallisation buffer. Only fractions containing the complex were pooled and concentrated to 20 mg/mL protein concentration.

The initial screening took place in a 364 well plate using the mosquito crystal robot (sptlabtech). Crystallisation took place in a 24-well plate using the hanging drop method using different reservoir buffer conditions, crystallisation temperatures, seeding methods, protein concentrations and ratios between protein solution and reservoir buffer. No three-dimensional crystals could be observed under any conditions tested.

2.2.8.2 Crystallisation of A10-SUMO

The complex of A10 and SUMO was purified by incubating equal amounts of DARPin and SUMO for 30 min on ice and subsequently running a size exclusion column (S75, 0.5 mL/min). Only fractions containing the complex were pooled and concentrated to 20 mg/mL protein concentration.
The initial screening took place in a 364-well plate using the mosquito crystal robot (sptlabtech). Crystallisation took place in a 24-well plate using the hanging drop method. Crystals formed at 20 ℃ using 0.1 M Bis-Tris pH 6.5 supplemented with 23 % (v/v) Peg3350 as reservoir conditions. 5 mg/mL protein were mixed 2:1, 1:1, or 0.5:1 with reservoir solution. Drops were directly macro-seeded with 1–3 crystals from a previous plate with the same conditions to induce crystal formation. The cryo-protection used for snap-freezing the crystals contained 0.1 mM Bis-Tris pH 6.5, 23 % (v/v) Peg3350 and 10 % (v/v) Peg200.

2.2.8.3 Crystallisation of C10-SUMO

The complex of C10 and SUMO was purified by incubating an equal amount of DARPin and SUMO for 30 min on ice and subsequently running a size exclusion column (S75, 0.5 mL/min). Only fractions containing the complex were pooled and concentrated to 20 mg/mL protein concentration.
The initial screening took place in a 364-well plate using the mosquito crystal robot (sptlabtech). Crystallisation took place in a 24-well plate using the hanging drop method. Crystals formed at 20 ℃ using 0.1 M Bis-Tris pH 6.5 supplemented with 16 % (v/v) Peg3350 as reservoir conditions. 20 mg/mL protein were mixed 2:1, 1.5:1, or 1:1 with reservoir solution. Drops were directly macro-seeded with 1–3 crystals from a previous plate with the same conditions to induce crystal formation. The cryo-protection used for snap-freezing the crystals contained 0.1 mM Bis-Tris pH 6.5, 16 % (v/v) Peg3350 and 10 % (v/v) Peg200.

2.2.8.4 Analysis of the interaction interface using PyMol

The interaction interface between the DARPin and SUMO was analysed by three different methods:
1. By calculating the amino acids that lie within 3.5 Åto each other using the "pairwise distance" function from pymol (function: pairwise_dist).
2. By looking for close amino acid residues, by calculating the interaction interface with the "interfaceResidue" function from pymol.
3. By using the PDBePISA tool from EMBL, uploading the crystal structure as a pdb file (https://www.ebi.ac.uk/pdbe/prot_int/pistart.html).

2.2.9 Nuclear magnetic resonance (NMR) experiments

2.2.9.1 NMR of DARPin-SUMO complexes

50 µM ^{15}N-labelled SUMO was mixed with 64–148 µM DARPin (A10: 95 µM, C10: 148 µM, F10: 75 µM, E11: 64 µM, G11: 119 µM, B12: 108 µM in NMR buffer (50 mM $NaPO_4$, 100 mM NaCl, 1-2 mM ^{15}N-Imidazole (as internal reference) in 95:5 H_2O:D_2O)). Measurement took place for 12 h at 25 ℃ on a Bruker599 NMR, as a ^{1}H-^{15}N-BEST-TROSY experiment with the TopSpin 3.0 Sparky software.

2.2.9.2 NMR of Ubiquitin variant and Spc24-glob/Spc25-CTD

25 µM or 50 µM (2 different experiments) ^{15}N-labelled A12 was mixed with 100 µM or 500 µM Spc24-glob/Spc25-CTD in NMR buffer. Measurement took place for 24 h at 4 ℃ on a Bruker599 NMR, as a ^{1}H-^{15}N-HSQC experiment with the TopSpin 3.0 Sparky software.

2.2.10 Preparation of mass spectrometry (MS) samples

2.2.10.1 Mass spectrometry with Pib1-TAP

Pib1-TEV-tandem-affinity-purification-tag (TAP) and Yal6B *WT* yeast strains were inoculated into L-lysine-U-$^{13}C_6$-$^{15}N_2$-SC-media or unlabelled SC-complete media. Precultures were grown overnight at 30 ℃. In the evening, an optical density at 600 nm (OD_{600}) 0.004 was inoculated in 1 L of the respective media (one sample per construct,

both directions) and grown for 16 h until OD_{600} 2 was reached. Cells were harvested at 5000 g for 15 min at RT, washed with 25 mL lysis buffer and finally resuspended in 20–25 mL lysis buffer. Cells were opened using a high-pressure cell disruption system (35000 psi, 3 rounds, 4 °C). After the addition of SIGMAFAST Protease Inhibitor Cocktail, samples were spun at 300 g for 5 min at 4 °C. Now, 10 mM NEM, 0.5 % (v/v) Igepal and 0.25 % (v/v) Triton X100 were added to the supernatant. Samples were incubated for 1 h at 4 °C rolling, spun down at 20000 g for 30 min at 4 °C, and the protein concentration was determined as described in section 2.2.4.6. Protein concentration and volume of all samples were adjusted and samples were incubated for 16 h at 4 °C rotating with 40 µL equilibrated IgG slurry per 5 mg protein. Afterwards, beads were washed 5x with extract buffer and labelled and unlabelled samples were combined in the last wash. Now, beads were resuspended in 10x bead volume of lysis buffer (with the same amount of Igepal, Triton X100, SIGMAFAST Protease Inhibitor Cocktail and NEM as above) and Pib1 and its interactors were released from the beads by the addition of 2 µg TEV-Protease per 5 mg protein and cleavage for 3 h at 16 °C, 800 rpm shaking. The beads were washed twice with 10 times the bead volume of extract buffer and the FT from the washes was added to the FT from the cleavage. Samples were reduced by the addition of 1 mM DTT (in 1x NuPage LDS buffer), boiling at 65 °C and alkylated with 5.5 mM chloroacetamide before being submitted for mass spectrometry.

2.2.10.2 Mass spectrometry with Pib1-GFP

Mass spectrometry samples for Pib1-GFP were preprepared as described under section 2.2.10.1. With the following changes: Before addition of beads, samples were diluted with 2 volumes of dilution buffer. Then 100 µL equilibrated anti-GFP bead slurry per 75 mg protein were added and incubated for 90 min, at 4 °C with rotation. Beads were washed 5x with extract buffer and light and heavy labelled samples were combined in the last wash. Elution and reduction was done by the addition of 1 mM dithiothreitol (in 1x NuPage LDS buffer), boiling at 65 °C and samples were alkylated with 5.5 mM chloroacetamide before being submitted for mass spectrometry.

2.2.10.3 Mass spectrometry with Ubait constructs

TAP-TEV-Pib1 (Lys^0), TAP-TEV-Pib1-ubi (Lys^8), and TAP-TEV-Pib1-ΔGG (Lys^4) constructs expressing yeast strains were inoculated to OD_{600} 0.001 in 0.5 L SC -URA media containing 2 % (w/v) raffinose as carbon source and grown for 16 h until OD_{600} 0.5 was reached. Cells were washed with 50 mL SC-URA containing 2 % (w/v) galactose and grown for 3 h, 30 °C in 500 mL SC -URA containing 2 % (v/v) galactose

to induce protein expression. Lysis was done as described in section 2.2.10.1. After adjusting the protein concentrations and volumes of all samples, 30 µL equilibrated IgG slurry per 10 mg protein were added and samples were incubated for 16 h at 4 ℃, with rotation. Beads were washed 3–5x with extract buffer and 10x bead volume of denaturing buffer were added. To elute the bound fraction, samples were boiled for 5 min at 95 ℃ and the supernatant was added to new IgG slurry. The beads from the first incubation were washed with 500 µL NP40 wash buffer and the supernatants were added as well to the new beads. Samples were incubated for 2 h at 4 ℃, rotating. Beads were washed 3x with lysis buffer, and in the last wash, beads of light, medium and heavy samples were combined. Samples were reduced by the addition of 1 mM dithiothreitol (in 1xNuPage LDS buffer), boiling at 65 ℃ and alkylated with 5.5 mM chloroacetamide before being submitted for mass spectrometry.

3 Results and Discussion

3.1 Characterisation of biological functions of the Pib1 ubiquitin ligase

Pib1 is a poorly characterized E3 enzyme of the RING-type family, which acts together with the heterodimeric E2 Ubc13/Mms2 in *S. cerevisiae* to form K63-linked ubiquitin chains on substrates. Through its N-terminal FYVE domain Pib1 localises to vacuoles, and most likely plays a role in the endocytic system. However, the exact ubiquitination targets on which Pib1 acts are not known so far. Previous findings by our lab and others suggest different substrates for Pib1. To see if Pib1 is the corresponding E3 for their ubiquitination, I performed denaturing His-ubiquitin Ni^{2+}-NTA pull-downs followed by western blots in *WT*, *PIB1*, *TUL1* deletion strains and *PIB1/TUL1* double deletion strains. Additionally, I attempted to find further Pib1 interactors and substrates of Pib1 using different mass-spectrometry approaches. All in all my results go in line with the previous findings from our lab and others that Pib1 is specifically acting in K63-linked polyubiquitination of proteins at endosomal and vacuolar membranes marking proteins for their vacuolar degradation. However, I was not able to identify any direct substrates or interactors for Pib1 in my work. The three main reasons for that are: Firstly, the redundancy between the ubiquitinating enzymes in the MVB pathway, which might even extend over the described ones for Rsp5, Pib1 and Tul1. Secondly, Pib1 is an E3 that extends an existing ubiquitin moiety by K63-linkage, but does not initiate *de novo* ubiquitination on a substrate. And finally, the difficult isolation of Pib1, because of its low abundance and bad solubility.

3.1.1 Background and aim of this project

Previous work from our lab has found that the E3 Pib1 specifically interacts with Ubc13/Mms2 to enhance its K63-linked ubiquitin chain formation activity at endosomal and vacuolar membranes,[99] but the exact substrates, on which Pib1 is active are not clear so far. [redacted], a former lab member of the [redacted] lab, has performed a yeast two-hybrid screen (Y2H) to find interactors of Pib1. In this screen, he identified

COPII vesicle components like Yop1, Yif1, Yip1 and Yip3. He also found the t-SNAREs Pep12 and Tlg1 to interact with Pib1 (unpublished work, fig. 10). Additionally to our work, Silva *et al.* (2015) performed a large mass spectrometry screen where they looked for K63-ubiquitinated proteins after induction of oxidative stress in budding yeast. They found one of the proteins identified by Thomas Albert (the t-SNARE Pep12) and some direct interactors of the proteins identified in the Y2H analysis described before, to be modified with K63-linked ubiquitin chains. The proteins of interest to us, which they identified, are the Rab GTPases Vps21, Sec4 and Ypt1, and the v-SNAREs Vti1, Snc1 and Gos1 (fig. 10).[389,390]

All these proteins play a role in vesicle trafficking in budding yeast and might therefore be interactors and substrates of Pib1 for their recycling, degradation or other means. Additionally, I included the exocyst subunit Sec3 as a potential substrate of Pib1, as its homologue was described to be marked with ubiquitin for proteasomal degradation by Pib1 in *Schizosaccharomyces pombe.*[391] To confirm the hypothesis that the listed proteins are ubiquitination targets of Pib1, I first wanted to verify that these proteins are ubiquitinated in *S. cerevisiae* and secondly see if Pib1 is the corresponding E3 for their ubiquitination. For testing this, GFP- or HA-tagged constructs of these proteins were coexpressed with His-tagged ubiquitin in wild-type and *PIB1* deletion strains. Denaturing His-ubiquitin Ni^{2+}-NTA pull-downs followed by western blots were performed to look for ubiquitinated proteins.

Xu *et al.* (2017) described that Pib1 shares a redundant function with Tul1 as an E3 for ubiquitination of the v-SNARE protein Snc1 in COPI-mediated protein trafficking.[117] To check for its redundant function with Pib1, also *TUL1* deletion strains and *PIB1/TUL1* double deletion strains were constructed and included in the pull-down assays.

Additionally, I attempted to find further Pib1 interactors using a SILAC based MS analysis with natively expressed Tandem Affinity Purification tagged (TAP) or GFP-tagged Pib1 as a substrate for pull-down. Moreover, I tried to identify further Pib1 substrates using the Ubait approach followed by MS, which was described by O'Connor *et al.* (2015).[392]

3.1.2 Analysis of potential Pib1 substrates by denaturing His-ubiquitin Ni^{2+}-NTA pull-downs after H_2O_2 treatment

To verify the possible substrates of Pib1 (fig. 10), I was performing denaturing His-ubiquitin Ni^{2+}-NTA pull-downs (PD, see section 2.2.3.7) with lysate from strains expressing His-tagged ubiquitin and my protein of interest tagged with an affinity tag for detection.[393] If the proteins of interest were conjugated with His-ubiquitin they should be detected in the blot after PD. If the detection is no longer possible in *PIB1* deletion strains, this would indicate the involvement of Pib1 as an E3 in their ubiquitination. As

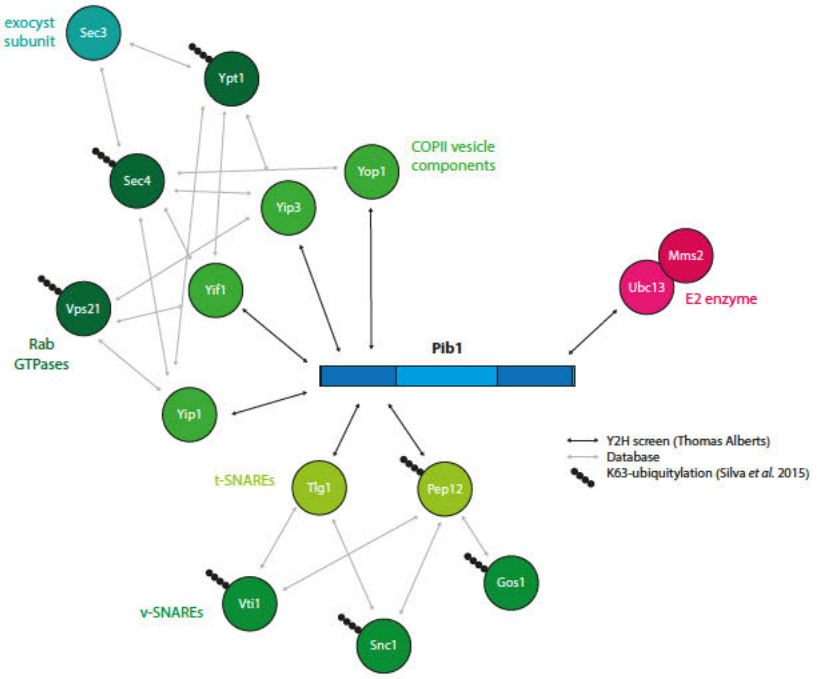

Figure 10: Possible interactors and substrates of Pib1. Pib1 specifically interacts with Ubc13/Mms2 (right).[99] Additionally, Thomas Albert performed a Y2H screen to find interactors of Pib1. In this screen, he identified Yop1, Yif1, Yip1, Yip3, Pep12 and Tlg1 to interact with Pib1 (black arrows). Silva *et al* (2015) found in a large MS screen, after induction of oxidative stress, Pep12, Vps21, Sec4, Ypt1, Vti1, Snc1 and Gos1 to be modified with K63-linked ubiquitin chains (black dots).[389,390] Interactions between the proteins found by Thomas Albert and by Silva *et al* were identified by searching the Saccharomyces Genome Database (SGD)[40] (grey arrows, figure adapted from Christian Renz).

the putative substrates of Pib1 were found to be ubiquitinated under oxidative stress conditions,[389] I also tested their ubiquitination after treatment of cells with 2.4 mM H_2O_2 for 45 min.

3.1.2.1 No detection of ubiquitination of endogenous GFP-tagged candidate substrates

In the first experiment, I created strains (see section 2.2.3.4) where the proteins of interest (Sec3, Sec4, Vps21, Vti1, Ypt1, Pep12, Gos1 or Snc1) were C-terminally tagged with GFP. I was able to tag all genes besides Ypt1. To look for proper localisation of the proteins, I analysed the strains by fluorescence microscopy (fig. 11a and table 13). As described in the literature (table 13), GFP-tagged Gos1 localized to the Golgi, endoplasmic reticulum (ER), and cell membrane.[394] Also Sec3 seems to localize correctly to the bud neck, and cell membrane.[394,395] GFP-tagged Snc1 and Vti1 seem to localise to the plasma membrane, vacuolar membrane, and bud, or to the Golgi, vacuolar membrane, cell membrane, and vesicles, respectively, as observed for the native proteins.[394] However, the described localisation of Pep12 to the Golgi, vacuole, or MVB[394] could not be reproduced with the C-terminally GFP-tagged construct, as expression levels

were too low to be analysed. Also, Sec4 and Vps21 were not detected at their native locations at the Golgi, ER, and cell membrane,[394] or at the endosomes, mitochondria, and vacuolar membrane, respectively.[394] Sec4 accumulated in the mitochondria and Vps21 showed a diffuse cytoplasmic localisation.
Therefore, I got yeast strains expressing N-terminally GFP-tagged versions of Sec4, Pep12, Vps21 and Ypt1 under control of their endogenous promoters, from the lab of [redacted].[396] I again tested them for the localisation of the tagged proteins by microscopy. Except for Sec4, which was not detectable in the microscope, the localisation of Pep12 (Golgi, vacuole, and MVB), Vps21 (endosomes, mitochondria, and vacuolar membrane) and Ypt1 (Golgi, ER, and cytoplasmic vesicles) looked correct in these strains (fig. 11b).

To detect ubiquitination of the GFP-tagged substrates, I coexpressed His-tagged ubiquitin and performed a denaturing His-ubiquitin Ni^{2+}-NTA pull-down and a WB probing for GFP (see section 2.2.3.7). Unfortunately, I was not able to detect any ubiquitinated species of my proteins of interest (fig. 12, lanes 3–10), besides for Snc1 (fig. 12, lane 11). This was possible due to the low expression of the proteins under their respective endogenous promoter.

Table 13: Localisation of possible substrates of Pib1. Localisations are received from the protein database UniProtKB.[394] ER, endoplasmic reticulum; MVB, multivesicular bodies.

Protein name	published localisation
Gos1	Golgi, ER, cell membrane
Pep12	Golgi, vacuole, MVB
Sec3	bud neck, cell membrane
Sec4	Golgi, ER, cell membrane
Snc1	plasma membrane, vacuolar membrane, bud
Vps21	endosomes, mitochondria, vacuolar membrane
Vti1	Golgi, vacuolar membrane, cell membrane, vesicles
Ypt1	Golgi, ER, vesicles

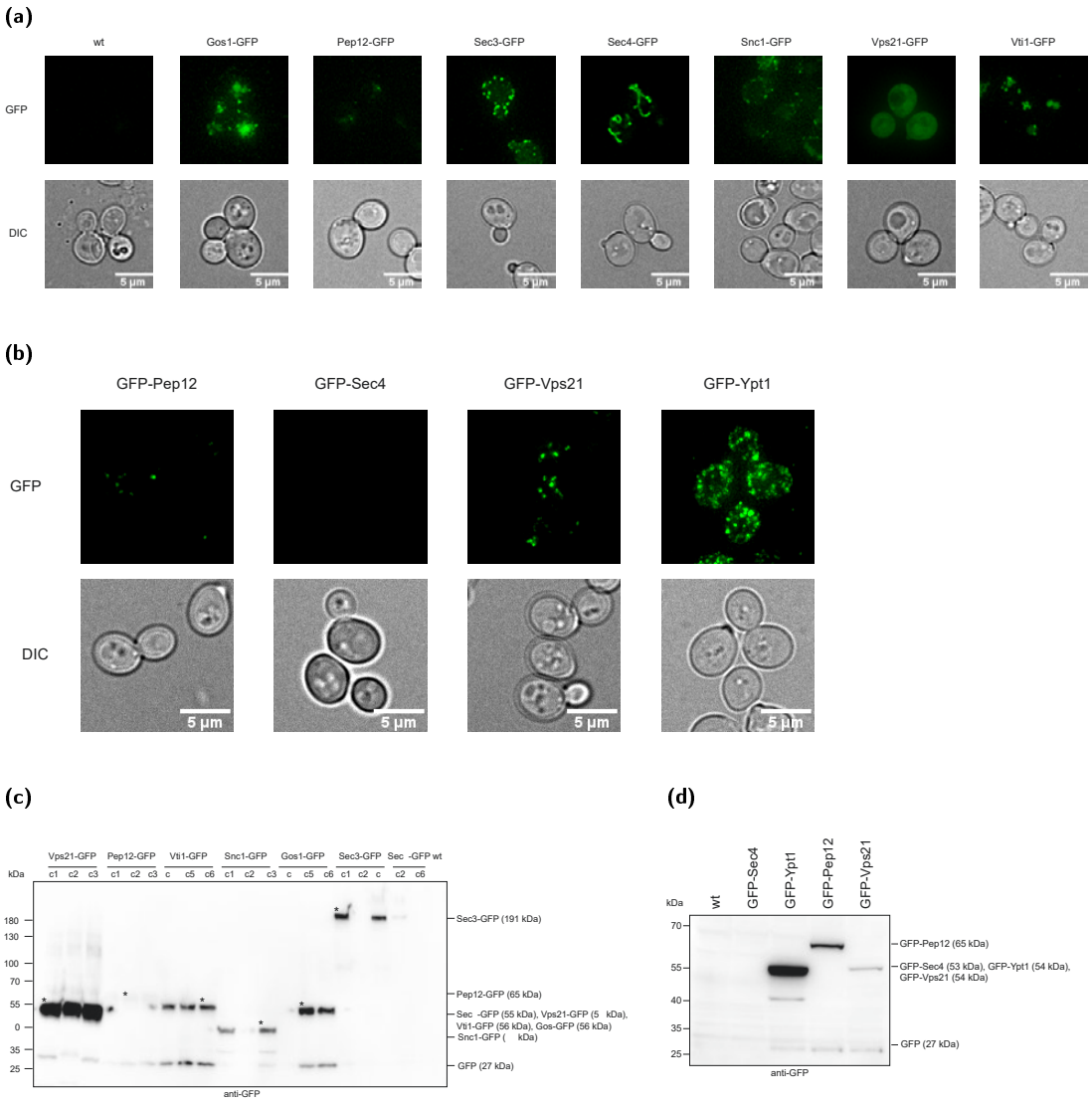

Figure 11: (a) Localisation of C-terminal tagged putative Pib1 substrates in yeast. Genes of interest were endogenously tagged with GFP. Fluorescence signal (GFP) and differential interference contrast (DIC) microscopy images of exponential growing living cells were taken. Gos1, Sec3, Snc1 and Vti1 seem to localize correctly. Pep12, Sec4 and Vps21 show an aberrant localisation. **(b) Localisation of N-terminal tagged putative Pib1 substrates in yeast.** Genes of interest were endogenously tagged with GFP.[396] Fluorescence signal (GFP) and differential interference contrast (DIC) microscopy images of exponential growing living cells were taken. Pep12, Vps21 and Ypt1 seem to localize correctly. GFP-Sec4 was not detectable. **Expression of C-terminally (c) and N-terminally (d) tagged putative Pib1 substrates.** Cultures for microscopy experiments were subject to cell lysis and Western blot. Substrate expression was detected using an anti-GFP antibody. In **(c)** three clones (c1-c$_n$) from tagging of each substrate were loaded. Clones marked with an asterisk (*) were used for microscopy. For Sec4-GFP a different clone, not depicted here that showed better protein expression, was used for microscopy.

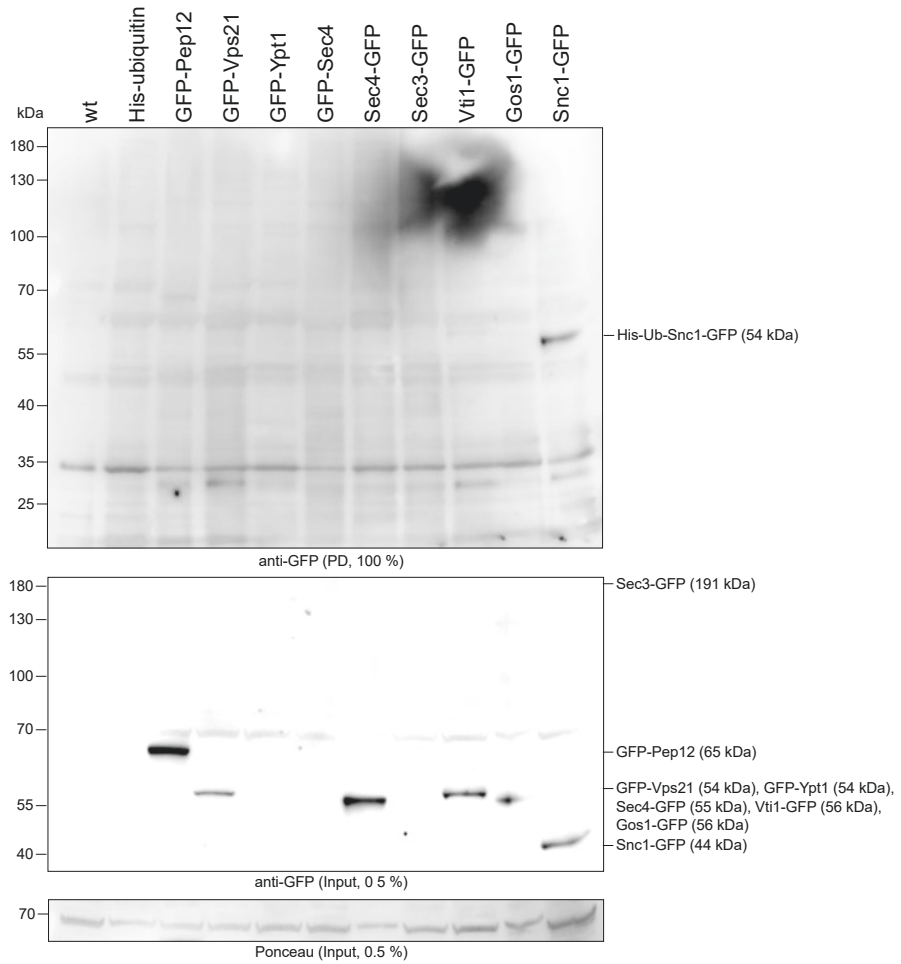

Figure 12: Denaturing His-ubiquitin Ni^{2+}-NTA pull-downs for detection of GFP-tagged putative Pib1 substrates. Expression of GFP-tagged constructs was performed in yeast strain BY4741. Expression of His-ubiquitin was induced with 0.1 mM $CuSO_4$. Lysis and denaturing His-ubiquitin pull-down from 80 OD of an exponentially growing culture was performed. On the lower blot input samples (0.5 % from the PD volume, 0.4 OD) were loaded. On the upper blot samples after a denaturing His-ubiquitin Ni^{2+}-NTA pull-downs (100 % volume) are shown. Both blots were developed with a GFP antibody to detect putative Pib1 substrates. No ubiquitinated species besides from Snc1 could be detected.

3.1.2.2 Successful detection of ubiquitination after overexpression of some putative substrates

To be able to detect ubiquitination of the possible substrates of Pib1 in yeast cells despite their low abundance, they were overexpressed from a centromeric plasmid under a constitutive promotor (see section 2.2.3.3). From these strains, I performed a TCA-lysis followed by a denaturing His-ubiquitin Ni^{2+}-NTA pull-down (see section 2.2.3.7). The overexpressed constructs were tagged with a 3xHA-tag (Snc1) or 2xHA-tag (all other proteins) to allow for their detection by Western blot. The results of the PD for each individual protein will be discussed in the following parts.

Ubiquitination of 3xHA-Snc1 is not influenced by Pib1

Xu *et al.* (2017) hypothesized Snc1 to be K63-ubiquitinated by Pib1 and Tul1, as upon deletion of both, Snc1 mislocalizes. Moreover, they fused Pib1 and Tul1 to an unspecific deubiquitinase, which resulted in a reduction of Snc1 ubiquitination.[117] I received their vectors for expression of HA-tagged Snc1 and its lysine mutant form, which cannot be ubiquitinated (Snc1-8KR) under control of the *TPI1* promoter, from Todd Graham.[117] I tested for Snc1 ubiquitination in untreated cultures and after treatment of cells with 2.4 mM H_2O_2 to induce oxidative stress. For detection of Snc1 ubiquitination, an enrichment by PD was not necessary, as it could already be nicely detected after cell lysis. Although, the ubiquitination of Snc1 was clearly visible (fig. 13a, lane 2), neither a knockout of *PIB1* nor of *TUL1* nor even a double knockout of both E3 enzymes showed any effect on the ubiquitination pattern of Snc1 (fig. 13a, lanes 4–9). The treatment of cells with H_2O_2 before PD increased Snc1 ubiquitination as described by Silva *et al.* (2015) (fig. 13b, lanes 2–5). However, again no reduction was visible in *PIB1*, *TUL1* or *PIB1/TUL1* double deletion strains (fig. 13b, lanes 6–11).

Additionally, I wanted to see if the heterodimeric E2 Ubc13-Mms2 that was described to specifically act together with Pib1,[99] has any influence on the ubiquitination of Snc1. Using a *UBC13* deletion strain, no reduction of ubiquitination was detected neither with H_2O_2 treatment nor without (fig. 13c, lane 4 and fig. 13d, lane 4). However, the modification was completely abolished in an *RSP5* mutant (fig. 14a, lane 4–6), but not in a mutant of one of its adapter proteins, Bsd2 (fig. 13c, lane 5 and fig. 13d, lane 5), indicating for a *RSP5* dependent ubiquitination of Snc1. As Rsp5 is an essential protein a temperature-sensitive (ts) strain (*rsp5-2*) at a restrictive temperature was used for these experiments.

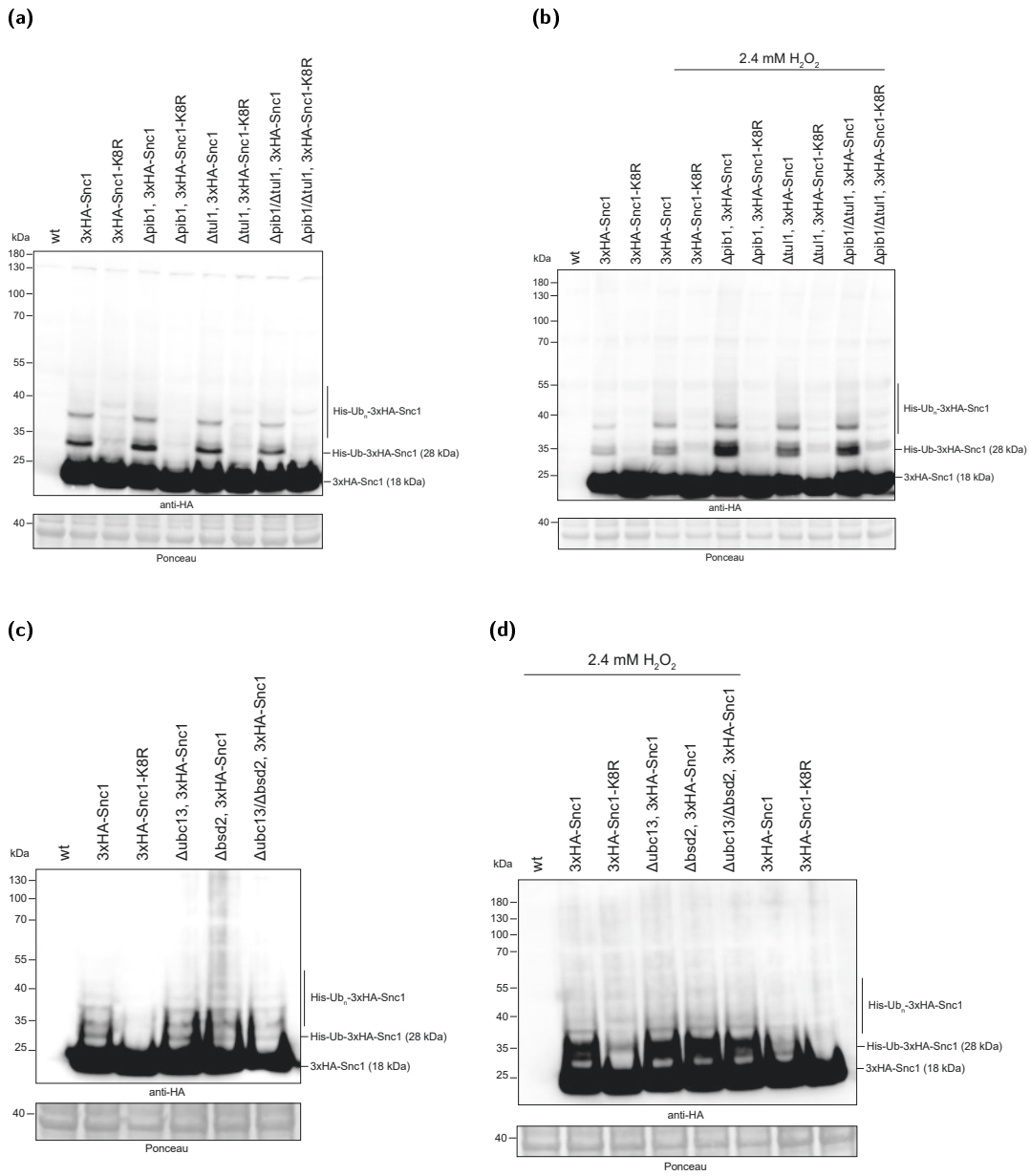

Figure 13: (a) Ubiquitination of Snc1 in *PIB1*, *TUL1* or *PIB1/TUL1* double deletion strains. *WT* cells or cells, in which the indicated gene was deleted, were transformed with a plasmid for expression of 3xHA-tagged Snc1 or the ubiquitination resistant mutant 3xHA-Snc1-K8R. TCA preparation of 0.3 OD of cells was done. The Western blot was developed with an antibody against the HA-tag. As a loading control, the membrane was stained with Ponceau. Ubiquitination of Snc1 is clearly visible in *WT*, *PIB1*, *TUL1* and *PIB1/TUL1* double knockout strains. **(b) Ubiquitination of Snc1 in *PIB1*, *TUL1* or *PIB1/TUL1* double deletion strains after H_2O_2 treatment.** Same experiment as in (a) only that cultures were treated with 2.4 mM H_2O_2 for 45 min before harvesting. For comparison, one culture was left untreated. Ubiquitination of Snc1 increased after H_2O_2 treatment, but again no difference in *PIB1*, *TUL1* and *PIB1/TUL1* double knockout strains is visible. **(c) Ubiquitination of Snc1 in *UBC13*, *BSD2* or *UBC13/BSD2* double deletion strains.** *WT* cells or cells, in which the indicated gene was deleted, were transformed with a plasmid for expression of 3xHA-tagged Snc1. TCA preparation of 0.3 OD of cells was done. The Western blot was developed with an antibody against the HA-tag. As a loading control the membrane was stained with Ponceau. Ubiquitination of Snc1 is clearly visible in *WT*, *UBC13*, *BSD2* and *UBC13/BSD2* double knockout strains. **(d) Ubiquitination of Snc1 in *UBC13*, *BSD2* or *UBC13/BSD2* double deletion strains after H_2O_2 treatment.** Same experiment as in (c) only that cultures were treated with 2.4 mM H_2O_2 for 45 min before harvesting. For comparison one culture was left untreated. Ubiquitination of Snc1 increased after H_2O_2 treatment, but again no difference in *UBC13*, *BSD2* and *UBC13/BSD2* double knockout strains is visible.

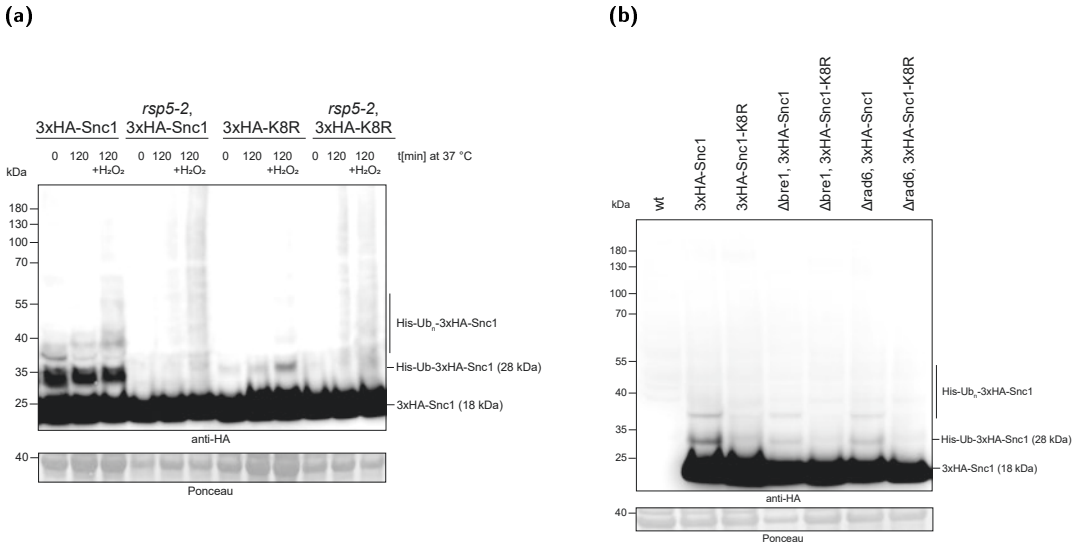

Figure 14: (a) Ubiquitination of Snc1 in *rsp5-2* strains. *WT* cells or the temperature-sensitive *rsp5-2* strain were grown for the indicated times at 37 °C and either treated for 45 min with 2.4 mM H_2O_2 or left untreated. TCA preparation of 0.3 OD of cells was done. The Western blot was developed with an antibody against the HA-tag. As a loading control, the membrane was stained with Ponceau. Ubiquitination of Snc1 is clearly visible in *WT* cells, but vanished in the *rsp5-2* strain. **(b) Ubiquitination of Snc1 in *BRE1* and *RAD6* deletion strains.** *WT* cells or cells, in which the indicated gene was deleted, were transformed with a plasmid for expression of 3xHA-tagged Snc1 or the ubiquitination resistant mutant 3xHA-Snc1-K8R. TCA preparation of 0.3 OD of cells was done. The Western blot was developed with an antibody against the HA-tag. As a loading control, the membrane was stained with Ponceau. A weaker signal for Snc1 ubiquitination in the *BRE1* and *RAD6* deletion strains can be observed, however, clear conclusions cannot be drawn, as also the signal of unmodified Snc1 was weaker in these strains. **(c) Ubiquitination of Snc1 in *BRE1* and *RAD6* deletion strains after H_2O_2 treatment.** Same experiment as in (b) only that cultures were treated with 2.4 mM H_2O_2 for 45 min before harvesting. For comparison, one culture was left untreated. Again, no clear conclusions can be drawn, as the signal of unmodified Snc1 was weaker in the *BRE1* and *RAD6* deletion strains.

To complete the analysis of Snc1 ubiquitination, I tested for a change of Snc1 ubiquitination in *BRE1* and *RAD6* deletion strains. Silva *et al.* (2015) described Rad6 as the E2 enzyme and Bre1 as the E3 responsible for K63-polyubiquitination in response to H_2O_2.[389] I observed a weaker signal for Snc1 ubiquitination in the *BRE1* and *RAD6* deletion strains, however, clear conclusions cannot be drawn, as also the signal of unmodified Snc1 was weaker in these strains (fig. 14b, lanes 4–7 and fig. 14c, lanes 6–9). Indicating the Snc1 levels are lower in the *BRE1* and *RAD6* deletion strains compared to *WT* strains.

Ubiquitination of 2xHA-Pep12 is visible in *DOA4* knockout strains

Reggiori *et al.* (2000, 2001, 2002)[116,397,398] found that the introduction of a polar residue into the transmembrane domain (TMD) of Pep12 (Pep12-L271D) enhances its ubiquitination and vacuolar degradation. The observed ubiquitination was lower in a *TUL1* deletion strain and the sorting of Pep12-L271D into MVB was partly abolished in strains lacking Ubc13/Mms2. As Pep12 was found to interact with Pib1 in the Y2H screen described above, I tested its ubiquitination in *WT*, *PIB1*, *TUL1* and *PIB1/TUL1* double deletion cells after TCA lysis and pull-down.

For the *WT* Pep12 construct, I was not able to see any ubiquitinated species (fig. 15a, lanes 4–8) after performing a denaturing His-ubiquitin PD with or without H_2O_2 treatment. Therefore, I cloned the L271D variant of Pep12, which was described by Reggiori *et al.* (2002)[116] Moreover, I constructed *PIB1*, *TUL1* and *PIB1/TUL1* deletion strains, in which additionally *DOA4* was deleted, as Reggiori *et al.* also did their experiments in strains lacking Doa4. Doa4 is the deubiquitinase responsible for removing K63-linked chains in the endocytic pathway, before substrates enter the MVB.[399–401] Therefore, K63-linked ubiquitination accumulated in this background (data not shown). A faint band, possibly corresponding to ubiquitinated Pep12 and Pep12-L271D, was visible after PD from *DOA4* strains (fig. 15b, lanes 4 and 6). The putative band for ubiquitinated Pep12-L271D was no longer visible in samples from *DOA4/PIB1*, *DOA4/TUL1* or *DOA4/PIB1/TUL1* deletion strains (fig. 15b, lanes 7–9). However, considering the position of the band in the gel, it represents more the size of unmodified Pep12 than the expected size of ubiquitinated Pep12.

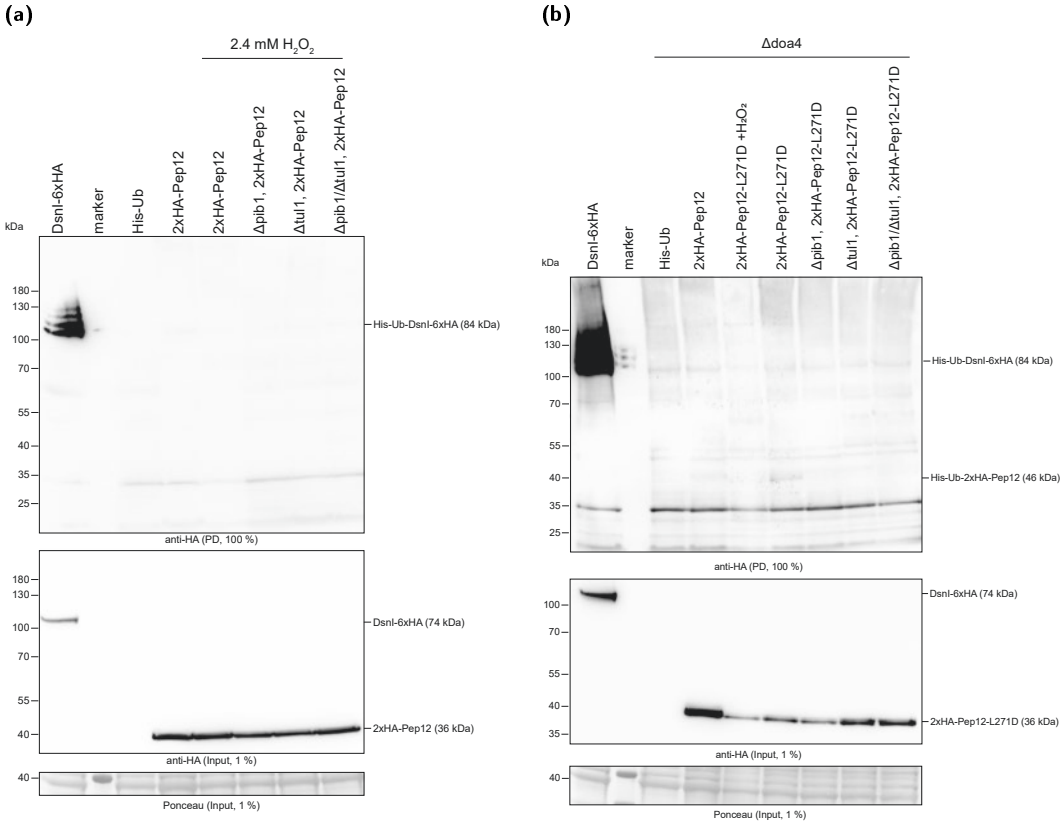

Figure 15: (a) Ubiquitination of Pep12 in *PIB1*, *TUL1* or *PIB1/TUL1* double deletion strains. Strains, in which the indicated gene was deleted, were co-transformed with plasmids for expression of 2xHA-tagged Pep12 and His-ubiquitin. His-ubiquitin expression was induced with 0.1 mM $CuSO_4$. Where indicated, cultures were treated with 2.4 mM H_2O_2 for 45 min. Lysis and denaturing His-ubiquitin Ni^{2+}-NTA pull-down from 80 OD of an exponentially growing culture was performed. The Western blot from the PD was developed with an antibody against the HA-tag. Dsnl-6xHA was used as a control for successful pull-down. Input samples (1 %, 0.8 OD) after cell lysis were loaded in parallel and developed against the HA-tag on Pep12. As a loading control, the membrane with the input samples was stained with Ponceau. No ubiquitination of Pep12 was visible under the tested conditions. **(b) Ubiquitination of Pep12 in *DOA4* deletion background and Pep12-L271D in *DOA4*, *DOA4/PIB1*, *DOA4/TUL1* or *DOA4/PIB1/TUL1* deletion strains.** Treatment, PD and blotting were performed as described in (a) only with strains expressing the Pep12-L271D mutant and having an additional *DOA4* deletion. For comparison, one strain expressing *WT* Pep12 was included as well. A faint band, possibly corresponding to ubiquitinated Pep12 and Pep12-L271D, was visible after PD from *DOA4* strain, but no ubiquitination of Pep12-L271D was visible after PD from *DOA4/PIB1*, *DOA4/TUL1* or *DOA4/PIB1/TUL1* deletion strains.

Ubiquitination of 2xHA-Sec3 is not influenced by Pib1

Kampmeyer *et al.* (2017) showed that in *Schizosaccharomyces pombe* partial unfolded Sec3, a subunit of the exocyst, is targeted for proteasomal degradation through attachment of K48-linked ubiquitin chains by Pib1.[391] I tested the ubiquitination status of *WT* Sec3 in *WT*, *PIB1*, *TUL1* or *PIB1/TUL1* double deletion *S. cerevisiae* strains with and without hydrogen peroxide treatment after denaturing His-ubiquitin PD. I was able to detect Sec3 ubiquitination (fig. 16a, lane 4), however, it did not change, if *PIB1*, *TUL1* or *PIB1/TUL1* were deleted in the strain (fig. 16a, lanes 5–7).

Ubiquitination of 2xHA-Gos1 is not influenced by Pib1, while ubiquitination of 2xHA-Vti1, 2xHA-Ypt1, 2xHA-Sec4 and 2xHA-Vps21 was not detected

Gos1 was found to be ubiquitinated after oxidative stress by Silva *et al.* (2015).[389] I saw its ubiquitination also in untreated cultures after His-ubiquitin PD (fig. 16b, lanes 4–5). Nevertheless, neither a knockout of *PIB1*, nor of *TUL1*, or the double deletion *PIB1/TUL1* led to a reduction of ubiquitination after pull-down in both conditions (fig. 16b, lanes 6–8).

Vti1 was found by O'Connor *et al.* (2015)[392] in a mass spectrometry screen, when they used an Rsp5-Ubait construct (described as in section 3.1.4). Unfortunately, I was not able to find conditions, in which I saw ubiquitination of Vti1 (fig. 17b, lanes 4–5).

Ypt1, Sec4 and Vps21 have been described to be ubiquitinated in high-throughput mass spectrometry-based screens.[115,389,402,403] Neither in untreated cultures nor after oxidative stress induction, I was able to see ubiquitination of these proteins after TCA-preparation and denaturing His-ubiquitin Ni^{2+}-NTA pull-downs (fig. 17a, lanes 6–9 and fig. 17b, lanes 6–7).

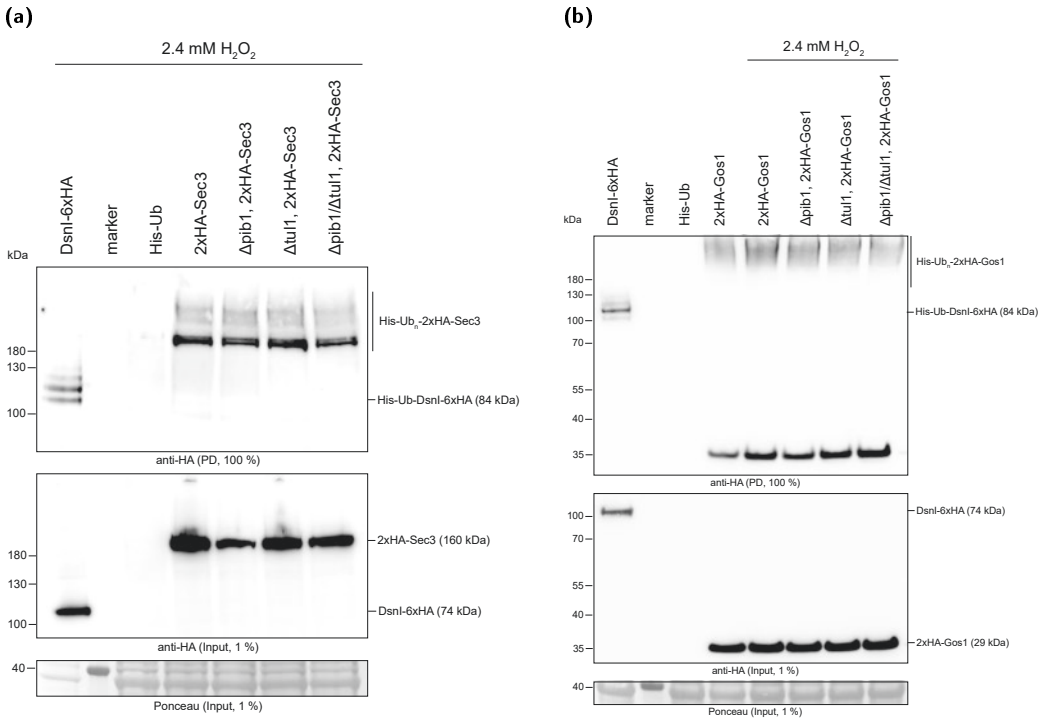

Figure 16: **(a) Ubiquitination of Sec3 in *PIB1*, *TUL1* or *PIB1/TUL1* double deletion strains.** Strains, in which the indicated gene was deleted, were co-transformed with plasmids for expression of 2xHA-tagged Sec3 and His-ubiquitin. His-ubiquitin expression was induced with 0.1 mM $CuSO_4$. All cultures were treated with 2.4 mM H_2O_2 for 45 min. Lysis and denaturing His-ubiquitin Ni^{2+}-NTA pull-downs were performed from 80 OD of exponentially growing cultures. The Western blot from the PD was developed with an antibody against the HA-tag. DsnI-6xHA was used as a control for successful pull-down. Input samples (1 %, 0.8 OD) after cell lysis were loaded in parallel and also developed against the HA-tag on Sec3. As a loading control, the membrane with the input samples was stained with Ponceau. No change in the ubiquitination of Sec3 was visible in the tested strains. **(b) Ubiquitination of Gos1 in *PIB1*, *TUL1* or *PIB1/TUL1* double deletion strains.** Treatment, PD and blotting were performed as described in (a), only with strains expressing 2xHA-Gos1 instead of Sec3. No change in the ubiquitination of Gos1 was visible in the tested strains.

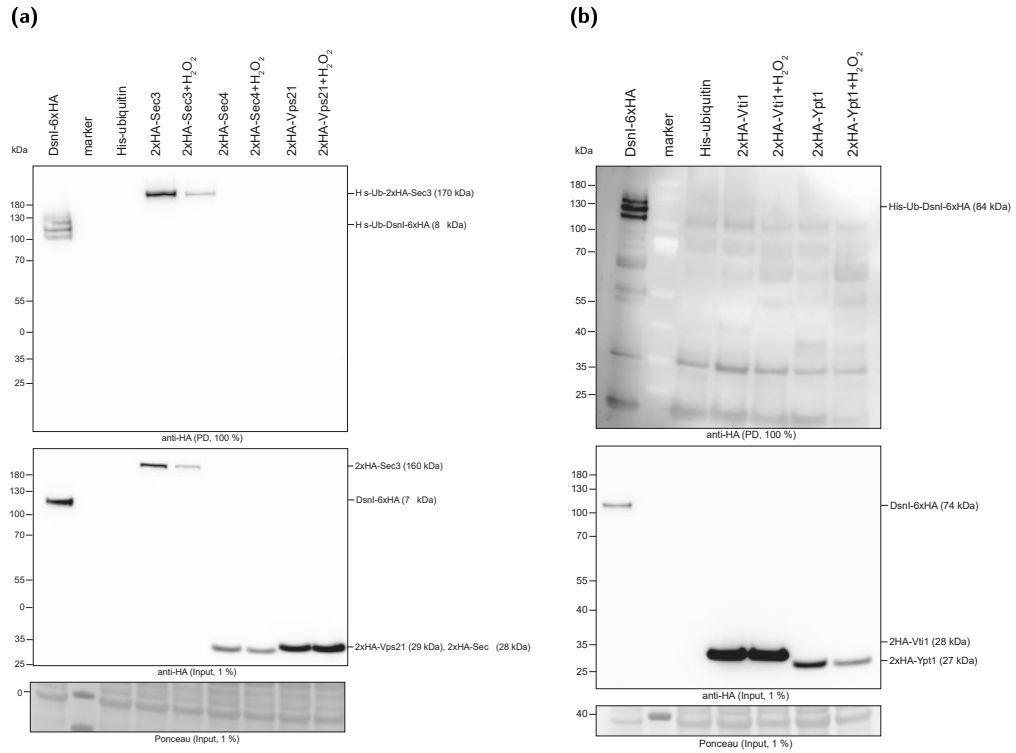

Figure 17: (a) Analysis of ubiquitination of Sec4 and Vps21 with and without H_2O_2 treatment. Treatment, PD and blotting were performed as described in fig. 16a, with strains expressing 2xHA-Sec3, 2xHA-Sec4 or 2xHA-Vps21. No ubiquitination of Sec4 or Vps21 was visible under the tested conditions. **(b) Analysis of ubiquitination of Vti1 and Ypt1 with and without H_2O_2 treatment.** Treatment, PD and blotting were performed as described under fig. 16a, with strains expressing 2xHA-Vti1or 2xHA-Ypt1 and H_2O_2 added only to half of the cultures. No ubiquitination of Vti1 and Ypt1 was visible in the tested conditions.

3.1.3 Pib1 and Tul1 have no role in autophagy

Autophagy is a process, during which ubiquitinated protein aggregates, organelles or other cytoplasmic structures are targeted for vacuolar degradation. Ubiquitin-binding autophagic receptors select targets and autophagy-related (ATG) protein complexes arrange the formation of the autophagosome, which fuses with the vacuole for degradation of their cargo.[404]

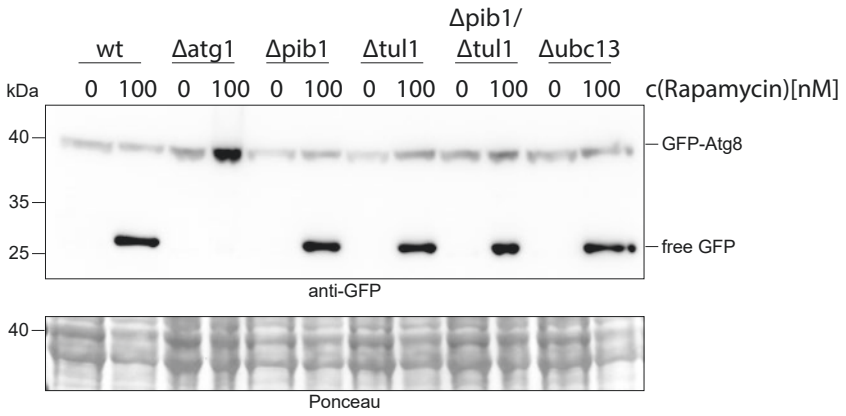

Figure 18: Autophagy assay with *UBC13*, *PIB1*, *TUL1* or *PIB1/TUL1* double deletion strains. GFP-Atg8 was expressed in the depicted strains. The autophagy pathway was induced by treating exponentially growing cultures with 100 nM rapamycin for 3 h. Cells were lysed and the Western blot was developed with an antibody against GFP. Cells lacking Atg1 were used as a positive control for autophagy failure. Ponceau staining is used as a loading control. No defect in autophagy could be observed in *UBC13*, *PIB1*, *TUL1* or *PIB1/TUL1* double deletion strains.

Autophagy, like endocytosis, is a ubiquitin-dependent degradation process via the vacuole, therefore we looked into a possible role of Pib1 during autophagy. [redacted] a postdoc of the [redacted] lab found that Pib1 is not involved in autophagy. To test that, he used an established assay (see section 2.2.3.15), in which GFP-Atg8 is expressed in yeast cells. These are then treated with rapamycin to induce autophagy. Lysates are examined by Western blot with an anti-GFP antibody. If autophagy is induced, the GFP-Atg8 construct is transported to the vacuole, where Atg8 is quickly degraded, while GFP is very stable and therefore accumulates in the vacuole. The failure to generate free GFP after rapamycin treatment indicates a defect in autophagy. An autophagy-defective mutant-like $\Delta atg1$ can be used as a positive control for autophagy failure.[405] To exclude a role for the E3 enzyme Tul1 or the E2 Ubc13 in autophagy, I used the same strategy as described above. I expressed GFP-Atg8 in *TUL1* and *UBC13* deletion strains and looked for autophagy induction after rapamycin treatment. In the control strain lacking Atg1 expression, an accumulation of GFP-Atg8 and no free GFP was observed (fig. 18, lanes 3–4). However, *UBC13*, *PIB1*, *TUL1* or *PIB1/TUL1* double deletion strain (fig. 18, lanes 5–12) accumulated free GFP to a level similar as in *WT* cells (fig. 18, lanes 1–2). Overall, I confirmed that Pib1 is not involved in autophagy. The same is true for Tul1 and Ubc13 and for the double mutant of *PIB1/TUL1*.

3.1.4 Mass spectrometry studies to identify interactors and substrates of Pib1 were not successful

For identification of further possible interactors of Pib1, I performed a pull-down of endogenously expressed tagged Pib1 followed by MS in collaboration with [redacted] from the group of [redacted] (IMB Mainz). Using TAP-tagged Pib1 (see section 2.2.10.1), I was not able to enrich for Pib1 as the mass spectrometric analysis done by [redacted] could not detect Pib1 over background levels (table 21). The putative band visible at the expected size in the Coomassie gel (fig. 20a, lanes 1 and 3) was therefore most likely not Pib1.
Using endogenously GFP-tagged Pib1 as bait (see section 2.2.10.2), I was also not able to enrich the protein enough and reproducible over the background for submitting samples to MS (fig. 20b, lane 3). Pib1-GFP was only detectable by Western blot, but not in the Coomassie gel.

Additionally, I tried to identify substrates of Pib1 using the Ubait approach.[392] Hereby, the E3 is fused to a ubiquitin molecule. The E3 assists in adding this ubiquitin to a protein, thereby getting covalently attached to its substrate. My Ubait constructs are composed of either *WT* Pib1 or a ligase dead Pib1 mutant (Pib1-I227A) fused to either *WT* ubiquitin or to a mutant that can not be conjugated (ubiquitin-ΔGG).
I first analysed the correct localisation of the Ubait constructs after expression in yeast cells. Although, they were massively overexpressed compared to the native Pib1 molecule, they still mostly localise to the vacuolar membrane (fig. 19) as was described before for Pib1.[112,113]
I performed two MS screens using the Ubait constructs (see section 2.2.10.3), again in collaboration with [redacted]. The experiments differed mostly in the amount of extract used (first time 40 mg, second time 320 mg protein) and a higher protein to IgG bead ratio used in the second experiment (first screen 30 µL slurry per 10 mg, second screen 15 µL slurry per 10 mg protein). The changes were made to enhance the amount of pulled-out Ubait construct, and its enrichment over the background. In both experiments, I could detect enrichment of the Ubait construct and its attachment to substrates by Western blot or Coomassie (fig. 20c and fig. 20d). Unfortunately, the Ubait constructs do not seem to be active *in vivo*, as both MS performed by [redacted] could identify Pib1 and ubiquitin as top hits, indicating a successful pull-down (table 22 and table 23), but in the first PD, no other proteins were identified with a high peptide count. The identified proteins from the second PD (e.g. Nucleolar protein 56 (NOP56), 1,3-beta-glucan synthase components FKS1 and GSC2 (FKS1/GSC2), V-type proton ATPase catalytic subunit (VMA1), ATP-dependent molecular chaperone 82 (HSC82), Nucleolar protein 58 (NOP58), Heat shock proteins (SSA1 and SSA2) and High-affinity hexose transporter (HXT6)) were not likely to be substrates of Pib1 as their normal-

ized heavy (ubiquitin-WT) to light (ubiquitin-ΔGG) ration is not higher than 1, like it would be expected for proteins that are conjugated with the Ubait construct.
All in all the results show that the Ubait construct was most likely not conjugated to any substrates by Pib1. Therefore Pib1 seems not active in the tested fusion construct or was not activated by the growth condition that was used.

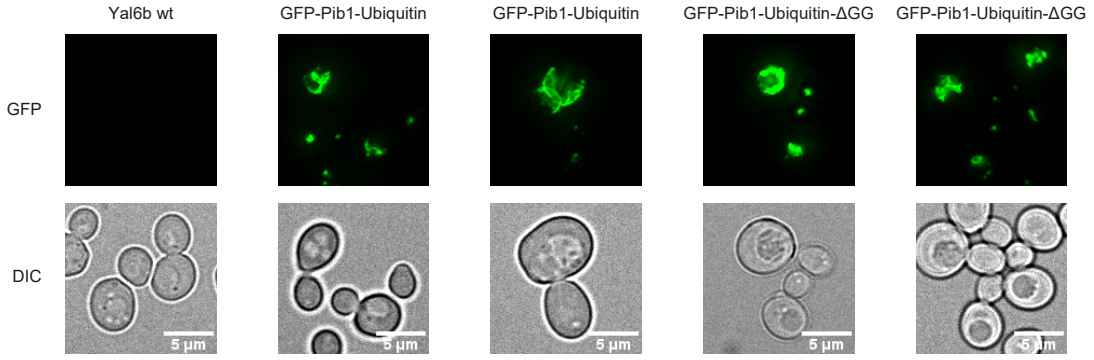

Figure 19: Localisation of GFP-tagged Ubait constructs. GFP-Pib1-ubiquitin and GFP-Pib1-ubiquitin-ΔGG Ubait constructs expression was induced by switching cells to Galactose containing media for 4 h. Fluorescent and light microscopy images of exponential growing living cells were taken. Ubait constructs seem to localize to the vacuolar membrane like it is described for Pib1.

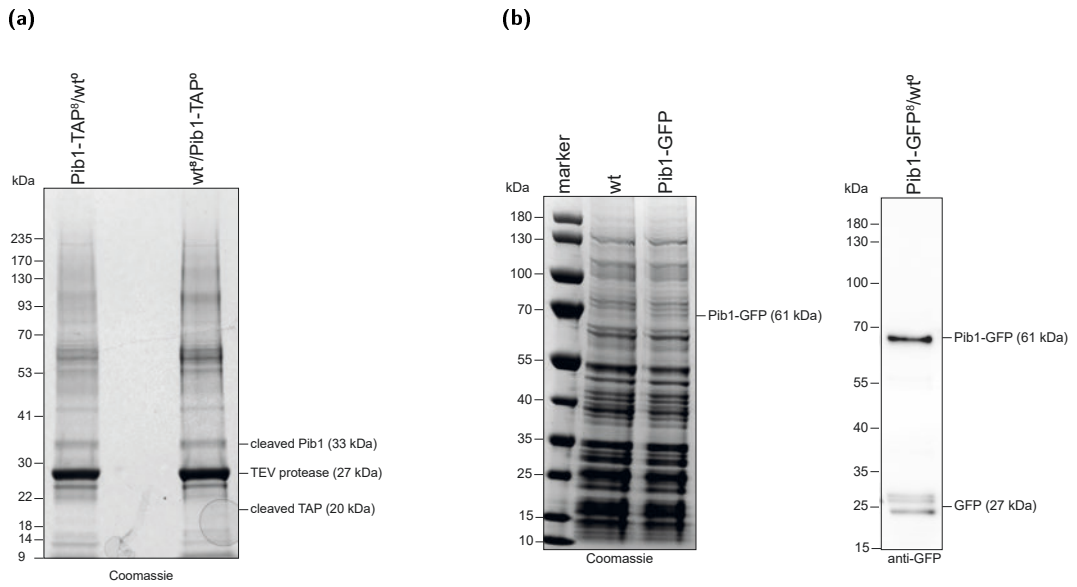

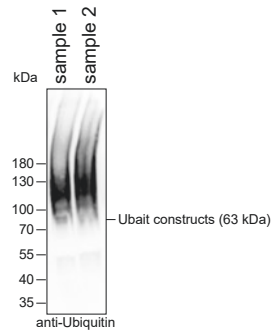

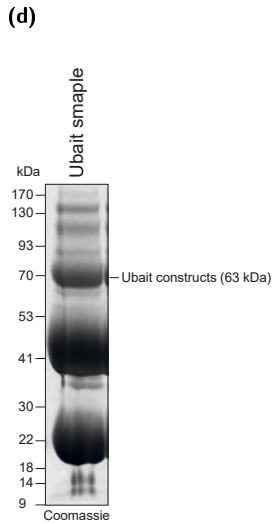

Figure 20: (a) PD for MS screen to identify interactors of endogenously TAP-tagged Pib1. Coomassie-stained gel with elutions of Pib1-TAP constructs and their interactors after pull-down with IgG sepharose beads from yeast lysate using 80 µL slurry per 10 mg protein. Elution was done by cleavage of the TAP tag with a TEV protease. Samples on the Coomassie gel contain the mixed elutions from beads incubated with an extract from strains expressing TAP-Pib1^{8} and *WT*^{0} or the label swap experiment. Cleaved Pib1 should be is visible at 33 kDa. **(b) PD for MS screen to identify interactors of endogenously GFP-tagged Pib1.** Coomassie-stained gel (left) and Western blot (right) with elutions of Pib1-GFP constructs and their interactors after pull-down with GFP nanobody coupled agarose beads from yeast lysate using 13 µL slurry per 10 mg protein. Elution was done by heating samples at 65 °C for 10 min in 2x NuPage loading dye containing 1 mM DTT. Samples on the Coomassie gel contain the elution from the extract from *WT* cells or cells expressing the Pib1-GFP construct loaded separately. Pib1-GFP should be visible at 63 kDa. Western blot samples contain the mixed elutions from beads incubated with an extract from strains expressing TAP-Pib1^{8} and *WT*^{0}. The blot was developed with an antibody against GFP. The Pib1-GFP construct is visible at 61 kDa. **(c) Western blot from first MS screen to identify substrates of Pib1 using the Ubait method.** Western blot with elution of Ubait constructs after two rounds of pull-down with IgG sepharose from yeast lysate using 30 µL slurry per 10 mg protein. Elution was done by heating samples at 65 °C for 10 min in 2x NuPage loading dye containing 1 mM DTT. Sample 1 contains mixed elution from beads incubated with an extract from strains expressing TAP-Pib1^{0}, TAP-Pib1-I227A-ubi^{4} and TAP-Pib1-ubi^{8} constructs. Sample 2 contains mixed elution from beads incubated with an extract from strains expressing TAP-Pib1^{0}, TAP-Pib1-ubi-ΔGG^{4} and TAP-Pib1-ubi^{8} constructs. The blot is developed with an antibody against ubiquitin. Ubait constructs might be conjugated and therefore visible as a smear above 63 kDa. **(d) Coomassie gel from second MS screen to identify substrates of Pib1 using the Ubait method.** pull-down was done as described in (c). Only that a higher amount of extract (320 mg) and 15 µL slurry per 10 mg protein were used. Coomassie gel, which contains mixed elution from IgG beads incubated with an extract from strains expressing TAP-Pib1^{0}, TAP-Pib1-ubi-ΔGG^{4} and TAP-Pib1-ubi^{8} constructs. Ubait constructs are visible at 63 kDa.

3.1.5 Discussion about difficulties while identifying substrates or interactors of Pib1 and outlook

Unfortunately, I was not able to confirm any of the interactors (or interactors of interactors) identified by Y2H as substrates of Pib1-dependent ubiquitination (table 14). Moreover, new substrates that are specifically ubiquitinated by Pib1 were not found in this work. The main suspect Snc1 turned out not to be ubiquitinated directly by Pib1 in my hands.
An earlier claim regarding K63-linked Snc1 ubiquitination by Pib1 was made by Xu *et al.* (2017),[117] who observed a redundant function of Pib1 and Tul1 in COPI-mediated vesicle sorting of ubiquitinated Snc1, for its recycling to the plasma membrane. Deletion of *PIB1* and *TUL1* inhibited Snc1 recycling, and fusion of a non-specific deubiquitinating enzyme to Pib1 or Tul1 interfered with Snc1 ubiquitination and trafficking.
However, by direct observation of its modification pattern, I found no defect in Snc1 ubiquitination in the *PIB1* and *TUL1* single and *PIB1/TUL1* double deletion strains, which suggests an indirect effect of the ligases on vesicle trafficking rather than any involvement in ubiquitin conjugation to the v-SNARE. Moreover, the observed effect on Snc1 ubiquitination by the E3-DUB fusions could be caused by the proximity of the ligases to Snc1, in the membranes of the endosomes, but they do not prove an enzyme-substrate relationship. The mislocalization of Snc1 in a *PIB1/TUL1* double deletion strain might also result from indirect effects on protein trafficking through the abolishment of the two E3s and not from direct ubiquitination defects on Snc1.
My results suggest a Bsd2 independent ubiquitination of Snc1 by Rsp5, rather than a direct action of Pib1 and/or Tul1 for modification of Snc1 with K63-linked ubiquitin chains.

Reggiori *et al.* (2000, 2001, 2002)[116,397,398] found that the introduction of a polar residue into the TMD of Pep12 (Pep12-L271D) enhances its ubiquitination and vacuolar degradation. The observed ubiquitination was partly abolished in a *TUL1* deletion strain and the sorting of Pep12-L271D into MVB was partly abolished in strains lacking Ubc13/Mms2. Assuming that the band I observed in the PD samples really originated from ubiquitinated Pep12 and not from background binding of the unmodified proteins to the beads, I was able to confirm ubiquitination of Pep12 or Pep12-L271D mutant in cells lacking *DOA4*. Ubiquitination was abolished in *DOA4/PIB1*, *DOA4/TUL1* or *DOA4/PIB1/TUL1* deletion strains, indicating for a redundant role for Pib1 and Tul1 in Pep12 ubiquitination, and explaining why Reggiori *et al.* could only see a partial effect when deleting *TUL1*.
Additionally, these results point me to the idea to repeat the PD for the other possible Pib1 interactors in *DOA4* deletion strains, as Pep12 ubiquitination was only visible in these samples, but not in *WT* strains (compare fig. 15a, lane 4 with fig. 15b, lane 4).

This would make sense as Doa4 is the deubiquitinase responsible for removing K63-linked chains in the endocytic pathway, before substrates enter the MVB[399–401] and its deletion would therefore prevent deubiquitination of Pib1s substrates. Therefore, an effect of Pib1 deletion would be more prominently visible as it could not be masked by deubiquitination of the substrates.

Table 14: Results from PD experiments of possible substrates of Pib1.

Protein name	Published ubiquitination	Ubiquitination detected	Ubiquitination dependent on Pib 1
Gos1	ubiquitinated after oxidative stress detected in MS by Silva *et al.* (2015)[389]	Yes	No
Pep12	Pep12-L271D mutation enhances ubiquitination and vacuolar degradation, partly dependent on Tul1 and Ubc13/Mms2 by Reggiori *et al.* (2000, 2001, 2002)[116,397,398]	Yes	possibly
Sec3	K48-linked ubiquitination by Pib1 for proteasomal degradation in *Schizosaccharomyces pombe* by Kampmeyer *et al.* (2017).[391]	Yes	No
Sec4	ubiquitination detected in MS screens[115,389,402,403]	No	not determined
Snc1	K63-linked ubiquitination by Pib1 and Tul1 by Xu *et al.* (2017)[117]	Yes	No
Vps21	ubiquitination detected in MS screens[115,389,402,403]	No	not determined
Vti1	ubiquitination detected in a MS screen using Rsp5-Ubait by O'Connor *et al.* (2015)[392]	No	not determined
Ypt1	ubiquitination detected in MS screens[115,389,402,403]	No	not determined
Ypl162c	ubiquitinated by Pib1 for degradation via the MVB pathway by Yang *et al.* (2020)[119]	not determined	not determined

The Pib1 homologue from *Schizosaccharomyces pombe* was reported to target a subunit of the exocyst, Sec3, for proteasomal degradation. This degradation was thought to be caused by partial unfolding and the attachment of K48-linked ubiquitin chains to the protein.[391] However, I could not identify any reduction in ubiquitination of Sec3 in *S. cerevisiae* strains lacking Pib1, Tul1 or both. These results point to the conclusion that Sec3 is not ubiquitinated by Pib1 or Tul1 in *S. cerevisiae*, or at least not exclusively. This is supported by the fact that Pib1 has never been described as playing a role in K48-ubiquitination for proteasomal degradation, as it seems to be specific for the formation of K63-linked ubiquitin chains.[99] A degree of redundancy between Pib1 and other E3s (including Rsp5) was noted in the described study by Kampmeyer *et al.* (2017),[391] and a contribution of vacuolar degradation was not rigorously excluded, thus leaving open the possibility that multiple degradation systems act on Sec3.

In my PD experiments, I could confirm the described observation that Gos1 is ubiquitinated after oxidative stress.[389] I even saw Gos1 ubiquitination without oxidative stress

treatment, but neither a deletion of *PIB1* or *TUL1* or both abolished it. Therefore, it is likely that these are not the corresponding E3 enzymes for its ubiquitination or at least not exclusively.
For Vti1, Ypt1, Sec4 and Vps21, which have only been described to be ubiquitinated in mass spectrometry-based screens,[115,389,392,402,403] I could not find conditions, in which their ubiquitination was visible. This might be caused by a very low abundance of ubiquitination in untreated or H_2O_2 treated cells. A repetition of the experiment under different conditions to induce more vacuolar degradation or upon deletion of *DOA4* could be considered.

In a newer study, Yang *et al.* (2020) describe Ypl162c, a putative vacuolar membrane transporter, as a substrate of Pib1. Supposedly, it is ubiquitinated by Pib1 for its degradation via the MVB pathway and that the protein levels of Pib1 were modestly increased after natural starvation.[119] These observations further support our suggestion that Pib1 plays a role in K63-linked ubiquitination of proteins for vacuolar degradation. However, as described in other studies before,[114,115,117,118] the authors also observed a high (but not complete) redundancy of Pib1 with Rsp5 and Tul1 for the ubiquitination of Ypl162c. This redundant action makes it very difficult to identify specific substrates for Pib1.

All in all, my described results go in line with previous findings from our lab and others that provide evidence for the action of Pib1, and possibly additional E3s, in K63-linked polyubiquitination at endosomal and vacuolar membranes marking proteins for their vacuolar degradation.[99,116,117,119]
However, my several attempts using proteomic analysis have failed to reveal any direct physiological interactors and substrates of Pib1. I identified three main reasons for that.
First of all, it is well established that delivery of membrane proteins to the vacuole requires multiple ubiquitination events at various stages and on many different targets, not limited to the cargo proteins themselves. One possible reason for the deficiency in identifying interactors or substrates of Pib1 might therefore be a high degree of redundancy between the ubiquitin conjugation factors involved in the endocytic pathway, possibly even extending over the described ones for Rsp5, Pib1 and Tul1.[114]
Secondly, Pib1 is an E3 that extends an existing ubiquitin moiety by K63-linkage but does not initiate *de novo* ubiquitination on a substrate,[99] making it difficult to pinpoint Pib1s actions to a specific target besides ubiquitin itself.
And finally, a technical difficulty derives from the fact that Pib1 is a membrane-associated protein, which is a class of proteins that have been reported to be difficult to analyse by MS, because of their low abundance and solubility.[406]
Targets of Pib1 might be found by repeating the pull-down of GFP-tagged Pib1 after isolating vacuoles,[407] using more detergent during cell lysis, or other described methods for membrane protein isolation.[408,409] Furthermore, better results might be gained

by overexpressing Pib1 prior to the extraction, using a physiological (so far unidentified) stimulus to induce Pib1-dependent ubiquitination, or performing the experiment in *DOA4* deletion strains to prevent deubiquitination of Pib1s substrates.

3.2 Characterisation of the ubiquitin-binding properties of Spc25

The Spc24/Spc25 heterodimer is part of the Ndc80 complex in the central kinetochore. In previous work from the [redacted] lab, the essential kinetochore component Spc25 has been identified as harbouring a so-far unknown ubiquitin-binding domain. Additionally, ubiquitination of various kinetochore proteins was found, but the type of ubiquitination was not analysed. This raises the possibility of a proteasome-independent function of ubiquitin at kinetochores. In this context ubiquitin binding of Spc25 might be required for maintaining the stability of the kinetochore complex.
This project aimed to uncover the interaction interface and exact binding site between Spc25 and ubiquitin variants (Ub*), that were raised to have a stronger binding affinity to Spc25 than *WT* ubiquitin. Pull-down assays, size exclusion chromatography and affinity determination by fluorescence polarisation assays showed that the ubiquitin variants have a stronger binding ability to Spc25 compared to *WT* ubiquitin. However, the interaction is still too weak to determine an exact biding constant. Moreover, the identification of the binding site of Spc25 on variant A12 was not successful, because the purified Spc24/25 protein complex was not stable enough in the high concentration that is needed for NMR measurements.
The knowledge of the exact interaction site between Spc25 and ubiquitin could be applied to analyse the physiological relevance of this interaction including the substrates, and ubiquitinating enzymes. Spc25 mutants that do not bind *WT* ubiquitin, could be used for phenotypic analysis in yeast to gain insights into the functional aspects of ubiquitin-binding at kinetochores. Moreover, dominant-negative expression of the better binding ubiquitin variants could elucidate details about the function of ubiquitin-binding of Spc25 *in vivo*.

3.2.1 Background and aim of this project

Previous lab members have started to characterize the binding of Spc25 to ubiquitin *in vitro* and *in vivo*. Spc25 was identified as a ubiquitin binding protein in a Y2H screen conducted by [redacted] in our lab ([redacted] lab). As its structure does not show any similarity to known ubiquitin-binding domains, [redacted] aimed on determining the minimal region required for the interaction of Spc25 with ubiquitin. According to his Y2H experiments, the flexible linker (aa107-132), as well as the globular domain (aa133-221), are necessary for binding (fig. 5c). His experiments in *S. cerevisiae* showed an interaction only with tetra-ubiquitin molecules, in which the single molecules were connected by a linker region (aa sequence VQIQ).[148] A binding of human Spc25 to ubiquitin tetramers could not be detected in Y2H assays so far (experiments by [redacted]

and [redacted], [redacted] lab).[149,410]
To confirm the presence of a direct interaction [redacted] also performed binding experiments with a purified Spc24/25 complex and different purified ubiquitin constructs. In the pull-down assays again an interaction was visible, not only with the linear tetra-ubiquitin construct but also with mono-ubiquitin and di-ubiquitin molecules. Further *in vitro* experiments showed a weakening of the interaction if Isoleucine-44 of ubiquitin was mutated to Alanine (I44A), and no interaction with K48- or K63-linked ubiquitin chains. [redacted] therefore, concluded that Spc25 binds preferably mono-ubiquitin and the interaction with linear tetra-ubiquitin chains could be caused by the availability of multiple mono-ubiquitin units, while in naturally linked chains (K48- and K63-chains) are not recognized because of their different conformation compared to the artificial linear construct.[148]
Many UBD-containing proteins bind to the conserved "hydrophobic pocket" on ubiquitin, which is located around Isoleucine-44 (I44).[68] The failure of binding after the induction of an I44A mutation, gives indications about a hydrophobic interaction mode between the β-sheets around I44A of ubiquitin and the Spc25 complex.[148] An additionally identified disruption of the interaction between Spc25 and ubiquitin in Y2H, if Leucine-109, Leucine-113 and Arginine-116 or Leucine-109, Leucine-112 and Valine-121 of the flexible linker region in Spc25 were mutated to Arginine, was not confirmed *in vitro*. Even, if all three residues were mutated the binding ability was still present, yet weaker, indicating for a second important interaction surface, within the globular domain of Spc25 (experiments by [redacted], [redacted] lab).[410,411]

Altogether these *in vitro* results suggest a role for proteasome-independent ubiquitin signalling at kinetochores. In this context ubiquitin binding of Spc25 might be required for maintaining the stability of the kinetochore complex. This was supported by the finding of [redacted], who showed that budding yeast cells expressing Spc25 with an L109A mutation exhibited a growth defect when combined with GFP-tagged Mcm21 (protein of the COMA complex). Furthermore, Spc25 L109A mutation increased the temperature sensitivity for mutant alleles of *DSN1, SPC105, NUF2, NDC80* and *SPC24*.[149]
Finally, [redacted] found that the Spc25 L109A mutant shows chromosome segregation defects, if the spindle assembly checkpoint (SAC) was perturbed as well. However, the Spc25 L109A mutant alone or the described triple mutants were viable, showed no differences in colony sizes compared to *WT* strains, no temperature sensitivity and did not have defects in spindle checkpoint function or chromosome segregation.

Nevertheless, many open questions remain regarding the function of ubiquitin at kinetochores. Relating to the previous findings, it would be interesting to find the functional link between all the phenotypes that were observed and ubiquitin-binding. Previous

trials to identify the interaction interface between Spc25 and *WT* ubiquitin by NMR (cooperation between [redacted] ([redacted] lab, IMB Mainz) and [redacted] ([redacted] lab, University of Frankfurt)) have not been successful. Therefore, [redacted] ([redacted] lab, University of Toronto) conducted a phage display assay with the Spc24-FL/Spc25-FL complex (FL full length protein) and the Spc24-glob/Spc25-CTD complex (CTD C-terminal domain) as the bait protein. From these, he provided us with six ubiquitin variants with a higher affinity for Spc25 (fig. 21).

This project aimed to uncover the interaction interface and exact binding site using Spc25 and a ubiquitin variant, as we expected this interaction interface to resemble the native interface. The methodical outline involved pull-down assays and affinity determination by FP-Assay to confirm the binding of the ubiquitin variants to the different Spc25 constructs. If a considerable better binding of the variants to Spc25 compared to wild-type ubiquitin could be observed, the characterisation of the binding interface and the amino acids responsible for binding by NMR should be repeated.
After their *in vitro* characterization, the ubiquitin variants could be used for phenotypical studies in yeast by expressing dominant-negative versions. If the binding interface was known, further functional studies could be performed using mutated versions of Spc25 and ubiquitin to elucidate functional aspects of ubiquitin binding at kinetochores and the function of the ubiquitin system around Spc25. Therefore, strains expressing Spc25 mutants that do not bind *WT* ubiquitin would be created followed by their phenotypic analysis.

The C-terminal part of the Ub* variants harbours several amino acids with a high divergence from *WT* ubiquitin and low variabiliy

We compared the amino acid sequence of *WT* Ub and the Ub* variants, to gain insights into the changes in the ubiquitin variants that might have influenced their binding strength to Spc25 (alignment performed by [redacted]). The comparison was based on the information in the publication describing the original phage screen (fig. 21).[166]
In the structural model of *WT* ubiquitin we tried to localize the stronger binding ability of the variants on the surface of ubiquitin. However, this was quite difficult as they were highly mutated.
The amino acids in the C-terminal part of ubiquitin, with high divergence, but low variability (shown in purple, fig. 21) were of most interest here, as they are different from the *WT* Ub sequence in all variants, but very similar in their mutations in the different variants, indicating that they play a role in improving the binding to Spc25 when mutated. In the structural model, they are located next to the Isoleucine-44 and therefore in the hydrophobic patch of ubiquitin. Additionally, amino acids with low variability, but high divergence can be found in the last 4–5 positions of each variant sequence, indicating that this part might be involved in Spc25 binding as well.

It should also be noticed that the strong interactors B16 and A12 (see section 3.2.2) both have a mutation in Isoleucine-44, which was previously shown to weaken the interaction with Spc25 if mutated to Alanine. In accordance with what was described for other ubiquitin variants,[179] the mutations they harbour mostly do not change the charge, but influence the size of the amino acids. In variant B16, I44 is mutated to Valine. This does not change the polarity of the residue but is a bit bulkier. In A12 the change in the size of the amino acid was even more pronounced as I44 was mutated to phenylalanine. The amino acids that lie in the folded protein next to I44 (T66 and V70) were mutated in both variants to Serine and Leucine. This does not change the polarity of the residues but again makes them bulkier.
In all variants, the C-terminus is extended by one to two amino acids. This is caused by the fact that the initial PCR template, which was used for mutagenesis in the Sidhu lab was elongated by two residues. In contrast to the normal glycine residues, the new amino acids in the variants make their C-terminus polar and negatively charged (with Serine and Aspartate/Glutamate at positions 74 and 75) and more bulky (with residues Leucine/Phenylalanine and Tryptophane at positions 76 and 77).

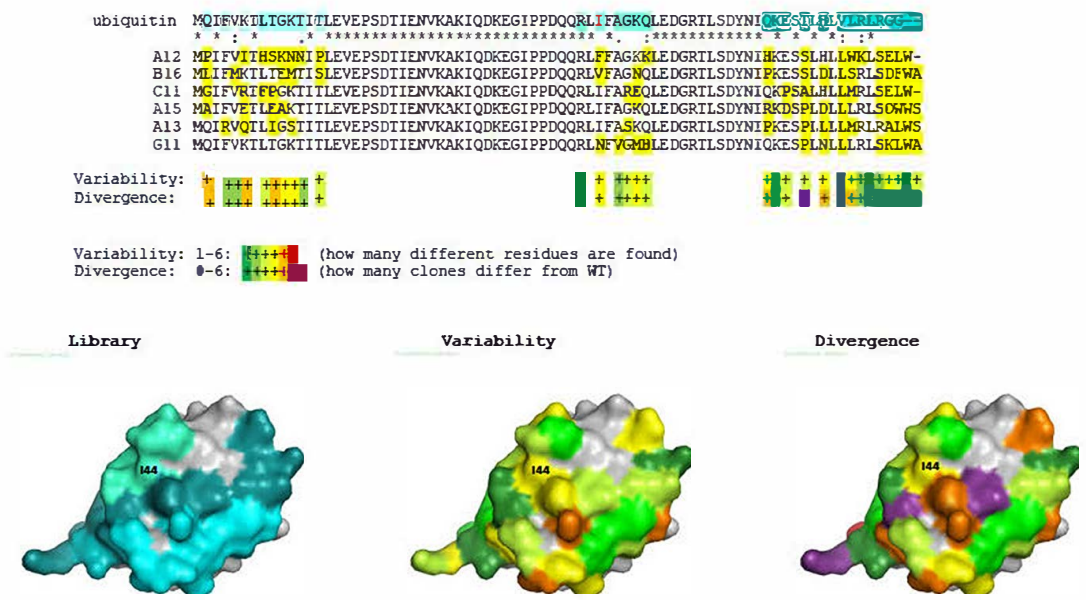

Figure 21: Alignment of ubiquitin variants and wild-type ubiquitin and structural models of ubiquitin. Colours are showing the variability (how many different residues are found) and divergence (how many clones differ from *WT*) of the ubiquitin variants compared to *WT* ubiquitin (adapted from a figure made by Helle Ulrich and based on information from Ernst *et al.* (2013)).[166] In the sequence alignment identical amino acids in all proteins are marked by an asterisk (*). A colon (:) indicates conservation between groups of strongly similar properties and a period (.) indicates conservation between groups of weakly similar properties. The lower panel shows the structural view focused on the hydrophobic patch of ubiquitin. The structures were generated by Helle Ulrich using PyMol.

3.2.2 Ubiquitin variants have a stronger binding affinity to Spc25 compared to wild-type ubiquitin

First of all pull-down assays with different Spc24/25 constructs and ubiquitin were performed to confirm its interaction with *WT* ubiquitin and binding of the received ubiquitin variants. Therefore, GST-tagged, as well as His-tagged Spc25, was purified (table 15). Spc25 is only stable during purification in complex with Spc24 as shown by [redacted] (2005) and [redacted] (2010).[144,148] As binding partners *WT* mono- and di-ubiquitin and the received ubiquitin variants were purified as GST-FLAG tagged and FLAG-tagged versions (section 2.2.5). The triple mutant of Spc25 (L109A, L112A, V121A), as well as the I44A mutant of ubiquitin, were shown to weaken the interaction between Spc25 and ubiquitin. Therefore these two constructs were also included in the analysis.
Pull-down assays were performed with each binding partner coupled to GST, while the other binding partner was free in solution and *vice versa* (section 2.2.7). Analysis of bound proteins was done by SDS-PAGE followed by Western blotting. In figure 22a the binding of His-Spc25-FL to the GST immobilised ubiquitin or ubiquitin variants is shown. In figure 22b the binding of His-Spc25-C-terminal domain (CTD) to the FLAG immobilised ubiquitin or ubiquitin variants is shown. Figures 23a and 23b represent the results from the assays in the other direction. Here the FLAG-tagged ubiquitin or ubiquitin variants were free in solution, while the globular domain or the C-terminal domain of Spc25 were immobilised on GST. Also, the triple mutant of Spc25-CTD was included in some experiments (fig. 23b). The experiments have been conducted with Spc24/25 constructs of various lengths, to limit the binding site of the variants to the CTD, as was shown for *WT* ubiquitin by [redacted].[148] Additionally, experiments in both directions were conducted to overcome possible unspecific interaction with the immobilisation material or blocking of binding sites by immobilisation. Moreover, the PD was conducted using differently tagged proteins, to avoid interaction resulting from binding to the tag.

Overall the conducted pull-down assays confirmed the binding of Spc25 to mono- and di-ubiquitin (fig. 22a lanes 5 and 6). As shown in earlier experiments the affinity of Spc25 to di-ubiquitin was slightly higher compared to mono-ubiquitin (fig. 22a lanes 5 and 6). As described before the I44A mutation in ubiquitin weakens the interaction between ubiquitin and Spc25 (fig. 22a lanes 3 and 4), indicating for an interaction on the hydrophobic patch of ubiquitin by Spc25.
The main outcome from the pull-down assays was, however, that the ubiquitin variants showed stronger binding to Spc25 than wild-type ubiquitin. This increased binding is visible regardless if the variants or the Spc24/25 complex is immobilised and even so if the variants are GST or FLAG-tagged (figs. 22a, 22b, 23a and 23b). In contrast to wild-

Table 15: Proteins purified for pull-down assays. Proteins written in the same row were co-expressed and purified as a complex. *WT*, wild-type; Ub, wild-type ubiquitin; 2Ub, dimeric wild-type ubiquitin; Ub*, ubiquitin variant; FL, full-length protein; CTD, C-terminal domain; glob, globular domain; 3M, triple mutant of Spc25 (L109A, L112A, V121A).

protein 1	protein 2
His-Spc25-FL-*WT*	Spc24-FL
His-Spc25-CTD-*WT*	His-Spc24-glob
His-Spc25-glob	His-Spc24-glob
GST-Spc25-CTD-*WT*	His-Spc24-glob
GST-Spc25-CTD-3M	His-Spc24-glob
GST-Spc25-FL-*WT*	Spc24-FL
GST-Spc25-glob	His-Spc24-glob
GST-FLAG-Ub*	–
GST-FLAG-Ub-*WT*	–
GST-Ub-*WT*	–
GST-2Ub	–
GST-Ub-I44A	–
FLAG-Ub*	–
FLAG-Ub-*WT*	–

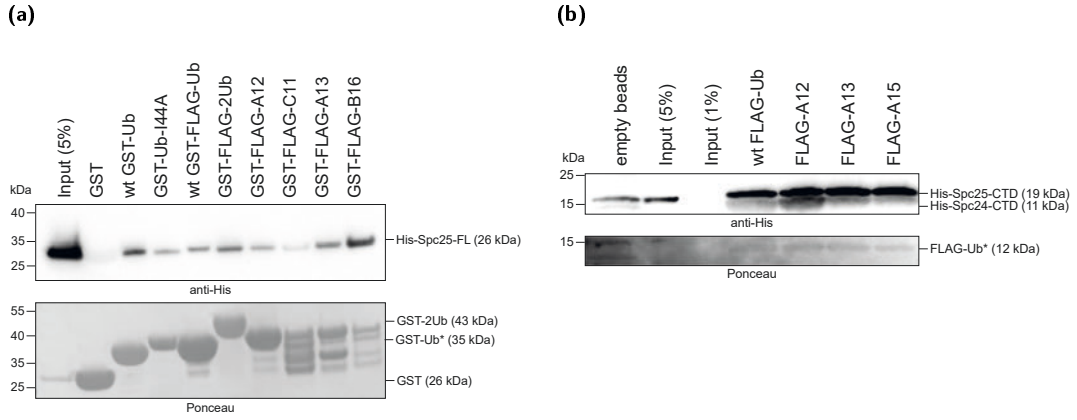

Figure 22: **(a) Pull-down assay of GST immobilised ubiquitin incubated with His-Spc25-FL/Spc24-FL.** 10 µM ubiquitin variants (Ub*), *WT* ubiquitin (Ub) or dimeric *WT* ubiquitin (diUb) were immobilized on 25 µL equilibrated GSH-beads and 10 µM Spc24/25-full-length (FL) constructs were added. Elution was performed by boiling the samples for 5 min at 95 °C. 5 % input of the Spc24/25-FL constructs were loaded additionally to the samples. The western blots were developed with an anti-His-tag antibody. As a loading control, the membrane was stained with Ponceau red after exposure. All ubiquitin variants, *WT* ubiquitin and di-ubiquitin pull out Spc25-FL. No background binding to beads with GST only was detectable. **(b) Pull-down assay of FLAG immobilised ubiquitin incubated with His-Spc25-CTD/His-Spc24-glob.** The assay was performed as under (a) only that anti-FLAG beads were used for immobilisation and the C-terminal domain of Spc24/25 was used. All tested variants and *WT* ubiquitin were able to pull out His-Spc24/25-CTD from the solution. Some background binding to empty beads was detected. Ub, wild-type ubiquitin; diUb, dimeric ubiquitin; Ub*/A12/A13/A15/B16/C11, ubiquitin variants; CTD, C-terminal domain; FL, full-length protein.

type ubiquitin, which only interacts with Spc25 full-length and C-terminal constructs (fig. 22a lane 3 and fig. 22b lane 4), the variants even bind to the globular domain of Spc25 (fig. 23a lanes 4 and 7).
Contrary to the results obtained by Y2H experiments with *WT* Ubiquitin, in pull-down assays the triple mutant of Spc25 interacts to the same extent with the ubiquitin variants as *WT* Spc25 (fig. 23b lanes 5–20). An interaction between *WT* ubiquitin and the triple mutant of Spc25 could not be analysed in this experiment (fig. 23b lanes 1–4), because the exposure was adjusted to the intensity of the pulled-out variants and not *WT* ubiquitin. Therefore the weaker interaction of Spc25 *WT* or the triple mutant with *WT* ubiquitin does not give any signal in the blot. However, [redacted] has shown in his bachelor thesis that the triple mutant of Spc25 does not abolish binding to ubiquitin *in vitro*.[410] Interestingly in the experiment shown here the triple mutant does not show an interaction with A13 (fig. 23b lane 15), while it did so in other repetitions of the pull-down.
Variants B16 and A12 appear to have the strongest binding ability to all Spc24/Spc25 constructs (fig. 23a lanes 5–12). However, B16 was partly insoluble during purification and unstable upon freezing (data not shown), and therefore it was no good candidate for downstream experiments. As a result variant, A12 was used for further assays.

All in all the pull-down experiments show that the ubiquitin variants have a stronger binding affinity to Spc25 compared to the *WT* ubiquitin. The *WT* ubiquitin shows binding to the full-length as well as the C-terminal domain of the Spc25 protein in *in vitro* pull-down experiments, but not to the globular domain of Spc25. In contrast, the variants also bind the globular domain of Spc25 in the performed pull-down assays.

Confirming the PD results that the ubiquitin variants bind to the Spc24/25 complex, I performed size exclusion chromatography for the strong binding variant A12 alone, Spc24-FL/His-Spc25-FL alone and the complex of both (fig. 24a and fig. 24b). In the gel filtration profile of the complex, a third earlier eluting peak was appearing, containing all three proteins (Peak 1). This indicates for complex formation to happen, as larger protein complexes elute earlier from the column. Although the third peak was very small and the binding therefore does not seem to be very strong.

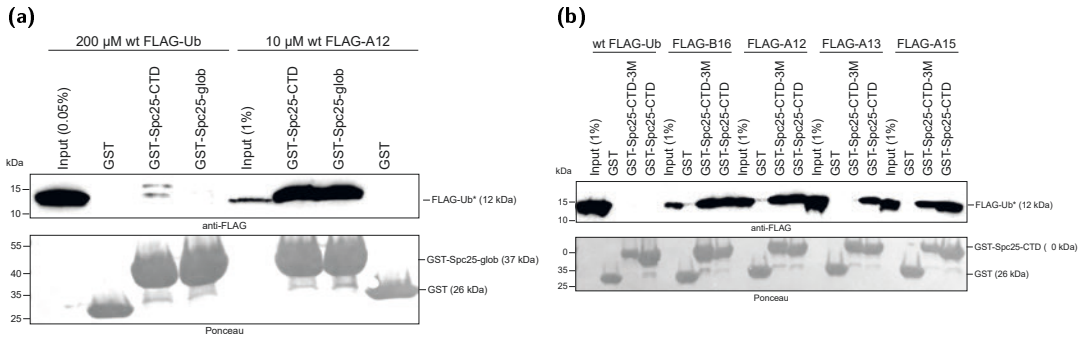

Figure 23: (a) Pull-down assay of GST immobilised Spc25-CTD/His-Spc24-glob and GST bound Spc25-glob/His-Spc24-glob incubated with FLAG-tagged wild type ubiquitin or ubiquitin variant A12. 10 µM C-terminal domain or globular domain (glob) of Spc24/25 were immobilized on 15 µL GSH bead slurry and 200 µM of ubiquitin (Ub) or 10 µM of the ubiquitin variant (A12) were added. Bound proteins were eluted by boiling in NuPAGE buffer at 95 °C. 0.05 % or 1 % input of the ubiquitin constructs were loaded additionally to the samples. The western blots were developed with an anti-FLAG antibody. As a loading control, the membrane was stained with Ponceau red after exposure. *WT* ubiquitin is only weakly pulled out by the Spc25-CTD/His-Spc24-glob, but not by the globular domain of Spc25. The ubiquitin variant A12 binds to the CTD and globular domain of Spc25 equally good. **(b) Pull-down assay of GST immobilised Spc25-CTD/His-Spc24-glob and the triple mutant (3M) of Spc25-CTD-3M/His-Spc24-glob incubated with FLAG tagged Ub variants or *WT* ubiquitin.** 10 µM Spc24/25 constructs were immobilized on 15 µL GSH bead slurry and 10 µM of ubiquitin (Ub) or of the ubiquitin variant (Ub*, A12, A13 or A15) were added. Bound proteins were eluted by boiling in NuPAGE buffer at 95 °C. 1 % input of the ubiquitin constructs were loaded additionally to the samples. The western blots were developed with anti-FLAG antibody. As a loading control, the membrane was stained with Ponceau red after exposure. All ubiquitin variants besides A13, showed an nearly equally strong interaction with Spc25-CTD/His-Spc24-glob and the triple mutant Spc25-CTD-3M/His-Spc24-glob. Unfortunately, *WT* ubiquitin did not show any interaction in this repetition. Ub, wild-type ubiquitin; Ub*/A12/A13/A15, ubiquitin variants; CTD, C-terminal domain; glob, globular domain; 3M, triple mutant of Spc25 (L109A, L112A, V121A).

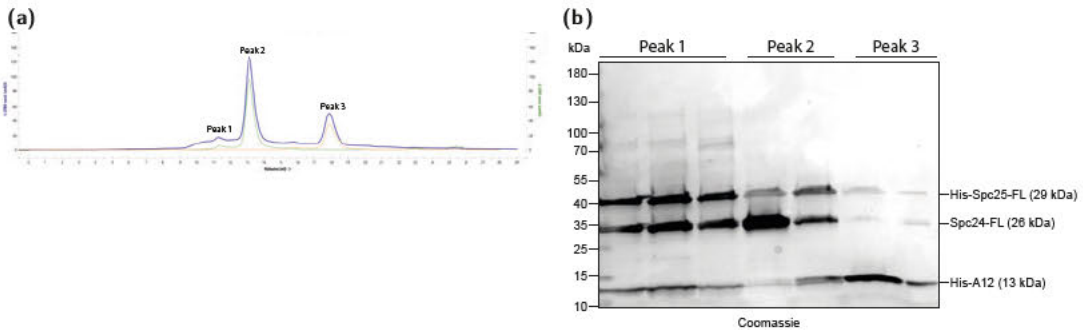

Figure 24: (a) Size exclusion analysis of the ubiquitin variant A12 pre-incubated with His-Spc25-FL/Spc24-FL. 100 µM ubiquitin variant A12 was mixed with 100 µM His-Spc25-full-length (FL)/Spc24-FL and run over a S200 Increase size exclusion column (blue). In addition, runs with the single proteins (His-Spc25-FL/Spc24-FL: green, A12: orange) were performed. The mixture of interaction partners resulted in a small additional peak (Peak 1) in the elution profile indicating for complex formation. **(b) Gel from size exclusion analysis of the ubiquitin variant A12 pre-incubated with His-Spc25-FL/Spc24-FL.** Peak fractions from the blue gel filtration profile run shown in (a) were loaded onto an SDS-gel. Proteins were stained using RunBlue reagent. Peak 1 contains both the Spc24/25 complex and the ubiquitin variant A12. Peak 2 only consists of the Spc24/25 complex and Peak 3 consists of only the ubiquitin variant A12. A12, ubiquitin variant; FL, full-length protein.

3.2.3 The stronger binding affinity is difficult to quantify by fluorescence polarization measurements

Using fluorescence polarization measurements, I wanted to confirm the observations from the pull-down experiments, which showed that the ubiquitin variants have a stronger binding ability to Spc25 compared to *WT* ubiquitin. Moreover, I attempted to measure the exact binding constants between His-Spc25-FL/Spc24-FL and the variant A12 or *WT* ubiquitin.

Wild type ubiquitin and all gained variants do not harbour a cysteine residue. For using maleimide chemistry to attach a fluorophore to the ubiquitin variants, constructs with a CGS sequence between the GST tag and the FLAG tag were cloned and purified. Labelling was done with Bodiby™ TMR C_5-maleimide dye (Thermo Fischer) and measurement was performed in the Tecan fluorescence plate reader (section 2.2.7.6).

Unfortunately, the binding was not strong enough to reach substrate saturation (fig. 25), so no exact K_D determination was possible. The data, however, indicates that in fact, the binding of the A12 variant is much stronger compared to the *WT* ubiquitin. The variant A12 is showing a dissociation constant in the low µM range (approximately 15 µM), while the binding constant to *WT* ubiquitin was determined with 89 µM. As the determination of maximum binding was very rough for both interactions, the calculated K_D are just an approximation. For the interaction between *WT* ubiquitin and Spc25, Shengkai had previously measured a K_D 14.2 µM using surface plasmon resonance measurements. However, this value could not be reproduced in my experiments using the solution-based fluorescence polarisation method.

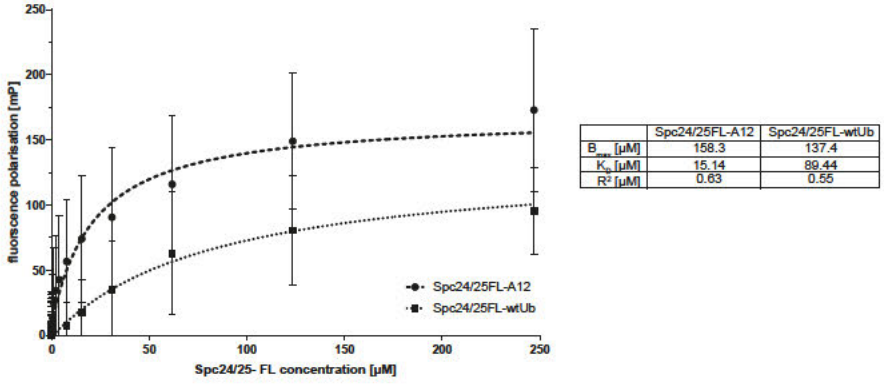

	Spc24/25FL-A12	Spc24/25FL-wtUb
B_{max} [µM]	158.3	137.4
K_D [µM]	15.14	89.44
R^2 [µM]	0.63	0.55

Figure 25: Fluorescence polarisation data of binding between His-Spc25-FL/Spc24-FL and Bodipy-labelled FLAG-A12 ubiquitin variant or FLAG-Ubiquitin (*WT*). A 1:2 dilution series of Spc24/25-FL with a start concentration of 250 µM was mixed with 40 nM of the labelled ubiquitin variant A12 or *WT* ubiquitin. The analysis was performed using the TecanSPARK fluorescence plate reader. Maximal polarisation (B_{max}) and dissociation constants (K_D) were calculated using the GraphPad Prism software, one sided specific, non-linear regression fit. The ubiquitin variant A12 shows an enhanced binding strength (K_D= 15 µM) to the Spc25/24 complex, compared to *WT* ubiquitin (K_D= 89 µM). wtUb, wild-type ubiquitin; A12, ubiquitin variant; FL, full-length protein; B_{max}, maximal polarisation; K_D dissociation constants.

3.2.4 The Spc24/25-C-terminal domain is not stable enough for determining the interaction interface by NMR

We used NMR spectroscopy in collaboration with [redacted] from the [redacted]ab in Frankfurt, to locate the exact binding site of Spc25 on the variant A12 (section 2.2.9). The NMR structure of ubiquitin was solved by Cornilescu *et al.* (1998) [412] and therefore, we expected that annotation of the amino acids responsible for binding in ^{15}N-labelled A12 would be easy. However, by overlaying the HSQC spectrum of ^{15}N-A12 with ^{15}N-Ub *WT* it became clear that the two spectra cannot be directly compared, as the location of the peaks in the spectra was highly different (fig. 26c). Therefore, a complete new annotation would be needed to identify the residues on A12 involved in the interaction with Spc25. Given that this requires deeper knowledge of the NMR technique and is quite time-intensive, this would go beyond the scope of this PhD project.

We attempted to use the CTD of Spc25 (in complex with the globular domain of Spc24) for NMR measurements as it is smaller than the FL protein, but binds better than the globular domain. We used 25 µM or 50 µM ^{15}N-labelled A12, respectively in two different experiments, and mixed it with 100 µM or 500 µM Spc24-glob/Spc25-CTD, respectively. During the measurements, we realised that the C-terminal domain of Spc25/Spc24 was not stable in a concentration adequate for NMR measurements (above 100 µM). It precipitated during concentrating and measurement, and the leftover protein did not appear to be folded, if analysed for its proton spectrum (see supplementary material section 5.2). In the depicted spectra therefore only the signals from the labelled ^{15}N-A12 were visible (experiment 1, fig. 26a).

Even when using freshly purified Spc24/Spc25 and ^{15}N-A12 that was not frozen prior to the measurement, Spc24/Spc25 was behaving in the same way as in the first experiment conducted with thawed proteins. Again, only signals from the labelled A12 variant were detected (experiment 2, fig. 26b).

However, in the NMR spectra from both experiments small chemical shift perturbations (CSP) were visible, which might result from either weak specific interactions or strong unspecific interactions. Yet, small differences in the pH and salt concentration have been detected in both experiments as well, which could also be causing the observed shifts, especially if hydrophobic interactions occur or if the proteins tend to aggregate. Therefore, we were not able to detect any binding between the A12 variant and Spc24-glob/25-CTD by NMR.

A chance to identify at least the binding site of the variants, and most likely also *WT* ubiquitin, on Spc25, would be to do the reverse experiment, using labelled Spc24/25-glob complex and adding highly concentrated A12 for NMR measurements. This would have the advantage that only a concentration of 25 µM of Spc25/Spc24 would be needed, and the more stable ubiquitin variant would be used in a high concentration as a binding

partner. The NMR structure of the Spc24/25 globular domains was solved by Wei *et al.* (2006).[145]

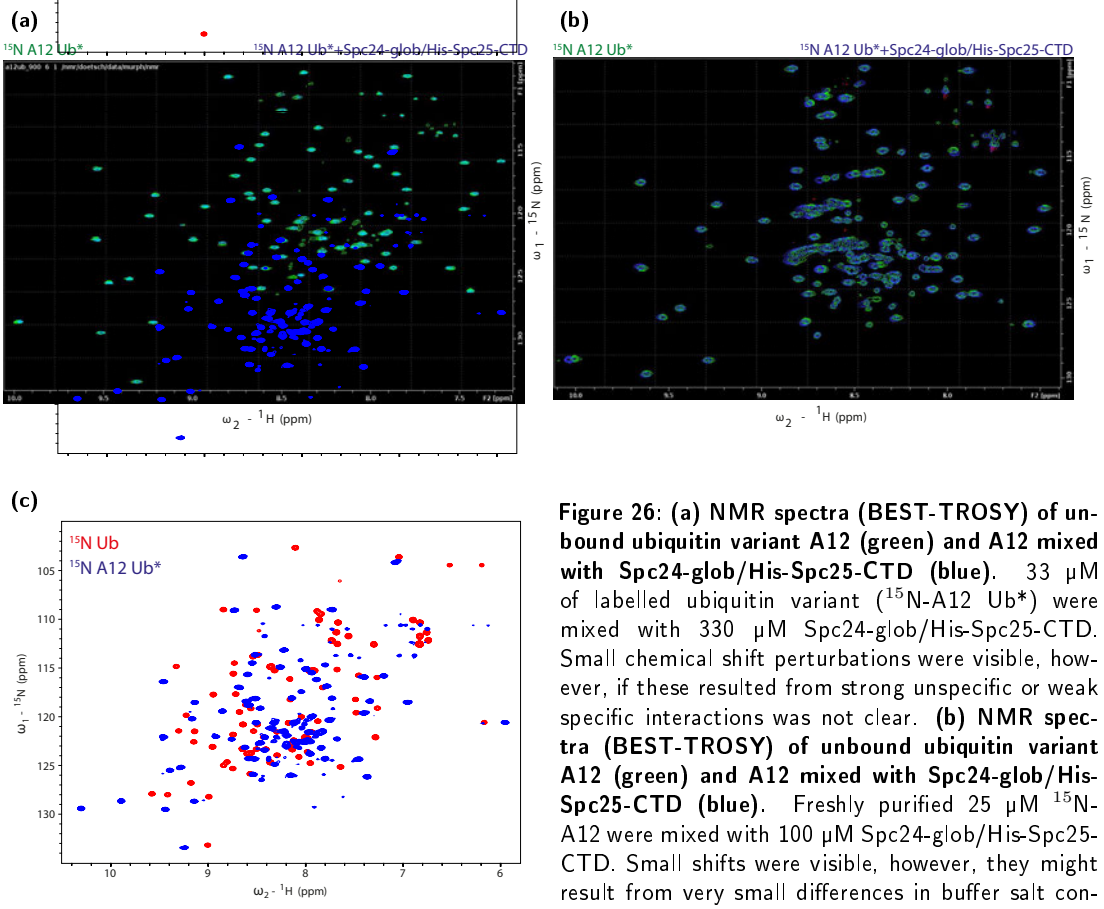

Figure 26: (a) NMR spectra (BEST-TROSY) of unbound ubiquitin variant A12 (green) and A12 mixed with Spc24-glob/His-Spc25-CTD (blue). 33 µM of labelled ubiquitin variant (^{15}N-A12 Ub*) were mixed with 330 µM Spc24-glob/His-Spc25-CTD. Small chemical shift perturbations were visible, however, if these resulted from strong unspecific or weak specific interactions was not clear. **(b) NMR spectra (BEST-TROSY) of unbound ubiquitin variant A12 (green) and A12 mixed with Spc24-glob/His-Spc25-CTD (blue).** Freshly purified 25 µM ^{15}N-A12 were mixed with 100 µM Spc24-glob/His-Spc25-CTD. Small shifts were visible, however, they might result from very small differences in buffer salt concentrations or pH, as the Spc24/25 construct was not properly folded and tended to aggregate. **(c) Overlay of NMR spectra (HSQC) from *WT* ubiquitin and ubiquitin variant A12.** Both proteins were labelled with ^{15}N and used in a concentration of 200 µM. Spectrum of A12 Ub* (blue) differs significantly from the spectrum of *WT* ubiquitin (red), making a new annotation for A12 necessary. Ub, wild-type ubiquitin; Ub*, ubiquitin variant; CTD, C-terminal domain; glob, globular domain.

3.2.5 Discussion and outlook on the ubiquitin binding properties of Spc25

The characterization of the interaction between Spc25 and ubiquitin turned out to be very challenging. The reason for that is that the binding is very weak. Therefore, [redacted] lab, University of Toronto) generated five ubiquitin variants with a higher affinity for Spc25 than *WT* ubiquitin, using a phage display assay.

Previous experiments have shown that Spc25 interacts preferably with mono-ubiquitin or non-native ubiquitin multimers, which are coupled to each other with some distance (linker), but not head-to-tail fusions of ubiquitin. For that reason, the current model predicts mono-ubiquitin as the preferred binding partner of Spc25. Interaction with non-native ubiquitin multimers most likely occurs through the binding of multiple Spc25 to the single-containing ubiquitin subunits.[148,410] Despite the strong indications for Spc25 interacting preferably with mono-ubiquitin, it is not solved yet if it also binds ubiquitin chains with a specific linkage. As a result, mono-ubiquitin or single ubiquitin variants were used for the assays.

I first tested the received variants for their affinity to Spc25 in comparison with wild-type ubiquitin. For this purpose, I performed pull-down experiments and fluorescence polarisation assays. These indeed showed that the ubiquitin variants have a stronger binding ability to Spc25 compared to *WT* ubiquitin.

WT ubiquitin shows binding to the full-length, as well as the C-terminal domain of the Spc25 protein, but not to its globular domain. In contrast, the variants additionally bind the globular domain of Spc25 in the pull-down assays. This different binding behaviour could either be explained by the hypothesis that the interface between the variants and Spc25 is not formed by the same amino acids as with wild-type ubiquitin, or that the binding of the variants is so much stronger than the contribution of the amino acids in the linker region is no longer needed for interaction. The second hypothesis is supported by the proposed model of Spc25 interaction with ubiquitin being mediated on one hand by amino acids in its linker region (especially L109A, L112A and V121A) and on the other hand by amino acids in its globular domain.[148] The model is backed up by the findings that the triple mutant of Spc25 with three mutations in the linker region (L109A, L112A and V121A or L109A, L113A and R116A) only abolishes binding in Y2H, but not in *in vitro* pull-down assays.[148,410] Reasoning that the mutations in the linker only reduced the binding ability of Spc25 to ubiquitin, so that the interaction *in vivo*, where ubiquitin concentrations are much lower than in *in vitro* experiments, is abolished.

In conclusion, I assume that the binding ability of the ubiquitin variants compared to *WT* ubiquitin is still strong enough for interaction with the globular domain even though the participation of the amino acids in the linker are missing.

In a size exclusion chromatography profile a third peak was visible if the strongest binding variant A12 was added to the Spc24/25 complex. This indicates for complex

formation to happen. The third peak was very small, adding to the assumption that the binding is not very strong even with the ubiquitin variant A12.
Fluorescence polarization measurements have been performed to show the exact binding constant between Spc25 and variant A12. Unfortunately, the binding was not strong enough to reach substrate saturation, so no exact K_D determination was possible. However, a considerable better binding of the variant A12 to Spc25 was observed compared to *WT* ubiquitin.
Therefore, the characterisation of the binding interface on A12 and the amino acids responsible for binding in the variant was attempted using NMR. The NMR experiment showed that the CTD of the Spc25 was not stable enough in the concentration used for the unlabelled binding partner for NMR. Moreover, the spectra of the ubiquitin variant A12 differ significantly from the spectra of *WT* ubiquitin, making a new annotation of the peaks necessary. This requires deeper knowledge of protein NMR and is quite time-consuming and therefore goes beyond the scope of this PhD work.
Even though the identification of the binding site on the variant A12 was not successful, it would still be possible to perform the reverse experiment, which determines the binding site of the variant on Spc25, using the construct Wei *et al.* (2006)[145] used for determining the NMR structure of Spc24/25. This construct corresponds to the globular domains of Spc24 and Spc25. As the ubiquitin variants also show binding to these constructs, one should be able to detect their binding site by NMR. Moreover, if the Spc25 complex is labelled instead of the ubiquitin variant, one might be able to directly compare the shifted peaks in the bound form of Spc25 to the unbound form without a new annotation needed.

Once the interaction sites of A12 on Spc25 are known, they need to be confirmed by pull-down assay with A12 and Spc25 harbouring more specific mutations of the responsible residues. Additionally, pull-down experiments with a non-interacting Spc25 mutant could be used to confirm that *WT* ubiquitin binds to the same site on Spc25 like the variant.
Most strikingly, the physiological relevance of this interaction including the substrates, and ubiquitinating enzymes have not been elucidated up to now. As described at the beginning of this chapter (section 3.2.1) previous findings by [redacted] and [redacted],[148,149,411] resulting from His-ubiquitin PD from cell extracts and genetic interactions of the Spc25 L109A mutant, support a model, in which the ubiquitin system around Spc25 might act specifically within the KMN network and other proteins nearby and is important for the stability of kinetochore complexes.
[redacted] showed that Dsn1, Nsl1 and Spc105 of the KMN network and other kinetochore proteins (Mcm21, Mad1, Mad2, Mps1, Ame1, Okp1, Mcm21, Mtw1, Cnn1 and Nuf2) are ubiquitinated. [redacted] further confirmed that mono-ubiquitination of Dsn1 and Spc105 is independent of proteasomal activity. However, the specific ubiquitinated interactor(s) of Spc25 remain unknown.

[redacted] found the E2 and E3 enzymes responsible for attaching ubiquitin chains to Dsn1, however, she could not finally determine, if Ubr2/Rad6 are also responsible for the mono-ubiquitination of Dsn1, as they might act redundantly with other E2/E3s in this case. A throughout analysis of the regulation of other kinetochore-associated ubiquitin targets was not performed so far. This could be done by pull-down of candidates from knockout strains for E2/E3-enzymes, followed by the confirmation of their ubiquitination by Western blot and an optional identification of ubiquitination sites using mass spectrometry.

Spc25 mutants that do not bind *WT* ubiquitin, could further be used for phenotypic analysis in yeast to gain insights into the functional aspects of ubiquitin-binding at kinetochores. Moreover, dominant-negative expression of the better binding ubiquitin variants could elucidate details about the function of ubiquitin-binding of Spc25, by repressing the endogenous ubiquitin signalling at this site. The analysis could also be performed in the different cell cycle stages of yeast or in arrested mutant strains, to elucidate the ubiquitin-binding function throughout the different steps of the cell cycle.

An approach to address whether the ubiquitin-binding of Spc25 is important for the stability of the kinetochore could be, to compare the composition and ubiquitination status of kinetochores in wild-type versus ubiquitin variant expressing strains by mass spectrometry after purification of the kinetochores from yeast cells using a method described by Akiyoshi *et al.* (2009, 2010).[413,414]

A way to further characterise the observed chromosome segregation defects after Spc25 L109A mutant expression, would be live imaging of GFP-labelled chromosomes as described by Straight *et al.* (1996), again using strains expressing the non-ubiquitin binding Spc25 mutant.[415]

Alternatively, in case the NMR approach is not successful, a random mutagenesis of Spc25 could be performed and analysed in a yeast two-hybrid screen with mono-ubiquitin to obtain non-binders that would reveal the interaction surface on Spc25.

Another open question which needs to be answered in the long run, besides the identification of the number and exact location of the binding sites between Spc25 and ubiquitin, is the role of Spc24 in binding ubiquitin. However, so far there has been no direct interaction of Spc24 with ubiquitin or a ubiquitination of Spc24 detected.[148,411]

3.3 Characterization of binders (DARPins) to the yeast SUMO protein

DARPins are genetically engineered antibody mimicking proteins, which can be selected by *in vitro* display techniques. They allow for monitoring and manipulation of targets inside the cell. A set of six DARPins selected for their affinity to the yeast SUMO protein, Smt3, was analysed for the influence on SUMO conjugation, deconjugation and binding *in vitro*. Kinetic measurements and crystallographic approaches complemented these studies. The binders were also analysed for their usefulness and versatility as *in vivo* sensors or inhibitors of SUMO-related processes. Overall, we could show that these DARPins cover a range of affinities and vary concerning their influence on SUMO-related processes. Therefore, the different probes might be used as sensors, inhibitors or affinity reagents to further investigate sumoylation in living yeast cells.

3.3.1 Background and aim of this project: Selection of DARPin candidates for further characterization

When I started on the project we had received 19 DARPin constructs from the [redacted] group in Zurich. They were raised against the SUMO protein from *S. cerevisiae* by ribosome display. [redacted] had started to characterize the binding affinity of these small proteins *in vitro*. He, therefore, purified the constructs and performed pull-down assays with the DARPins. In these, he tried to pull out an overexpressed SUMO construct from *E.coli* lysate, or a purified His-SUMO or His-SUMO-GFP construct from a buffer solution. For each pull-down experiment, the DARPins were immobilised on beads while the SUMO constructs were used as analytes in solution. Nearly all SUMO-specific DARPins showed a high ability to pull out SUMO constructs in all PD set-ups. Moreover, [redacted] performed analytical gel filtration runs (SEC, Size exclusion chromatography) for the complex of SUMO with the DARPins. In the PD as well as in the SEC, all tested constructs except for E10 showed strong affinities to SUMO. DARPin E3.5 was always used as a negative control, as it was not raised against SUMO. Additionally, [redacted] undertook fluorescence polarisation measurements with labelled SUMO and the DARPins. He found their binding affinity to be in the nanomolar range but did not determine the exact binding constants.
[redacted] further characterized the influence of DARPins on the biological functions of SUMO. She found that the binders inhibited the sumoylation of an example substrate *in vitro*, but clearly to a different extent. Her results show that while some DARPins (C10, E11 and G11) still allowed mono-sumoylation of an example substrate (PCNA), poly-sumoylation was affected by all DARPins besides C10. Moreover, [redacted] started to characterize the behaviour of some DARPins, when expressed in *S. cerevisiae*.

All tested DARPins lead to a failure in colony formation after induction of expression from an episomal plasmid under a galactose inducible promotor.
Based on [redacted] results, I selected six SUMO-specific DARPins to further characterise their usability for *in vitro* and *in vivo* experiments.

3.3.1.1 Objective of this project

This part of my thesis aims to characterise selected SUMO-specific DARPins, showing their usability for different approaches in yeast cells. For that their characteristics *in vitro* (section 3.3.2) should be analysed using, on one hand, interaction assays (like pull-down assays or SPR measurements) and activity assays (like de-/sumoylation assays and thioester formation assays) *in vitro*. Moreover, the exact binding site of selected DARPins to SUMO should be determined (section 3.3.3). To characterize the properties of the DARPins *in vivo* (section 3.3.4) growth analysis and detection of sumoylated species *in vivo* should be performed. Finally, their versatility for inhibition of sumoylation (section 3.3.4.4) and detection of sumoylated species (section 3.3.4.5) in *S. cerevisiae* should be proven in exemplary experiments.

3.3.2 *In vitro* characterization of DARPins

A thorough characterization of the DARPins *in vitro* is important to be able to select highly specific DARPins with either inhibitory effects to use them for blocking sumoylation in cells, or DARPins without effect on the sumoylation cascade for using them as sensors or affinity reagents in yeast. Moreover, it is essential to be able to interpret observations from *in vivo* experiments and identify and exclude unwanted behaviour, such as inhibition of (de-) sumoylation or SIM interaction by DARPins used as sensors or off-target binding that resulted from the probes.

3.3.2.1 SUMO-specific DARPins pull out native SUMO from cell extracts

This section aims on showing the specificity of the DARPins for SUMO and on completing the picture gained from [redacted] pull-down experiments, in which he showed the interaction of DARPins with different recombinantly expressed and purified SUMO constructs.
Therefore, I immobilized the purified DARPins on beads and incubated them with native yeast cell extract (section 2.2.7.4, fig. 27). Beads without DARPin conjugated to them or with the control DARPin E3.5 conjugated, do not pull out SUMO from

the extract (fig. 27 lanes 1 and 2). All selected SUMO-specific DARPins were able to pull-down free SUMO from, and thereby reduce the amount of it in, yeast extract as determined by Western blot. A10 and F10 deplete mono-SUMO nearly completely from the extract (fig. 27 lanes 3 and 5), while C10, E11, G11 and B12 do not (fig. 27 lanes 4, 6, 7, 8). This result gives indications that A10 and F10 are more strongly interacting with SUMO than E11, G11, B12 and especially C10.

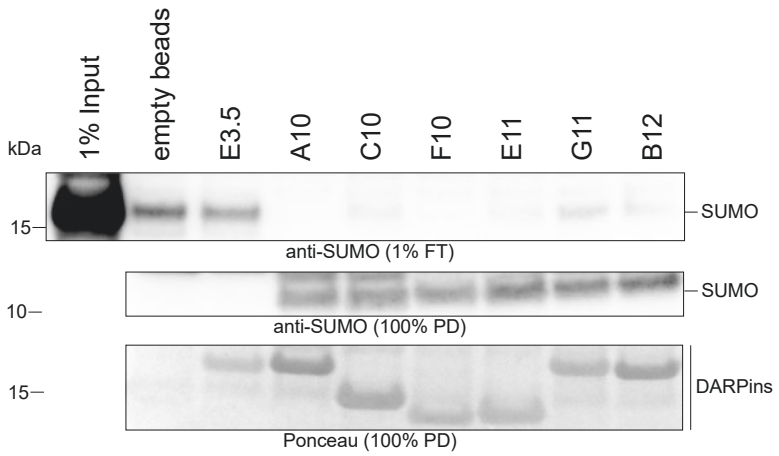

Figure 27: Pull-down (PD) of endogenous SUMO from yeast extract. An excess of DARPins were coupled to Ni^{2+}-NTA-agarose beads and incubated with 1 mg yeast extract for 2 h. Elution was done by boiling in SDS loading buffer. 1 % input and 1 % flow through (FT) were loaded additionally to the samples. Both Western blots were developed with yeast SUMO-specific antibodies. Beads without DARPin conjugated to them or with the control DARPin E3.5 conjugated, do not pull out SUMO from the extract. The other tested DARPins were able to pull out SUMO.

3.3.2.2 DARPins show different affinities and kinetics for SUMO binding

Already the SEC, which were performed by [redacted] indicated very different affinities of the different DARPins to SUMO. To determine the exact binding constant and kinetics surface plasmon resonance experiments were performed using a BIACORE instrument. SUMO was biotinylated using an AVI-tagged template gene and coexpressing it with the BirA enzyme in the presence of biotin in *E. coli* (section 2.2.5.2). The resulting SUMO protein was immobilised on a streptavidin-coated chip (coated by streptavidin conjugated with the complementary single-strand DNA molecule binding to the pre-immobilized single-strand DNA molecule on the chip) and increasing concentrations of the different DARPins were run over it (section 2.2.7.5).
The measurements showed that the DARPins have dissociation constants (K_D) in the low nM to low µM range (table 16). Dependent on the binding properties and the association and dissociation speed of the DARPins, the K_D value was either calculated from the kinetic (for A10, F10, G11) or affinity (for C10, E11, B12) measurements.
The strongest binders were A10 and F10 with an K_D of 0.3 or 3 nM, respectively. A10

seems not to come of SUMO at all or only very slowly (k_{off} 0.00024 s^{-1}), F10 has a faster off-rate (k_{off} 0.0126 s^{-1}). The off-rates of E11, G11 and B12 were similar or even faster compared to F10 (off-rates for E11 and B12 were too fast to be measured by the instrument, k_{off}(G11) 0.0034 s^{-1}) and their affinities were lower. E11 has a K_D of 43 nM, while G11 and B12 have dissociation constants of 197 and 356 nM, respectively. The weakest binder was C10, which has a dissociation constant of 1400 nM and it dissociates from the target protein very fast (outside of instrument range).

Table 16: Affinity and kinetics of SUMO binding by DARPins. Affinity and kinetics were determined using surface plasmon resonance in a BIACORE system. Biotinylated SUMO was immobilized on the chip, while the respective DARPin was washed over it in concentrations ranging from a non-detectable signal to a saturated binding signal. The affinity constant (K_D) and kinetic parameters (k_{off}/k_{on}) were calculated from three independent measurements. Kinetic parameters for C10, E11 and B12 could not be determined, as the dissociation from SUMO lies outside of the instrument range. Dependent on the binding properties and the association and dissociation speed of the DARPins, the K_D value was either calculated from the kinetic (for A10, F10, G11) or affinity (for C10, E11, B12) measurements.

	A10	C10	F10	E11	G11	B12	E3.5
K_D [nM]	0.27 ± 0.03	1433.50 ± 94.05	3.07 ± 0.72	42.81 ± 6.02	197.40 ± 45.34	355.93 ± 17.46	–
k_{off} [10^{-3} s^{-1}]	0.24 ± 0.02	–	12.6 ± 6.1	–	3.4 ± 1.5	–	–
k_{on} [10^5 $M^{-1}s^{-1}$]	8.8 ± 12	–	34.7 ± 18.7	–	0.60 ± 0.3	–	–

The small modifier ubiquitin shares 18 % sequence identity with ySUMO, but the fold of both is very similar. hSUMO1 and hSUMO2 have a high sequence identity with ySUMO (42 %/38 % respectively, fig. 28).[416] In order to show the specificity of the yeast SUMO DARPins, I measured their affinity towards biotinylated yeast ubiquitin, hSUMO1 and hSUMO2 by SPR. None of the DARPins binds ubiquitin in an affinity measurement, in which 10 or 20 µM of each DARPin was tested against 25 nM immobilized ubiquitin (table 17).

C10, G11 and B12 show good affinities to hSUMO1 (G11 even with a K_D of 530 nM) (table 17) and G11 shows additionally some affinity to hSUMO2 (K_D in the low µM range, table 17). The other tested DARPins (A10, F10 and E11) do not bind these two human SUMO isoforms. The exact K_D values were only exemplarily determined for G11. For the other DARPins, 6.6 µM and the 10 fold concentration of the K_D to ySUMO were tested on 20 nM immobilized hSUMO1 or hSUMO2.

```
SMT3      MSDSEVNQEAKPEVK--PEVKPETHINLKVS-DGSSEIFFKIKKTTPLRRLMEAFAKRQGKEMDSLRFLYDGIRIQADQTPEDLDMEDNDIIEAHREQIGGATY- 101
SUMO1     MSDQ----EAKPSTEDLGDKKEGEYIKLKVIGQDSSEIHFKVKMTTHLKKLKESYCQRQGVPMNSLRFLFEGQRIADNHTPKELGMEEEDVIEVYQEQTGGHSTV 101
SUMO2     MADE----KPK----EGVKTENNDHINLKVAGQDGSVVQFKIKRHTPLSKLMKAYCERQGLSMRQIRFRFDGQPINETDTPAQLEMEDEDTIDVFQQQTGGVY-- 95
          *:*.    : *       . :   :*:***  :..* : **:*  * * :* :::.:***  * .:** ::*  *   .** :* **::* *:..::* **
```

Figure 28: Alignment of yeast SUMO (SMT3) with hSUMO1 and hSUMO2 isoforms. Identical amino acids in all three proteins are marked by an asterisk (*). A colon (:) indicates conservation between groups of strongly similar properties and a period (.) indicates conservation between groups of weakly similar properties. Alignment was performed using the Clustal Omega tool from EMBL-EBI.

Table 17: Binding of yeast SUMO-specific DARPins to yeast ubiquitin and hSUMO isoforms. Affinity was determined using SPR in a BIACORE system. Biotinylated ubiquitin or SUMO was immobilized on the chip, while the respective DARPin was washed over it in different concentrations (see main text). An exact affinity constant was only exemplarily determined for G11 on hSUMO1, as this binding was the strongest.

	ubiquitin	hSUMO1	hSUMO2
bound by:	–	C10, G11 (K_D 530 nM) and B12	G11

3.3.2.3 The selected DARPins have distinct effects on SUMO conjugation and deconjugation

In this section, the effects of the different DARPins on the sumoylation cascade and desumoylation are characterized. With this knowledge, DARPins with different properties can be selected for use as either inhibitors, sensors or affinity reagents in yeast. As described above [redacted] started to characterize the influence of DARPins on the biological functions of SUMO. She found that some of the DARPins that bind to SUMO also inhibited sumoylation *in vitro*, but clearly to a different extent.
I aimed to follow up on this observation by analysing, which step of the conjugation cascade is influenced by the different binders. As discussed in section 1.2.6.1, conjugation of SUMO to a lysine residue in a substrate protein requires a cascade of different enzymatic activities. These enzymatic steps can be divided into E1 and E2 thioester formation, substrate conjugation, SUMO chain formation and desumoylation. To analyse the influence of the DARPins on each reaction individually, I purified the enzymes needed for simulation of the different steps of the sumoylation cascade *in vitro* (section 2.2.5).

I performed an E1 thioester formation assays by incubating the yeast E1 enzyme (Aos1/Uba2), SUMO and ATP in the presence of a five times excess of the different DARPins, and resolved the products on an SDS gel without reducing agents (section 2.2.6.1). The formation of a thioester between Aos1/Uba2 and SUMO resulted in a shift of the Uba2 protein band by ∼15 kDa. The quantification of the shifted band shows that only A10 completely abolished E1 thioester formation (fig. 29a lanes 11–13 and fig. 29b), while F10 and E11 slow it (fig. 29a lanes 14–16 and 20–22 and fig. 29b). The other binders (C10, G11 and B12) did not show any influence on E1 thioester formation (fig. 29a lanes 17–19 and 23–25 and fig. 29b). These reactions run equally fast as in the positive control (fig. 29a lanes 8–10 and fig. 29b).

The candidates that did not inhibit E1 thioester formation, were further tested for their influence on E2 thioester formation. The set-up of the experiment was the same as for the E1 thioester formation assay, only that additionally Ubc9 (the yeast SUMO E2) was added to the reaction (section 2.2.6.2). However, a quantification of the gel was not possible as the DARPins, SUMO and free Ubc9 run at the same height in the gel and

therefore their bands cannot be distinguished. Additionally, covalent SUMO conjugation to Aos1/Uba2 and Ubc9 occurred, even so, a SUMO mutant (SUMO-K11/15/19R)[417] and an Ubc9 mutant (Ubc9-K153/157R)[418] with the most important sumoylation sites mutated, were used. Nevertheless, one can conclude that none of the tested DARPins showed an observable influence on this second step of the conjugation cascade (fig. 30 lanes 10–18).

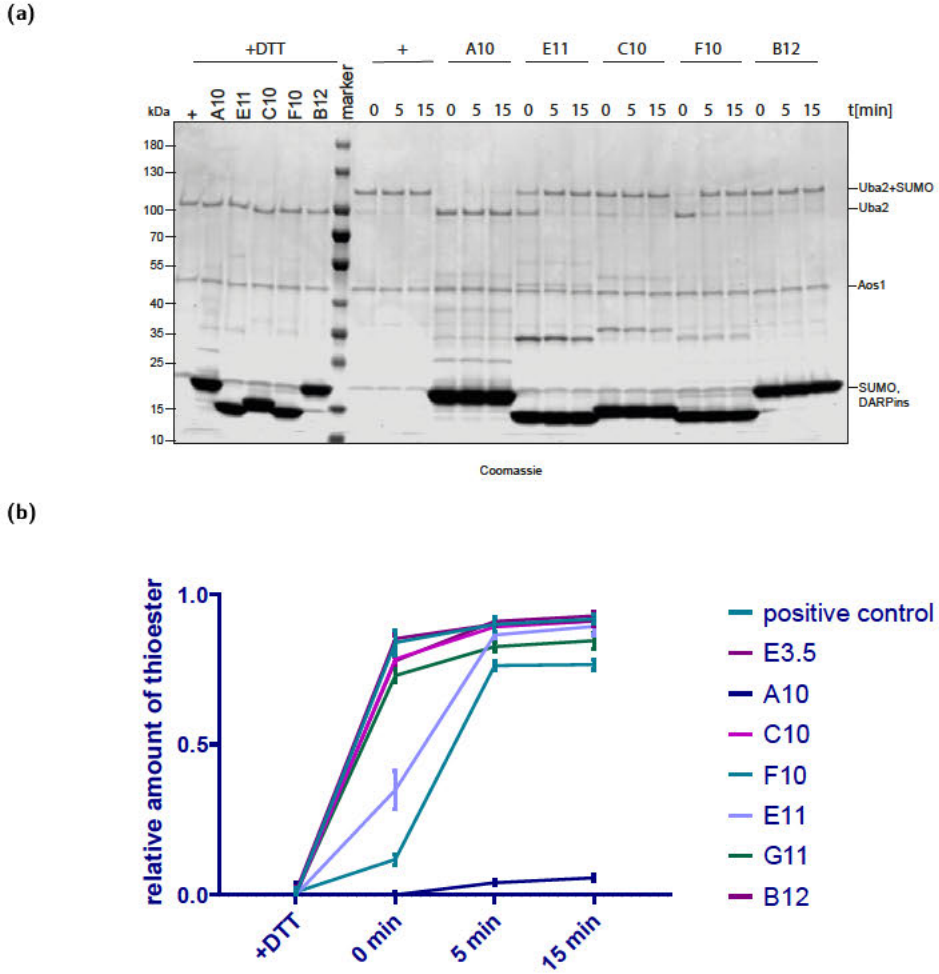

Figure 29: (a) E1 thioester formation assay. SUMO was pre-incubated with 5x excess of the different DARPins before Aos1/Uba2 and ATP were added to the reaction. Samples were taken after 0, 5 and 15 min. After separation on an SDS gel, staining was performed using Instant Blue reagent. As a control one set of samples was boiled in the presence of DTT (+DTT), to resolve the thioester. A positive control (+) without DARPin was run in parallel. **(b) Quantification of E1 thioester formation.** The mean of three to six independent experiments and the standard deviation is shown. The relative E1 thioester signal was calculated by dividing the thioester signal band by the amount of total Uba2 (thioester plus free Uba2). DARPin A10 nearly completely inhibits E1 thioester formation, while F10 and E11 slow it. C10, G11, B12 and the control DARPin E3.5 do not seem to influence thioester formation.

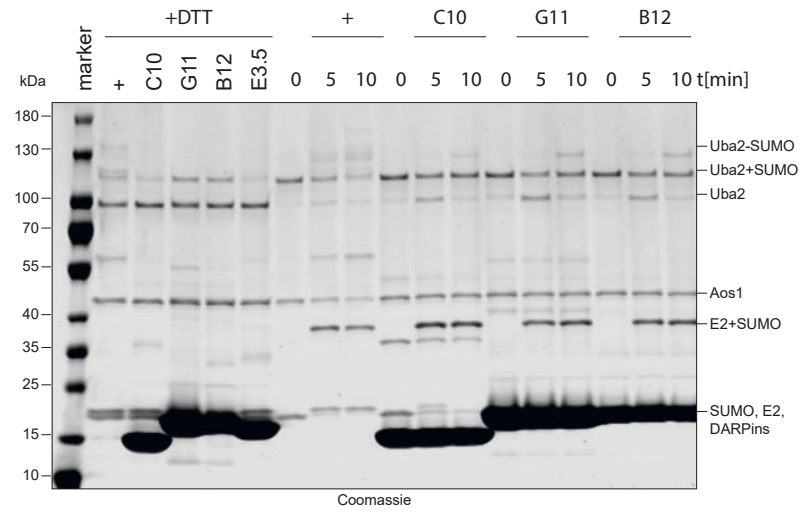

Figure 30: E2 thioester formation assay. The E1 thioester was pre-formed, before 5x excess of the DARPins were added. Only DARPins that did not affect E1 thioester formation were included. After a short incubation, the E2 thioester formation reaction was started by adding Ubc9. Samples were taken after 0, 5 and 10 minutes. Again one set of samples, taken after 10 min, was boiled in the presence of DTT to resolve thioester bondings. A positive control (+) without DARPin was run in parallel. Samples were separated on an SDS gel and stained with Instant Blue. A quantification was not possible as SUMO conjugation to Aos1/Uba2 and Ubc9 occurred, even so, a SUMO-K11/15/19R mutant and a Ubc9-K153/157R mutant were used. None of the tested DARPins shows an influence on E2 thioester formation.

Furthermore, I performed a free SUMO chain formation assay by incubating a reaction containing purified Aos1/Uba2, Ubc9, SUMO, ATP and a five times excess of one of the DARPins and blotting for SUMO. SUMO chain reaction can happen *in vitro* in the absence of a SUMO E3, however, it is enhanced in its presence (reviewed in Pichler *et al.* (2017))[203]. Therefore, I tested the reaction in the presence and absence of Siz1 (section 2.2.6.3).

None of the DARPins that did not influence thioester formation (C10, G11 and B12) showed any strong inhibitory effect on chain formation, regardless of the presence or absence of the E3 (Siz1) (exemplarily shown for C10 in fig. 31a lanes 5, 9, 13, 17, 21 and 25). The candidates that already had an impact on thioester formation (A10, F10 and E11, exemplarily shown for A10 and E11 in fig. 31a lanes 4, 6, 8, 10, 12, 14, 16, 18, 20, 22, 24, 26) showed the consequential effect also in the free chain formation assay. In the early time-points of the non-inhibitory DARPins containing samples, one can also see that the addition of Siz1 increases the speed of free chain formation (fig. 31a compare lane 11 with lane 15).

Tatham and Hay (2009)[316] and Stankovic-Valentin (2009)*et al.*[334] have described a FRET assay, with which sumoylation can be quantitatively monitored. For that SUMO is tagged with YFP and a sumoylation model substrate (RanGAP1(418–587)) with CFP. During the assay, CFP is excited with a light pulse in its specific excitation wavelength. If YFP-tagged SUMO is conjugated to the CFP-tagged substrate an energy transfer between CFP and YFP happens and the fluorescence emission of YFP is detectable. To prevent SUMO chain formation on the substrate a SUMO mutant with K11/K15/K19

mutated to Arginine was used (section 2.2.6.6).[417]
When the SUMO-specific DARPins were used in ten-fold molar excess over SUMO (fig. 31b), all SUMO-specific DARPins prevented its conjugation to a substrate. Using a lower concentration of DARPins (five-fold molar excess (fig. 31c)) conjugation was visible for C10 at the later time points. Also for E11 inhibition of sumoylation was not as strong as for the other DARPins. Using the same amount of SUMO and DARPin (fig. 31d), the inhibition was weakened for C10, G11 and B12. With the control DARPin E3.5, no inhibition was visible compared to the reaction without DARPin, regardless of its concentration.

Sumoylation can be removed by the action of the SUMO-specific proteases Ulp1 and Ulp2. Ulp2 mainly cleaves poly-SUMO chains, while Ulp1 shows a broad specificity *in vitro*.[206] Therefore, I tested the ability of purified Ulp1 to cleave a C-terminal fusion protein of GFP and SUMO in the presence of a five-fold molar excess of the different DARPins (section 2.2.6.5). I quantified the assay by determining the ratio of the intensities of the SUMO-GFP fusion protein to the free GFP signal. In this assay, only A10 showed a medium-strong inhibitory effect (fig. 32a lane 10–13 and fig. 32b dark blue line), while all other DARPins were not influencing Ulp1's ability to cleave the construct.

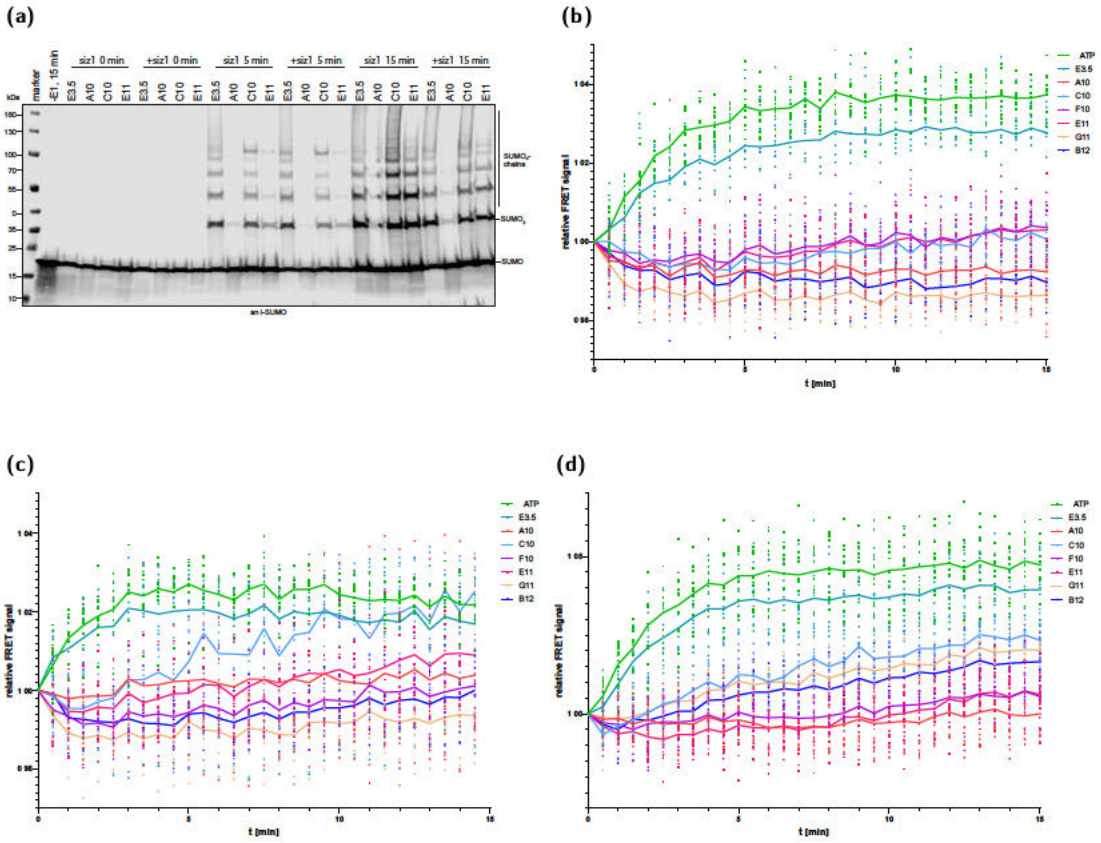

Figure 31: (a) Formation of free SUMO chains in the presence of DARPins with/-out an E3. SUMO was pre-incubated with 5x excess of the DARPins, before the enzymes and ATP were added to start the reaction. One reaction was performed without ATP to prevent chain formation. Samples were taken after 0, 5 and 15 min. Samples were separated on an SDS gel, followed by Western blotting. The blot was developed with an anti-SUMO antibody. Free chain formation was not blocked much further than seen in the E1 thioester formation assay. **(b) Conjugation of YFP-SUMO-3R to an example substrate (CFP-RanGAP1(418–587)) in the presence of 10x DARPins.** The reaction components were pre-incubated with the 10x excess of DARPins to SUMO, before ATP was added to start the reaction. One reaction was performed without ATP to prevent chain formation. This reaction was used for correcting the baseline of all other samples. Samples were analysed for FRET signals in a fluorescence plate reader every 30 s up to 15 min. The relative FRET signal was calculated by dividing the YFP by the CFP signal and normalizing the result to the time point 0 min and taking the -ATP control time course as a baseline. Shown are the single measurement points per reaction and their mean. At this concentration, all DARPins inhibited substrate conjugation of SUMO. **(c) Conjugation of YFP-SUMO-3R to an example substrate (CFP-GAP(418–587)) in the presence of 5x DARPins.** The reaction was performed as described under b, only that 5 times excess of DARPins to SUMO was added. Conjugation was visible for C10 at the later time points. Also for E11 inhibition of sumoylation was not as strong as for the other DARPins. **(d) Conjugation of YFP-SUMO-3R to an example substrate (CFP-GAP(418–587)) in the presence of 1x DARPins.** The reaction was performed as described under b, only that 1 times the amount of DARPins to SUMO was added. The conjugation of SUMO to its substrates is strongly inhibited by A10, F10 and E11. The inhibition is weaker for C10, G11 and B12.

(a)

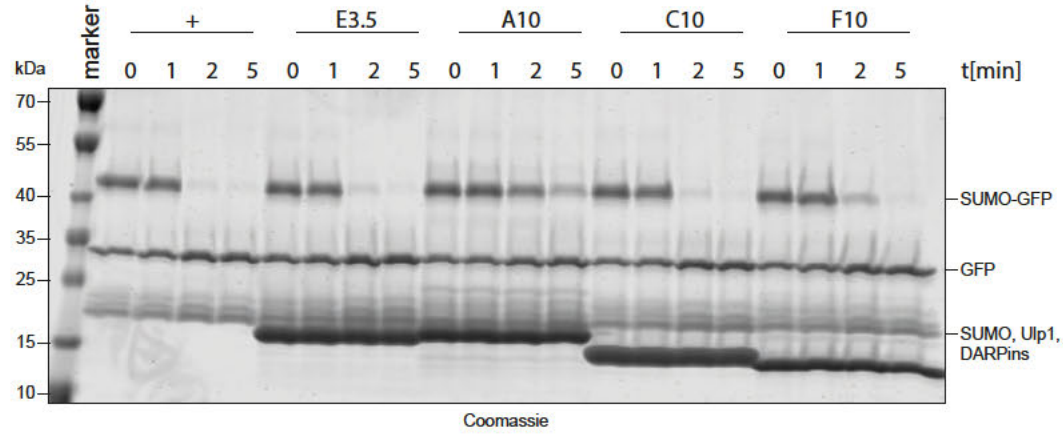

(b)

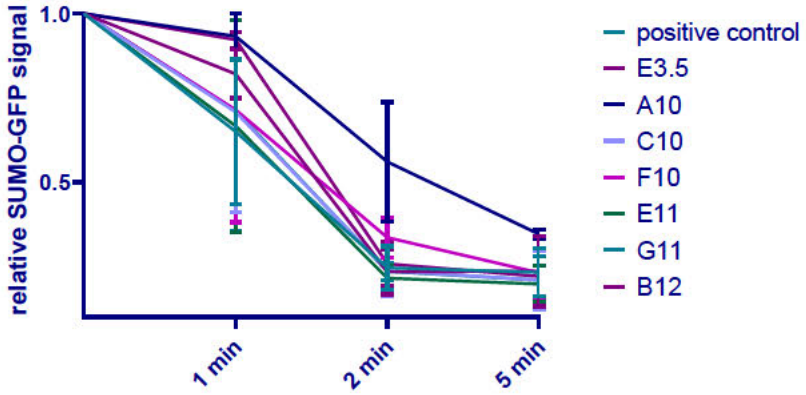

Figure 32: (a) Ulp1 cleavage of a SUMO-GFP construct in the presence of DARPins. The SUMO-GFP construct was pre-incubated with 5x excess of DARPins, before the SUMO protease Ulp1 was added. A positive control (+) without DARPin was run in parallel. Samples were taken after 0, 1, 2 and 5 minutes. Samples were separated on an SDS gel and stained with Instant Blue. **(b) Quantification of Ulp1 cleavage assay.** The relative SUMO-GFP signal was calculated by dividing the amount of uncleaved SUMO-GFP by the amount of free GFP and normalizing it to the relative amount at time point 0 min. The mean and standard deviation was calculated from three independent experiments. Only A10 seems to influence Ulp1 cleavage.

3.3.2.4 The selected DARPins show different effects on SIM–SUMO interaction

To transmit the SUMO signals in the cell, sumoylation is recognized by SIM-containing proteins. As a consequence, we were interested in determining, if the ability of SIM-containing proteins to bind to SUMO was abolished in the presence of the different DARPins. In the first experiment, I tried to use a well-characterized SIM peptide[209,246] with the sequence KVDVIDLTIE in a PD or a surface plasmon resonance set-up. However, no detection of interaction between the peptide and SUMO was possible in my hands.

To still be able to test the ability of a SIM-containing protein to bind SUMO in the presence of the DARPins, RNF4 was purified. RNF4 harbours four SIM motifs and it preferentially binds to hSUMO2 chains, but it can also bind mono-SUMO and SUMO from *S. cerevisiae*.[256] The interaction in the presence of the DARPins was tested by immobilizing 2.5 µM SUMO on beads, pre-incubation it with 50 µM of a DARPin, before adding 5 µM RNF4. The elution was analysed for the presence of RNF4 in a Western blot (section 2.2.7.3, fig. 33).

In this experiment, the DARPins A10 and F10 show a very strong inhibition of SIM binding (fig. 33a lane 7 and 11 and fig. 33b), C10 and B12 show an intermediate level of inhibition (fig. 33a lane 9 and 17 and fig. 33b), while E11 and G11 show very weak to no inhibition (fig. 33a lane 13 and 15 and fig. 33b). For comparison, reactions without DARPin or with the control DARPin E3.5 were run in parallel (fig. 33a lane 3 and 5 and fig. 33b).

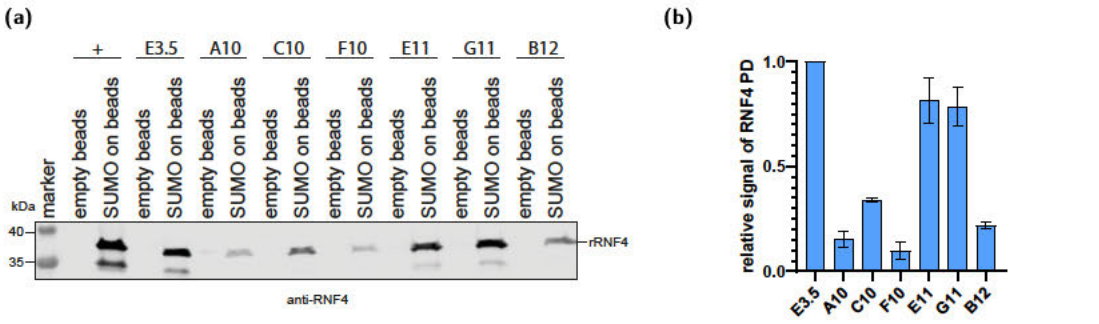

Figure 33: (a) Pull-down of RNF4 in the presence of DARPins. 2.5 µM SUMO was immobilized on Streptavidin agarose beads. 50 µM of the DARPins was allowed to bind to the immobilized SUMO, before 5 µM RNF4 purified RNF4 was added to either empty beads or beads with immobilized SUMO. Samples were blotted against RNF4. E3.5 was used as a control, as it was not raised against SUMO. **(b) Quantification of the SIM-containing protein to SUMO interaction in the presence of the DARPins.** The signal of both bands visible in the anti-RNF4 WB was quantified, subtracted by the signal detected with empty beads and normalized to the signal from the PD, in which the control DARPin E3.5 is present. The graph shows the mean and standard deviation from three replicates. DARPins A10 and F10 show very strong inhibition of SIM binding, C10 and B12 show an intermediate level of inhibition, while E11 and G11 show very weak to no inhibition.

3.3.3 Structural analysis of the binding site between DARPins A10 or C10 and SUMO

Different DARPins have distinct effects on the function of SUMO (fig. 60). Therefore, it was interesting to see if they bind to different surfaces of the molecule. NMR measurements were done by [redacted] the [redacted] group in Frankfurt to characterize the interaction interface of the DARPins and SUMO. The NMR structure of unbound SUMO was solved and published by Sheng and Liao in 2002.[419]
All measured DARPins showed a strong binding behaviour in the NMR experiment (low to high nanomolar range, section 2.2.9, see supplementary information section 5.2). This very strong binding leads to a slow exchange. This means that the peaks influenced by the binding of a DARPin in the NMR spectra vanish and appear again in a different place and therefore cannot be directly annotated to the corresponding peak from the unbound protein. An additional difficulty in comparing the structure of the bound to the free SUMO protein was that the DARPins seem not to bind to a single or few residues, but to a larger area in the protein or cause a conformational change in the SUMO structure as many amino acids peaks shift in the spectra. These results show that an easy annotation of the binding interface by comparing the bound and the annotated unbound spectra was not possible. A complete new annotation of all DARPin bound forms would be needed.

In order to still be able to get insights into the binding site of selected DARPins to SUMO, we have crystallised and solved the structure of the strong binding DARPin A10 in complex with SUMO and the weak binding DARPin C10 with SUMO (section 2.2.8). This was done in collaboration with [redacted] from the [redacted] group of the University of Mainz. The first 19 amino acids of SUMO were deleted from the crystallisation construct, as they are disordered.[233] An attempt to also crystallize the intermediate binder E11 in complex with SUMO was not successful.
Crystals were obtained from fractions after size exclusion chromatography showing the right size of the DARPin SUMO complex and displaying the corresponding protein bands of both proteins in a Coomassie gel (fig. 34 and fig. 35). The phase problem for both complexes was solved by [redacted] using molecular displacement with known structures of SUMO and DARPins (protein data bank (pdb): 1MJ0 and 1L2N).

The crystal structure of the A10-SUMO complex showed a 1:1 binding of the proteins. The structure was refined to 2.51 Å and includes 149 amino acid residues of the 165 possible residues of the used DARPin A10 construct and 74 of the possible 80 amino acids residues of the used SUMO construct (table 18). As described before by Sheng *et al.* (2002), Mossessova *et al.* (2000) and Duda *et al.* (2007)[233,419,420] the secondary structure of SUMO includes five anti-parallel β-strands forming a twisted β-sheet and

one (or two dependent on the annotation) α-helix. The DARPin A10 consists of three library modules each containing a variable loop and two α-helices. They are capped by an N-capping and one C-capping module with two α-helices each (fig. 36a).
SUMO does not undergo large conformational changes when bound to the DAPRin. A10 makes contacts with its variable loops and variable residues in the library modules to the hydrophobic patch between α-helix 1 and the β-sheet on SUMO (fig. 36a and fig. 38c). Analysing the interface between SUMO and the DARPin was performed using the PISA tool from EMBL[421] and the interface residue code and pairwise distance code from pymol (InterfaceResidues.py and pairwise_dist).[422]
The interface covers 13.6 % of the solvent-accessible area of the DARPin and 20.5 % of the solvent-accessible area of SUMO. The interactions include side chain to main chain hydrogen bondings, van der Waals (VdW) contacts, and salt bridges (fig. 36b). Hydrogen bonds occur between Arg36 of the DARPin and Ser32 and Glu34 of SUMO (in the following the first amino acid is always from A10 and the second amino acid(s) from SUMO), between Asn46 and Phe36, between His115 and Lys38 , between Arg112 and Glu50 and Arg47, between Trp135 and Glu59, between Asn46 and Phe36, between Val79 and Lys38, between Leu113 and Arg47, between Asn148 and Arg47, between Asn146 and Arg47, and between Asp67 and Arg55 and possibly between Gly114 and Lys40 (only found with one method). Salt bridges were identified between Arg36 in A10 and Glu34 in SUMO, between Asp67 and Arg55 and between Arg112 and Glu50 (fig. 36b). Other amino acids in the interaction interface include on the DARPin site Arg13, Phe38, Leu43, Ser47, Asn68, Tyr69, Trp71, Leu76, Ile80, Gly81, Asp100, Phe102, Ser104, Leu109, Gly114, Leu116, Asp133, Glu137, Asp143, Gly147, Ile151 and on the SUMO site His13, Asn15, Ser37, Ile39, Phe41, Ile43, Lys44, Thr47, Arg50, Leu52, Ala55, Phe57, Lys58, Gln60 Gly61, and Lys62.

The crystal structures for SUMO in complex with Aos1/Uba2, Ubc9, a SIM peptide, Siz1 and Ulp1 are available from pdb (entry references: 1y8r, 2eke, 3v62, 5jne and 1euv, respectively). By overlaying these structures with the one of A10 bound to SUMO (fig. 37a), it became obvious that the interaction of the DARPin with SUMO clashes with the interaction site for the Aos1/Uba2 (fig. 37b). Ubc9 and the SUMO-specific protease Ulp1 bind to a different interface of SUMO (fig. 37c, e). The hydrophobic patch, to which A10 binds is also the interaction site for SIM-containing proteins, as for example the E3 Siz1 (fig. 37d, f).

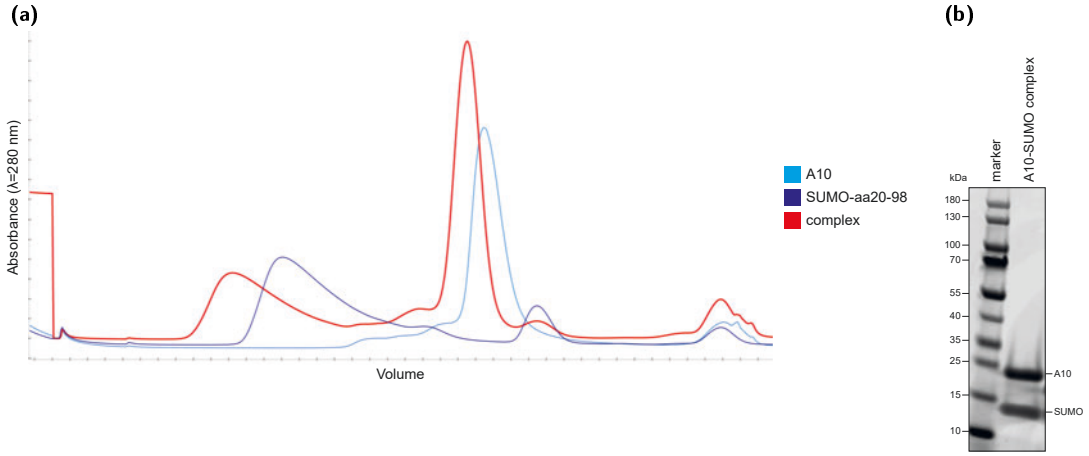

Figure 34: **(a) Gel filtration profile of the complex between DARPin A10 and SUMO(20–98)**. In red the run of the complex is shown. In dark blue a run of only SUMO is shown and in light blue a run of only A10 is represented. **(b) Complex between A10 and SUMO(20–98) after gel filtration**. Clean peak fractions of the gel filtration representing the complex between A10 and SUMO were loaded onto a denaturing gel and stained with Instant Blue. The two bands represent the DARPin A10 and SUMO. No contaminations are visible.

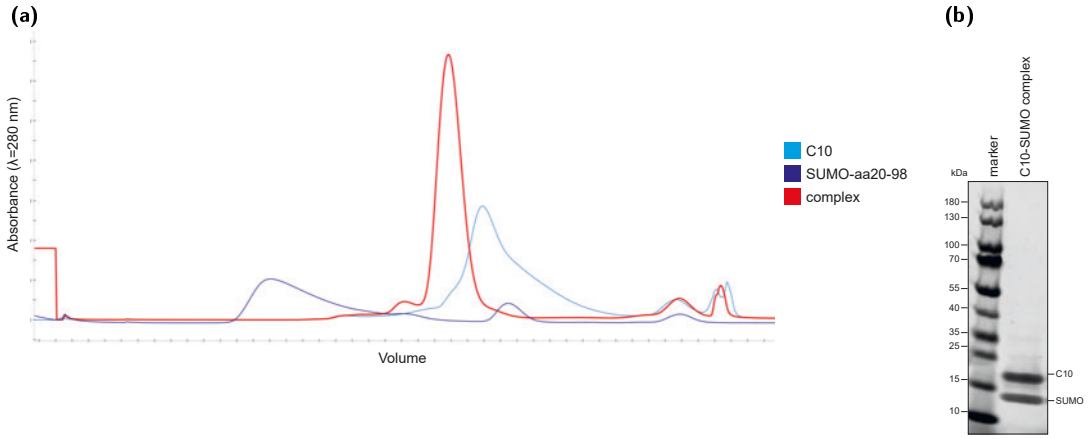

Figure 35: **(a) Gel filtration profile of complex between DARPin C10 and SUMO(20–98)**. In red the run of the complex is shown. In dark blue a run of SUMO only is shown and in light blue a run of only C10 is represented. **(b) Complex between C10 and SUMO(20–98) after gel filtration**. Clean peak fractions of the gel filtration representing the complex between C10 and SUMO were loaded onto a denaturing gel and stained with Instant Blue. The two bands represent the DARPin C10 and SUMO.

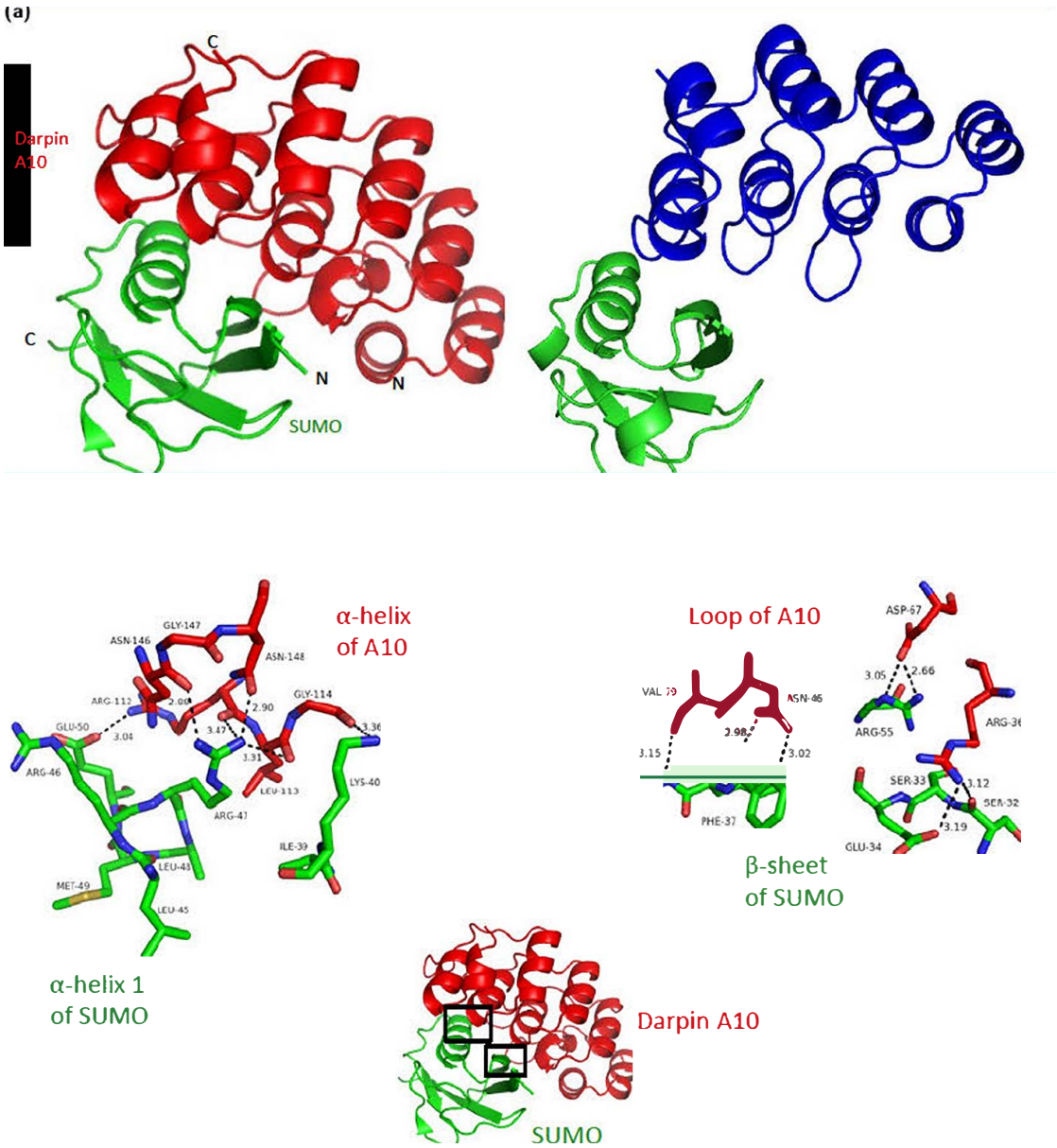

Figure 36: (a) Cartoon representation of DARPin A10 bound to SUMO(20–98) with A10 in red and SUMO in green. N- and C-termini are labelled. X-ray data collection and refinement statistics can be found in table 18. **(b) Contact sites between A10 and SUMO(20–98).** DARPin A10 contacts SUMO with its variable residues in the loops and α-helices of the library modules. On SUMO the contact site is located in the hydrophobic patch between α-helix 1 and β-sheet 2. Hydrogen bonds and salt bridges are labelled (dashed, black lines). Distances are given in Å. The A10 residues are shown in red, the residues from SUMO are shown in green. Nitrogens are coloured blue. Oxygens are coloured bright red.

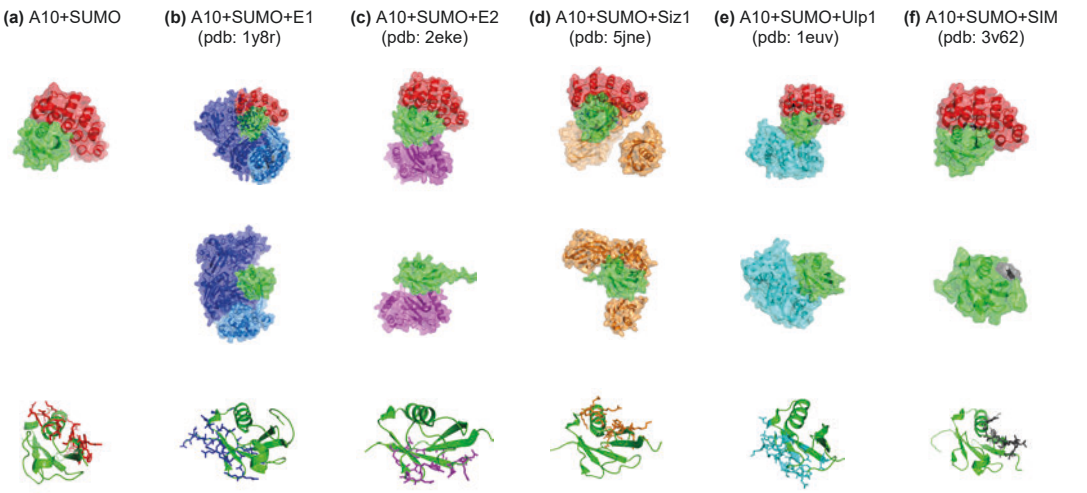

Figure 37: Merge of the structures between A10 (red) bound to SUMO(20–98) (a, green) and Aos1/Uba2 (b, blue), Ubc9 (c, violet), Siz1 (d, orange), Ulp1 (e, bright blue) or SIM (f, grey). The upper row shows the merge of SUMO, DARPin A10 and the respective enzyme in a surface model. The middle row shows the merge between SUMO and the respective enzyme and the lowest row shows the secondary structure model of SUMO with the residues for interaction with A10 or the respective enzyme as coloured sticks. All structures are represented in the same orientation. The structures of Aos1/Uba2, Ubc9, Siz1, Ulp1 or SIM-bound SUMO are published and accessible on pdb (entry references: 1y8r, 2eke, 5jne, 1euv, and 3v62 respectively). The overlay was done using pymol. The A10 binding site clashes with the one for Aos1/Uba2, Siz1 and SIM binding. Ulp1 and Ubc9 interactions happen on the opposite side of SUMO compared to the A10 binding site.

The crystal structure of the C10-SUMO complex showed a 1:1 binding of the proteins. The structure was refined to 2.64 Å. It includes 121 amino acid residues of the possible 143 amino acids of DARPin C10 and 73 of the possible 80 amino acid residues of SUMO (table 18). The DARPin C10 consists of two library modules with a variable loop and two α-helices each. It is capped by an N-capping and a C-capping module with two α-helices each.

SUMO does not undergo large conformational changes when bound to the DAPRin. Like A10, C10 makes contacts with its variable loops and variable residues in the library modules, to the hydrophobic patch between α-helix1 and the β-sheet of SUMO (fig. 38a, fig. 38c). The interface covers 11.4 % of the solvent-accessible area of SUMO and 8.9 % of the solvent-accessible area of the DARPin. The interactions include side chain to main chain hydrogen bondings and mainly VDW contacts (fig. 38b). Hydrogen bonds were formed between His92 in C10 and Thr22 in SUMO and between Trp84 in C10 and Lys38 in SUMO. Other amino acids in the interaction interface include on the DARPin site Gln49, Arg51, Gln59, Gln81, Tyr82, Leu89, Asp114, Trp115, Ile116, Gly117, Val118, Leu123, Asp126 and Asp127 and on the SUMO site His23, Asn25, Ile35, Phe36, Phe37, Ile39, Lys40, Thr43, Arg47, Leu48, Ala51, Arg55 and Asn86 (fig. 38b).

The overlay of the C10-SUMO complex with the different enzymes of the sumoylation cascade was performed as described above (data not shown). As for A10, the structure shows a clash between C10 binding and Aos1/Uba2, Siz1 and SIM binding. While Ubc9 and Ulp1 binding occur on a different site of SUMO.

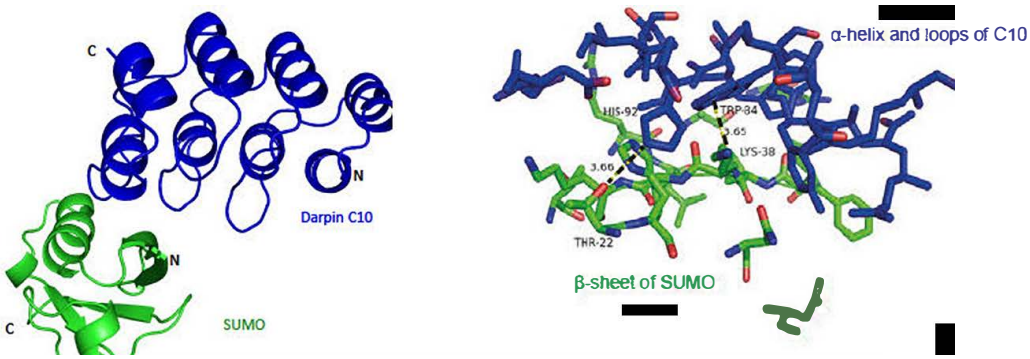

(c)

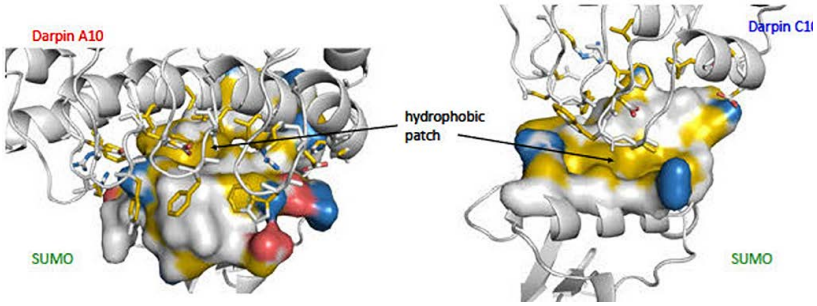

Figure 38: (a) Cartoon representation of DARPin C10 bound to SUMO(20–98) with C10 in blue and SUMO in green. N- and C-termini are labelled. X-ray data collection and refinement statistics can be found in table 18. **(b) Interaction interface between C10 and SUMO(20–98).** DARPin C10 contacts SUMO with its variable residues in the loops and α-helices of the library modules. On SUMO the contact site is located in the hydrophobic patch between α-helix 1 and β-sheet 2. Hydrogen bonds are labelled (dashed, black lines). Distances are given in Å. The amino acids in the interaction interface are represented. Residues from C10 are shown in blue, the residues from SUMO are shown in green. Nitrogens are coloured blue. Oxygens are coloured red. **(c) Contact sites between A10 and SUMO(20–98) (left) or C10 and SUMO(20–98) (right).** Both complexes are represented with SUMO in the same orientation. DARPins A10 and C10 are shown as a cartoon with the amino acids that make contact to SUMO being highlighted. SUMO is represented as a cartoon with the interaction surface being colour-coded according to the properties of the amino acids. Carbon atoms that can form hydrophobic interactions are coloured in yellow, while nitrogen atoms in the side chains of arginine and lysine are coloured blue and oxygen atoms in the side chains of glutamate and aspartate are red.[423] The DARPins contact SUMO with their variable residues in the loops and α-helices of the library modules. On SUMO the contact site was located to the hydrophobic patch between α-helix 1 and β-sheet 2.

Table 18: X-Ray data collection and refinement statistics.

	SUMO(20–98)-A10 complex	SUMO(20–98)-C10 complex
Wavelength [Å]	1.000033	0.979
Resolution range [Å]	47.31-2.51 (2.61-2.51)	47.05-2.64 (2.83-2.64)
Space group	P 21 21 21	C 2 2 21
a, b, c [Å]	42.97, 94.75, 120.96	90.46 , 44.69, 47.60
α, β, γ (°)	90, 90, 90	90, 89.757, 90
Unique reflections	17608	82807
Multiplicity	13.1 (11.3-12.8)	5.7 (6.4)
Completeness (%)	100 (99.5-99.9)	99.8 (86.1)
Mean I/σ(I)	17.6 (1.8-63.2)	38.7 (3.1)
$CC_{1/2}$	1 (0.891-1)	0.998 (0.861)
R_{merge}	0.032	0.043 (0.585)
Protein atoms	3336	1443
Solvent ions	15	–
R_{work}	0.217	0.270
R_{free}	0.341	0.304
RMSD bonds [Å]	0.0219	0.0047
RMSD angles (°)	2.893	1.380
Favored (%)	94.84	88.48
Allowed (%)	4.49	8.90
Outliers (%)	0.67	2.62

3.3.3.1 Verification of structural data of DARPin/SUMO complexes

This section aims on verifying the interaction sites between DARPins and SUMO, using different biotinylated mutant SUMO proteins, which according to the solved structures should prevent SUMO interaction. They were purified and their interaction with A10 and C10 was tested by surface plasmon resonance in the same set-up as for kinetic measurements (section 2.2.7.5). For each complex a mutant SUMO protein was found that prevents binding of the respective DARPin (fig. 39a, table 19 and table 20).
A disruption of the interface residues (from the C10/SUMO complex) in the hydrophobic SIM interaction site, as in mutant SUMO-C10mut (T22A-I35S-F37S-K38E-K40E-T43A-L48S-R55E-N86A), prevented both DARPins from binding. The mutation of the SIM interaction site surrounding interface residues (from the A10/SUMO complex) (as in SUMO-S1-all (H23Y-N25K-F36H-I39V-K41M-R46K-R47K-A51S-K54Q-K58V-E59P)) only prevented DARPin A10 from binding. All tested SUMO mutants with a reduced number of mutant residues, compared to the non-interacting SUMO protein, lead to a regain of binding of the DARPins to SUMO (table 19 and table 20). Also a mutant in which the main hydrophobic residues (SUMO-I35D-F36D-F37D) of the interaction interface, the main charged residues (SUMO-E34A-E50A-E59A) or a mixture of both (SUMO-F36H-R47K-E59P) are mutated lead only to a reduced affinity, but no inhibition of interaction.
These results suggest that the binding site of the different DARPins involves several distinct amino acids and that only deletion of all of them abolishes the binding of the DARPin to SUMO.

The SUMO-C10mut, in which part of the SIM interaction site was mutated, was also tested for its ability to form SUMO chains (fig. 39b), however, it did not show any SUMO conjugation (fig. 39b lane 3). Most likely because some of the mutated residues (I35S, F37S) were destabilizing the protein.[312]
While both mutants contain mutations involved in SIM recognition (R47K-A51S in SUMO-S1-all or I35S-F37S-K38E-K40E-T43A-R55E in SUMO-C10mut), none of the mutated residues in the two SUMO mutants were important for recognition by Aos1/Uba2, Ubc9 or SUMO proteases. An idea of replacing the native SUMO by the mutants in yeast to create DARPin-resistant strains was abstained from, as both mutants contain residues that were shown to be either lethal if mutated in living yeast (R47K in SUMO-S1-all and R55E in SUMO-C10mut) or conditional for yeast growth under stress conditions (H23Y-K58V in SUMO-S1-all and I35S-F37S-K38E-K40E in SUMO-C10mut, fig. 39a).[312]

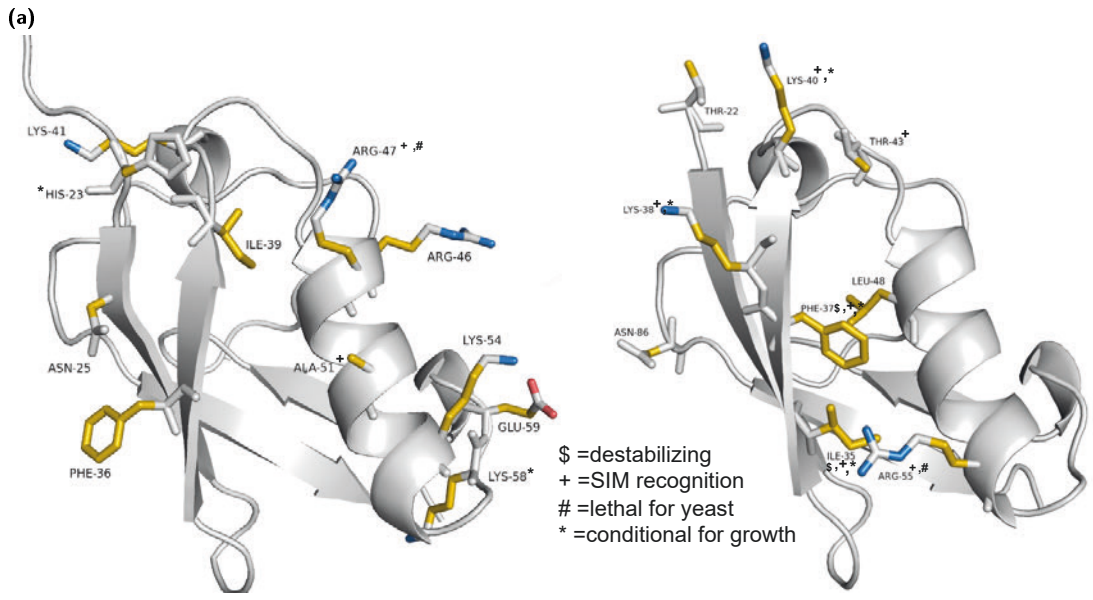

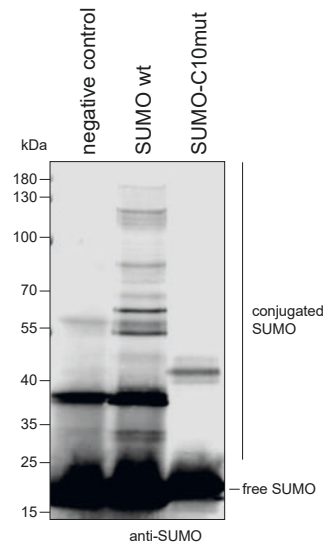

Figure 39: (a) Structure of SUMO from the complex between DARPin A10 and SUMO (right) or the complex of C10 and SUMO (left). Residues that were mutated to prevent the respective DARPin from binding are labelled. Carbon atoms that can form hydrophobic interactions are coloured in yellow, while nitrogen atoms in the site chains of arginine and lysine are coloured blue and oxygen atoms in the site chains of glutamate and aspartate are red.[423] Residues that destabilize the protein structure if mutated are marked with a dollar sign ($). Residues that are involved in SIM interaction are marked with a plus (+). Residues that are either lethal if mutated in living yeast or conditional for yeast growth under stress conditions are marked with a hash key (#) or a asterisk (*), respectively.[312] **(b) Chain formation with SUMO *WT* and SUMO-C10-mutant.** SUMO or the SUMO mutant that does not allow for C10 binding (SUMO-C10mut) was mixed with Aos1/Uba2, Ubc9 and ATP. As a negative control a sample without ATP was loaded. Reactions were blotted against SUMO. Chain formation is visible with SUMO-*WT* but not with the SUMO-C10-mutant.

Table 19: Binding kinetics of A10 to SUMO and SUMO mutants determined by surface plasmon resonance.

	K_D [nM]	k_a [$*10^5$ $*M^{-1}*s^{-1}$]	k_d [s^{-1}]
SUMO-*WT*	0.27	8.83	0.0002
SUMO-R47A	0.06	7.11	0.0003
SUMO-E34A-E50A-E59A	4.49	1.69	0.0014
SUMO-F36H-R47K-E59P	25.21	2.96	0.0074
SUMO-8M (S32A-F36A-K38A-K40A-R47A-E50A-R55A-E59A)	114.00	0.10	0.0115
SUMO-I35D-F36D-F37D	1.87	9.35	0.0011
SUMO-H23Y-N25K-I39V-A51S	2.15	3.88	0.0008
SUMO-H23Y-N25K-I39V-A51S-F36H-R47K	48.38	4.4	0.0165
SUMO-S1-all (H23Y-N25K-F36H-I39V-K41M-R46K-R47K-A51S-K54Q-K58V-E59P)	no binding detected		
SUMO-C10mut (T22A-I35S-F37S-K38E-K40E-T43A-L48S-R55E-N86A)	no binding detected		

Table 20: Binding kinetics of C10 to SUMO and SUMO mutants determined by surface plasmon resonance.

	K_D [nM]	k_a [$*10^5$ $*M^{-1}*s^{-1}$]	k_d [s^{-1}]
SUMO-*WT*	1433.50	no kinetics calculated, because outside of instrument range	
SUMO-S1-all (H23Y-N25K-F36H-I39V-K41M-R46K-R47K-A51S-K54Q-K58V-E59P)	63	0.925	0.0011
SUMO-C10mut (T22A-I35S-F37S-K38E-K40E-T43A-L48S-R55E-N86A)	no binding detected		

3.3.4 *In vivo* characterization of the properties of DARPins

The *in vitro* experiments described in section 3.3.2, have given indications, on which DARPin could be used for what purpose *in vivo*. The strong binding DARPin A10 seemed to be a good inhibitor of sumoylation, while the DARPins with fast off-rates could be better used as a sensor or affinity reagent, as they have less effect on the functions of SUMO *in vitro*. To test how this behaviour holds true *in vivo*, the following section describes growth analysis and detection of sumoylated species from yeast expressing the DARPins. Moreover, optimization of expression constructs and conditions are described.

3.3.4.1 Optimization of experimental system 1: DARPin expression shows a concentration dependent impact on sumoylation in yeast

In this first part, the expression system of DARPins is optimized and the impact of DARPin expression on the sumoylation landscape in yeast is analysed. [redacted] started to characterize the behaviour of some DARPins, when expressed in *S. cerevisiae*. All tested DARPins lead to a failure in colony formation after induction of expression, when overexpressed from an episomal plasmid.
I looked at the overall sumoylation status of yeast cells after overexpression of DARPins from an episomal plasmid (section 2.2.3.6). However, no or only a very slight change in the overall sumoylation was visible (fig. 40a lanes 5–10) compared to cells expressing the control DARPin E3.5 or an empty vector (fig. 40a lanes 3–4). The same holds true when I performed a denaturing pull-down of an example substrate (PCNA) and looked for its sumoylation (section 2.2.3.7). Again no changes can be observed after expression of DARPins (fig. 40b lanes 3–8) compared to *WT* cells or cells expressing the control DARPin (fig. 40b lanes 1 and 9). These observations might be caused by the fact that the yeast cells tend to lose the episomal plasmids for DARPin expression, because of their toxicity to the cells. Even though, I can still observe the expression of DARPins on a Western blot, most cells might already have lost DARPin expression or died due to its expression. Therefore, the SUMO signal of non-expressing cells might mask the expected reduction of sumoylation after DARPin expression. Therefore, I switched to expressing the DARPins from an integrated plasmid to overcome the problem of cells losing it. The plasmid contains a promotor with a mutated Tetracycline-inducible repressor (TetR) moiety that is activated through the binding of an antibiotic effector molecule (in our case doxycycline (dox)).[424] Moreover, my DARPin constructs were tagged with GFP, allowing their detection using flow cytometry, Western blot or microscopy.

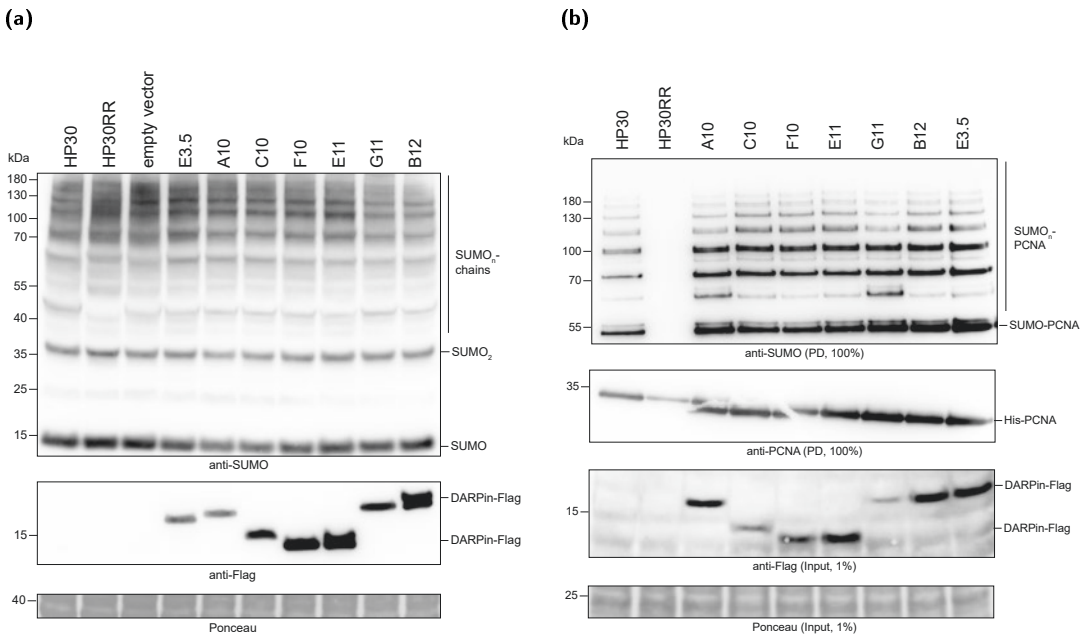

Figure 40: (a) The overall sumoylation in yeast cells does not change significantly after overexpression of DARPins from an episomal plasmid. DARPin constructs were expressed under a galactose inducible promotor. After 90 minutes of growth in galactose-containing media, cells were lysed by TCA preparation. The lysate was applied on an SDS gel and blotted. The blot was developed with an antibody against the Flag-tag on the DARPin construct, to check for DARPin expression. Additionally, it was checked for the presence of sumoylated species using an anti-SUMO antibody. For all DARPins expression was detectable after galactose induction. Overall sumoylation level in the cells was only very slightly reduced after DARPin expression. Cells only expressing His-PCNA (HP30) or the PCNA-K127/164R mutant (HP30RR) and cells transformed with the empty vector or with the non-binding DARPin (E3.5) were used as a control. **(b) Sumoylation of PCNA after over-expression of DARPins.** The DARPins were overexpressed from a galactose inducible promoter in cells also expressing His-tagged PCNA (HP30). 2 h after galactose induction samples were taken, with which a denaturing pull-down was performed. The samples from the pull-down were loaded twice and blotted for either PCNA or SUMO. On a third membrane input samples (1 %, before pull-down) were probed with an anti-Flag antibody to check for DARPin expression. All DARPins were expressed, but clearly to different levels. As expected the PCNA-K127/164R mutant (HP30RR) does not show any sumoylation. The sumoylation of PCNA was not changed after DARPin expression. Cells only expressing His-PCNA (HP30) and cells transformed with the non-binding DARPin (E3.5) were used as a control.

When I expressed the DARPins from an integrated plasmid with a dox inducible promotor, I saw that even without dox induction a high background expression level of the DARPin was visible. Similar to the episomal expression, I also observed that the expression visible in a Western blot only resulted from very few highly expressing yeast cells, while most cells shut off DARPin expression (section 2.2.3.11, section 2.2.3.12, seen in a flow cytometric analysis for GFP positive cells and microscopy, see supplementary information section 5.2). Therefore, a constitutively expressed TetR-Ssn6 repressor gene was added to the cells, which protein product represses DARPin expression as long as no dox was added to the culture.[424]

With this expression system in hand, I analysed different expression times and induction conditions by Western blot, microscopy and flow cytometry. For all following experiments, I used clones from each strain that express the different DARPins to the same

low level (quantified by Western blot) and induced DARPin expression for 20 h with either an high amount of dox (2 µg/mL) or a low dose of dox (0.5 µg/mL) if not stated otherwise.

Side note: DARPins were described to be resistant to denaturation by boiling or guanidine hydrochloride.[344,425] I observed that they are such stable that even after being blotted onto a membrane, they can bind to SUMO (tested with purified SUMO, fig. 41 lanes 3–8). As a result, DARPins will be visible in the following blots after incubation with an anti-SUMO antibody. Presumably, the DARPins bind to SUMO, which was released from the membrane during washing of the blot.

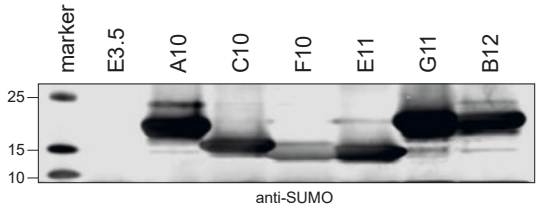

Figure 41: DARPins bind to SUMO after being blotted onto a membrane. 450 ng purified DARPins were loaded onto a SDS gel. After transfer to a membrane and blocking, 6.25 µg His-SUMO were added. After incubation, the blot was developed with an anti-SUMO antibody. All SUMO-specific DARPins can be detected here, while this is not the case for the control DARPin E3.5.

Initially, the effect of the DARPins on the overall sumoylation in the cells was analysed (section 2.2.3.6). For that whole cell extracts of DARPin expressing strains were blotted against SUMO and the amount of free and conjugated SUMO was quantified (fig. 42a and fig. 42b). Conjugated SUMO levels were reduced, while free SUMO levels were increased in all DARPin expressing strains compared to the control DARPin expressing or parental strains. A10 and G11 show the strongest effect on sumoylation (fig. 42a lanes 5 and 9), while F10 and E11 have the least effect (fig. 42a lanes 7 and 8).
When using different clones with different expression levels of a transformation with the same DARPin, the level of sumoylation was highly dependent on the amount of DARPin in the cell (fig. 42c). To investigate the DARPin concentration dependency of the sumoylation pattern further, the strong binding DARPin A10 and the medium binding DARPin E11 were induced with different doxycycline concentrations (0, 0.005, 0.01, 0.05, 0.1, 0.5, 2 µg/mL dox). The cell extracts from logarithmic growing cultures were subjected to Western blotting, detecting, on one hand, the DARPin expression and on the other hand free and conjugated SUMO (fig. 43a). The intensity of the DARPin band and the mono-SUMO band was quantified.
Quantification showed a clear connection between rising DARPin levels and rising amounts of unconjugated SUMO in the cell (fig. 43b). Hence, for quantification of the sumoylation assays, the conjugated SUMO intensities were normalised to the expression level of the respective DARPin. An effect on sumoylation was seen with dox concentrations of 0.05 µg/mL and more (fig. 43a lane 8), when also the expression of

the DARPins was visible. The amount of DARPin A10 in the cell rises slightly faster upon dox induction, compared to the amount of E11 and thus the free SUMO levels increase faster (fig. 43b). Dividing the mono-SUMO signal by the DARPin signal did not give a clear difference between the different DARPins (fig. 43c).

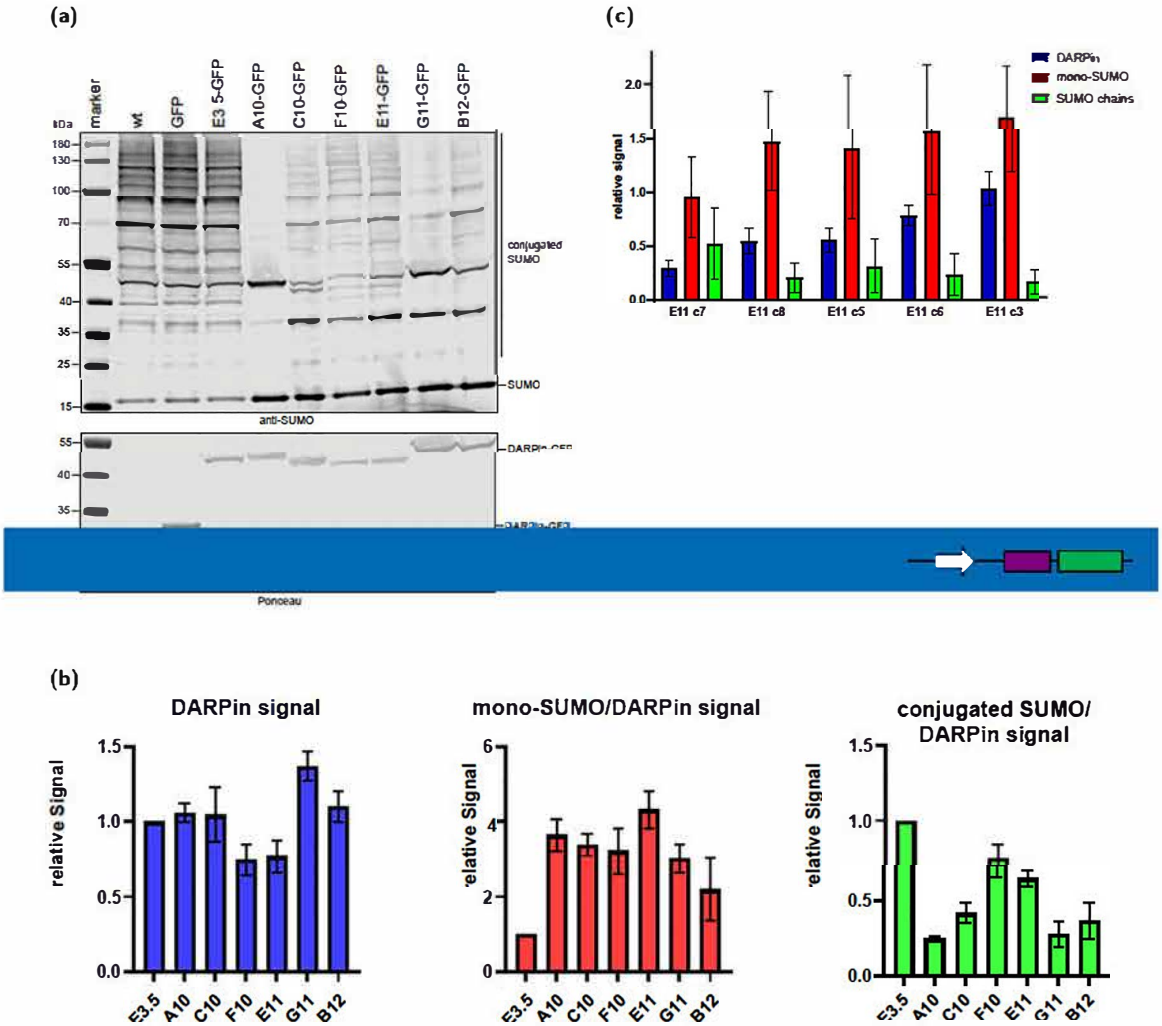

Figure 42: (a) Sumoylation levels in the presence of the different DARPins induced with 2 µg/mL dox. DARPin constructs were expressed under a doxycycline-inducible promotor. After 20 h of induction (rapidly diluted 4 h before harvesting), cells were lysed by TCA preparation and blotted with an antibody against GFP, to check for DARPin expression, or for the presence of sumoylated species using an anti-SUMO antibody. The prominent band of the DARPin in the SUMO blot results from the DARPins on the blot binding to SUMO again after blotting. It is excluded for quantification. The different DARPins influence the sumoylation level to different degrees. **(b) Quantification of DARPin expression and sumoylation of cells expressing the different DARPins induced with 2 µg/mL dox.** DARPin signal (blue), mono-SUMO signal (red) and conjugated SUMO signal (green) were quantified. Sumoylation was divided by DARPin expression levels and normalized to ponceau staining. The sumoylation level is shown relative to the sumoylation of cells expressing the control DARPin E3.5. Represented is the mean of three to five quantifications. Conjugated SUMO levels were reduced in all DARPin expressing strains compared to the control DARPin expressing strain, while free SUMO levels were increased. **(c) Quantification of DARPin expression and sumoylation of different clones expressing the DARPin E11.** Whole-cell lysates from clones expressing the DARPin E11 in different amounts induced for 20 h with 2 µg/mL dox, were blotted and sumoylation was detected using a SUMO-specific antibody and the DARPins were detected using a GFP-specific antibody. DARPin signal (blue), mono-SUMO signal (red) and conjugated SUMO signal (green) were quantified. Sumoylation was normalized to ponceau staining. The sumoylation level is shown relative to the sumoylation of cells expressing the control DARPin E3.5. Represented is the mean of four quantifications. Sumoylation was highly dependent on the DARPin expression level.

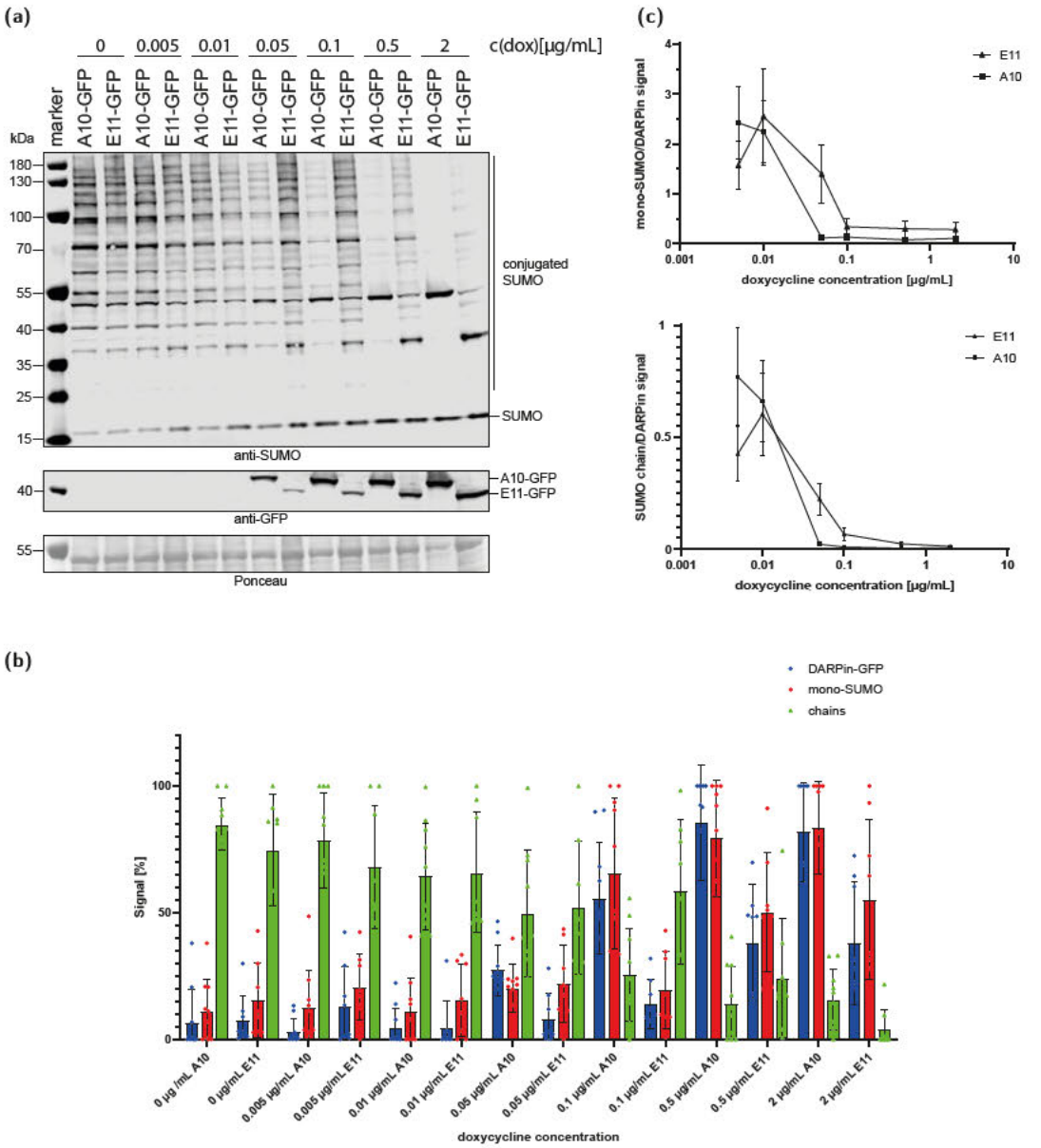

Figure 43: (a) Sumoylation levels in the presence of the DARPins A10 and E11 under different induction conditions. DARPin constructs were expressed under a doxycycline inducible promotor. After 20 h of induction (freshly diluted 4 h before harvesting) with 0.005–2 µg/mL dox, cells were lysed by TCA preparation and blotted with an antibody against GFP, to check for DARPin expression, or for the presence of sumoylated species using an anti-SUMO antibody. The prominent band of the DARPin in the SUMO blot results from the DARPins on the blot binding to SUMO again after blotting. It is excluded for quantification. The sumoylation level is highly dependent on DARPin expression levels. **(b) Quantification of DARPin expression and sumoylation in cells expressing the DARPin A10 or E11 with 0.005–2 µg/mL dox.** Whole cell lysates from clones expressing the DARPin A10 or E11 in different amounts were blotted and sumoylation was detected using a SUMO-specific antibody and the DARPins were detected using the GFP-specific antibody. DARPin signal (blue), mono-SUMO signal (red) and conjugated SUMO signal (green) were quantified. Sumoylation was normalized to ponceau staining. The signal in % that is shown, is relative to the highest (100 %) and lowest (0 %) measured DARPin, mono-SUMO or conjugated SUMO signal. Represented is the mean of 8 to 10 quantifications (represented by single dots). Sumoylation was highly dependent on the DARPin expression level. **(c) Relative free SUMO level (top) and conjugated SUMO level (bottom) in A10 and E11 expressing strains.** The free SUMO level and conjugated SUMO level from (b) are shown relative to the DARPin expression level. No clear difference between the two DARPins is visible.

3.3.4.2 Optimization of experimental system 2: DARPin expression shows an impact on cell growth

Secondly, DARPin expressing strains were analysed for their growth and cell cycle. Growth analysis was done by monitoring the OD_{600} of a culture using the Tecan Spark plate reader and spot assays with different dilutions of cells (section 2.2.3.8, section 2.2.3.10, fig. 44a and fig. 44b).
The replication of yeast cells was differently affected by the different DARPins. While F10 and E11 show the weakest effect on growth (fig. 44a purple curve and fig. 44b rows 5 and 6), G11 shows the strongest effect (fig. 44a green curve and fig. 44b row 7) compared to *WT* cells, cells expressing the control DARPin or GFP only (fig. 44a black, green and blue curve and fig. 44b rows 1 and 2). However, this observation might also result from the slightly different expression levels of the DARPins, as the influence of the DARPins on cell growth was highly dependent on expression levels (fig. 44c).
Using lower dox concentrations, I investigated, if a concentration could be found, with which no influence on the growth of the yeast cells was observed. In concentrations below 1 µg/mL dox the growth defect of the yeast strains was nearly abolished (fig. 44b first three panels), while DARPin expression was detectable in a Western blot from 0.05 µg/mL dox onwards (fig. 43b). However, one has to keep in mind that in a spot assay, it can not be determined if the cells that were growing well were still positive for DARPin expression.
Therefore, I further analysed the percentage of GFP-positive cells at different dox concentrations using flow cytometry (section 2.2.3.11). Here, I observed that a dox concentration of 0.1 µg/mL and above gives over 80 % GFP positive cells when used for 20 h (see supplementary information section 5.2). Shorter induction times again lead to a drop in the percentage of DARPin expressing cells (20–60 % after 4 h) and in the intensity of the DARPin signal. From these experiments, I concluded that for the chosen clones an induction time of 20 h with 0.5 µg/ mL dox and using DARPins F10 or E11 is optimal to have a good amount of DARPin expression without affecting cell growth. In addition, I could conclude that for the analysis of inhibitory effects of the DARPins on yeast, as indicated by the *in vitro* experiments, using DARPin A10 at a higher dox concentration (2 µg/mL) is optimal.

To investigate if the growth defect observed at high dox concentrations was caused by DARPins binding to SUMO or sumoylated substrates inside the nucleus or in the cytoplasm, I repeated the spot assay in strains expressing DARPins harbouring a double nuclear localisation (NLS) or nuclear export sequence (NES). Hence, expressed DARPins localise either inside the nucleus or in the cytoplasm. For comparison, I also spotted strains expressing DARPins without a localisation signal.
Strains expressing the control DARPin E3.5 do not show any growth defect regardless

of the localisation and induction strength compared to the parental strain (fig. 45a rows 2, 3 and 4). Using the SUMO-specific DARPins F10 and E11, I could observe that untagged and NLS-tagged DARPin expressing strains show a similar growth defect (fig. 45a rows 6 and 9), while NES-tagged DARPin expressing strains (fig. 45a rows 7 and 10) grow comparable to the parental strain (fig. 45a row 1). The effect was less pronounced for E11 compared to F10. Hence, we can co

Quantification: Sumoylation is reduced after D

sumoylation of nuclear targets by DARPins has a higher impact on cell growth than the binding of DARPins to cytoplasmic targets.

Method: SUMO signal (minus DARPin band) divided by DARPin DARPin (E3.5) expressing cells (mean of 4 experiments).

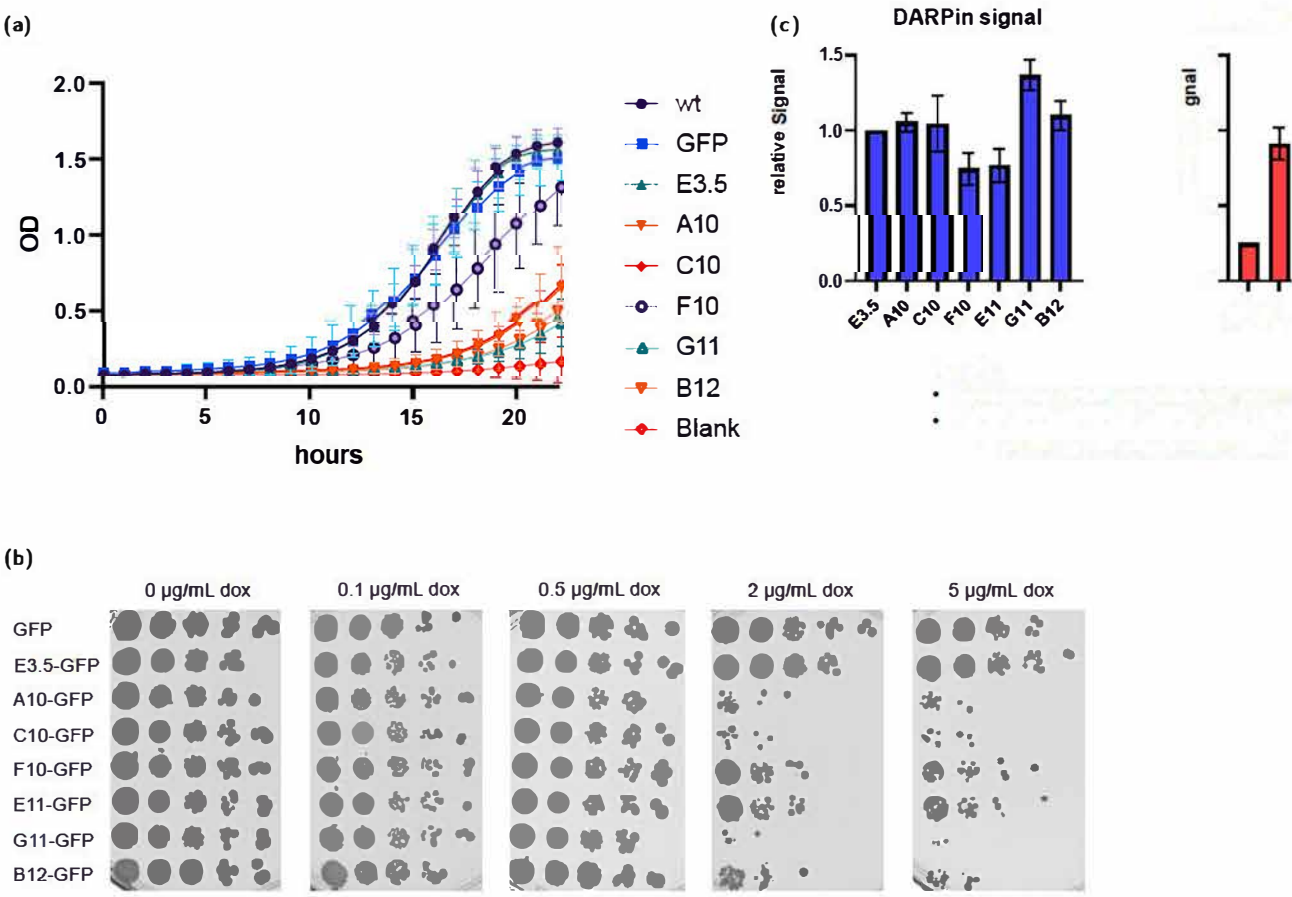

Figure 44: (a) Growth curves of DARPin expressing strains. The OD of yeast expressing the DARPins for 20 h with 2 µg/mL dox was monitored for 24 h. The graph shows the mean and standard deviation from three independent replicas. All DARPins besides E3.5 show an effect on cell growth. The weakest effect is visible for DARPin F10. **(b) Spot assay looking for yeast growth under different DARPin expression conditions.** Different dilutions of yeast strains expressing the different DARPins were spotted onto plates containing 0, 0.1, 0.5, 2 or 5 µg/mL dox. Plates were incubated for 3 days at 30 °C. Cells transformed with the empty vector (GFP) or the non-specific DARPin (E3.5) were used as a control. DARPin expression allows colony formation at low dox concentrations, but growth is influenced from 2 µg/mL dox upwards. **(c) Quantification of DARPin expression in the yeast strains used for *in vivo* experiments.** DARPin-GFP expression was quantified from three independent Western blots against GFP. The signal is shown relative to the signal of cells expressing the control DARPin E3.5. The construct for DARPin expression contains a FLAG- and GFP-tagged DARPin under a doxycycline inducible promotor. For tight expression control, a repressor was introduced into the strains used for *in vivo* analysis.

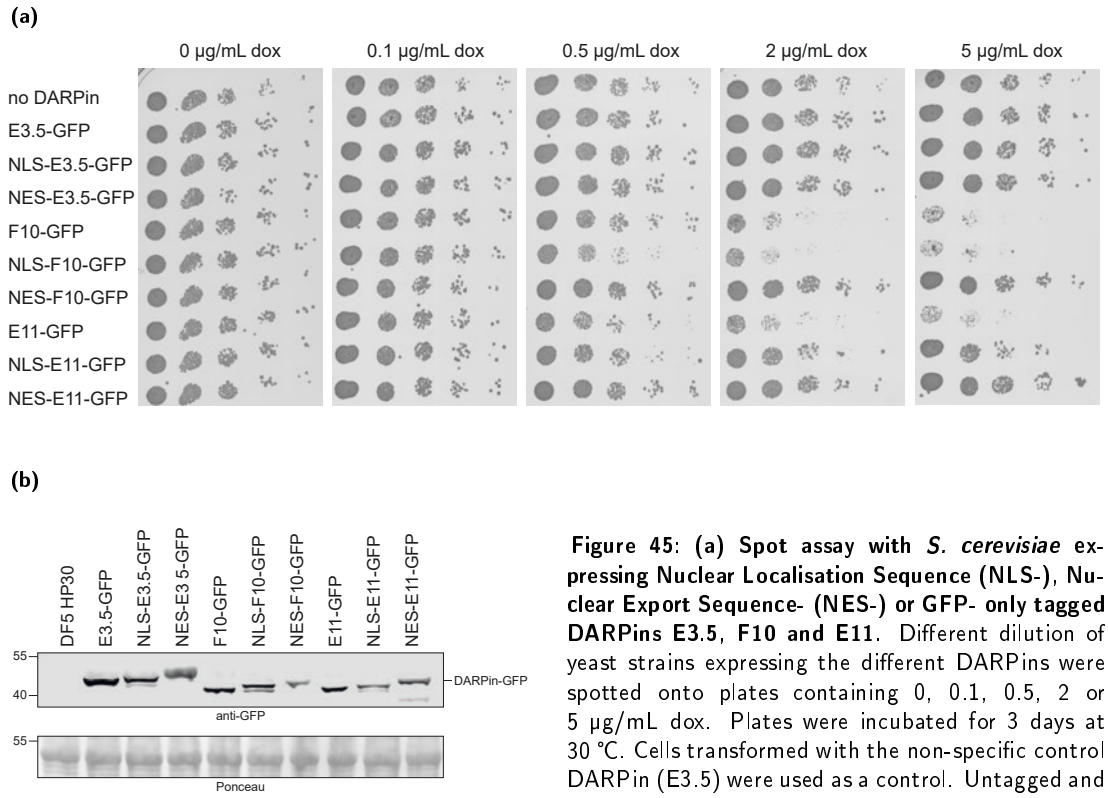

Figure 45: (a) Spot assay with *S. cerevisiae* expressing Nuclear Localisation Sequence (NLS-), Nuclear Export Sequence- (NES-) or GFP- only tagged DARPins E3.5, F10 and E11. Different dilution of yeast strains expressing the different DARPins were spotted onto plates containing 0, 0.1, 0.5, 2 or 5 µg/mL dox. Plates were incubated for 3 days at 30 °C. Cells transformed with the non-specific control DARPin (E3.5) were used as a control. Untagged and NLS-tagged DARPin expressing strains show a similar growth defect, while NES-tagged DARPins expressing strains grow comparable to the parental strain. **(b) Expression of DARPins for spot assay.** Yeast cultures used for the spot assay were subjected to cell lysis and Western blot. The DARPins were detected using a GFP-specific antibody. The strains express the DARPins to similar level.

The cell cycle of DARPin expressing strains was analysed using formaldehyde-fixed cells stained with propidium iodide and analysed for their DNA content in the flow cytometer (section 2.2.3.11). In this experiment, it was possible to distinguish between DARPin expressing and non-expressing yeast, by gating for GFP positive cells. In the following section, only the results for the GFP-positive cells are discussed.

Again, the highest percentage of cells expressing the DARPin was seen after 20 h induction with 0.1–2 µg/mL dox (70–90 % GFP positive cells, see supplementary information section 5.2). However, under the high dox induction conditions (2 µg/mL) the cells expressing the DARPins were severely impaired in cell cycle progression (fig. 48a). From a comparison with the cell cycle profile of α-factor or nocodazole arrested cells (G_1- and G_2-/M-Phase arrest, respectively) one can assume that they were stuck in late S-Phase or G_2/M-Phase (fig. 48b).

This goes in hand with previous results, where I have seen that under these induction conditions (2 µg/mL dox), the DARPin expressing strains were growing much slower compared to cells expressing the control DARPin (fig. 44b), and the sumoylation levels in the cells were highly reduced (fig. 42b).

3.3.4.3 Optimization of experimental system 3: DARPins localise mostly nuclear and sometimes form bright spots

This section aims on analysing the localisation of DARPins inside yeast and to determine the exact cell cycle phase, in which the DARPin expression induces arrest. For detecting DARPins *in vivo* they were fused to the fluorescence marker GFP that can be detected in the microscope (section 2.2.3.12). Using an integrated plasmid with a titratable promoter, I was looking for the localisation of a strong binding DARPin (F10) fused to GFP in yeast cells (fig. 46a).

At a high induction level (2 µg/mL dox) and with a short induction time (90 min) of the DARPin, many cells seemed not to express the DARPin construct. In the most healthy-looking cells, the DARPin was localized equally throughout the nucleus (fig. 46a panels 2–4). Sometimes it was also localized to bright spots in the nucleus (fig. 46a panels 2–3) or to the bud neck (fig. 46a panel 4). An high number of cells expressing the DARPin construct became big and round. This indicates that they were cell cycle arrested. These cells often have a strong nuclear DARPin signal (fig. 46a panel 5) or a signal in long structures in the cytoplasm (fig. 46a panel 6), which possibly represent mitochondria or the endoplasmic reticulum.

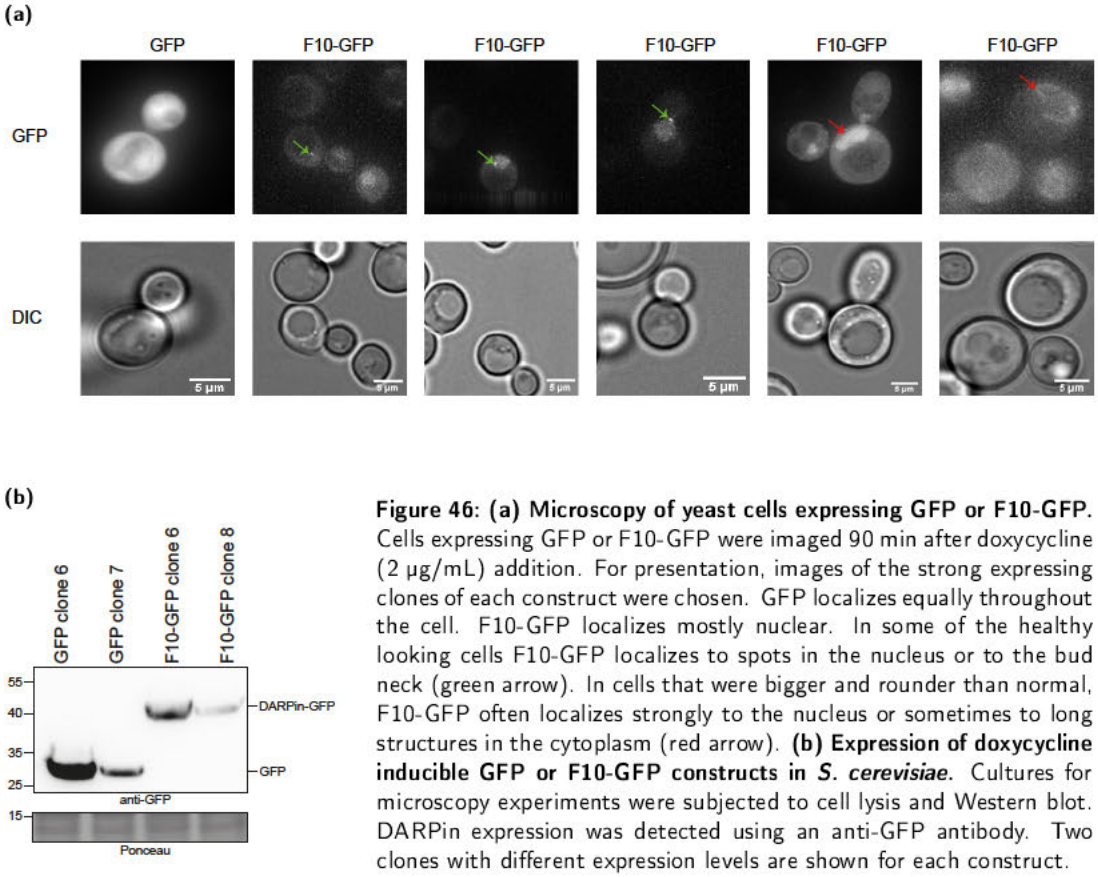

Figure 46: (a) Microscopy of yeast cells expressing GFP or F10-GFP. Cells expressing GFP or F10-GFP were imaged 90 min after doxycycline (2 µg/mL) addition. For presentation, images of the strong expressing clones of each construct were chosen. GFP localizes equally throughout the cell. F10-GFP localizes mostly nuclear. In some of the healthy looking cells F10-GFP localizes to spots in the nucleus or to the bud neck (green arrow). In cells that were bigger and rounder than normal, F10-GFP often localizes strongly to the nucleus or sometimes to long structures in the cytoplasm (red arrow). **(b) Expression of doxycycline inducible GFP or F10-GFP constructs in *S. cerevisiae*.** Cultures for microscopy experiments were subjected to cell lysis and Western blot. DARPin expression was detected using an anti-GFP antibody. Two clones with different expression levels are shown for each construct.

Using low induction conditions (0.5 µg/mL dox) all DARPins besides the control DARPin E3.5 show strong nuclear staining, and a slightly lesser cytoplasmic staining (fig. 47a). E3.5 was equally distributed in the cell (fig. 47a column 1). Using the strong binder A10 no distinct foci were visible in the yeast cells, only a strong diffuse staining of the nucleus (fig. 47a column 2). This is probably caused by its high affinity to SUMO and the strong inhibitory effect on sumoylation processes in the cell. Using the weaker binding DARPins C10, F10, E11, G11 and B12 with a fast off-rate, in some yeast cells distinct nuclear foci were visible (fig. 47a column 3–7). With DARPins F10 and E11 sometimes a ring-like structure around the bud neck was visible. Both observed structures represent most likely sumoylated proteins in the cell that were detected with the DARPins. Identification of these structures was followed up in section 3.3.4.5 and section 3.3.4.5.

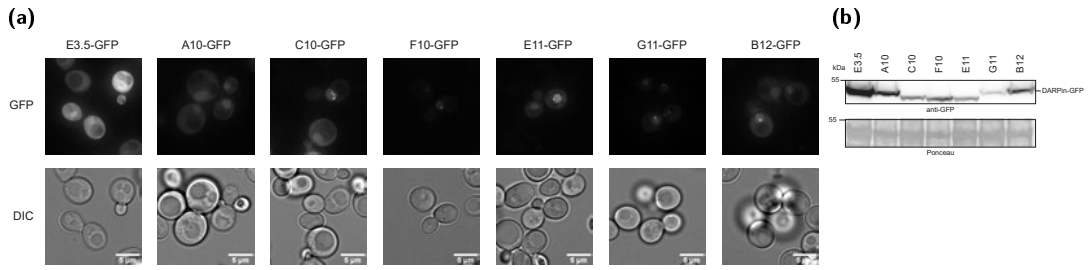

Figure 47: (a) Localisation of SUMO-specific DARPins in yeast. DARPin expression (upper panel) was induced with 0.5 µg/mL dox for 20 h. Microscopy images of exponential growing living cells were taken. All DARPins besides the control DARPin E3.5 show a strong nuclear staining, and a slightly lesser cytoplasmic staining **(b) Expression of DARPins in cultures used for microscopy.** Cultures for microscopy experiments were subjected to cell lysis and Western blot. DARPin expression was detected using an anti-GFP antibody.

In the microscope highly DARPin expressing cells (20 h in 2 µg/mL dox) show a phenotype similar to an *ubc9 temperature-sensitive* (*ubc9ts*) strain grown at the restrictive temperature and therefore losing the expression of the SUMO E2 enzyme. All SUMO-specific DARPin expressing strains and the *ubc9ts* strain show mainly large budded cells under the microscope (fig. 48d panels 2, 3 and 4).
Additionally, a cell cycle analysis by flow cytometry showed that the *ubc9ts* and in the DARPin expressing strains are arrested in the same cell cycle phase (fig. 48c). Moreover, in *ubc9ts* as well as the DARPin expressing strains the whole cell cycle profile shifts to the right when grown at 37 °C, while that was not the case for the parental or control DARPin expressing strains (fig. 48c).

To analyse the exact cell cycle phase, in which the DARPin expressing strains were arrested, I performed immunofluorescence microscopy (section 2.2.3.14) including staining for the microtubules, the GFP-tag on the DARPins and the nucleus (DAPI).
Through the cell cycle microtubules form very distinct patterns in each stage. In G_1-phase the spindle pole body (SPB) can be seen as a bright dot, from which one or more microtubules stretch out. In S-phase, the SPB has duplicated but is still visible as one dot, as it has not separated yet. It lies completely within the mother cell. A spindle is

not visible. At G_2-/M-phase the mitotic spindle can be seen as a short bright stretch, with an area of lower intensity at its centre, corresponding to the two halves of the mitotic spindle. It is orientated towards the bud neck. Cytoplasmic microtubules extend from the end of the spindle into different dictions. During mitosis the spindle becomes elongated through the bud neck, spanning from the mother to the daughter cell. At the exit from mitosis, the spindle separates and cells enter G_1-phase.[426]

The cells expressing the control DARPin show equal DARPin staining throughout the cell, and the microtubule staining indicates that cells are in all different cell cycle phases with most cells being in G_1-phase (fig. 49a row 1). Cells that have lost Ubc9 after a switch to restrictive temperature and cells that express a high amount of the strong binding DARPin A10 were mostly arrested in G_2-/M-Phase transition (fig. 49a row 2 and 3). This can be seen by the microtubules forming a short spindle oriented towards the bud neck in most of the cells (fig. 49a column 1). The GFP staining here was more prominent in the nucleus compared to the cytoplasm, indicating that the DARPin localizes mostly nuclear (fig. 49a column 2).

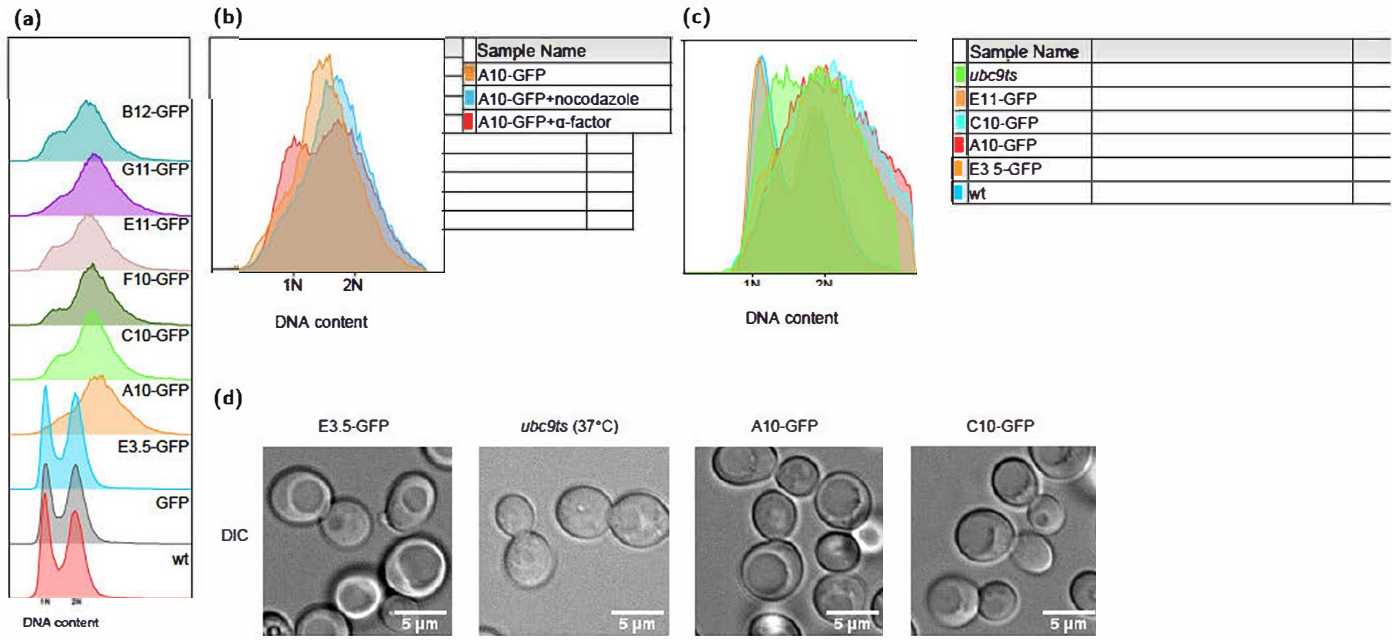

Figure 48: (a) Cell cycle analysis of DARPin expressing strains. Yeast strains expressing the DARPins or an empty vector were grown overnight in 2 µg/mL dox. Before analysis cultures were diluted and grown to exponential phase. Cells were fixed with formaldehyde and the DNA was stained with PI, before subjected to analysis by flow cytometry. Only GFP positive cells were analysed. Cells not transformed with the DARPin expression plasmid (*WT*, red), with an empty vector (GFP, grey) or the control DARPin (E3.5, blue) were used as a control. DARPin expression for 20 h at high dox concentration shifts the cell cycle profile and arrests the cells. **(b) Comparison of cell-cycle profiles to α-factor or nocodazole arrested cells.** Overlay of non-treated A10 (orange) expressing yeast with G_1- (red) or G_2-arrested (blue) cells shows an arrest of DARPin expressing cells in late S- or G_2-/M-phase. **(c) Comparison of cell cycle profile of DARPin expressing and *ubc9ts* strains.** Overlay of the cell cycle profile of the DARPin expressing cells and the *ubc9ts* strains (green) grown at restrictive temperatures, shows a growth arrest in the same cell cycle phase. The *ubc9ts* strain does not show a complete arrest at the point of analysis. Compared to the non-transformed or control DARPin expressing strain the cell cycle profiles of the *ubc9ts* and DARPin expressing strains are shifted to the right. **(d) Comparison of phenotype of DARPin expressing cells to *ubc9ts* strain.** A *ubc9ts* strain was grown at restrictive temperature for 4 h. This leads to the prevention of the expression of the E2 enzyme for sumoylation. Light microscopic pictures were taken from the *ubc9ts* as well as DARPin expressing strains which were induced with 2 µg/mL dox for 20 h. DARPin expressing strains show a similar phenotype like cells defective for sumoylation.

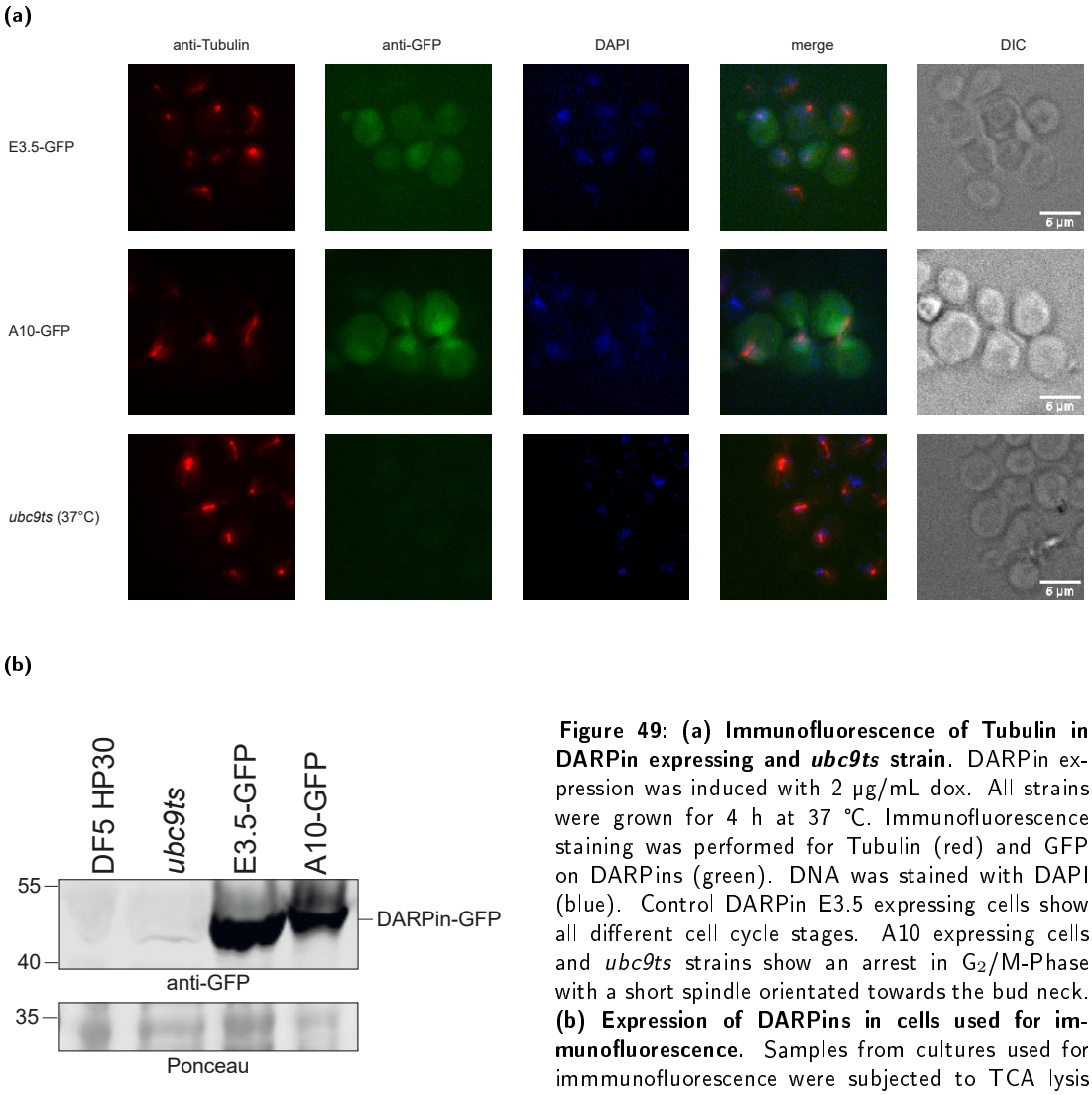

Figure 49: (a) Immunofluorescence of Tubulin in DARPin expressing and *ubc9ts* strain. DARPin expression was induced with 2 µg/mL dox. All strains were grown for 4 h at 37 °C. Immunofluorescence staining was performed for Tubulin (red) and GFP on DARPins (green). DNA was stained with DAPI (blue). Control DARPin E3.5 expressing cells show all different cell cycle stages. A10 expressing cells and *ubc9ts* strains show an arrest in G_2/M-Phase with a short spindle orientated towards the bud neck. **(b) Expression of DARPins in cells used for immunofluorescence.** Samples from cultures used for immmunofluorescence were subjected to TCA lysis and Western blot. DARPins were detected using a GFP-specific antibody.

3.3.4.4 Usability of DARPins as tools for inhibiting SUMO functions *in vivo*

In vitro data, as well as detection of whole-cell sumoylation patterns by Western blot, have shown that especially DARPin A10 can be used to inhibit sumoylation, desumoylation or SIM interaction as summarized in fig. 60. *In vivo* the influence of these affinity probes was not only dependent on the characteristics of the DARPin, but also on its concentration in the cell (section 3.3.4.1). This section will now show the usability of the DARPins to inhibit sumoylation *in vivo*.

Proof of concept 1: Inhibition of cell growth under stress conditions

SUMO has been shown to play a vital role in many stress response pathways of yeast,[312] as a consequence an inhibition of sumoylation in yeast would make cells sensitive to different stress conditions. Therefore, I also tested the growth of DARPin expressing cells after induction with 0.5 µg/mL dox under osmotic (NaCl), DNA damaging (MMS/UV), temperature or oxidative (H_2O_2) stress conditions (section 2.2.3.8, fig. 50a and fig. 50c). None of the DARPins had any influence on cell growth in the various temperatures tested (fig. 50a columns 4 and 5). G11 showed a strong effect under all other conditions tested (fig. 50a row 7), while F10 and E11 showed only weak effects on cell growth under all conditions (fig. 50a rows 6 and 5). The other DARPins (A10, C10 and B12) showed medium to strong effects under the different tested conditions besides temperature (fig. 50a rows 3, 4 and 8). A10 was having more effect after osmotic stress and C10 after UV treatment conditions.

Proof of concept 2: Inhibition of PCNA sumoylation

To complete the picture of how DARPins can be used as inhibitors for sumoylation *in vivo*, I performed denaturing pull-downs for His-tagged PCNA in DARPin expressing strains to look for their effect on PCNA sumoylation (section 2.2.3.7). Therefore, the DARPins were induced with 0.5 µg/mL dox for 20 h and cells were treated with 0 %, 0.02 % or 0.3 % MMS for 90 min to induce DNA damage. PCNA is sumoylated during normal replication. Low doses of MMS mainly induce PCNA ubiquitinylation, while high doses cause additional PCNA sumoylation.[44,198]
The Western blot after denaturing PD of PCNA showed that A10, C10, G11 and B12 decrease PCNA sumoylation upon expression (fig. 50b lanes 5 and 6), while in F10 and E11 expressing cells the sumoylation pattern was comparable to *WT* cells (fig. 50b lanes 2, 4 and 7). These results confirm previous observations that especially A10 is a very good inhibitor of sumoylation, not only *in vitro* but also *in vivo*.

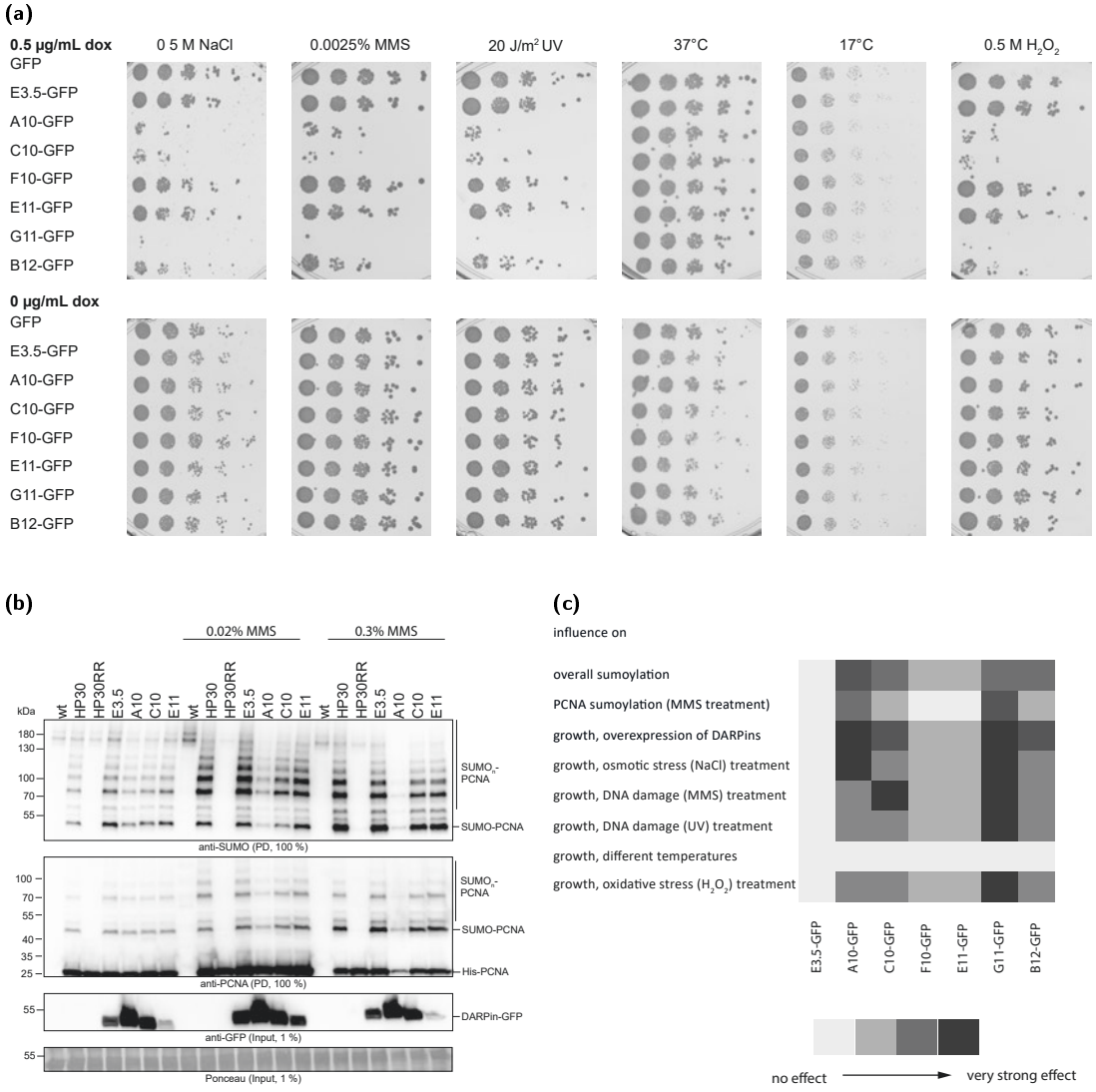

Figure 50: **(a) Spot assay of DARPin expressing strains under different stress conditions.** Different dilutions of yeast strains expressing the DARPins of interest were spotted onto plates containing 0.5 µg/mL dox (upper panel) or no dox (lower panel). Plates were supplemented with 0.5 M NaCl, 0.0025 % MMS, 0.5 mM H_2O_2, 20 J/m^2 UV radiation or grown at 37 °C, or 17 °C. Plates were incubated for 3 days at 30 °C (if not indicated otherwise). Cells transformed with the empty vector (GFP) or the non-SUMO specific DARPin (E3.5) were used as a control. Without dox induction, no growth defect is visible for any strain. DARPin expression has a negative impact on growth under all stress conditions besides high and low temperature. **(b) Denaturing pull-down of PCNA in DARPin expressing strains.** Yeast strains were grown in the presence of 0.5 µg/mL dox to induce DARPin expression. Where indicated strains were treated with low (0.02 %) or high (0.3 %) doses of MMS. 50 OD cells were harvested, lysed and a denaturing pull-down of His-PCNA was performed. Each sample was blotted twice and either developed against SUMO or PCNA. Input samples (1 %) after cell lysis, were loaded in parallel and probed for DARPin expression with an anti-GFP antibody. Different DARPins inhibit the sumoylation of PCNA to a different degree. **(c) Summary of *in vivo* characteristics of the SUMO specific DARPins.** The graphic shows that the different DARPins have distinct influences on sumoylation and colony formation. The colour coding spans from light grey (no effect) to dark grey (strong effect).

3.3.4.5 Usability of DARPins as detection tools *in vivo*

In vitro data (fig. 60), as well as the previosly described *in vivo* experiments have shown that the strong binding DARPins F10 and E11 with fast off-rates (table 16) have the most promising properties to be used as sensors to detect sumoylation *in vivo*. *In vivo* they show the least effect on cell growth, cell cycle progression, phaenotypic appearance of yeast cells, the overall sumoylation of the cells and sumoylation of an example substrate (section 3.3.4). This section will now show the usability of the DARPins to detect sumoylation *in vivo*.

Proof of concept 1: Colocalisation with SUMO

For using DARPins F10 and E11 to detect sumoylation or sumoylated proteins *in vivo* they were fused to the fluorescence marker GFP that can be detected in the microscope (section 2.2.3.12). Using low induction conditions (0.5 µg/mL dox) the different DARPins were tested for their usability as sensors. As the first proof of concept experiment, this section shows the colocalisation of DARPins and SUMO in the cell.
Newman *et al.* (2017) showed that SUMO can be found mostly nuclear in the cell with some cytoplasmic localisation.[312] To show colocalisation with the SUMO-specific DARPins, they were co-expressed with mCherry-SUMO, expressed from an episomal plasmid under a copper inducible promotor. In a logarithmic growing culture a colocalisation of mCherry-SUMO with the SUMO-specific DARPins F10 and E11 (fig. 51a row 2 and 3), but not with the control DARPin E3.5 (fig. 51a row 1) was observed.

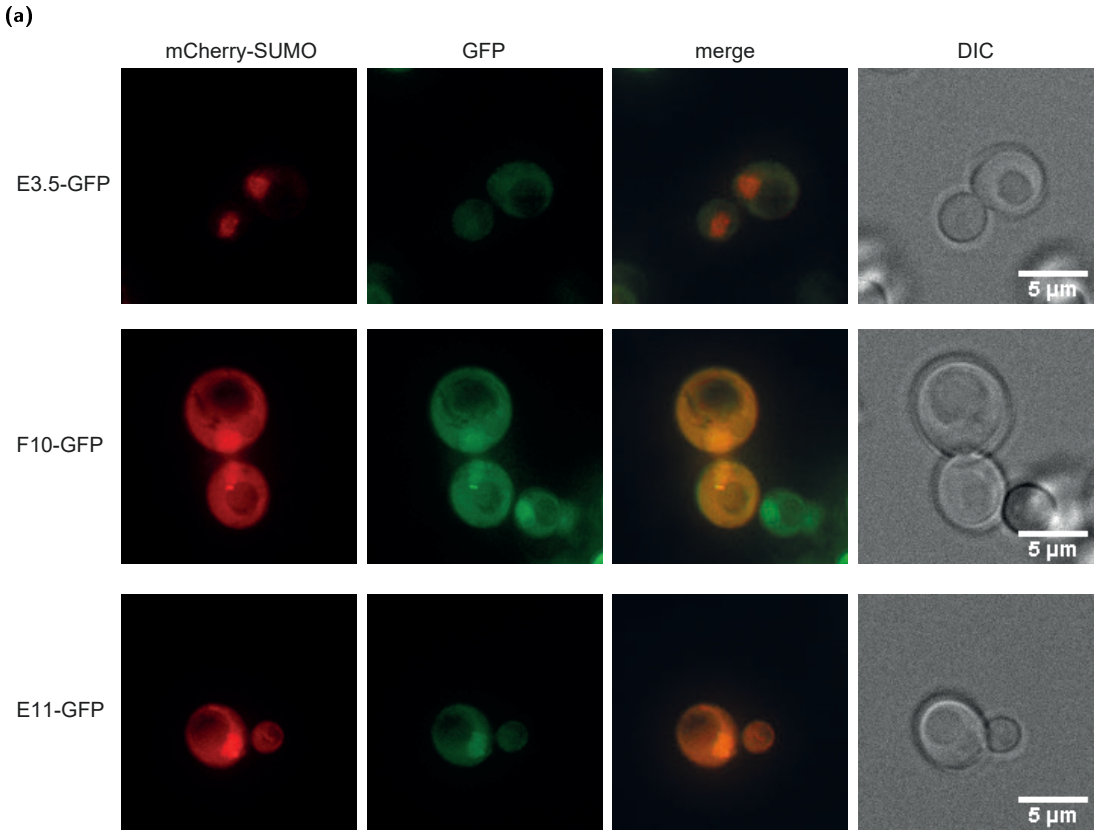

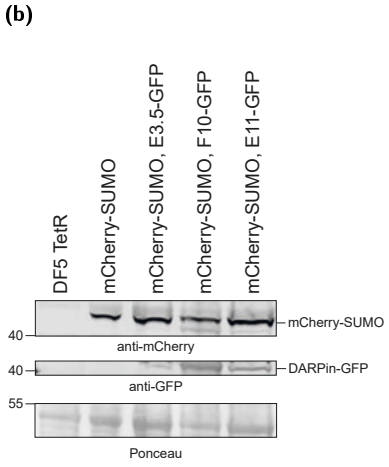

Figure 51: (a) Colocalisation of DARPins-GFP (green) with mCherry-SUMO (red). Integrated DARPins F10-GFP and E11-GFP were induced for 20 h with 0.5 µg/mL doxycycline. mCherry-SUMO was coexpressed from an episomal plasmid under a leaky copper inducible promotor without induction. A logarithmic growing culture was taken for microscopy. Red and green channels were merged for the detection of colocalisation. SUMO-specific DARPins F10 and E11, but not the control DARPin E3.5, colocalize with SUMO in the cell. **(b) Expression of DARPins and SUMO in cultures used for colocalisation studies.** Cultures from microscopy experiments were subjected to cell lysis and Western blot. DARPin expression was detected using an anti-GFP antibody. mCherry-SUMO was detected using a mCherry-specific antibody.

Proof of concept 2: Colocalisation with mitotic Septins

As a second proof of principle, I wanted to show colocalisation of my SUMO-specific DARPins with the well-described sumoylation signal on the mother bud neck side of the Septin ring during mitotic cell division (section 1.2.5.3). The DARPins were tagged with GFP and expressed (0.5 µg/mL dox) in a strain where the non-essential Septin Shs1, was tagged with a red fluorophore (Shs1-mCherry). Tagging of Shs1 with mCherry does not interfere with its functionality during mitosis as shown before by Renz *et al.* (2016).[301] I observed that in an asynchronous growing culture an high percentage of cells show the Septin ring being stained with mCherry at the bud neck. However, the GFP-tagged DARPins were detected mostly in the nucleus and only rarely at the bud neck (data not shown).

To force the DARPins to localise to the cytoplasm rather than to the nucleus, I cloned constructs expressing a 2xNES in front of the DARPin. Now, nice colocalisation with the Septin ring was visible with the SUMO-specific DARPins F10 and E11 (fig. 53a lanes 2 and 3), but not with the control DARPin E3.5 (fig. 53a lane 1). In accordance with results from other groups[197,300] this signal forms only after the Septins form an hourglass shape around the bud neck and vanishes after splitting of the Septin ring (fig. 53b). As only the Septins of the mother site of the Septin ring are sumoylated, we exclusively observed Septin ring staining by DARPins on one side of the bud neck.

In denaturing pull-down experiments (section 2.2.3.7) with His-tagged Shs1, I was able to show that the used DARPins (F10 and E11) do not interfere with Septin sumoylation (fig. 52 lanes 5 and 6), compared to *WT* cells or cells expressing the control DARPin E3.5 (fig. 52 lanes 3 and 4) and were therefore useful tools for the detection of sumoylation *in vivo*.

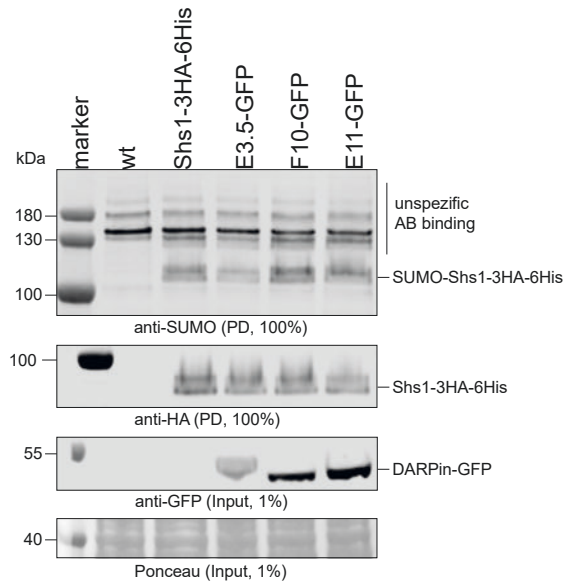

Figure 52: Denaturing pull-down of Shs1-3xHA-6xHis from NES-DARPin-GFP expressing cells. Yeast strains were grown in the presence of 0.5 µg/mL dox for 20 h. 50 OD cells were harvested, lysed and a denaturing pull-down of Shs1-His was performed. Each sample was blotted twice and either developed against SUMO or the HA-tag on Shs1. Input samples after cell lysis were loaded in parallel (1 %) and probed for DARPin expression with an anti-GFP antibody. DARPins E3.5, F10 and E11 do not interfere with Septin sumoylation.

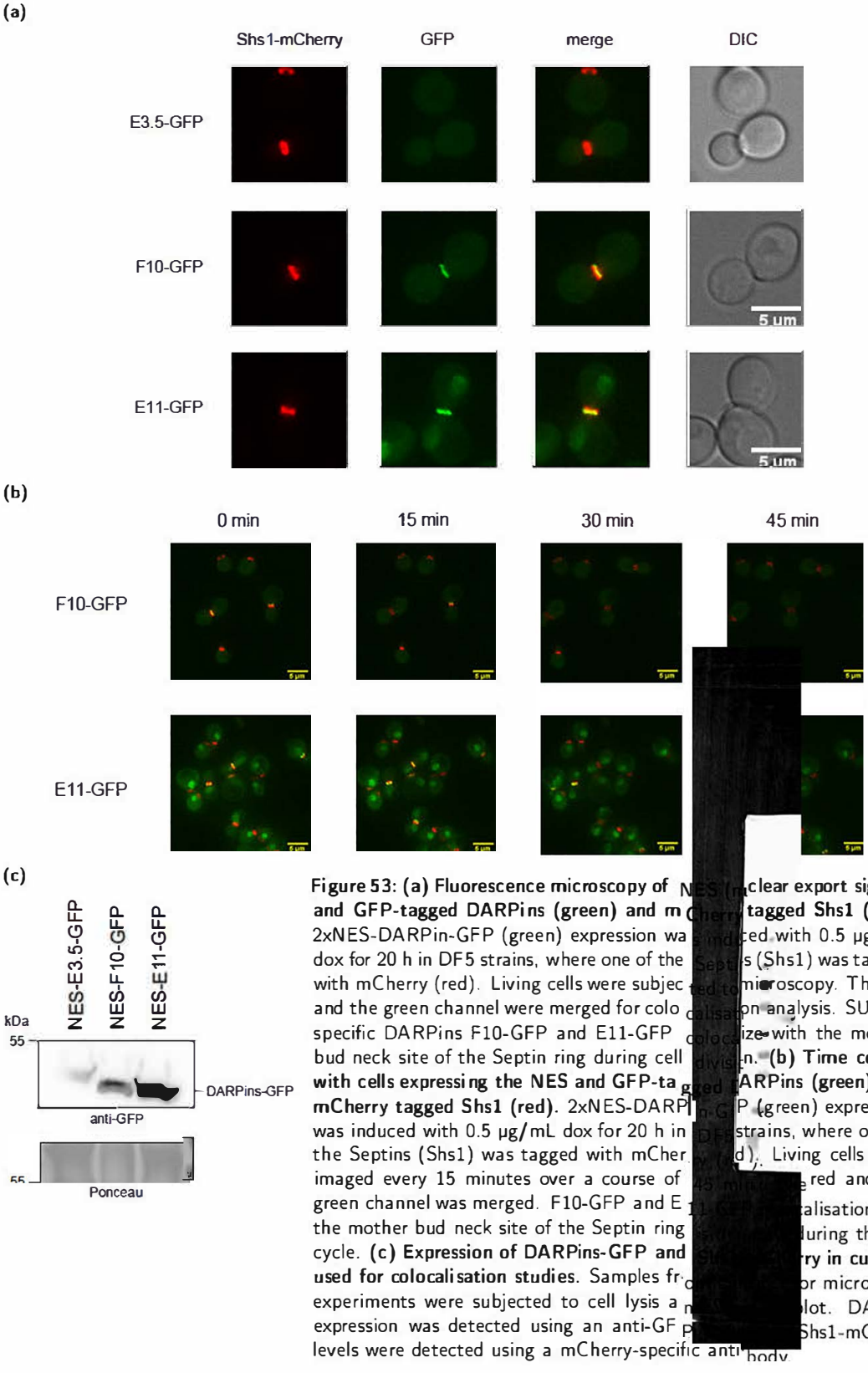

Figure 53: (a) Fluorescence microscopy of N[illegible]clear export signal) and GFP-tagged DARPins (green) and m[illegible]tagged Shs1 (red). 2xNES-DARPin-GFP (green) expression wa[illegible]ced with 0.5 µg/mL dox for 20 h in DF5 strains, where one of the [illegible]s (Shs1) was tagged with mCherry (red). Living cells were subjec[illegible]ted to microscopy. The red and the green channel were merged for colo[illegible]on analysis. SUMO-specific DARPins F10-GFP and E11-GFP [illegible]ize with the mother bud neck site of the Septin ring during cell [illegible]n. **(b) Time course with cells expressing the NES and GFP-ta[illegible]ARPins (green) and mCherry tagged Shs1 (red).** 2xNES-DARP[illegible]P (green) expression was induced with 0.5 µg/mL dox for 20 h in [illegible]strains, where one of the Septins (Shs1) was tagged with mCher[illegible]). Living cells were imaged every 15 minutes over a course of [illegible]e red and the green channel was merged. F10-GFP and E[illegible]alisation with the mother bud neck site of the Septin ring [illegible]during the cel cycle. **(c) Expression of DARPins-GFP and [illegible]ry in culture used for colocalisation studies.** Samples fr[illegible]or microscopy experiments were subjected to cell lysis a[illegible]lot. DARPin expression was detected using an anti-GF[illegible]Shs1-mCherry levels were detected using a mCherry-specific anti[illegible]body.

Experiment 1: Vain detection of sumoylation of meiotic Septins

The regulation of Septin structure formation during mitosis is widely clear, however, how localisation of Septins is regulated during meiosis is not known so far (section 1.2.5.3). It is known that Septins play an important role during meiotic cell division in *S. cerevisiae*.[308] Though, the only reported regulation so far is a possible involvement of the Gip1p-Glc7p phosphatase complex and therefore dephosphorylation might be important for septin localisation during meiosis.[427] I now wanted to investigate if sumoylation plays a role in the regulation of meiotic Septin structure formation.
The SK1 strain is routinely used for meiotic experiments in yeast because it can be driven very synchronously into sporulation by a switch from glucose to acetate as a carbon source and a lack of nitrogen in the medium (section 2.2.3.17).[428] In preliminary experiments I saw that high levels of DARPin-GFP expression or tagging of the meiotic Septin Spr3 with mCherry prevents sporulation of diploids (data not shown). Hence, I expressed Spr3-mCherry from a centromeric plasmid (as done in Pablo-Hernando *et al.* (2008))[306] and selected clones with lower DARPin expression levels for my experiments (fig. 54b). Additionally, I used diploid strains, where Shs1 was tagged on one allele with mCherry and that expressed low levels of DARPin-GFP constructs. These strains I received by mating the DF5 strains used for the mitotic Septin colocalisation with the SK1 strain of an opposite mating type. With the described strains I performed a time-course experiment taking microscopy pictures every hour up to 11 h and at 24 h after the switch to sporulation media.
However, neither Spr3 nor Shs1 seems to localise normally under the tested conditions, even without DARPin expression (fig. 54a lanes 1 and 4), as no expected microtubules or PSM-like structures were visible in the microscope.

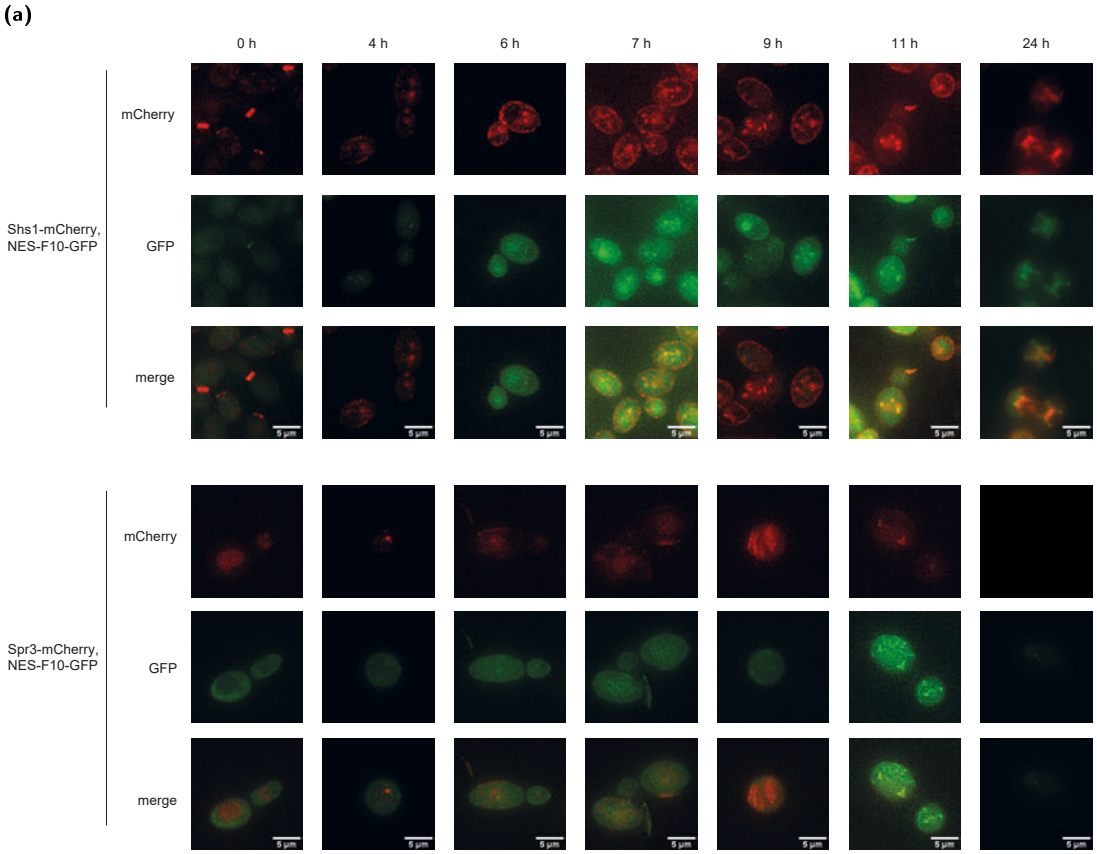

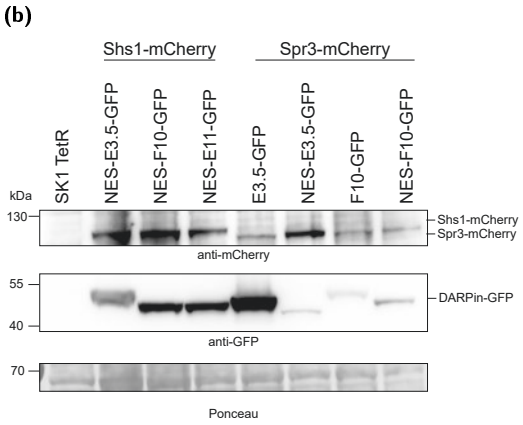

Figure 54: (a) Fluorescence microscopy of NES and GFP tagged DARPin F10 and mCherry-tagged Septins Shs1 (upper panel) and Spr3 (lower panel). 2xNES-DARPin-GFP (green) expression was induced with 0.5 µg/mL dox in diploid SK1 strains, where either one allele of Shs1 was tagged with mCherry (red) or Spr3-mCherry is expressed from a centromeric plasmid (red). Meiosis was induced in a logarithmic growing culture by a switch from pre-sporulation to sporulation media. Living cells were imaged every 60 minutes for 11 h and then again 24 h after the medium switch. Exemplary time points are presented here. The red and the green channel were merged. The Septins do not show any characteristic localisation to the microtubule or the prospore membrane during meiosis. Also, the DARPins do not show any specific localisation pattern. **(b) Expression of DARPins-GFP, Spr3-mCherry and Shs1-mCherry in cultures used for colocalisation studies.** Cultures from microscopy experiments were subjected to cell lysis and Western blot 24 h after sporulation induction. DARPin expression was detected using an anti-GFP antibody. Shs1-mCherry and Spr3-mCherry levels were detected using a mCherry-specific antibody.

Experiment 2: Identification of spots visible after DNA damage treatment

As described above some cells expressing the SUMO-specific DARPins with fast off-rates (F10 and E11) show one or more prominent nuclear foci (fig. 47a). This section aims on identifying these foci. DARPin containing foci appear in more cells if cultures were treated for 90 min with a low dose of MMS (fig. 55a column 2) or if they were released for 30 min from α-factor treatment (from G_1 phase arrest (fig. 56a upper panel, column 4). The foci vanish in a strain were the genes for the expression of the E3 enzymes Siz1 and Siz2 were deleted (fig. 55a columns 3 and 4). This indicated that the DARPins detect sumoylation targets in the nucleus that were sumoylated to a higher degree after DNA damage or during S-phase, and their sumoylation was dependent on the SUMO ligases Siz1 and/or Siz2. To identify the proteins that are detected by the DARPins, I performed colocalisation studies with fluorescence tagged known sumoylation targets or proteins that are described to form nuclear foci. The following experiments are performed with low induction of expression with 0.5 µg/mL dox and using the medium binders F10 and E11.

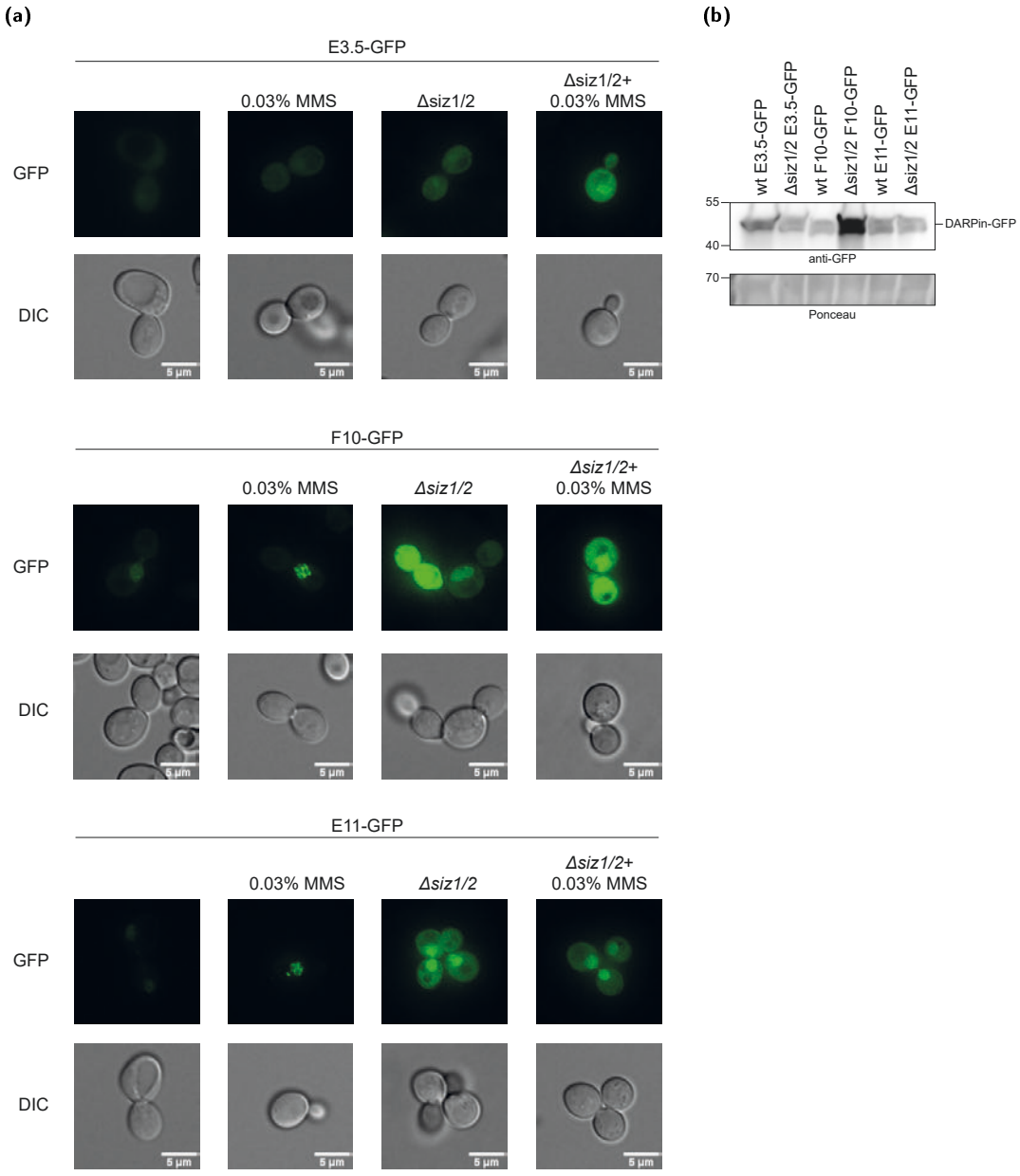

Figure 55: (a) Microscopy of SUMO-specific DARPins F10-GFP and E11-GFP expressing strains in *WT* and *siz1/siz2* deletion strains after MMS treatment. DARPin expression (green) was induced with 0.5 µg/mL dox for 20 h in a DF5 *WT* stain or strains were the E3 enzymes Siz1 and Siz2 were deleted (Δ *siz1/2*). Where indicated cells were treated with a low dose of MMS (0.03 %) for 90 min. SUMO-specific DARPins F10-GFP and E11-GFP form distinct foci in the cell, which were stronger and more frequent after MMS treatment and lost in *siz1/siz2* deletion strains. **(b) Expression of DARPins in cultures used for microscopy.** Samples from cultures for microscopy experiments were subjected to cell lysis and Western blot. DARPin expression was detected using an anti-GFP antibody.

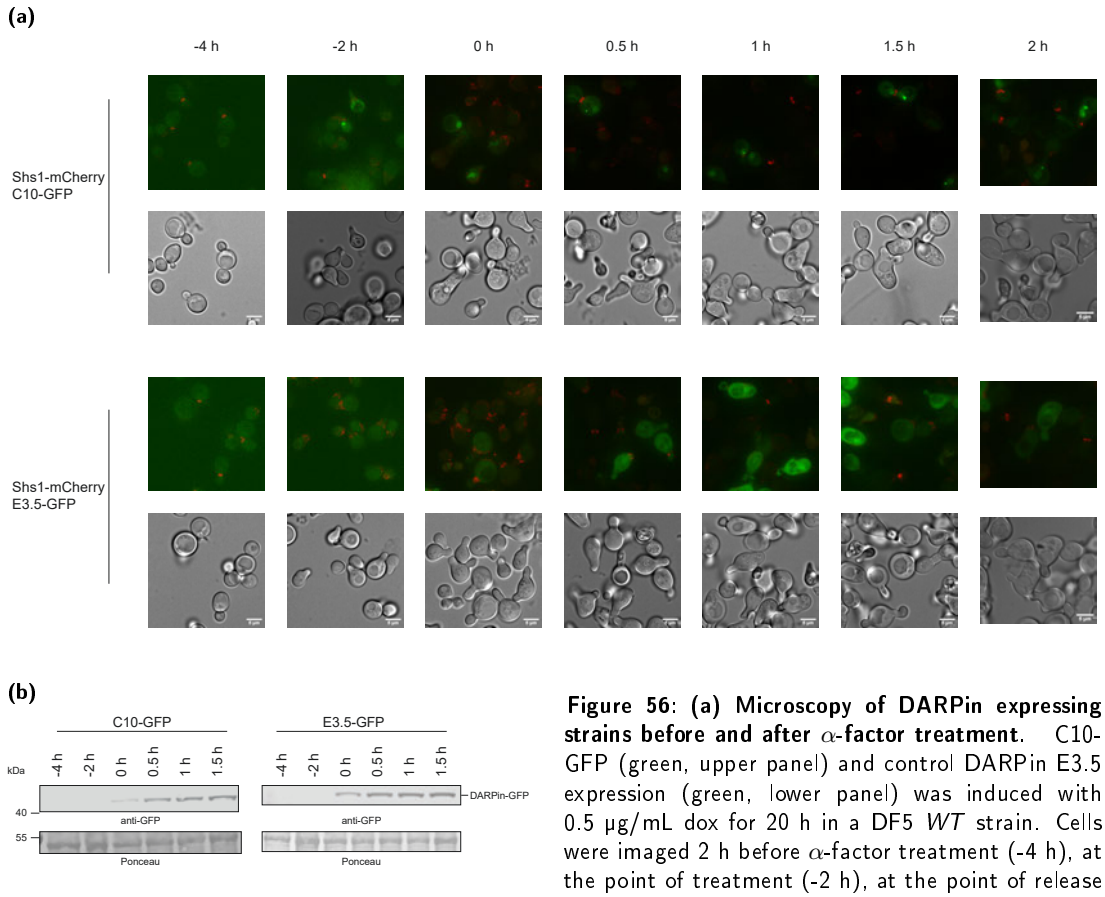

Figure 56: (a) Microscopy of DARPin expressing strains before and after α-factor treatment. C10-GFP (green, upper panel) and control DARPin E3.5 expression (green, lower panel) was induced with 0.5 µg/mL dox for 20 h in a DF5 *WT* strain. Cells were imaged 2 h before α-factor treatment (-4 h), at the point of treatment (-2 h), at the point of release from α-factor (0 h) and every 30 min up to 2 h after α-factor release. In the SUMO-specific DARPin C10 expressing strains foci appear after cultures were released for 30 min from α-factor treatment (from G_1-phase arrest). In red the Septin ring around the bud neck is stained (Shs1-mCherry). **(b) Expression of DARPins in cultures used for microscopy.** Samples from cultures for microscopy experiments were subjected to cell lysis and Western blot. DARPin expression was detected using an anti-GFP antibody.

To identify the sumoylated protein, to which the DARPins localise after damage treatment, fluorescence-tagged possible substrates were coexpressed.

Cdc48 is an AAA-ATPase with protein-unfoldase activity. As a subunit of the poly-ubiquitin-selective segregase complex, it is involved in endoplasmic-reticulum-associated protein degradation, inner nuclear membrane-associated degradation, mitotic spindle disassembly, macroautophagy, Skp/Cullin/F-box containing complex disassembly and other processes.[429] Studies performed in *Schizosaccharomyces pombe* showed that the SUMO targeted ubiquitin ligase mutant, *slx8-29*, forms nuclear foci containing SUMO and the Cdc48 segregase.[430] Newman *et al.* (2017) reported that in *S. cerevisiae* cells expressing wild-type SUMO, the Cdc48 signal is equally distributed throughout the cell. However, when a SUMO mutant with a mutation in the SIM interaction interface (F65A) was coexpressed, Cdc48 foci formed in the nucleus and co-localized with the SUMO-F65A foci.[312]

Unfortunately, when I expressed a Cdc48-mCherry construct in the DARPin-GFP expressing cells, I was not able to observe any prominent foci formation of Cdc48 with or without a low dose of MMS treatment (fig. 57a column 1). Hence, the DARPins did not have a similar effect on Cdc48 localisation as the SUMO-F65A mutant.

Spc42 is a central plaque component of the spindle pole body and is involved in SPB duplication and attachment of the SPB to the nuclear membrane.[431] It is detected as one or two bright nuclear spots in cells dependent on their cell cycle state.[432,433]
Tagging of Spc42 with mCherry and observing it in MMS treated cultures, does not show any colocalisation between the DARPins and the spindle pole body (fig. 57b column 3), although for both proteins nice foci formation was observed (fig. 57b column 1).

The subunit of the kinetochore-microtubule binding complex Kre28 is known to be modified by sumoylation. The complex bridges centromeric heterochromatin and kinetochore microtubule-associated proteins and is required for sister chromatid bi-orientation and kinetochore binding of spindle assembly checkpoint components.[434] It is detected as one or two nuclear spots inside the budding cell, but follows different cell cycle regulated kinetics than Spc42.[433]
Again, nice foci formation (fig. 58a column 1), but no colocalisation with the GFP-tagged DARPins was visible in MMS treated cultures that express Kre28-mCherry (fig. 58a column 3).

PCNA's main function is its role as a sliding replication clamp for DNA polymerase δ, but it is also involved in other processes during DNA replication and DNA repair. It is known to be sumoylated on K164 and K127 during normal S-Phase and in response to replication stress (section 1.2.5.1). In consequence of this sumoylation, resolution of DNA damage by recombination pathways is inhibited and ubiquitin-dependent damage bypass is favoured.[130,187]
The N-terminal fusion protein of mCherry and PCNA was expressed additionally to the native PCNA. It did not localise properly after its expression and therefore no foci of PCNA could be detected after MMS treatment (fig. 59a column 1). Hence, no final conclusion about a colocalisation between the DARPins and PCNA can be drawn.

Rfa1 is a subunit of the heterotrimeric RPA complex. The single-stranded DNA binding protein RPA is involved in DNA replication, repair, and recombination, and is modified by SUMO upon treatment with MMS.[103] After cultures expressing the mRuby-tagged Rfa1 protein were treated with MMS, foci formation was visible (fig. 58b column 1). These foci partly colocalise with the foci from F10-GFP and E11-GFP (fig. 58b column 3). Therefore, it is likely that the sumoylation that is detected by the DARPins might occur either on RPA or on other proteins at the RPA-covered single-strand gaps after DNA damage treatment.

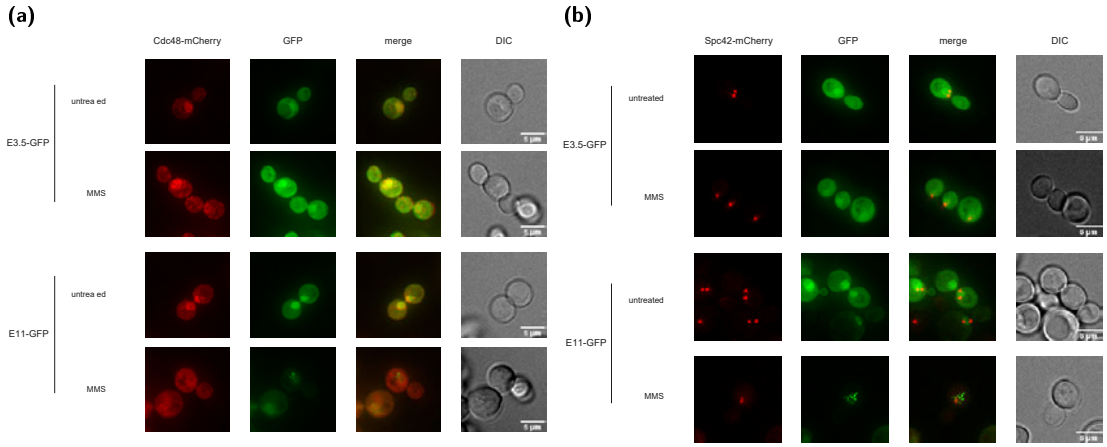

Figure 57: **(a) Colocalisation studies of DARPins with Cdc48 after MMS treatment**. Strains expressing the SUMO-specific DARPin E11-GFP or the control DARPin E3.5-GFP (green) and mCherry-tagged native Cdc48 (red) were either untreated or treated with 0.02 % MMS (+MMS) for 90 min and subjected to microscopy. Red and green channels were merged for detection of colocalisation. No foci formation by Cdc48 is visible in any of these strains. **(b) Colocalisation studies of DARPins with the spindle pole body (Spc42) after MMS treatment**. Strains expressing the SUMO-specific DARPin E11-GFP or the control DARPin E3.5-GFP (green) and mCherry tagged native Spc42 (red) were either untreated or treated with 0.02 % MMS (+MMS) for 90 min and subjected to microscopy. Red and green channels were merged for the detection of colocalisation. No colocalisation between the DARPins and the spindle pole body is visible, although for both proteins nice foci formation was observed.

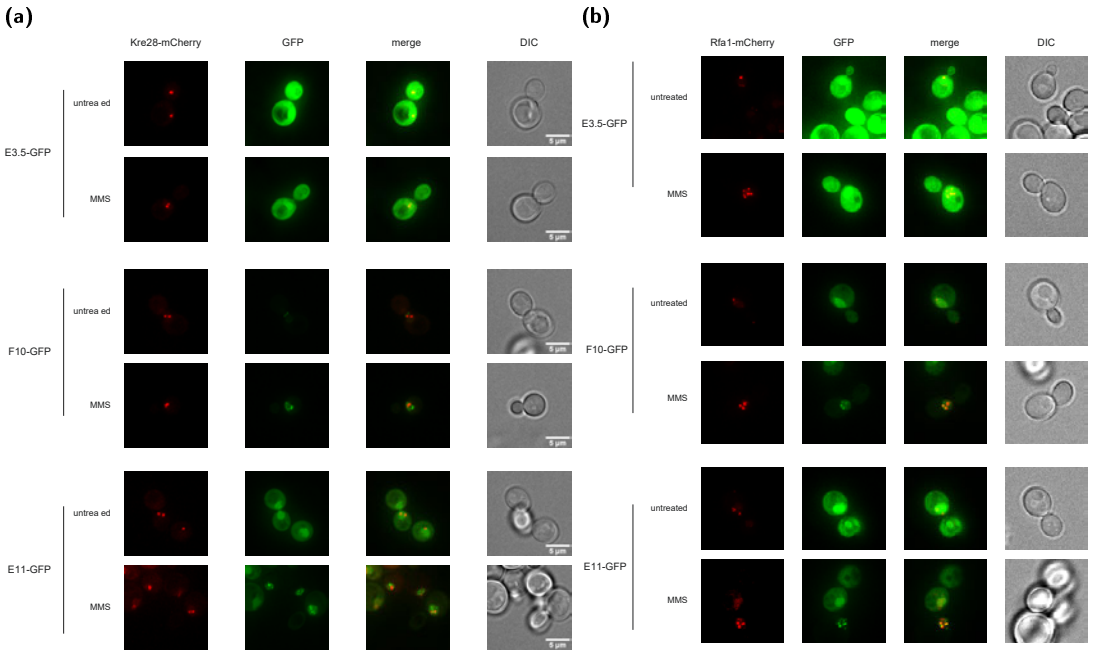

Figure 58: (a) Colocalisation studies of DARPins with the kinetochore (Kre28) after MMS treatment. Strains expressing the SUMO-specific DARPins F10-GFP, E11-GFP or the control DARPin E3.5-GFP (green) and mCherry-tagged native Kre28 (red) were either untreated or treated with 0.02 % MMS (+MMS) for 90 min and subjected to microscopy. Red and green channels were merged for the detection of colocalisation. No colocalisation between the SUMO-specific DARPins and the kinetochore is visible, although for both proteins nice foci formation was observed. **(b) Colocalisation studies of DARPins with RPA (RFA1) after MMS treatment.** Strains expressing the SUMO-specific DARPins F10-GFP, E11-GFP or the control DARPin E3.5-GFP (green) and mRuby-tagged native RFA1 (red) were either untreated or treated with 0.02 % MMS (+MMS) for 90 min and subjected to microscopy. Red and green channels were merged for the detection of colocalisation. The RPA foci partly colocalise with the foci from F10-GFP and E11-GFP.

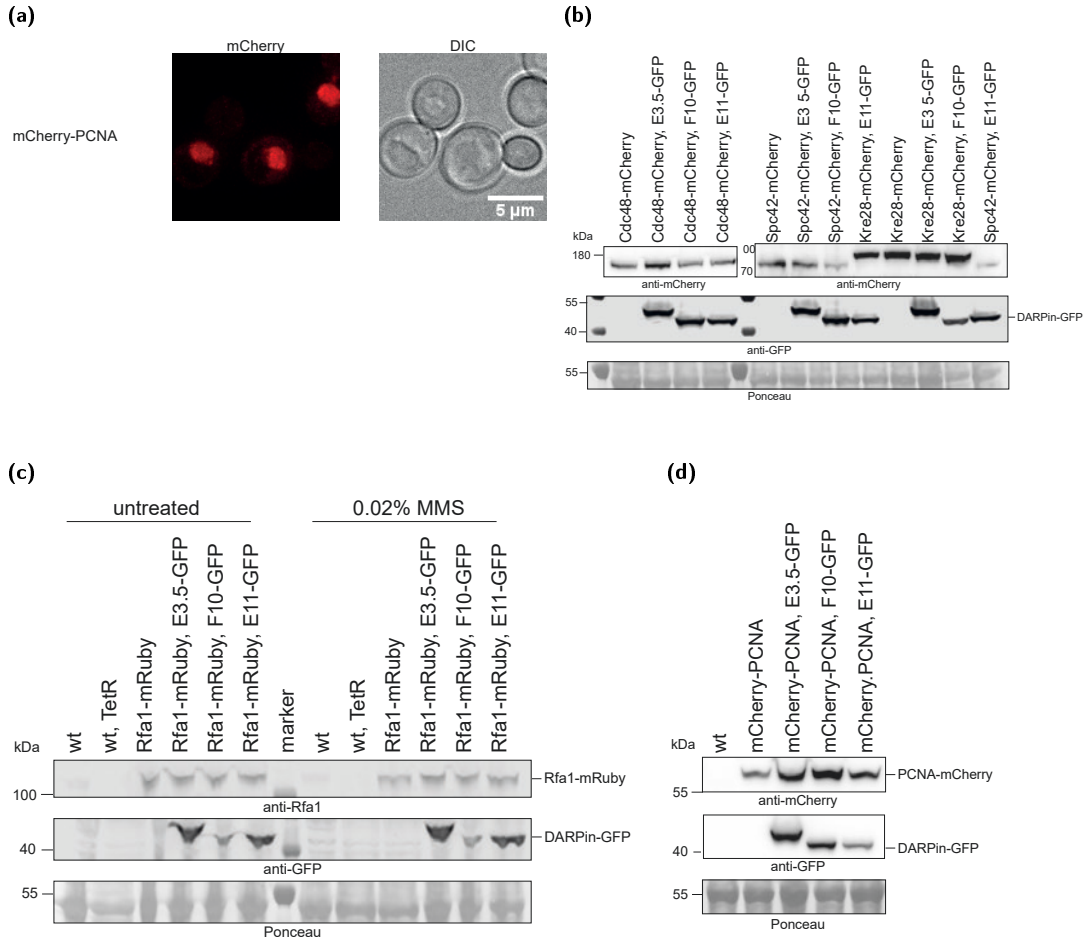

Figure 59: **(a) Colocalisation studies of DARPins with PCNA after MMS treatment**. Strains expressing integrated mCherry-PCNA (red) were treated with 0.02 % MMS for 90 min and subjected to microscopy. No foci formation by PCNA is visible in any of this strain. **(b) Expression of DARPins-GFP and Cdc48-mCherry, Spc42-mCherry or Kre28-mCherry in cultures used for colocalisation studies.** Samples from cultures for microscopy experiments were subjected to cell lysis and Western blot. DARPin expression was detected using an anti-GFP antibody. Cdc48, Spc42 and Kre28 levels were detected using a mCherry-specific antibody. **(c) Expression of DARPins-GFP and Rfa1-mRuby in cultures used for colocalisation studies.** Samples from cultures for microscopy experiments were subjected to cell lysis and Western blot. DARPin expression was detected using an anti-GFP antibody. Rfa1-mRuby levels were detected using a RFA1-specific antibody. **(d) Expression of DARPins-GFP and mCherry-PCNA in cultures used for colocalisation studies.** Samples from cultures for microscopy experiments were subjected to cell lysis and Western blot. DARPin expression was detected using an anti-GFP antibody. mCherry-PCNA levels were detected using a mCherry-specific antibody.

3.3.5 Discussion and outlook: DARPin A10 is a useful inhibitor of sumoylation and DARPin F10 and E11 can be used as sensors to detect sumoylation

This part of my thesis aimed to characterise selected SUMO-specific DARPins, showing their usability for inhibition of sumoylation and detection of sumoylated species in *S. cerevisiae* in exemplary experiments.
From the *in vitro* experiments investigating the influence of the DARPins on the sumoylation cascade (fig. 60), I can conclude that A10 inhibits all steps of the sumoylation cascade as well as SUMO cleavage. In line, it prevents the model substrate PCNA from being mono- or poly-sumoylated and it prevents free SUMO chain formation. Hence, it could be used as an inhibitor of sumoylation in yeast.
DARPin F10 also affects mono- and poly-sumoylation of PCNA, substrate conjugation and free chain formation, which most likely results from its influence on E1 thioester formation.
E11 inhibits E1 thioester formation, and therefore also substrate conjugation. However, on PCNA it only influences poly-sumoylation.
DARPins G11 and B12 do not have any effect on the single steps of the sumoylation cascade, although they influence PCNA sumoylation and if used in excess, also substrate conjugation.
C10 does not show any effect on PCNA sumoylation and had the weakest effect on substrate conjugation. In line with that, it showed no effect on the single steps of the sumoylation cascade. From these experiments, C10 seems to be the best candidate to be used as a sensor or affinity reagent *in vivo*.

To transmit the sumoylation signal in the cell it is recognized by SIM-containing proteins like for example RNF4. The DARPins A10 and F10 show very strong inhibition of RNF4 binding to SUMO, C10 and B12 show an intermediate level of inhibition, while E11 and G11 show very weak to no inhibition. This might hint toward E11 and G11 binding to a different site on SUMO than the other DARPins.
Reading on the problem that I could not detect binding of SUMO to the well-characterized SIM peptide[209,246] in the surface plasmon resonance experiment, I found out that to detect an interaction of a peptide in the Biacore system, a higher amount of SUMO would need to be immobilized on the Chip than I used.

The selected DARPins have dissociation constants (K_D) in the low nM to low µM range (table 16). This is comparable to the dissociation constants of high-affinity antibodies.[435] The affinity of the DARPins nicely agrees with their behaviour towards the conjugation cascade of SUMO. The strongest binders were A10 and F10 with an K_D of 0.3 or 3 nM, respectively. The difference in the functional behaviour of these two can-

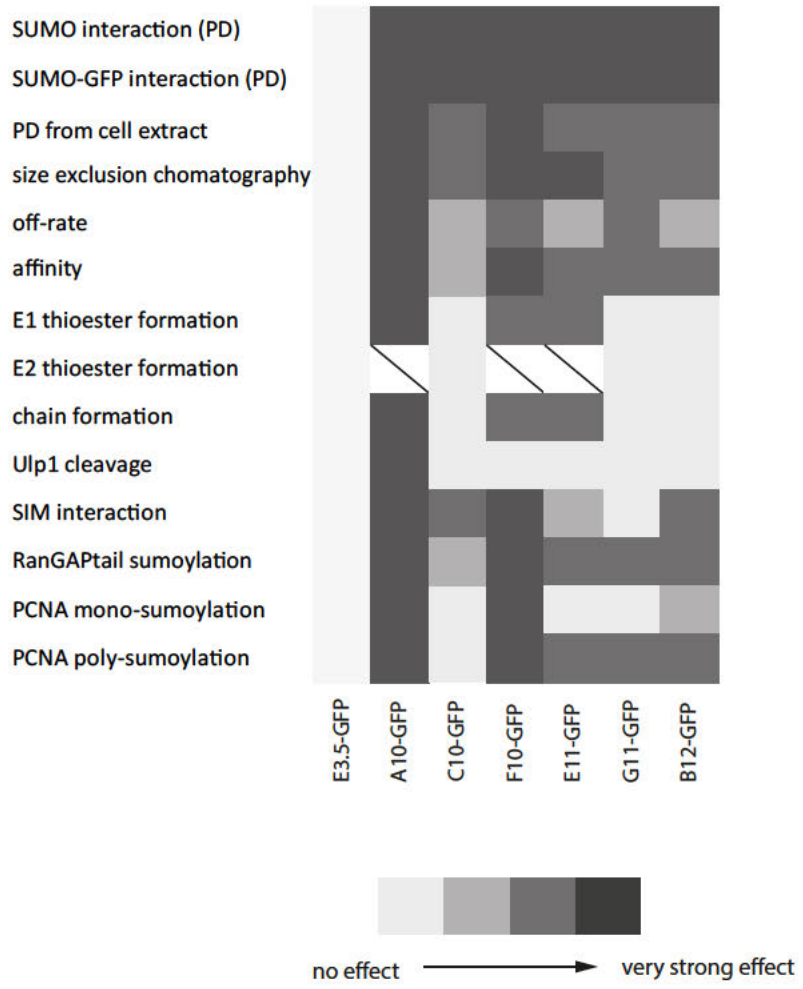

Figure 60: Summary of the *in vitro* characteristics of the SUMO-specific DARPins. The colour coding spans from light grey (no effect) to dark grey (strong effect).

didates is most likely mainly caused by their different off-rates. A10, which negatively influences all steps of SUMO conjugation and deconjugation, also shows the strongest binding with nearly no off-rate. The DARPins E11 and F10, which were also strong binders, and slow E1 thioester formation, but still allow for some SUMO conjugation and cleavage, possible due to their medium off-rates. The weakest binders with very fast off-rates, C10, G11 and B12 did not show any influence on thioester formation and had weaker effects on substrate sumoylation.

hSUMO1 and hSUMO2 have 42 %/38 % sequence identity with ySUMO respectively. C10, G11 and B12 show good affinities to hSUMO1 and G11 shows some affinity to hSUMO2. A10, F10 and E11 do not bind these two human SUMO isoforms. This binding analysis hints toward C10, G11 and B12 binding to more conserved residues in hSUMO1 than A10, F10 and E11 (fig. 28). G11 most likely binds to residues conserved in hSUMO1 and hSUMO2 (fig. 28). The small modifier ubiquitin shares only 18 % sequence identity with ySUMO, but the fold of both is very similar. None of the tested

DARPins binds ubiquitin. Therefore, the fold alone does not seem to be enough for recognition by DARPins.

Also, the NMR interface hints at the fact that the individual DARPins bind to different sites on the SUMO molecules, as the peaks of the bound SUMO shift in different directions. This goes in hand with their varying effects on the function of SUMO (fig. 60). For example, the very strong binders A10 and F10 have a strong influence on the sumoylation cascade and SUMO interaction and they show shifts of the SUMO peaks in the same direction in their NMR spectra. While for example E11, which was also a strong binder, but does not inhibit SIM interaction, shifts the peaks in a different direction.

The results of the structural analysis of A10 mostly represent what we would expect from the observations in the *in vitro* assays (fig. 60). In line with the crystal structure, A10 inhibits E1 thioester formation and free SUMO chain formation. However, according to its binding site on SUMO, we would not expect Ulp1 cleavage to be affected by DARPin binding. Indeed there was not a complete inhibition of Ulp1 cleavage, but only a slowing of the reaction.
In contrast, the *in vitro* behaviour of C10 was very different from what we would expect from its binding site. As it interacts with the same site on SUMO as A10, we would assume the whole sumoylation cascade, besides Ubc9 interaction and Ulp1 cleavage, to be inhibited. However, C10 only influences SIM interaction, but not the other steps of the sumoylation cascade. In contrast to A10, C10 was also able to interact with hSUMO1.
As A10 and C10 are both binding to the SIM interaction site, where also Aos1/Uba2 binds, but not Ubc9 and the desumoylases, it is rather likely that not the interaction site alone determines the effect of the DARPins on SUMO, but also their interaction strength and kinetics. As shown in table 16, A10 is a very strong interactor with a K_D of 0.3 nM and a very slow off-rate (k_{off} 0.0002 s^{-1}). C10 only interacts with a K_D of 1400 nM with a very fast off-rate (k_{off} too fast to be determined). In consequence, A10 binds to SUMO and prevents other interactors from binding by blocking their accessibility. While C10 binds SUMO, but dissociates quickly, allowing for an exchange with other interactors even at the same site.

In contrast to what we have seen *in vitro*, the *in vivo* experiments show that F10 and E11 have the weakest effect on cell growth, cell cycle progression, overall sumoylation, substrate sumoylation and phenotypic appearance of the expressing cells. The strongest inhibitor of these processes is DARPin A10. This might be caused by the very slow off-rate of A10, resulting in its binding to SUMO without allowing any exchange with other enzymes. The weaker effect of F10 and E11, compared to C10, might either be caused by the weaker binding affinity and faster off-rate of C10 that would make it less well interacting with SUMO in the crowded environment of the cell. Furthermore, a slightly

higher expression of C10 could cause a possible inhibitory effect, as detected by *in vitro* sumoylation assays with a high excess of DARPin to SUMO.

Through quantification of the overall sumoylation level in DARPin expressing cells, I concluded that the amount of DARPin has a greater influence on the sumoylation landscape of the cell, than the type of DARPin. Cells showed a relation between DARPin levels and the amounts of unconjugated SUMO in the cell. This was not different for DARPin A10 and E11 expressing strains.
To test the DARPins as inhibitors of sumoylation not only the overall sumoylation level was analysed, but also the sumoylation of an example substrate (PCNA). A10, C10, G11 and B12 decrease PCNA sumoylation upon expression, while in F10 and E11 expressing cells the sumoylation pattern was comparable to *WT* cells. These results confirm previous observations that especially A10 is a very good inhibitor of sumoylation, not only *in vitro* but also *in vivo*.
Under high induction conditions, the DARPin expressing strains were growing much slower, and the sumoylation levels in the cells were highly reduced. The growth defect mostly resulted from the inhibition of sumoylation targets in the nucleus, as shown by spot assays using NES- or NLS-tagged DARPin constructs. From a comparison with the cell cycle profile of G_1- or G_2/M-Phase arrested cells one can assume that the DARPin expressing yeast strains were stuck in late S-Phase or G_2/M-Phase. This goes in hand with the results, that the DARPin expressing cells show an arrest in the same cell cycle phase as cells having lost the sole yeast E2 Ubc9, which were described to arrest in G_2/M-Phase.[309] Immunofluorescence staining of the cytoskeleton confirmed the observation.

All DARPins showed an influence on cell growth under various stress conditions (osmotic stress, DNA damage by UV or MMS, and oxidative stress), besides low- or high-temperature. The weakest effect was seen for DARPins F10 and E11, while the strongest effect was shown with DARPin G11. The other DARPins (A10, C10 and B12) showed medium to strong effects under the different tested conditions besides temperature. This again supports our hypothesis that the different DARPins have a distinct influence on the sumoylation landscape in cells (fig. 50c). However, one has to take into account that slight variations in the expression levels of the DARPins might have an effect on the cell viability as well. These results again show that DARPin A10 is the most potent inhibitor of sumoylation in yeast cells.

The results described, indicate not only that A10 is the DARPin best suitable to be used as an inhibitor, but also that F10 and E11 are the weakest inhibitors of sumoylation in the cell. This gives indications that F10 and E11 are good candidates to be used as sensors for sumoylation *in vivo*. To confirm that, I performed mainly microscopy experiments using GFP-tagged DARPins.

Using the strong binder A10 no distinct foci were visible in the yeast cells, only a strong diffuse staining of the nucleus. This is probably caused by its high affinity to SUMO and the strong inhibitory effect on sumoylation processes in the cell. DARPins F10 and E11 localise also mostly nuclear. However, sometimes a ring-like structure around the bud neck was visible or they localized to distinct bright spots in the nucleus. Through colocalisation studies, I identified the structures at the bud necks as Septins, which are known to be sumoylated during mitosis.[197] In the colocalisation experiments with mCherry-tagged Septin Shs1, I observed that the DARPin signal forms only after the Septins form an hourglass shape around the bud neck and vanishes after splitting of the Septin ring. This is in accordance with results from other groups, who described the dynamic sumoylation of Septins as a signal for their correct localisation during mitosis.[197,300] As only the Septins of the mother site of the Septin ring are sumoylated,[197,300] I exclusively observed Septin ring staining by DARPins on one side of the bud neck. Denaturing pull-down experiments with His-tagged Shs1, confirmed that DARPins F10 and E11 do not interfere with Septin sumoylation.
Additionally to the colocalisation with Septins, in a logarithmic growing culture a colocalisation of mCherry-SUMO with the SUMO-specific DARPins F10 and E11, but not with the control DARPin E3.5 was observed. These two experiments support my former claim, that the DARPins F10 and E11 are useful tools for the detection of sumoylation *in vivo*.

The attempt to use the DARPins F10 or E11 to investigate if sumoylation plays a role in the regulation of meiotic Septin structure formation was not successful. This was, however, not caused by the DARPins, but by the failure of tagged Spr3 or Shs1 to localise normally under the tested conditions. Even without DARPin expression no expected microtubules- or PSM-like structures were visible in the microscope.

In a second attempt to use the DARPins as sensors, I aimed on identifying the bright nuclear spots that formed in some DARPin-expressing cells. They were more frequent in their appearance and number in cells treated for 90 min with a low dose of MMS or after strains were released for 30 min from α-factor treatment (from G_1-phase arrest). The foci vanished in a strain where the E3 enzymes Siz1 and Siz2 were absent. This indicated that the DARPins detect sumoylation targets in the nucleus that are sumoylated to a higher degree after DNA damage or during S-phase, and their sumoylation is dependent on the SUMO ligases Siz1 and/or Siz2. To identify the proteins that are detected by the DARPins, I performed again colocalisation studies with fluorescence-tagged proteins. The examined proteins tested, are all known to form prominent nuclear foci or to be sumoylated in the nucleus (see section 3.3.4.5). However, Cdc48 and PCNA did not form any nuclear foci under the conditions tested. Indicating an interference with their functionality through tagging of the protein. The SPB protein Spc42 and the kinetochore protein Kre28 showed nice foci formation when tagged with mCherrry.

However, no colocalisation with the DARPins F10 and E11 was visible. Indicating, that the sumoylation detected in the MMS-treated cells is not occurring at the SPB or the kinetochore.
In MMS-treated cultures expressing a mRuby-tagged Rfa1 protein, foci formation was visible. These foci partly colocalise with the foci from F10-GFP and E11-GFP. Therefore, it is likely that the sumoylation that is detected by the DARPins occurs either on RPA or on other proteins at the RPA-covered single-strand gaps after DNA damage treatment. This observation agrees with the results of other groups that sumoylation is used by the cell as a signal for DNA damage (section 1.2.5.2).

Overall, in this part of my project I was able to thoroughly characterize the SUMO-specific DARPins with regard to their characteristics *in vitro* (section 3.3.2) using interaction assays (like pull-down assays or SPR measurements) and activity assays (like de-/sumoylation assays and thioester formation assays). Moreover, I identified the exact binding site of selected DARPins to SUMO using a crystallographic approach (section 3.3.3).
Finally, I also characterize the properties of the DARPins *in vivo* (section 3.3.4) by growth analysis and detection of sumoylated species *in vivo*. Using the knowledge gained through my *in vitro* and *in vivo* studies, I identified the DARPin A10 as a potent inhibitor of sumoylation in cells (section 3.3.4.4). I confirmed this characteristic by the quantification of sumoylated species after A10 expression in yeast extract. Additionally, I identified F10 and E11 as versatile tools for the detection of sumoylated species (section 3.3.4.5), which I verified in colocalisation and PD studies.
In conclusion, I could prove the selected SUMO-specific DARPins as useful and versatile tools for different approaches in living yeast cells. They can be used as sensors to target previously unknown sumoylation substrates in living cells. The big advantage of this *in vivo* analysis, compared to antibody-based studies, is that it allows analysing the localisation and timing of the sumoylation signal in real time and space. DARPins can also be used as inhibitors to target the sumoylation of a cell in a spacial and temporal regulated manner, by using timed expression systems or targeted DARPin localisation using a localisation tag. Moreover, it would be possible to use NES- and NLS-tagged DARPins to isolate sumoylated proteins and investigate and compare the sumoylation landscape in- and outside of the nucleus by mass spectrometry. Moreover, other targeted mass-spectrometric approaches could be performed by using localisation-tagged DARPins or timed expression followed by pull-down and identification of sumoylated proteins by mass spectrometry.

4 Bibliography

[1] Knorre, D. G., Kudryashova, N. V. & Godovikova, T. S. Chemical and functional aspects of posttranslational modification of proteins. *Acta naturae* **1**, 29–51 (2009).

[2] Lothrop, A. P., Torres, M. P. & Fuchs, S. M. Deciphering post-translational modification codes. *FEBS Letters* **587**, 1247–1257 (2013).

[3] Swatek, K. N. & Komander, D. Ubiquitin modifications. *Cell research* **26**, 399–422 (2016).

[4] Cappadocia, L. & Lima, C. D. Ubiquitin-like Protein Conjugation: Structures, Chemistry, and Mechanism. *Chemical Reviews* **118**, 889–918 (2018).

[5] Heride, C., Urbé, S. & Clague, M. J. Ubiquitin code assembly and disassembly. *Current Biology* **24** (2014).

[6] Kwon, Y. T. & Ciechanover, A. The Ubiquitin Code in the Ubiquitin-Proteasome System and Autophagy. *Trends in Biochemical Sciences* **42**, 873–886 (2017).

[7] Asimaki, E., Petriukov, K., Renz, C., Meister, C. & Ulrich, H. D. Fast friends – Ubiquitin-like modifiers as engineered fusion partners. *Seminars in Cell and Developmental Biology* **21** (2021).

[8] Goldstein, G. *et al.* Isolation of a polypeptide that has lymphocyte differentiating properties and is probably represented universally in living cells. *Proceedings of the National Academy of Sciences of the United States of America* **72**, 11–15 (1975).

[9] Liao, Y., Sumara, I. & Pangou, E. Non-proteolytic ubiquitylation in cellular signaling and human disease. *Communications Biology 2022 5:1* **5**, 1–15 (2022).

[10] Bonifacino, J. S. & Weissman, A. M. Ubiquitin and the control of protein fate in the secretory and endocytic pathway. *Annual Review of Cell and Developmental Biology* **14**, 19–57 (1998).

[11] Leestemaker, Y. & Ovaa, H. Tools to investigate the ubiquitin proteasome system. *Drug Discovery Today: Technologies* **26**, 25–31 (2017).

[12] Komander, D. & Rape, M. The Ubiquitin Code. *Annual Review of Biochemistry* **81**, 203–229 (2012).

[13] Vijay-kumar, S., Bugg, C. E. & Cook, W. J. Structure of ubiquitin refined at 1.8Å resolution. *Journal of Molecular Biology* **194**, 531–544 (1987).

[14] Doshi, A., Mishra, P., Sharma, M. & Prabha, C. R. Functional characterization of dosage-dependent lethal mutation of ubiquitin in Saccharomyces cerevisiae. *FEMS Yeast Research* **14**, 1080–1089 (2014).

[15] Ozkaynak, E., Finley, D., Solomon, M. J. & Varshavsky, A. The yeast ubiquitin genes: a family of natural gene fusions. *The EMBO journal* **6**, 1429–1439 (1987).

[16] Alfano, C., Faggiano, S. & Pastore, A. The Ball and Chain of Polyubiquitin Structures. *Trends in Biochemical Sciences* **41**, 371–385 (2016).

[17] Ronau, J. A., Beckmann, J. F. & Hochstrasser, M. Substrate specificity of the ubiquitin and Ubl proteases. *Cell Research* **26**, 441–456 (2016).

[18] Sloper-Mould, K. E., Jemc, J. C., Pickart, C. M. & Hicke, L. Distinct Functional Surface Regions on Ubiquitin. *Journal of Biological Chemistry* **276**, 30483–30489 (2001).

[19] Komander, D. The emerging complexity of protein ubiquitination. *Biochemical Society Transactions* **37**, 937–953 (2009).

[20] Hochstrasser, M. Origin and function of ubiquitin-like proteins. *Nature* **458**, 422–429 (2009).

[21] Li, W. & Ye, Y. Polyubiquitin chains: Functions, structures, and mechanisms. *Cellular and Molecular Life Sciences* **65**, 2397–2406 (2008).

[22] Mulder, M. P., Witting, K. F. & Ovaa, H. Cracking the ubiquitin code: The ubiquitin toolbox. *Current Issues in Molecular Biology* **37**, 1–20 (2020).

[23] Takahashi, T. S., Wollscheid, H. P., Lowther, J. & Ulrich, H. D. Effects of chain length and geometry on the activation of DNA damage bypass by polyubiquitylated PCNA. *Nucleic Acids Research* **48**, 3042–3052 (2020).

[24] Tokunaga, F. Linear ubiquitination-mediated NF-κB regulation and its related disorders. *Journal of Biochemistry* **154**, 313–323 (2013).

[25] Sumara, I., Maerki, S. & Peter, M. E3 ubiquitin ligases and mitosis: embracing the complexity. *Trends in Cell Biology* **18**, 84–94 (2008).

[26] Ciechanover, A. Proteolysis: From the lysosome to ubiquitin and the proteasome. *Nature Reviews Molecular Cell Biology* **6**, 79–86 (2005).

[27] McClellan, A. J., Laugesen, S. H. & Ellgaard, L. Cellular functions and molecular mechanisms of non-lysine ubiquitination. *Open Biology* **9**, 190147 (2019).

[28] Chen, Z. J. & Sun, L. J. Nonproteolytic Functions of Ubiquitin in Cell Signaling. *Molecular Cell* **33**, 275–286 (2009).

[29] Finley, D., Ulrich, H. D., Sommer, T. & Kaiser, P. The ubiquitin-proteasome system of Saccharomyces cerevisiae. *Genetics* **192**, 319–360 (2012).

[30] Ye, Y. & Rape, M. Building ubiquitin chains: E2 enzymes at work. *Nature Reviews Molecular Cell Biology* **10**, 755–764 (2009).

[31] McGrath, J. P., Jentsch, S. & Varshavsky, A. UBA1: An essential yeast gene encoding ubiquitin-activating enzyme. *EMBO Journal* **10**, 227–236 (1991).

[32] Ghaboosi, N. & Deshaies, R. J. A conditional yeast E1 mutant blocks the ubiquitin-proteasome pathway and reveals a role for ubiquitin conjugates in targeting Rad23 to the proteasome. *Molecular Biology of the Cell* **18**, 1953–1963 (2007).

[33] Haas, A. L., Warms, J. V., Hershko, A. & Rose, I. A. Ubiquitin-activating enzyme. Mechanism and role in protein-ubiquitin conjugation. *Journal of Biological Chemistry* **257**, 2543–2548 (1982).

[34] Haas, A. L., Bright, P. M. & Jackson, V. E. Functional diversity among putative E2 isozymes in the mechanism of ubiquitin-histone ligation. *Journal of Biological Chemistry* **263**, 13268–13275 (1988).

[35] Lee, I. & Schindelin, H. Structural Insights into E1-Catalyzed Ubiquitin Activation and Transfer to Conjugating Enzymes. *Cell* **134**, 268–278 (2008).

[36] Haldeman, M. T., Xia, G., Kasperek, E. M. & Pickart, C. M. Structure and function of ubiquitin conjugating enzyme E2-25K: The tail is a core-dependent activity element. *Biochemistry* **36**, 10526–10537 (1997).

[37] Middleton, A. J. & Day, C. L. The molecular basis of lysine 48 ubiquitin chain synthesis by Ube2K. *Scientific Reports* **5**, 1–14 (2015).

[38] Johnson, E. S., Schwienhorst, I., Dohmen, R. J. & Blobel, G. The ubiquitin-like protein Smt3p is activated for conjugation to other proteins by an Aos1p/Uba2p heterodimer. *The EMBO journal* **16**, 5509–19 (1997).

[39] Liakopoulos, D., Doenges, G., Matuschewski, K. & Jentsch, S. A novel protein modification pathway related to the ubiquitin system. *EMBO Journal* **17**, 2208–2214 (1998).

[40] Saccharomyces Genome Database | SGD. *https://www.yeastgenome.org/* (accessed: 2022-03-21).

[41] Eletr, Z. M., Huang, D. T., Duda, D. M., Schulman, B. A. & Kuhlman, B. E2 conjugating enzymes must disengage from their E1 enzymes before E3-dependent ubiquitin and ubiquitin-like transfer. *Nature Structural and Molecular Biology* **12**, 933–934 (2005).

[42] Dohmen, R. J., Madura, K., Bartel, B. & Varshavsky, A. The N-end rule is mediated by the UBC2(RAD6) ubiquitin-conjugating enzyme. *Proceedings of the National Academy of Sciences of the United States of America* **88**, 7351–7355 (1991).

[43] Bailly, V., Lamb, J., Sung, P., Prakash, S. & Prakash, L. Specific complex formation between yeast RAD6 and RAD18 proteins: A potential mechanism for targeting RAD6 ubiquitin-conjugating activity to DNA damage sites. *Genes and Development* **8**, 811–820 (1994).

[44] Hoege, C., Pfander, B., Moldovan, G. L., Pyrowolakis, G. & Jentsch, S. RAD6-dependent DNA repair is linked to modification of PCNA by ubiquitin and SUMO. *Nature* **419**, 135–141 (2002).

[45] Windheim, M., Peggie, M. & Cohen, P. Two different classes of E2 ubiquitin-conjugating enzymes are required for the mono-ubiquitination of proteins and elongation by polyubiquitin chains with a specific topology. *Biochemical Journal* **409**, 723–729 (2008).

[46] Petroski, M. D. & Deshaies, R. J. Function and regulation of cullin-RING ubiquitin ligases. *Nature Reviews Molecular Cell Biology* **6**, 9–20 (2005).

[47] Deshaies, R. J. & Joazeiro, C. A. RING domain E3 ubiquitin ligases. *Annual Review of Biochemistry* **78**, 399–434 (2009).

[48] Berndsen, C. E. & Wolberger, C. New insights into ubiquitin E3 ligase mechanism. *Nature Structural and Molecular Biology* **21**, 301–307 (2014).

[49] David, Y. *et al.* E3 ligases determine ubiquitination site and conjugate type by enforcing specificity on E2 enzymes. *Journal of Biological Chemistry* **286**, 44104–44115 (2011).

[50] Morreale, F. E. & Walden, H. Types of Ubiquitin Ligases. *Cell* **165**, 248–248 (2016).

[51] Lima, C. D. & Schulman, B. A. Structural biology: A protein engagement RING. *Nature* **489**, 43–44 (2012).

[52] Ohi, M. D., Vander Kooi, C. W., Rosenberg, J. A., Chazin, W. J. & Gould, K. L. Structural insights into the U-box, a domain associated with multi-ubiquitination. *Nature Structural Biology* **10**, 250–255 (2003).

[53] Huibregtse, J. M., Scheffner, M., Beaudenon, S. & Howley, P. M. A family of proteins structurally and functionally related to the E6-AP ubiquitin-protein ligase. *Proceedings of the National Academy of Sciences of the United States of America* **92**, 2563–2567 (1995).

[54] Eletr, Z. M. & Kuhlman, B. Sequence Determinants of E2-E6AP Binding Affinity and Specificity. *Journal of Molecular Biology* **369**, 419–428 (2007).

[55] Ries, L. K. *et al.* Analysis of ubiquitin recognition by the HECT ligase E6AP provides insight into its linkage specificity. *Journal of Biological Chemistry* **294**, 6113–6129 (2019).

[56] Wenzel, D. M. & Klevit, R. E. Following Ariadne's thread: A new perspective on RBR ubiquitin ligases. *BMC Biology* **10**, 1–8 (2012).

[57] Kim, H. C. & Huibregtse, J. M. Polyubiquitination by HECT E3s and the Determinants of Chain Type Specificity. *Molecular and Cellular Biology* **29**, 3307–3318 (2009).

[58] Clague, M. J., Urbé, S. & Komander, D. Breaking the chains: deubiquitylating enzyme specificity begets function. *Nature Reviews Molecular Cell Biology* **20**, 338–352 (2019).

[59] Reyes-Turcu, F. E., Ventii, K. H. & Wilkinson, K. D. Regulation and cellular roles of ubiquitin-specific deubiquitinating enzymes. *Annual Review of Biochemistry* **78**, 363–397 (2009).

[60] Nanduri, B., Suvarnapunya, A. E., Venkatesan, M. & Edelmann, M. J. Deubiq-

uitinating Enzymes as Promising Drug Targets for Infectious Diseases. *Current Pharmaceutical Design* **19**, 3234–3247 (2013).

[61] Mevissen, T. E. & Komander, D. Mechanisms of deubiquitinase specificity and regulation. *Annual Review of Biochemistry* **86**, 159–192 (2017).

[62] Dikic, I. Proteasomal and autophagic degradation systems. *Annual Review of Biochemistry* **86**, 193–224 (2017).

[63] Finley, D., Bartel, B. & Varshavsky, A. The tails of ubiquitin precursors are ribosomal proteins whose fusion to ubiquitin facilitates ribosome biogenesis. *Nature* **338**, 394–401 (1989).

[64] Hurley, J. H., Lee, S. & Prag, G. Ubiquitin-binding domains. *Biochemical Journal* **399**, 361 (2006).

[65] Husnjak, K. & Dikic, I. Ubiquitin-binding proteins: Decoders of ubiquitin-mediated cellular functions. *Annual Review of Biochemistry* **81**, 291–322 (2012).

[66] González-Prieto, R. *et al.* Global non-covalent SUMO interaction networks reveal SUMO-dependent stabilization of the non-homologous end joining complex. *Cell Reports* **34**, 108691 (2021).

[67] Fisher, R. D. *et al.* Structure and ubiquitin binding of the ubiquitin-interacting motif. *Journal of Biological Chemistry* **278**, 28976–28984 (2003).

[68] Hicke, L., Schubert, H. L. & Hill, C. P. Ubiquitin-binding domains. *Nature Reviews Molecular Cell Biology* **6**, 610–621 (2005).

[69] Dikic, I., Wakatsuki, S. & Walters, K. J. Ubiquitin-binding domains from structures to functions. *Nature Reviews Molecular Cell Biology* **10**, 659–671 (2009).

[70] Cardozo, T. & Pagano, M. The SCF ubiquitin ligase: Insights into a molecular machine. *Nature Reviews Molecular Cell Biology* **5**, 739–751 (2004).

[71] E. Hare, A. & D. Parvin, J. Processes that Regulate the Ubiquitination of Chromatin and Chromatin-Associated Proteins. In *Ubiquitin Proteasome System - Current Insights into Mechanism Cellular Regulation and Disease* (IntechOpen, 2019).

[72] Ohta, T. & Fukuda, M. Ubiquitin and breast cancer. *Oncogene* **23**, 2079–2088 (2004).

[73] Ramanathan, H. N. & Ye, Y. Cellular strategies for making monoubiquitin signals. *Critical Reviews in Biochemistry and Molecular Biology* **47**, 17–28 (2012).

[74] Sigismund, S., Polo, S. & Di Fiore, P. P. Signaling through monoubiquitination. *Current Topics in Microbiology and Immunology* **286**, 149–185 (2004).

[75] Chau, V. *et al.* A multiubiquitin chain is confined to specific lysine in a targeted short-lived protein. *Science* **243**, 1576–1583 (1989).

[76] Erpapazoglou, Z., Walker, O. & Haguenauer-Tsapis, R. Versatile Roles of K63-Linked Ubiquitin Chains in Trafficking. *Cells* **3**, 1027–1088 (2014).

[77] Ulrich, H. D. & Walden, H. Ubiquitin signalling in DNA replication and repair. *Nature Reviews Molecular Cell Biology* **11**, 479—-489 (2010).

[78] Kliza, K. & Husnjak, K. Resolving the Complexity of Ubiquitin Networks. *Frontiers in Molecular Biosciences* **7**, 21 (2020).

[79] Mendes, M. L., Fougeras, M. R. & Dittmar, G. Analysis of ubiquitin signaling and chain topology cross-talk. *Journal of Proteomics* **215**, 103634 (2020).

[80] Paul, A. & Wang, B. RNF8- and Ube2S-Dependent Ubiquitin Lysine 11-Linkage Modification in Response to DNA Damage. *Molecular Cell* **66**, 458–472 (2017).

[81] Thrower, J. S., Hoffman, L., Rechsteiner, M. & Pickart, C. M. Recognition of the polyubiquitin proteolytic signal. *EMBO Journal* **19**, 94–102 (2000).

[82] Smeenk, G. & Mailand, N. Writers, readers, and erasers of histone ubiquitylation in DNA double-strand break repair. *Frontiers in Genetics* **7**, 122 (2016).

[83] Oh, E., Akopian, D. & Rape, M. Principles of Ubiquitin- Dependent Signaling. *Annual Review of Cell and Developmental Biology* **34**, 137–162 (2018).

[84] Elia, A. E. *et al.* Quantitative Proteomic Atlas of Ubiquitination and Acetylation in the DNA Damage Response. *Molecular Cell* **59**, 867–881 (2015).

[85] Durcan, T. M. *et al.* USP 8 regulates mitophagy by removing K 6-linked ubiquitin conjugates from parkin. *The EMBO Journal* **33**, 2473–2491 (2014).

[86] Gatti, M. *et al.* RNF168 promotes noncanonical K27ubiquitination to signal DNA damage. *Cell Reports* **10**, 226–238 (2015).

[87] Yuan, W. C. *et al.* K33-Linked Polyubiquitination of Coronin 7 by Cul3-KLHL20

Ubiquitin E3 Ligase Regulates Protein Trafficking. *Molecular Cell* **54**, 586–600 (2014).

[88] Johnson, E. S., Ma, P. C., Ota, I. M. & Varshavsky, A. A proteolytic pathway that recognizes ubiquitin as a degradation signal. *Journal of Biological Chemistry* **270**, 17442–17456 (1995).

[89] Iwai, K. Discovery of linear ubiquitination, a crucial regulator for immune signaling and cell death. *FEBS Journal* **288**, 1060–1069 (2021).

[90] Emmerich, C. H. *et al.* Activation of the canonical IKK complex by K63/M1-linked hybrid ubiquitin chains. *Proceedings of the National Academy of Sciences of the United States of America* **110**, 15247–15252 (2013).

[91] Meyer, H. J. & Rape, M. Enhanced protein degradation by branched ubiquitin chains. *Cell* **157**, 910–921 (2014).

[92] Hershko, A. & Ciechanover, A. The ubiquitin system. *Annual Review of Biochemistry* **67**, 425–479 (1998).

[93] Finley, D. Recognition and processing of ubiquitin-protein conjugates by the proteasome. *Annual Review of Biochemistry* **78**, 477–513 (2009).

[94] Hicke, L. Protein regulation by monoubiquitin. *Nature Reviews Molecular Cell Biology* **2**, 195–201 (2001).

[95] Finley, D. *et al.* Inhibition of proteolysis and cell cycle progression in a multiubiquitination-deficient yeast mutant. *Molecular and Cellular Biology* **14**, 5501–5509 (1994).

[96] Xu, M., Skaug, B., Zeng, W. & Chen, Z. J. A Ubiquitin Replacement Strategy in Human Cells Reveals Distinct Mechanisms of IKK Activation by TNFα and IL-1β. *Molecular Cell* **36**, 302–314 (2009).

[97] Tasaki, T., Sriram, S. M., Park, K. S. & Kwon, Y. T. The N-End rule pathway. *Annual Review of Biochemistry* **81**, 261–289 (2012).

[98] Lu, Y., Lee, B. H., King, R. W., Finley, D. & Kirschner, M. W. Substrate degradation by the proteasome: A single-molecule kinetic analysis. *Science* **348**, 1250834 (2015).

[99] Renz, C. *et al.* Ubc13–Mms2 cooperates with a family of RING E3 proteins in budding yeast membrane protein sorting. *Journal of Cell Science* **133** (2020).

[100] Duncan, L. M. *et al.* Lysine-63-linked ubiquitination is required for endolysosomal degradation of class I molecules. *EMBO Journal* **25**, 1635–1645 (2006).

[101] Lauwers, E., Jacob, C. & Andre, B. K63-linked ubiquitin chains as a specific signal for protein sorting into the multivesicular body pathway. *Journal of Cell Biology* **185**, 493–502 (2009).

[102] Manzanillo, P. S. *et al.* The ubiquitin ligase parkin mediates resistance to intracellular pathogens. *Nature* **501**, 512–516 (2013).

[103] García-Rodríguez, N., Wong, R. P. & Ulrich, H. D. Functions of Ubiquitin and SUMO in DNA Replication and Replication Stress. *Frontiers in Genetics* **7**, 87 (2016).

[104] Panier, S. & Durocher, D. Regulatory ubiquitylation in response to DNA double-strand breaks. *DNA Repair* **8**, 436–443 (2009).

[105] Wu, X. & Karin, M. Emerging roles of Lys63-linked polyubiquitylation in immune responses. *Immunological Reviews* **266**, 161–174 (2015).

[106] Galan, J. M., Moreau, V., Andre, B., Volland, C. & Haguenauer-Tsapis, R. Ubiquitination mediated by the Npi1p/Rsp5p ubiquitin-protein ligase is required for endocytosis of the yeast uracil permease. *Journal of Biological Chemistry* **271**, 10946–10952 (1996).

[107] Springael, J. Y. & André, B. Nitrogen-regulated ubiquitination of the Gap1 permease of Saccharomyces cerevisiae. *Molecular Biology of the Cell* **9**, 1253–1263 (1998).

[108] Katzmann, D. J., Babst, M. & Emr, S. D. Ubiquitin-dependent sorting into the multivesicular body pathway requires the function of a conserved endosomal protein sorting complex, ESCRT-I. *Cell* **106**, 145–155 (2001).

[109] Mukhopadhyay, D. & Riezman, H. Proteasome-independent functions of ubiquitin in endocytosis and signaling. *Science* **315**, 201–205 (2007).

[110] Huang, F., Kirkpatrick, D., Jiang, X., Gygi, S. & Sorkin, A. Differential regulation of EGF receptor internalization and degradation by multiubiquitination within the kinase domain. *Molecular Cell* **21**, 737–748 (2006).

[111] Lauwers, E., Erpapazoglou, Z., Haguenauer-Tsapis, R. & André, B. The ubiquitin code of yeast permease trafficking. *Trends in Cell Biology* **20**, 196–204 (2010).

[112] Burd, C. G. & Emr, S. D. Phosphatidylinositol(3)-Phosphate Signaling Mediated by Specific Binding to RING FYVE Domains. *Molecular Cell* **2**, 157–162 (1998).

[113] Shin, M. E., Ogburn, K. D., Varban, O. A., Gilbert, P. M. & Burd, C. G. FYVE Domain Targets Pib1p Ubiquitin Ligase to Endosome and Vacuolar Membranes. *Journal of Biological Chemistry* **276**, 41388–41393 (2001).

[114] Nikko, E. & Pelham, H. R. B. Arrestin-Mediated Endocytosis of Yeast Plasma Membrane Transporters. *Traffic* **10**, 1856–1867 (2009).

[115] MacDonald, C., Winistorfer, S., Pope, R. M., Wright, M. E. & Piper, R. C. Enzyme reversal to explore the function of yeast E3 ubiquitin-ligases. *Traffic* **18**, 465–484 (2017).

[116] Reggiori, F. & Pelham, H. R. B. A transmembrane ubiquitin ligase required to sort membrane proteins into multivesicular bodies. *Nature Cell Biology* **4**, 117–123 (2002).

[117] Xu, P. *et al.* COPI mediates recycling of an exocytic SNARE by recognition of a ubiquitin sorting signal. *eLife* **6**, 1–22 (2017).

[118] Sardana, R., Zhu, L. & Emr, S. D. Rsp5 Ubiquitin ligase-mediated quality control system clears membrane proteins mistargeted to the vacuole membrane. *The Journal of cell biology* **218**, 234–250 (2019).

[119] Yang, X. *et al.* TORC1 regulates vacuole membrane composition through ubiquitin- And ESCRT-dependent microautophagy. *Journal of Cell Biology* **219** (2020).

[120] Vengayil, V., Rashida, Z. & Laxman, S. The E3 ubiquitin ligase Pib1 regulates effective gluconeogenic shutdown upon glucose availability. *Journal of Biological Chemistry* **294**, 17209–17223 (2019).

[121] Lewis, M. J., Nichols, B. J., Prescianotto-Baschong, C., Riezman, H. & Pelham, H. R. Specific retrieval of the exocytic SNARE Snc1p from early yeast endosomes. *Molecular Biology of the Cell* **11**, 23–38 (2000).

[122] Ma, M. & Burd, C. G. Retrograde trafficking and quality control of yeast synaptobrevin, Snc1, are conferred by its transmembrane domain. *Molecular Biology of the Cell* **30**, mbc.E19–02–0117 (2019).

[123] Best, J. T., Xu, P., McGuire, J. G., Leahy, S. N. & Graham, T. R. Yeast synaptobrevin, Snc1, engages distinct routes of post-endocytic recycling mediated by

a sorting nexin, Rcy1-COPI, and retromer. *Molecular biology of the cell* **31**, mbcE19050290 (2020).

[124] Bienko, M. *et al.* Biochemistry: Ubiquitin-binding domains in Y-family polymerases regulate translesion synthesis. *Science* **310**, 1821–1824 (2005).

[125] Ulrich, H. D. (ed.) *SUMO Protocols: Preface*, vol. 497 of *Methods in Molecular Biology* (Humana Press, Totowa, NJ, 2009).

[126] Stelter, P. & Ulrich, H. D. Control of spontaneous and damage-induced mutagenesis by SUMO and ubiquitin conjugation. *Nature* **425**, 188–191 (2003).

[127] Parker, J. L., Bielen, A. B., Dikic, I. & Ulrich, H. D. Contributions of ubiquitin- and PCNA-binding domains to the activity of Polymerase η in Saccharomyces cerevisiae. *Nucleic Acids Research* **35**, 881–889 (2007).

[128] Kannouche, P. L., Wing, J. & Lehmann, A. R. Interaction of human DNA polymerase η with monoubiquitinated PCNA: A possible mechanism for the polymerase switch in response to DNA damage. *Molecular Cell* **14**, 491–500 (2004).

[129] Davies, A. A., Huttner, D., Daigaku, Y., Chen, S. & Ulrich, H. D. Activation of Ubiquitin-Dependent DNA Damage Bypass Is Mediated by Replication Protein A. *Molecular Cell* **29**, 625–636 (2008).

[130] Parker, J. L., Ulrich, H. D., JL, P. & HD, U. A SUMO-interacting motif activates budding yeast ubiquitin ligase Rad18 towards SUMO-modified PCNA. *Nucleic acids research* **40**, 11380–8 (2012).

[131] Motegi, A. *et al.* Polyubiquitination of proliferating cell nuclear antigen by HLTF and SHPRH prevents genomic instability from stalled replication forks. *Proceedings of the National Academy of Sciences of the United States of America* **105**, 12411–12416 (2008).

[132] Parker, J. L. & Ulrich, H. D. Mechanistic analysis of PCNA poly-ubiquitylation by the ubiquitin protein ligases Rad18 and Rad5. *EMBO Journal* **28**, 3657–3666 (2009).

[133] Gallego-Sánchez, A., Andrés, S., Conde, F., San-Segundo, P. A. & Bueno, A. Reversal of PCNA ubiquitylation by Ubp10 in Saccharomyces cerevisiae. *PLoS Genetics* **8**, e1002826 (2012).

[134] Álvarez, V. *et al.* PCNA Deubiquitylases Control DNA Damage Bypass at Replication Forks. *Cell Reports* **29**, 1323–1335 (2019).

[135] McAinsh, A. D., Tytell, J. D. & Sorger, P. K. Structure, function, and regulation of budding yeast kinetochores. *Annu Rev Cell Dev Biol* **19**, 519–539 (2003).

[136] Santaguida, S. & Musacchio, A. The life and miracles of kinetochores. *The EMBO Journal* **28**, 2511–2531 (2009).

[137] Cleveland, D. W., Mao, Y. & Sullivan, K. F. Centromeres and Kinetochores: From Epigenetics to Mitotic Checkpoint Signaling. *Cell* **112**, 407–421 (2003).

[138] Cheeseman, I. M., Drubin, D. G. & Barnes, G. Simple centromere, complex kinetochore: linking spindle microtubules and centromeric DNA in budding yeast. *The Journal of Cell Biology* **157**, 199–203 (2002).

[139] Wei, R. R., Al-Bassam, J. & Harrison, S. C. The Ndc80/HEC1 complex is a contact point for kinetochore-microtubule attachment. *Nat Struct Mol Biol* **14**, 54–59 (2007).

[140] Cheeseman, I. M. *et al.* Phospho-Regulation of Kinetochore-Microtubule Attachments by the Aurora Kinase Ipl1p. *Cell* **111**, 163–172 (2002).

[141] Cheeseman, I. M., Chappie, J. S., Wilson-Kubalek, E. M. & Desai, A. The Conserved KMN Network Constitutes the Core Microtubule-Binding Site of the Kinetochore. *Cell* **127**, 983–997 (2006).

[142] De Wulf, P., McAinsh, A. D. & Sorger, P. K. Hierarchical assembly of the budding yeast kinetochore from multiple subcomplexes. *Genes and Development Development* **17**, 2902–2921 (2003).

[143] Janke, C. *et al.* The budding yeast proteins Spc24p and Spc25p interact with Ndc80p and Nuf2p at the kinetochore and are important for kinetochore clustering and checkpoint control. *The EMBO Journal* **20**, 777–791 (2001).

[144] Wei, R. R., Sorger, P. K. & Harrison, S. C. Molecular organization of the Ndc80 complex, an essential kinetochore component. *Proceedings of the National Academy of Sciences of the United States of America* **102**, 5363–5367 (2005).

[145] Wei, R. R. *et al.* Structure of a Central Component of the Yeast Kinetochore: The Spc24p/Spc25p Globular Domain. *Structure* **14**, 1003–1009 (2006).

[146] Ciferri, C. *et al.* Implications for Kinetochore-Microtubule Attachment from the Structure of an Engineered Ndc80 Complex. *Cell* **133**, 427–439 (2008).

[147] Westermann, S., Drubin, D. G. & Barnes, G. Structures and functions of yeast kinetochore complexes. *Annu Rev Biochem* **76**, 563–591 (2007).

[148] Zhao, S. & Shengkai, Z. *Signalling Functions of Polyubiquitin Chains and Ubiquitinbinding Domains*. Ph.D. thesis, University College London and Cancer Research UK London Research Institute (2010).

[149] Banerjee, J. J. *Developmental function of Drosophila RASSF9 and RASSF10*. Ph.D. thesis, University College London and Cancer Research UK London Research Institute (2015).

[150] Gestaut, D. R. *et al.* Phosphoregulation and depolymerization-driven movement of the Dam1 complex do not require ring formation. *Nature Cell Biology* **10**, 407–414 (2008).

[151] Akiyoshi, B. *et al.* The Mub1/Ubr2 Ubiquitin Ligase Complex Regulates the Conserved Dsn1 Kinetochore Protein. *PLOS Genetics* **9**, e1003216 (2013).

[152] Francisco, L., Wang, W. & Chan, C. S. Type 1 protein phosphatase acts in opposition to IpL1 protein kinase in regulating yeast chromosome segregation. *Molecular and Cellular Biology* **14**, 4731–4740 (1994).

[153] Montpetit, B., Hazbun, T. R., Fields, S. & Hieter, P. Sumoylation of the budding yeast kinetochore protein Ndc10 is required for Ndc10 spindle localization and regulation of anaphase spindle elongation. *The Journal of Cell Biology* **174**, 653–663 (2006).

[154] Newton, K. *et al.* Ubiquitin Chain Editing Revealed by Polyubiquitin Linkage-Specific Antibodies. *Cell* **134**, 668–678 (2008).

[155] Thermo Fisher Scientific. Ubiquitin Primary Antibodies. *https://www.thermofisher.com/antibody/primary/query/* (accessed: 2022-02-22).

[156] Hospenthal, M. K., Mevissen, T. E. & Komander, D. Deubiquitinase-based analysis of ubiquitin chain architecture using Ubiquitin Chain Restriction (UbiCRest). *Nature Protocols* **10**, 349–361 (2015).

[157] Hjerpe, R. *et al.* Efficient protection and isolation of ubiquitylated proteins using tandem ubiquitin-binding entities. *EMBO Reports* **10**, 1250 (2009).

[158] Yoshida, Y. *et al.* A comprehensive method for detecting ubiquitinated substrates

using TR-TUBE. *Proceedings of the National Academy of Sciences of the United States of America* **112**, 4630–4635 (2015).

[159] Ordureau, A., Münch, C. & Harper, J. W. W. Quantifying Ubiquitin Signaling. *Molecular Cell* **58**, 660–676 (2015).

[160] Terrell, J., Shih, S., Dunn, R. & Hicke, L. A Function for Monoubiquitination in the Internalization of a G Protein–Coupled Receptor. *Molecular Cell* **1**, 193–202 (1998).

[161] Wegmann, S. *et al.* Linkage reprogramming by tailor-made E3s reveals polyubiquitin chain requirements in DNA-damage bypass. *Molecular Cell* 1589–1602 (2022).

[162] Neklesa, T. K., Winkler, J. D. & Crews, C. M. Targeted protein degradation by PROTACs. *Pharmacology and Therapeutics* **174**, 138–144 (2017).

[163] Nishimura, K., Fukagawa, T., Takisawa, H., Kakimoto, T. & Kanemaki, M. An auxin-based degron system for the rapid depletion of proteins in nonplant cells. *Nature Methods* **6**, 917–922 (2009).

[164] Jin, L., Williamson, A., Banerjee, S., Philipp, I. & Rape, M. Mechanism of Ubiquitin-Chain Formation by the Human Anaphase-Promoting Complex. *Cell* **133**, 653–665 (2008).

[165] Deng, L. *et al.* Activation of the Iκb kinase complex by TRAF6 requires a dimeric ubiquitin-conjugating enzyme complex and a unique polyubiquitin chain. *Cell* **103**, 351–361 (2000).

[166] Ernst, A. *et al.* A Strategy for Modulation of Enzymes in the Ubiquitin System. *Science* **339**, 590–595 (2013).

[167] Teyra, J. *et al.* Structural and Functional Characterization of Ubiquitin Variant Inhibitors of USP15. *Structure* **27**, 590–605 (2019).

[168] Gabrielsen, M. *et al.* A General Strategy for Discovery of Inhibitors and Activators of RING and U-box E3 Ligases with Ubiquitin Variants. *Molecular Cell* **68**, 456–470 (2017).

[169] Brown, N. G. *et al.* Dual RING E3 Architectures Regulate Multiubiquitination and Ubiquitin Chain Elongation by APC/C. *Cell* **165**, 1440–1453 (2016).

[170] Gorelik, M. & Sidhu, S. S. Specific targeting of the deubiquitinase and E3 lig-

ase families with engineered ubiquitin variants. *Bioengineering and Translational Medicine* **2**, 31–42 (2016).

[171] Manczyk, N. *et al.* Structural and functional characterization of a ubiquitin variant engineered for tight and specific binding to an alpha-helical ubiquitin interacting motif. *Protein Science : A Publication of the Protein Society* **26**, 1060 (2017).

[172] Zhang, W. *et al.* System-Wide Modulation of HECT E3 Ligases with Selective Ubiquitin Variant Probes. *Molecular Cell* **62**, 121–136 (2016).

[173] Zhang, W. *et al.* Potent and selective inhibition of pathogenic viruses by engineered ubiquitin variants. *PLoS Pathogens* **13** (2017).

[174] Zhang, W. *et al.* Generation and Validation of Intracellular Ubiquitin Variant Inhibitors for USP7 and USP10. *Journal of molecular biology* **429**, 3546–3560 (2017).

[175] Middleton, A. J., Teyra, J., Zhu, J., Sidhu, S. S. & Day, C. L. Identification of Ubiquitin Variants That Inhibit the E2 Ubiquitin Conjugating Enzyme, Ube2k. *ACS Chemical Biology* **16**, 1745–1756 (2021).

[176] Tang, J. Q. *et al.* A Panel of Engineered Ubiquitin Variants Targeting the Family of Domains Found in Ubiquitin Specific Proteases (DUSPs). *Journal of Molecular Biology* **433**, 167300 (2021).

[177] Manczyk, N. *et al.* Dimerization of a ubiquitin variant leads to high affinity interactions with a ubiquitin interacting motif. *Protein Science* **28**, 848–856 (2019).

[178] Wiechmann, S. *et al.* Site-specific inhibition of the small ubiquitin-like modifier (SUMO)-conjugating enzyme Ubc9 selectively impairs SUMO chain formation. *The Journal of biological chemistry* **292**, 15340–15351 (2017).

[179] Cohen, A., Rosenthal, E. & Shifman, J. M. Analysis of Structural Features Contributing to Weak Affinities of Ubiquitin/Protein Interactions. *Journal of Molecular Biology* **429**, 3353–3362 (2017).

[180] Saitoh, H. & Hinchey, J. Functional heterogeneity of small ubiquitin-related protein modifiers SUMO-1 versus SUMO-2/3. *Journal of Biological Chemistry* **275**, 6252–6258 (2000).

[181] Bylebyl, G. R., Belichenko, I. & Johnson, E. S. The SUMO isopeptidase Ulp2 prevents accumulation of SUMO chains in yeast. *The Journal of biological chemistry* **278**, 44113–20 (2003).

[182] Zhao, X. SUMO-Mediated Regulation of Nuclear Functions and Signaling Processes. *Molecular Cell* **71**, 409–418 (2018).

[183] Bhagwat, N. R. *et al.* SUMO is a pervasive regulator of meiosis. *eLife* **10**, 1–89 (2021).

[184] Almedawar, S., Colomina, N., Bermúdez-López, M., Pociño-Merino, I. & Torres-Rosell, J. A SUMO-dependent step during establishment of sister chromatid cohesion. *Current Biology* **22**, 1576–1581 (2012).

[185] Flotho, A. & Melchior, F. Sumoylation: A Regulatory Protein Modification in Health and Disease. *Annual Review of Biochemistry* **82**, 357–385 (2013).

[186] Liebelt, F. & Vertegaal, A. C. Ubiquitin-dependent and independent roles of SUMO in proteostasis. *American Journal of Physiology - Cell Physiology* **311**, C284–C296 (2016).

[187] Papouli, E. *et al.* Crosstalk between SUMO and ubiquitin on PCNA is mediated by recruitment of the helicase Srs2p. *Molecular Cell* **19**, 123–133 (2005).

[188] Steinacher, R. & Schär, P. Functionality of human thymine DNA glycosylase requires SUMO-regulated changes in protein conformation. *Current Biology* **15**, 616–623 (2005).

[189] Wasik, U. & Filipek, A. Non-nuclear function of sumoylated proteins. *Biochimica et Biophysica Acta (BBA) - Molecular Cell Research* **1843**, 2878–2885 (2014).

[190] Jackson, S. P. & Durocher, D. Regulation of DNA Damage Responses by Ubiquitin and SUMO. *Molecular Cell* **49**, 795–807 (2013).

[191] Eifler, K. & Vertegaal, A. C. SUMOylation-Mediated Regulation of Cell Cycle Progression and Cancer. *Trends in Biochemical Sciences* **40**, 779–793 (2015).

[192] Anderson, D. B., Zanella, C. A., Henley, J. M. & Cimarosti, H. Sumoylation: Implications for Neurodegenerative Diseases. In *Advances in experimental medicine and biology*, vol. 963, 261–281 (Springer, Cham, 2017).

[193] Melchior, F. SUMO - Nonclassical ubiquitin. *Annual Review of Cell and Developmental Biology* **16**, 591–626 (2000).

[194] He, X. *et al.* Probing the roles of SUMOylation in cancer cell biology by using a selective SAE inhibitor. *Nature Chemical Biology* **13**, 1164–1171 (2017).

[195] Hughes, D. J. *et al.* Generation of specific inhibitors of SUMO-1- and SUMO-2/3-mediated protein-protein interactions using Affimer (Adhiron) technology. *Science Signaling* **10** (2017).

[196] Van Der Veen, A. G. & Ploegh, H. L. Ubiquitin-like proteins. *Annual Review of Biochemistry* **81**, 323–357 (2012).

[197] Johnson, E. S. & Blobel, G. Cell cycle-regulated attachment of the ubiquitin-related protein SUMO to the yeast septins. *The Journal of cell biology* **147**, 981–94 (1999).

[198] Windecker, H., Ulrich, H. D., H, W. & HD, U. Architecture and Assembly of Poly-SUMO Chains on PCNA in Saccharomyces cerevisiae. *Journal of Molecular Biology* **376**, 221–231 (2008).

[199] Jürgen Dohmen, R. SUMO protein modification. *Biochimica et Biophysica Acta - Molecular Cell Research* **1695**, 113–131 (2004).

[200] Gareau, J. R. & Lima, C. D. The SUMO pathway: Emerging mechanisms that shape specificity, conjugation and recognition. *Nature Reviews Molecular Cell Biology* **11**, 861–871 (2010).

[201] Jentsch, S. & Psakhye, I. Control of nuclear activities by substrate-selective and protein-group SUMOylation. *Annual Review of Genetics* **47**, 167–186 (2013).

[202] Johnson, E. S. Protein modification by SUMO. *Annual Review of Biochemistry* **73**, 355–382 (2004).

[203] Pichler, A., Fatouros, C., Lee, H. & Eisenhardt, N. SUMO conjugation - A mechanistic view. *Biomolecular Concepts* **8**, 13–36 (2017).

[204] Li, S. J. & Hochstrasser, M. A new protease required for cell-cycle progression in yeast. *Nature* **398**, 246–251 (1999).

[205] Li, S.-J. & Hochstrasser, M. The Yeast ULP2 (SMT4) Gene Encodes a Novel Protease Specific for the Ubiquitin-Like Smt3 Protein. *Molecular and Cellular Biology* **20**, 2367–2377 (2000).

[206] Hickey, C. M., Wilson, N. R. & Hochstrasser, M. Function and Regulation of SUMO Proteases. *Nature reviews. Molecular cell biology* **13** (2012).

[207] Sarangi, P. & Zhao, X. SUMO-mediated regulation of DNA damage repair and responses. *Trends in Biochemical Sciences* **40**, 233–242 (2015).

[208] Dhingra, N. & Zhao, X. Intricate SUMO-based control of the homologous recombination machinery. *Genes and Development* **33**, 1346–1354 (2019).

[209] Song, J., Durrin, L. K., Wilkinson, T. A., Krontiris, T. G. & Chen, Y. Identification of a SUMO-binding motif that recognizes SUMO-modified proteins. *Proceedings of the National Academy of Sciences of the United States of America* **101**, 14373–14378 (2004).

[210] Hecker, C. M., Rabiller, M., Haglund, K., Bayer, P. & Dikic, I. Specification of SUMO1- and SUMO2-interacting motifs. *Journal of Biological Chemistry* **281**, 16117–16127 (2006).

[211] Desterro, J. M., Rodriguez, M. S., Kemp, G. D. & Ronald T, H. Identification of the enzyme required for activation of the small ubiquitin-like protein SUMO-1. *Journal of Biological Chemistry* **274**, 10618–10624 (1999).

[212] Walden, H. *et al.* The Structure of the APPBP1-UBA3-NEDD8-ATP Complex Reveals the Basis for Selective Ubiquitin-like Protein Activation by an E1. *Molecular Cell* **12**, 1427–1437 (2003).

[213] Rodriguez, M. S., Dargemont, C. & Hay, R. T. SUMO-1 Conjugation in Vivo Requires Both a Consensus Modification Motif and Nuclear Targeting. *Journal of Biological Chemistry* **276**, 12654–12659 (2001).

[214] Sampson, D. A., Wang, M. & Matunis, M. J. The Small Ubiquitin-like Modifier-1 (SUMO-1) Consensus Sequence Mediates Ubc9 Binding and is Essential for SUMO-1 Modification. *Journal of Biological Chemistry* **276**, 21664–21669 (2001).

[215] Bernier-Villamor, V., Sampson, D. A., Matunis, M. J. & Lima, C. D. Smt3 modification appears critical for septin ring forma-tion, chromosomal segregation, and progression of the cell cycle through G 2-M. *Cell* **108**, 345–356 (2002).

[216] Hendriks, I. A. & Vertegaal, A. C. O. A comprehensive compilation of SUMO proteomics. *Nature Reviews Molecular Cell Biology* **17**, 581–595 (2016).

[217] Knipscheer, P., van Dijk, W. J., Olsen, J. V., Mann, M. & Sixma, T. K. Noncovalent interaction between Ubc9 and SUMO promotes SUMO chain formation. *The EMBO journal* **26**, 2797–807 (2007).

[218] Alontaga, A. & Chen, Y. Reply to function and structure of the RWD domain. *Journal of Biological Chemistry* **290**, 20628 (2015).

[219] Alontaga, A. Y. *et al.* Observation of an E2 (Ubc9)-homodimer by crystallography. *Data in Brief* **7**, 195–200 (2016).

[220] Page, R. C., Pruneda, J. N., Amick, J., Klevit, R. E. & Misra, S. Structural Insights into the Conformation and Oligomerization of E2-Ubiquitin Conjugates. *Biochemistry* **51**, 4175–4187 (2012).

[221] Werner, A., Flotho, A. & Melchior, F. The RanBP2/RanGAP1 *SUMO1/Ubc9 Complex Is a Multisubunit SUMO E3 Ligase. *Molecular Cell* **46**, 287–298 (2012).

[222] Streich, F. C. & Lima, C. D. Capturing a substrate in an activated RING E3/E2-SUMO complex. *Nature* **536**, 304–308 (2016).

[223] Johnson, E. S. & Gupta, A. A. An E3-like Factor that Promotes SUMO Conjugation to the Yeast Septins. *Cell* **106**, 735–744 (2001).

[224] Takahashi, Y., Toh-e, A. & Kikuchi, Y. A novel factor required for the SUMO1/Smt3 conjugation of yeast septins. *Gene* **275**, 223–231 (2001).

[225] Martin, N. *et al.* PARP-1 transcriptional activity is regulated by sumoylation upon heat shock. *EMBO Journal* **28**, 3534–3548 (2009).

[226] Reindle, A. *et al.* Multiple domains in Siz SUMO ligases contribute to substrate selectivity. *Journal of Cell Science* **119**, 4749–4757 (2006).

[227] Zhao, X. & Blobel, G. A SUMO ligase is part of a nuclear multiprotein complex that affects DNA repair and chromosomal organization. *Proceedings of the National Academy of Sciences of the United States of America* **102**, 4777–4782 (2005).

[228] Andrews, E. A. *et al.* Nse2, a Component of the Smc5-6 Complex, Is a SUMO Ligase Required for the Response to DNA Damage. *Molecular and Cellular Biology* **25**, 185–196 (2005).

[229] Varejão, N. *et al.* DNA activates the Nse2/Mms21 SUMO E3 ligase in the Smc5/6 complex. *The EMBO Journal* **37**, e98306 (2018).

[230] Agarwal, S. & Roeder, G. S. Zip3 provides a link between recombination enzymes and synaptonemal complex proteins. *Cell* **102**, 245–255 (2000).

[231] Cheng, C. H. *et al.* SUMO modifications control assembly of synaptonemal complex and polycomplex in meiosis of Saccharomyces cerevisiae. *Genes and Development* **20**, 2067–2081 (2006).

[232] Yunus, A. A. & Lima, C. D. Structure of the Siz/PIAS SUMO E3 ligase Siz1 and determinants required for SUMO modification of PCNA. *Molecular cell* **35**, 669–82 (2009).

[233] Mossessova, E. & Lima, C. D. Ulp1-SUMO Crystal Structure and Genetic Analysis Reveal Conserved Interactions and a Regulatory Element Essential for Cell Growth in Yeast. *Molecular Cell* **5**, 865–876 (2000).

[234] Nayak, A. & Müller, S. SUMO-specific proteases/isopeptidases: SENPs and beyond. *Genome Biology* **15**, 422 (2014).

[235] Shin, E. J. *et al.* DeSUMOylating isopeptidase: A second class of SUMO protease. *EMBO Reports* **13**, 339–346 (2012).

[236] Schulz, S. *et al.* Ubiquitin-specific protease-like 1 (USPL1) is a SUMO isopeptidase with essential, non-catalytic functions. *EMBO Reports* **13**, 930–938 (2012).

[237] Schwienhorst, I., Johnson, E. S. & Dohmen, R. J. SUMO conjugation and deconjugation. *Molecular and General Genetics* **263**, 771–786 (2000).

[238] Strunnikov, A. V., Aravind, L. & Koonin, E. V. Saccharomyces cerevisiae SMT4 encodes an evolutionarily conserved protease with a role in chromosome condensation regulation. *Genetics* **158**, 95–107 (2001).

[239] Li, S. J. & Hochstrasser, M. The Ulp1 SUMO isopeptidase: Distinct domains required for viability, nuclear envelope localization, and substrate specificity. *Journal of Cell Biology* **160**, 1069–1081 (2003).

[240] Leisner, C. *et al.* Regulation of Mitotic Spindle Asymmetry by SUMO and the Spindle-Assembly Checkpoint in Yeast. *Current Biology* **18**, 1249–1255 (2008).

[241] Schwartz, D. C., Felberbaum, R. & Hochstrasser, M. The Ulp2 SUMO Protease Is Required for Cell Division following Termination of the DNA Damage Checkpoint. *Molecular and Cellular Biology* **27**, 6948–6961 (2007).

[242] Takahashi, K., Chen, E. S. & Yanagida, M. Requirement of Mis6 centromere connector for localizing a CENP-A-like protein in fission yeast. *Science* **288**, 2215–2219 (2000).

[243] Baldwin, M. L., Julius, J. A., Tang, X., Wang, Y. & Bachant, J. The yeast SUMO isopeptidase Smt4/Ulp2 and the polo kinase Cdc5 act in an opposing fashion to regulate sumoylation in mitosis and cohesion at centromeres. *Cell Cycle* **8**, 3406–3419 (2009).

[244] Zhao, B. *et al.* SUMO-mimicking peptides inhibiting protein SUMOylation. *Chembiochem : a European journal of chemical biology* **15**, 2662–2666 (2014).

[245] Escobar-Cabrera, E. *et al.* Characterizing the N- and C-terminal small ubiquitin-like modifier (SUMO)-interacting motifs of the scaffold protein DAXX. *Journal of Biological Chemistry* **286**, 19816–19829 (2011).

[246] Song, J., Zhang, Z., Hu, W. & Chen, Y. Small ubiquitin-like modifier (SUMO) recognition of a SUMO binding motif: a reversal of the bound orientation. *The Journal of biological chemistry* **280**, 40122–9 (2005).

[247] Baba, D. *et al.* Crystal structure of thymine DNA glycosylase conjugated to SUMO-1. *Nature* **435**, 979–982 (2005).

[248] Reverter, D. & Lima, C. D. Insights into E3 ligase activity revealed by a SUMO-RanGAP1-Ubc9-Nup358 complex. *Nature* **435**, 687–92 (2005).

[249] Sekiyama, N. *et al.* Structure of the small ubiquitin-like modifier (SUMO)-interacting motif of MBD1-containing chromatin-associated factor 1 bound to SUMO-3. *Journal of Biological Chemistry* **283**, 35966–35975 (2008).

[250] Chang, C. C. *et al.* Structural and Functional Roles of Daxx SIM Phosphorylation in SUMO Paralog-Selective Binding and Apoptosis Modulation. *Molecular Cell* **42**, 62–74 (2011).

[251] Anamika & Spyracopoulos, L. Molecular basis for phosphorylation-dependent SUMO recognition by the DNA repair protein RAP80. *Journal of Biological Chemistry* **291**, 4417–4428 (2016).

[252] Yau, T. Y., Sander, W., Eidson, C. & Coure, A. J. Sumo interacting motifs: Structure and function. *Cells* **10**, 2825 (2021).

[253] Stehmeier, P. & Muller, S. Phospho-Regulated SUMO Interaction Modules Connect the SUMO System to CK2 Signaling. *Molecular Cell* **33**, 400–409 (2009).

[254] Ullmann, R., Chien, C. D., Avantaggiati, M. L. & Muller, S. An Acetylation Switch Regulates SUMO-Dependent Protein Interaction Networks. *Molecular Cell* **46**, 759–770 (2012).

[255] Sun, H. & Hunter, T. Poly-small ubiquitin-like modifier (PolySUMO)-binding proteins identified through a string search. *Journal of Biological Chemistry* **287**, 42071–42083 (2012).

[256] Keusekotten, K. *et al.* Multivalent interactions of the SUMO-interaction motifs in RING finger protein 4 determine the specificity for chains of the SUMO. *Biochemical Journal* **457**, 207–214 (2014).

[257] Xu, Y. *et al.* Structural insight into SUMO chain recognition and manipulation by the ubiquitin ligase RNF4. *Nature Communications* **5**, 4217 (2014).

[258] Aguilar-Martinez, E. *et al.* Screen for multi-SUMO-binding proteins reveals a multi-SIM-binding mechanism for recruitment of the transcriptional regulator ZMYM2 to chromatin. *Proceedings of the National Academy of Sciences of the United States of America* **112**, E4854–E4863 (2015).

[259] Danielsen, J. R. *et al.* DNA damage-inducible SUMOylation of HERC2 promotes RNF8 binding via a novel SUMO-binding Zinc finger. *Journal of Cell Biology* **197**, 179–187 (2012).

[260] Guzzo, C. M. *et al.* Characterization of the SUMO-binding activity of the myeloproliferative and mental retardation (MYM)-type zinc fingers in ZNF261 and ZNF198. *PLoS ONE* **9**, e105271 (2014).

[261] Jalal, D., Chalissery, J. & Hassan, A. H. Genome maintenance in Saccharomycescerevisiae: the role of SUMO and SUMO-targeted ubiquitin ligases. *Nucleic Acids Research* **45** (2017).

[262] Parker, J. L. & Ulrich, H. D. SIM-dependent enhancement of substrate-specific SUMOylation by a ubiquitin ligase in vitro. *Biochemical Journal* **457**, 435–440 (2014).

[263] Tatham, M. H. *et al.* RNF4 is a poly-SUMO-specific E3 ubiquitin ligase required for arsenic-induced PML degradation. *Nature Cell Biology* **10**, 538–546 (2008).

[264] Plechanovová, A. *et al.* Mechanism of ubiquitylation by dimeric RING ligase RNF4. *Nature Structural and Molecular Biology* **18**, 1052–1059 (2011).

[265] Chang, Y. C., Oram, M. K. & Bielinsky, A. K. Sumo-targeted ubiquitin ligases and their functions in maintaining genome stability. *International Journal of Molecular Sciences* **22** (2021).

[266] Fasci, D., Anania, V. G., Lill, J. R. & Salvesen, G. S. SUMO deconjugation is required for arsenic-triggered ubiquitylation of PML. *Science Signaling* **8** (2015).

[267] Rojas-Fernandez, A. *et al.* SUMO chain-induced dimerization activates RNF4. *Molecular Cell* **53**, 880–892 (2014).

[268] Nacerddine, K. *et al.* The SUMO pathway is essential for nuclear integrity and chromosome segregation in mice. *Developmental Cell* **9**, 769–779 (2005).

[269] Pfander, B., Moldovan, G. L., Sacher, M., Hoege, C. & Jentsch, S. SUMO-modified PCNA recruits Srs2 to prevent recombination during S phase. *Nature* **436**, 428–433 (2005).

[270] Robert, T., Dervins, D., Fabre, F. & Gangloff, S. Mrc1 and Srs2 are major actors in the regulation of spontaneous crossover. *EMBO Journal* **25**, 2837–2846 (2006).

[271] Parker, J. L. *et al.* SUMO modification of PCNA is controlled by DNA. *The EMBO journal* **27**, 2422–31 (2008).

[272] Armstrong, A. A., Mohideen, F. & Lima, C. D. Recognition of SUMO-modified PCNA requires tandem receptor motifs in Srs2. *Nature* **483**, 59–65 (2012).

[273] Krejci, L. *et al.* DNA helicase Srs2 disrupts the Rad51 presynaptic filament. *Nature* **423**, 305–309 (2003).

[274] Veaute, X. *et al.* The Srs2 helicase prevents recombination by disrupting Rad51 nucleoprotein filaments. *Nature* **423**, 309–312 (2003).

[275] Parnas, O. *et al.* Elg1, an alternative subunit of the RFC clamp loader, preferentially interacts with SUMOylated PCNA. *EMBO Journal* **29**, 2611–2622 (2010).

[276] Kubota, T., Nishimura, K., Kanemaki, M. T. & Donaldson, A. D. The Elg1 Replication Factor C-like Complex Functions in PCNA Unloading during DNA Replication. *Molecular Cell* **50**, 273–280 (2013).

[277] Sau, S., Liefshitz, B. & Kupiec, M. The yeast pcna unloader Elg1 RFC-like complex plays a role in eliciting the DNA damage checkpoint. *mBio* **10** (2019).

[278] Moldovan, G. L. *et al.* Inhibition of homologous recombination by the PCNA-interacting protein PARI. *Molecular Cell* **45**, 75–86 (2012).

[279] Leach, C. A. & Michael, W. M. Ubiquitin/SUMO modification of PCNA promotes replication fork progression in Xenopus laevis egg extracts. *Journal of Cell Biology* **171**, 947–954 (2005).

[280] Gali, H. *et al.* Role of SUMO modification of human PCNA at stalled replication fork. *Nucleic acids research* **40**, 6049–6059 (2012).

[281] Longhese, M. P., Plevani, P. & Lucchini, G. Replication factor A is required

in vivo for DNA replication, repair, and recombination. *Molecular and Cellular Biology* **14**, 7884–7890 (1994).

[282] Brill, S. J. & Stillman, B. Replication factor-A from Saccharomyces cerevisiae is encoded by three essential genes coordinately expressed at S phase. *Genes and Development* **5**, 1589–1600 (1991).

[283] Grandin, N. & Charbonneau, M. RPA provides checkpoint-independent cell cycle arrest and prevents recombination at uncapped telomeres of Saccharomyces cerevisiae. *DNA Repair* **12**, 212–226 (2013).

[284] Yates, L. A. *et al.* A structural and dynamic model for the assembly of Replication Protein A on single-stranded DNA. *Nature Communications* **9**, 1–14 (2018).

[285] Psakhye, I. & Jentsch, S. Protein group modification and synergy in the SUMO pathway as exemplified in DNA repair. *Cell* **151**, 807–820 (2012).

[286] Chung, I. & Zhao, X. Dna break-induced sumoylation is enabled by collaboration between a sumo ligase and the ssdnabinding complex rpa. *Genes and Development* **29**, 1593–1598 (2015).

[287] Dhingra, N., Wei, L. & Zhao, X. Replication protein A (RPA) SUMOylation positively influences the DNA damage checkpoint response in yeast. *Journal of Biological Chemistry* **294**, jbc.RA118.006006 (2018).

[288] Cappadocia, L., Kochańczyk, T. & Lima, C. D. DNA asymmetry promotes SUMO modification of the single-stranded DNA-binding protein RPA. *The EMBO Journal* **40** (2021).

[289] Bonner, J. N. *et al.* Smc5/6 Mediated Sumoylation of the Sgs1-Top3-Rmi1 Complex Promotes Removal of Recombination Intermediates. *Cell Reports* **16**, 368–378 (2016).

[290] Dou, H., Huang, C., Singh, M., Carpenter, P. B. & Yeh, E. T. Regulation of DNA Repair through DeSUMOylation and SUMOylation of replication protein A complex. *Molecular Cell* **39**, 333–345 (2010).

[291] Hartwell, L. H. Genetic control of the cell division cycle in yeast. IV. Genes controlling bud emergence and cytokinesis. *Experimental Cell Research* **69**, 265–276 (1971).

[292] Pan, F., Malmberg, R. L. & Momany, M. Analysis of septins across kingdoms reveals orthology and new motifs. *BMC Evolutionary Biology* **7**, 1–17 (2007).

[293] Dobbelaere, J. & Barral, Y. Spatial coordination of cytokinetic events by compartmentalization of the cell cortex. *Science* **305**, 393–396 (2004).

[294] Khan, A., McQuilken, M. & Gladfelter, A. S. Septins and Generation of Asymmetries in Fungal Cells. *Annual Review of Microbiology* **69**, 487–503 (2015).

[295] Frazier, J. A. *et al.* Polymerization of purified yeast septins: Evidence that organized filament arrays may not be required for septin function. *Journal of Cell Biology* **143**, 737–749 (1998).

[296] McMurray, M. A. *et al.* Septin Filament Formation Is Essential in Budding Yeast. *Developmental Cell* **20**, 540–549 (2011).

[297] Mino, A. *et al.* Shs1p: A novel member of septin that interacts with Spa2p, involved in polarized growth in Saccharomyces cerevisiae. *Biochemical and Biophysical Research Communications* **251**, 732–736 (1998).

[298] Bertin, A. *et al.* Saccharomyces cerevisiae septins: Supramolecular organization of heterooligomers and the mechanism of filament assembly. *Proceedings of the National Academy of Sciences of the United States of America* **105**, 8274–8279 (2008).

[299] Booth, E. A., Vane, E. W., Dovala, D. & Thorner, J. A förster resonance energy transfer (FRET)-based system provides insight into the ordered assembly of yeast septin hetero-octamers. *Journal of Biological Chemistry* **290**, 28388–28401 (2015).

[300] Glomb, O. & Gronemeyer, T. Septin Organization and Functions in Budding Yeast. *Frontiers in Cell and Developmental Biology* **4**, 123 (2016).

[301] Renz, C. *et al.* Identification of cell cycle dependent interaction partners of the septins by quantitative mass spectrometry. *PLoS ONE* **11** (2016).

[302] Finnigan Lab | Biochemistry and Molecular Biophysics | Kansas State University. *https://www.k-state.edu/bmb/department/directory/finnigan/lab/* (accessed: 2020-05-20).

[303] Ozsarac, N., Bhattacharyya, M., Dawes, I. W. & Clancy, M. J. The SPR3 gene encodes a sporulation-specific homologue of the yeast CDC3/10/11/12 family of bud neck microfilaments and is regulated by ABFI. *Gene* **164**, 157–162 (1995).

[304] C, D. V. *et al.* SPR28, a sixth member of the septin gene family in Saccharomyces cerevisiae that is expressed specifically in sporulating cells. *Microbiology* **142**, 2897–2905 (1996).

[305] Fares, H. *et al.* Identification of a developmentally regulated septin and involvement of the septins in spore formation in Saccharomyces cerevisiae. *Journal of Cell Biology* **132**, 399–411 (1996).

[306] Pablo-Hernando, M. E. *et al.* Septins localize to microtubules during nutritional limitation in Saccharomyces cerevisiae. *BMC Cell Biology* **9**, 55 (2008).

[307] Garcia, G. *et al.* Assembly, molecular organization, and membrane-binding properties of development-specific septins. *Journal of Cell Biology* **212**, 515–529 (2016).

[308] Nakamura, T. S. *et al.* Dynamic localization of a yeast development-specific PP1 complex during prospore membrane formation is dependent on multiple localization signals and complex formation. *Molecular Biology of the Cell* **28**, 3881–3895 (2017).

[309] Dieckhoff, P., Boite, M., Sancak, Y., Braus, G. H. & Irniger, S. Smt3/SUMO and Ubc9 are required for efficient APC/C-mediated proteolysis in budding yeast. *Molecular Microbiology* **51**, 1375–1387 (2004).

[310] Biggins, S., Bhalla, N., Chang, A., Smith, D. L. & Murray, A. W. Genes involved in sister chromatid separation and segregation in the budding yeast Saccharomyces cerevisiae. *Genetics* **159**, 453–470 (2001).

[311] Dasso, M. Emerging roles of the SUMO pathway in mitosis. *Cell Division* **3**, 5 (2008).

[312] Newman, H. A. *et al.* A high throughput mutagenic analysis of yeast sumo structure and function. *PLoS Genetics* **13**, e1006612 (2017).

[313] Srikumar, T. *et al.* Global analysis of SUMO chain function reveals multiple roles in chromatin regulation. *The Journal of cell biology* **201**, 145–63 (2013).

[314] Takahashi, Y. *et al.* Smt3, a SUMO-1 homolog, is conjugated to Cdc3, a component of septin rings at the mother-bud neck in budding yeast. *Biochemical and Biophysical Research Communications* **259**, 582–587 (1999).

[315] Sumo antibody | Sigma-Aldrich. *https://www.sigmaaldrich.com/DE/de/search/sumo-antibody* (accessed: 2022-03-11).

[316] Tatham, M. H. & Hay, R. T. FRET-based in vitro assays for the analysis of SUMO protease activities. *Methods in Molecular Biology* **497**, 253–268 (2009).

[317] Becker, J. *et al.* Detecting endogenous SUMO targets in mammalian cells and tissues. *Nature Structural and Molecular Biology* **20**, 525–531 (2013).

[318] Pirone, L. *et al.* A comprehensive platform for the analysis of ubiquitin-like protein modifications using in vivo biotinylation. *Scientific Reports* **7**, 1–17 (2017).

[319] Da Silva-Ferrada, E. *et al.* Strategies to identify recognition signals and targets of SUMOylation. *Biochemistry Research International* **2012**, 16 (2012).

[320] Barroso-Gomila, O. *et al.* Identification of proximal SUMO-dependent interactors using SUMO-ID. *Nature Communications* **12**, 2020.12.28.424528 (2021).

[321] Bruderer, R. *et al.* Purification and identification of endogenous polySUMO conjugates. *EMBO Reports* **12**, 142–148 (2011).

[322] Lopitz-Otsoa, F. *et al.* Sumo-binding entities (Subes) as tools for the enrichment, isolation, identification, and characterization of the sumo proteome in liver cancer. *Journal of Visualized Experiments* **2019**, e60098 (2019).

[323] Kim, D. H. *et al.* Mms21 SUMO ligase activity promotes nucleolar function in Saccharomyces cerevisiae. *Genetics* **204**, 645–658 (2016).

[324] Matic, I. *et al.* Site-Specific Identification of SUMO-2 Targets in Cells Reveals an Inverted SUMOylation Motif and a Hydrophobic Cluster SUMOylation Motif. *Molecular Cell* **39**, 641–652 (2010).

[325] Taupitz, K. F., Dörner, W. & Mootz, H. D. Covalent Capturing of Transient SUMO–SIM Interactions Using Unnatural Amino Acid Mutagenesis and Photocrosslinking. *Chemistry - A European Journal* **23**, 5978–5982 (2017).

[326] Ong, S. E. *et al.* Stable isotope labeling by amino acids in cell culture, SILAC, as a simple and accurate approach to expression proteomics. *Molecular and cellular proteomics* **1**, 376–386 (2002).

[327] Kirkpatrick, D. S., Denison, C. & Gygi, S. P. Weighing in on ubiquitin: The expanding role of mass-spectrometry-based proteomics. *Nature Cell Biology* **7**, 750–757 (2005).

[328] Impens, F., Radoshevich, L., Cossart, P. & Ribet, D. Mapping of SUMO sites and analysis of SUMOylation changes induced by external stimuli. *Proceedings of the National Academy of Sciences of the United States of America* **111**, 12432–12437 (2014).

[329] Hendriks, I. A. *et al.* Site-specific characterization of endogenous SUMOylation across species and organs. *Nature Communications* **9**, 2456 (2018).

[330] McManus, F. P., Altamirano, C. D. & Thibault, P. In vitro assay to determine SUMOylation sites on protein substrates. *Nature Protocols* **11**, 387–397 (2016).

[331] Eisenhardt, N., Ilic, D., Nagamalleswari, E. & Pichler, A. Biochemical characterization of SUMO-conjugating enzymes by in vitro sumoylation assays. In *Methods in Enzymology*, vol. 618, 167–185 (Academic Press, 2019).

[332] Bossis, G. *et al.* A fluorescence resonance energy transfer-based assay to study SUMO modification in solution. *Methods in Enzymology* **398**, 20–32 (2005).

[333] Martin, S. F., Hattersley, N., Samuel, I. D., Hay, R. T. & Tatham, M. H. A fluorescence-resonance-energy-transfer-based protease activity assay and its use to monitor paralog-specific small ubiquitin-like modifier processing. *Analytical Biochemistry* **363**, 83–90 (2007).

[334] Stankovic-Valentin, N., Kozaczkiewicz, L., Curth, K. & Melchior, F. An in vitro FRET-based assay for the analysis of SUMO conjugation and isopeptidase cleavage. *Methods in Molecular Biology* **497**, 241–251 (2009).

[335] Dudek, A. Z. *et al.* Phase 1/2 study of the novel SUMOylation inhibitor TAK-981 in adult patients (pts) with advanced or metastatic solid tumors or relapsed/refractory (RR) hematologic malignancies. *Journal of Clinical Oncology* **39**, TPS2667–TPS2667 (2021).

[336] Kroonen, J. S. & Vertegaal, A. C. Targeting SUMO Signaling to Wrestle Cancer. *Trends in Cancer* **7**, 496–510 (2021).

[337] Langston, S. P. *et al.* Discovery of TAK-981, a First-in-Class Inhibitor of SUMO-Activating Enzyme for the Treatment of Cancer. *Journal of Medicinal Chemistry* **64**, 2501–2520 (2021).

[338] Helma, J., Cardoso, M. C., Muyldermans, S. & Leonhardt, H. Nanobodies and recombinant binders in cell biology. *Journal of Cell Biology* **209**, 633–644 (2015).

[339] Binz, H. *et al.* Designing Repeat Proteins: Well-expressed, Soluble and Stable Proteins from Combinatorial Libraries of Consensus Ankyrin Repeat Proteins. *Journal of Molecular Biology* **332**, 489–503 (2003).

[340] Li, J., Mahajan, A. & Tsai, M. D. Ankyrin repeat: A unique motif mediating protein-protein interactions. *Biochemistry* **45**, 15168–15178 (2006).

[341] Bork, P. Hundreds of ankyrin-like repeats in functionally diverse proteins: Mobile modules that cross phyla horizontally? *Proteins: Structure, Function, and Bioinformatics* **17**, 363–374 (1993).

[342] Mosavi, L. K., Cammett, T. J., Desrosiers, D. C. & Peng, Z.-y. The ankyrin repeat as molecular architecture for protein recognition. *Protein Science* **13**, 1435–1448 (2004).

[343] Craig Venter, J. *et al.* The sequence of the human genome. *Science* **291**, 1304–1351 (2001).

[344] Plückthun, A. Designed Ankyrin Repeat Proteins (DARPins): Binding Proteins for Research, Diagnostics, and Therapy. *Annual Review of Pharmacology and Toxicology* **55**, 489–511 (2015).

[345] Malek, S., Huxford, T. & Ghosh, G. IκBα functions through direct contacts with the nuclear localization signals and the DNA binding sequences of NF-κB. *Journal of Biological Chemistry* **273**, 25427–25435 (1998).

[346] Sedgwick, S. G. & Smerdon, S. J. The ankyrin repeat: A diversity of interactions on a common structural framework. *Trends in Biochemical Sciences* **24**, 311–316 (1999).

[347] Walker, R. G., Willingham, A. T. & Zuker, C. S. A Drosophila mechanosensory transduction channel. *Science* **287**, 2229–2234 (2000).

[348] Kobe, B. & Kajava, A. V. When protein folding is simplified to protein coiling: The continuum of solenoid protein structures. *Trends in Biochemical Sciences* **25**, 509–515 (2000).

[349] Kohl, A. *et al.* Designed to be stable: Crystal structure of a consensus ankyrin repeat protein. *Proceedings of the National Academy of Sciences of the United States of America* **100**, 1700–5 (2003).

[350] Forrer, P., Binz, H. K., Stumpp, M. T. & Plückthun, A. Consensus design of repeat proteins. In *ChemBioChem*, vol. 5, 183–189 (Chembiochem, 2004).

[351] Binz, H. K. *et al.* High-affinity binders selected from designed ankyrin repeat protein libraries. *Nature Biotechnology* **22**, 575–582 (2004).

[352] Interlandi, G., Wetzel, S. K., Settanni, G., Plückthun, A. & Caflisch, A. Characterization and Further Stabilization of Designed Ankyrin Repeat Proteins by

Combining Molecular Dynamics Simulations and Experiments. *Journal of Molecular Biology* **375**, 837–854 (2008).

[353] Schilling, J. *et al.* Thermostable designed ankyrin repeat proteins (DARPins) as building blocks for innovative drugs. *Journal of Biological Chemistry* **298**, 101403 (2022).

[354] Plückthun, A. Ribosome Display: A Perspective. In *Methods in Molecular Biology*, vol. 805, 3–28 (Springer, New York, NY, 2012).

[355] Batchelor, A. H., Piper, D. E., Charles De La Brousse, F., McKnight, S. L. & Wolberger, C. The structure of GABPα/β: An ETS domain-ankyrin repeat heterodimer bound to DNA. *Science* **279**, 1037–1041 (1998).

[356] Wodak, S. J. & Janin, J. Structural basis of macromolecular recognition. *Advances in Protein Chemistry* **61**, 9–73 (2002).

[357] Binz, H. K. *et al.* Design and characterization of MP0250, a tri-specific anti-HGF/anti-VEGF DARPin® drug candidate. *mAbs* **9**, 1262–1269 (2017).

[358] Cattaneo, A. & Biocca, S. The selection of intracellular antibodies. *Trends in Biotechnology* **17**, 115–121 (1999).

[359] Tamaskovic, R., Simon, M., Stefan, N., Schwill, M. & Plückthun, A. Designed ankyrin repeat proteins (DARPins): From research to therapy. In *Methods in Enzymology*, vol. 503, 101–134 (Academic Press, 2012).

[360] Stumpp, M. T., Dawson, K. M. & Binz, H. K. Beyond Antibodies: The DARPin® Drug Platform. *BioDrugs* **34**, 423–433 (2020).

[361] Stahl, A. *et al.* Highly potent VEGF-A-antagonistic DARPins as anti-angiogenic agents for topical and intravitreal applications. *Angiogenesis* **16**, 101–111 (2013).

[362] Zahnd, C. *et al.* A Designed Ankyrin Repeat Protein Evolved to Picomolar Affinity to Her2. *Journal of Molecular Biology* **369**, 1015–1028 (2007).

[363] Huber, T., Steiner, D., Röthlisberger, D. & Plückthun, A. In vitro selection and characterization of DARPins and Fab fragments for the co-crystallization of membrane proteins: The Na+-citrate symporter CitS as an example. *Journal of Structural Biology* **159**, 206–221 (2007).

[364] Gilbreth, R. N. & Koide, S. Structural insights for engineering binding proteins

based on non-antibody scaffolds. *Current Opinion in Structural Biology* **22**, 413–420 (2012).

[365] Bukowska, M. A. & Grütter, M. G. New concepts and aids to facilitate crystallization. *Current Opinion in Structural Biology* **23**, 409–416 (2013).

[366] Ernst, P. *et al.* Rigid fusions of designed helical repeat binding proteins efficiently protect a binding surface from crystal contacts. *Scientific Reports* **9**, 16162 (2019).

[367] Kohl, A. *et al.* Allosteric inhibition of aminoglycoside phosphotransferase by a designed ankyrin repeat protein. *Structure* **13**, 1131–1141 (2005).

[368] Sennhauser, G., Amstutz, P., Briand, C., Storchenegger, O. & Grütter, M. G. Drug export pathway of multidrug exporter AcrB revealed by DARPin inhibitors. *PLoS Biology* **5**, 0106–0113 (2007).

[369] Thieltges, K. M. *et al.* Characterization of a drug-targetable allosteric site regulating vascular endothelial growth factor signaling. *Angiogenesis* **21**, 533–543 (2018).

[370] Kummer, L. *et al.* Structural and functional analysis of phosphorylation-specific binders of the kinase ERK from designed ankyrin repeat protein libraries. *Proceedings of the National Academy of Sciences of the United States of America* **109**, E2248–E2257 (2012).

[371] Molecular Partners – Building tomorrow's breakthroughs. *https://www.molecularpartners.com/* (accessed: 2022-01-25).

[372] Syed, B. A., Evans, J. B. & Bielory, L. Wet AMD market. *Nature Reviews Drug Discovery* **11**, 827–828 (2012).

[373] Kunimoto, D. *et al.* Efficacy and Safety of Abicipar in Neovascular Age-Related Macular Degeneration: 52-Week Results of Phase 3 Randomized Controlled Study. In *Ophthalmology*, vol. 127, 1331–1344 (Ophthalmology, 2020).

[374] Novartis and Molecular Partners report positive topline data from Phase 2 study for ensovibep (MP0420), a DARPin antiviral therapeutic for COVID-19 | Novartis. *https://www.novartis.com/news/media-releases/novartis-and-molecular-partners-report-positive-topline-data-from-phase-2-study-ensovibep-mp0420-darpin-antiviral-therapeutic-covid-19* (accessed: 2022-01-17).

[375] Walser, M. *et al.* Highly potent anti-SARS-CoV-2 multivalent DARPin therapeutic candidates. *bioRxiv* 2020.08.25.256339 (2021).

[376] Steiner, D. *et al.* Half-life extension using serum albumin-binding DARPin domains. In *Protein Engineering, Design and Selection*, vol. 30, 583–591 (Protein Eng Des Sel, 2017).

[377] Rothenberger, S. *et al.* Ensovibep, a novel trispecific DARPin candidate that protects against SARS-CoV-2 variants. *bioRxiv* 2021.02.03.429164 (2021).

[378] Zahnd, C. *et al.* Efficient tumor targeting with high-affinity designed ankyrin repeat proteins: Effects of affinity and molecular size. *Cancer Research* **70**, 1595–1605 (2010).

[379] Mattheakis, L. C., Bhatt, R. R. & Dower, W. J. An in vitro polysome display system for identifying ligands from very large peptide libraries. *Proceedings of the National Academy of Sciences of the United States of America* **91**, 9022–9026 (1994).

[380] Mattheakis, L. C., Dias, J. M. & Dower, W. J. Cell-free synthesis of peptide libraries displayed on polysomes. *Methods in Enzymology* **267**, 195–207 (1996).

[381] Hanes, J. *et al.* In vitro selection and evolution of functional proteins by using ribosome display. *Proceedings of the National Academy of Sciences* **94**, 4937–4942 (1997).

[382] Dreier, B. & Plückthun, A. Ribosome display: a technology for selecting and evolving proteins from large libraries. *Methods in molecular biology (Clifton, N.J.)* **687**, 283–306 (2011).

[383] Schindelin, J. *et al.* Fiji: An open-source platform for biological-image analysis. *Nature Methods* **9**, 676–682 (2012).

[384] Mullis, K. *et al.* Specific enzymatic amplification of DNA in vitro: The polymerase chain reaction. *Cold Spring Harbor Symposia on Quantitative Biology* **51**, 263–273 (1986).

[385] Louderback, A. L., City, T., Natland, M. C., Shanbrom, E. & Ana, S. Method of electrophoresis. *patent:* **US3497437A**, 437 (1967).

[386] Davies, A. A. & Ulrich, H. D. *DNA Repair Protocols* **920**, 543–567 (2012).

[387] Werner, A., Moutty, M. C., Möller, U. & Melchior, F. Performing in vitro sumoylation reactions using recombinant enzymes. *Methods in Molecular Biology* **497**, 187–199 (2009).

[388] Mcnew, J. A. *et al.* Compartmental speci city of cellular membrane fusion encoded in SNARE proteins. *Nature* **407**, 153–159 (2000).

[389] Silva, G. M., Finley, D. & Vogel, C. K63 polyubiquitination is a new modulator of the oxidative stress response. *Nature structural and molecular biology* **22**, 116–123 (2015).

[390] Silva, G. M. & Vogel, C. Mass spectrometry analysis of K63-ubiquitinated targets in response to oxidative stress. *Data in Brief* **4**, 130–134 (2015).

[391] Kampmeyer, C. *et al.* The exocyst subunit Sec3 is regulated by a protein quality control pathway. *J Biol Chem* **292**, 15240–15253 (2017).

[392] O'Connor, H. F. *et al.* Ubiquitin-Activated Interaction Traps (UBAITs) identify E3 ligase binding partners. *EMBO reports* **16**, 1699–1712 (2015).

[393] Davies, A. A. & Ulrich, H. D. Detection of PCNA modifications in saccharomyces cerevisiae. *Methods in Molecular Biology* **920**, 543–567 (2012).

[394] The UniProt Consortium. UniProtKB. *https://www.uniprot.org/* (accessed: 2021-12-03).

[395] Huh, W. K. *et al.* Global analysis of protein localization in budding yeast. *Nature* **425**, 686–691 (2003).

[396] Yofe, I. *et al.* One library to make them all: Streamlining the creation of yeast libraries via a SWAp-Tag strategy. *Nature Methods* **13**, 371–378 (2016).

[397] Reggiori, F., Black, M. W. & Pelham, H. R. Polar transmembrane domains target proteins to the interior of the yeast vacuole. *Molecular biology of the cell* **11**, 3737–3749 (2000).

[398] Reggiori, F. & R.B.Pelham, H. Sorting of proteins into multivesicular bodies: ubiquitin-dependent and -independent targeting. *The EMBO journal* **20**, 5176–86 (2001).

[399] Dupré, S. & Haguenauer-Tsapis, R. Deubiquitination step in the endocytic pathway of yeast plasma membrane proteins: crucial role of Doa4p ubiquitin isopeptidase. *Molecular and cellular biology* **21**, 4482–94 (2001).

[400] Nikko, E. & André, B. Evidence for a Direct Role of the Doa4 Deubiquitinating Enzyme in Protein Sorting into the MVB Pathway. *Traffic* **8**, 566–581 (2007).

[401] Amerik, A. Y., Nowak, J., Swaminathan, S. & Hochstrasser, M. The Doa4 Deubiquitinating Enzyme Is Functionally Linked to the Vacuolar Protein-sorting and Endocytic Pathways. *Molecular Biology of the Cell* **11**, 3365–3380 (2000).

[402] Mayor, T., Graumann, J., Bryan, J., MacCoss, M. J. & Deshaies, R. J. Quantitative profiling of ubiquitylated proteins reveals proteasome substrates and the substrate repertoire influenced by the Rpn10 receptor pathway. *Molecular and Cellular Proteomics* **6**, 1885–1895 (2007).

[403] Ziv, I. *et al.* A perturbed ubiquitin landscape distinguishes between ubiquitin in trafficking and in proteolysis. *Molecular and Cellular Proteomics* **10**, M111.009753 (2011).

[404] Lamark, T. & Johansen, T. Mechanisms of Selective Autophagy. *Annual Review of Cell and Developmental Biology* **37**, 143–169 (2021).

[405] Klionsky, D. J. For the last time, it is GFP-Atg8, not Atg8-GFP (and the same goes for LC3). *Autophagy* **7**, 1093–1094 (2011).

[406] Larance, M. *et al.* Global membrane protein interactome analysis using in vivo crosslinking and mass spectrometry-based protein correlation profiling. *Molecular and Cellular Proteomics* **15**, 2476–2490 (2016).

[407] Wiederhold, E. *et al.* The yeast vacuolar membrane proteome. *Molecular and Cellular Proteomics* **8**, 380–92 (2009).

[408] Kolkman, A. *et al.* Proteome analysis of yeast response to various nutrient limitations. *Molecular Systems Biology* **16** (2006).

[409] Mick Hitchcock, N. P. C. Protocol: Preparation of Soluble and Membrane Protein Fractions. *https://www.unr.edu/proteomics/sample-preparation/2d-protocols/protocol-protein-fractions* (accessed: 2018-07-17).

[410] Simon, A. M. *Biochemische Charakterisierung der Interaktion einer Kinetochor-Untereinheit mit Ubiquitin.* Bachelor's thesis, Institut für Molekulare Biologie (IMB, Mainz) (2016).

[411] Windecker, H. Private communication (2017).

[412] Cornilescu, G., Marquardt, J. L., Ottiger, M. & Bax, A. Validation of protein structure from anisotropic carbonyl chemical shifts in a dilute liquid crystalline phase. *Journal of the American Chemical Society* **120**, 6836–6837 (1998).

[413] Akiyoshi, B., Nelson, C. R., Ranish, J. A. & Biggins, S. Quantitative proteomic analysis of purified yeast kinetochores identifies a PP1 regulatory subunit. *Genes and Development* **23**, 2887–2899 (2009).

[414] Akiyoshi, B. *et al.* Tension directly stabilizes reconstituted kinetochore-microtubule attachments. *Nature* **468**, 576–579 (2010).

[415] Straight, A. F., Belmont, A. S., Robinett, C. C. & Murray, A. W. GFP tagging of budding yeast chromosomes reveals that protein-protein interactions can mediate sister chromatid cohesion. *Current Biology* **6**, 1599–1608 (1996).

[416] Su, H. L. & Li, S. S. Molecular features of human ubiquitin-like SUMO genes and their encoded proteins. *Gene* **296**, 65–73 (2002).

[417] Takahashi, Y., Toh-e, A. & Kikuchi, Y. Comparative analysis of yeast PIAS-type SUMO ligases in vivo and in vitro. *Journal of biochemistry* **133**, 415–422 (2003).

[418] Klug, H. *et al.* Ubc9 Sumoylation Controls SUMO Chain Formation and Meiotic Synapsis in Saccharomyces cerevisiae. *Molecular Cell* **50**, 625–636 (2013).

[419] Sheng, W. & Liao, X. Solution structure of a yeast ubiquitin-like protein Smt3: the role of structurally less defined sequences in protein-protein recognitions. *Protein science : a publication of the Protein Society* **11**, 1482–91 (2002).

[420] Duda, D. M. *et al.* Structure of a SUMO-binding-motif mimic bound to Smt3p-Ubc9p: conservation of a non-covalent ubiquitin-like protein-E2 complex as a platform for selective interactions within a SUMO pathway. *Journal of molecular biology* **369**, 619–30 (2007).

[421] PDBe < PISA < EMBL-EBI. *https://www.ebi.ac.uk/pdbe/pisa/pistart.html http://www.ebi.ac.uk/pdbe/pisa/* (accessed: 2021-08-13).

[422] Vertrees, J. InterfaceResidues - PyMOLWiki (2009). *https://pymolwiki.org/index.php/InterfaceResidues* (accessed: 2021-08-13).

[423] Hagemans, D., van Belzen, I. A., Luengo, T. M. & Rüdiger, S. G. A script to highlight hydrophobicity and charge on protein surfaces. *Frontiers in Molecular Biosciences* **2**, 56 (2015).

[424] Bellí, G., Garí, E., Piedrafita, L., Aldea, M. & Herrero, E. An activator/repressor dual system allows tight tetracycline-regulated gene expression in budding yeast. *Nucleic acids research* **26**, 942–7 (1998).

[425] Wetzel, S. K., Settanni, G., Kenig, M., Binz, H. K. & Plückthun, A. Folding and Unfolding Mechanism of Highly Stable Full-Consensus Ankyrin Repeat Proteins. *Journal of Molecular Biology* **376**, 241–257 (2008).

[426] Keeling, J. W. P. & Miller, R. K. Indirect Immunofluorescence for Monitoring Spindle Assembly and Disassembly in Yeast. *Methods in Molecular Biology* **782**, 231–244 (2011).

[427] Tachikawa, H., Bloecher, A., Tatchell, K. & Neiman, A. M. A Gip1p-Glc7p phosphatase complex regulates septin organization and spore wall formation. *Journal of Cell Biology* **155**, 797–808 (2001).

[428] Kane, S. M. & Roth, R. Carbohydrate metabolism during ascospore development in yeast. *Journal of Bacteriology* **118**, 8–14 (1974).

[429] CDC48 | Saccharomyces Genome Database | SGD. *https://www.yeastgenome.org/locus/S000002284* (accessed: 2021-11-02).

[430] Nie, M. *et al.* Dual recruitment of Cdc48 (p97)-Ufd1-Npl4 ubiquitin-selective segregase by small ubiquitin-like modifier protein (SUMO) and ubiquitin in SUMO-targeted ubiquitin ligase-mediated genome stability functions. *Journal of Biological Chemistry* **287**, 29610–29619 (2012).

[431] SPC42 | Saccharomyces Genome Database | SGD. *https://www.yeastgenome.org/locus/S000001525* (accessed: 2021-11-02).

[432] Drennan, A. C. *et al.* Structure and function of Spc42 coiled-coils in yeast centrosome assembly and duplication. *Molecular Biology of the Cell* **30**, 1505–1522 (2019).

[433] Killinger, K. *et al.* Auto-inhibition of Mif2/CENP-C ensures centromere-dependent kinetochore assembly in budding yeast. *The EMBO Journal* **39**, e102938 (2020).

[434] KRE28 | Saccharomyces Genome Database | SGD. *https://www.yeastgenome.org/locus/S000002940* (accessed: 2021-11-02).

[435] Abcam. KD value: a quantitative measurement of antibody affinity | Abcam (2018). *https://www.abcam.com/primary-antibodies/kd-value-a-quantitive-measurement-of-antibody-affinity* 375 (accessed: 2021-10-28).

5 Appendices

5.1 Mass spectrometry results

Table 21: Results of mass spectrometry studies to identify interactors of Pib-TAP. Pull-down of endogenously expressed TAP-tagged Pib1 followed by MS performed in collaboration with [redacted] from the group of [redacted] (IMB Mainz). No detection of Pib1 over background levels was possible. The complete list of identified proteins can be found on the attached DVD. H/L, intensity ratio of "heavy"-to-"light"; NaN, „Not a Number" value equal to background.

Gene name	Unique peptides	Ratio H/L	Ratio H/L normalized
...	...	...	...
SSB2	3	NaN	NaN
RTT102	1	NaN	NaN
PIB1	11	NaN	NaN
STO1	2	NaN	NaN
ATP7	2	NaN	NaN
PIN4	3	NaN	NaN
...	...	...	...

Table 22: Results of mass spectrometry studies to identify substrates of Pib (Experiment 1). Pull-down of overexpressed TAP-Pib1^{0}, TAP-Pib1-I227A-ubi^{4} and TAP-Pib1-ubi^{8} and TAP-Pib1^{0}, TAP-Pib1-ubi-ΔGG^{4} and TAP-Pib1- ubi^{8} followed by MS performed in collaboration with [redacted] from the group of [redacted] (IMB Mainz). Besides Pib1 and ubiquitin, no proteins were identified with a high unique peptide count. The complete list of identified proteins can be found on the attached DVD. H/L, intensity ratio of "heavy"-to-"light"; NaN, „Not a Number" value equal to background.

Gene name	Unique peptides	Ratio H/L	Ratio H/L normalized
YDR029W	1	11.97	19.97
SAP1	1	7.73	18.00
UBI4	16	2.63	2.04
PIB1	25	1.02	1.02
NOP58	4	0.27	0.29
ECM5	2	NaN	NaN
PDC1;PDC6	2	NaN	NaN
...	...	...	...

Table 23: Results of mass spectrometry studies to identify substrates of Pib (Experiment 2). Pull-down of overexpressed TAP-Pib1^{0}, TAP-Pib1-ubi-ΔGG^{4} and TAP-Pib1-ubi^{8} followed by MS performed in collaboration with [redacted] from the group of [redacted] (IMB Mainz). Identified proteins were not likely to be substrates of Pib1 as their normalized heavy to light ratio is not higher than 1. The complete list of identified proteins can be found on the attached DVD. H/L, intensity ratio of "heavy"-to-"light"

Gene name	Unique peptides	Ratio H/L	Ratio H/L normalized
PIB1	34	3.00	1.31
UBI4	12	1.53	0.77
NOP58	7	1.02	0.77
HSC82;HSP82	8	1.19	0.60
VMA1	6	1.31	0.56
FKS1;GSC2	12	1.48	0.55
NOP56	8	1.04	0.50
HXT7;HXT6	9	1.31	0.49
SSA1;SSA2	10	1.17	0.47
...	...	...	...

5.2 Supplementary information

The following supplementary information is included on the DVD, located on the last page of this thesis:

- Crystallisation data: complex A10-SUMO and complex C10-SUMO.
- full MS results tables: Pib1-TAP, Ubait experiment 1, Ubait experiment 2.
- raw NMR data: complex A12-Spc24/Spc25 and DARPin-SUMO complexes.
- FACS data: cell cycle analysis of DARPin expressing cells and comparison to Ubc9 defective cells.
- plotted BIACORE data: binding curves of DARPin to SUMO, DARPins to SUMO mutants, DARPins to ubiquitin, and DARPins to hSUMO proteins.

5.3 Curriculum vitae: Vera Tröster

Personal

Date of birth **15.02.1992**

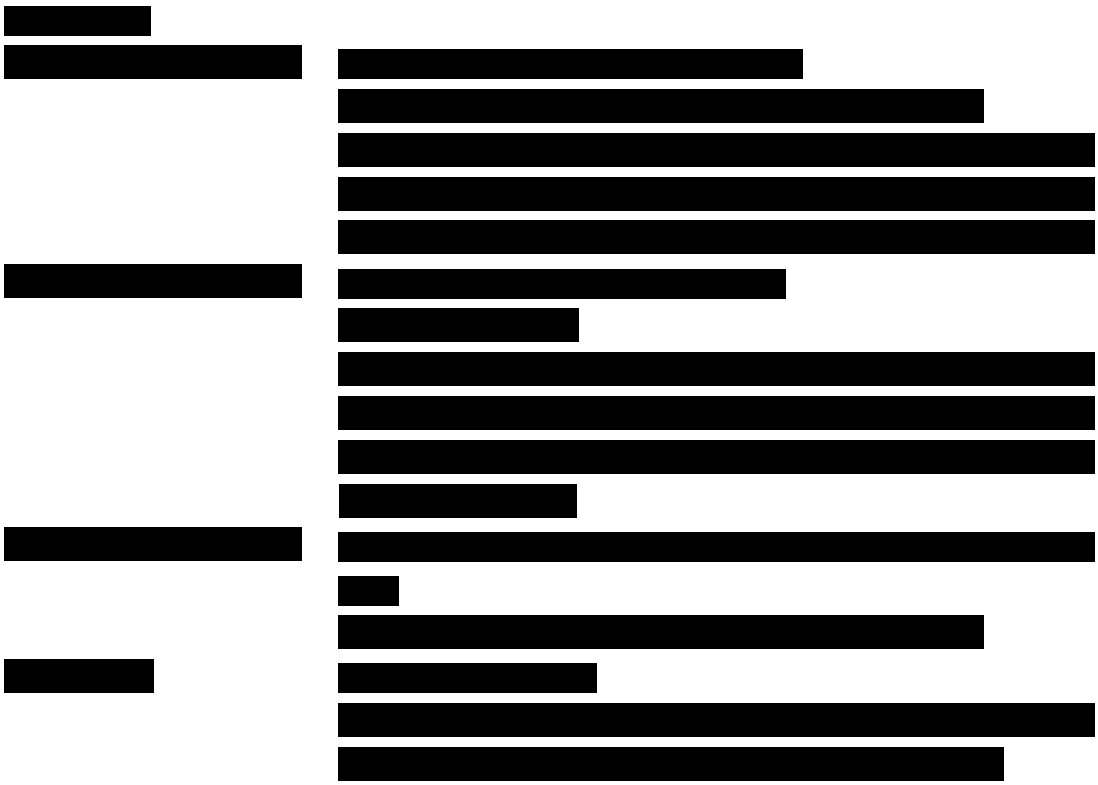

5.4 Publications

Christian Renz, Vera Tröster, Thomas K. Albert, Olivier Santt, Susan C. Jacobs, Anton Khmelinskii, and Helle D. Ulrich. The ubiquitin-conjugating enzyme Ubc13-Mms2 cooperates with a family of FYVE-type-RING ubiquitin protein ligases in K63-polyubiquitylation at internal membranes. *bioRxiv* **575241** (2019).

Christian Renz, Véronique Albanèse, Vera Tröster, Thomas K. Albert, Olivier Santt, Susan C. Jacobs, Anton Khmelinskii, Sébastien Léon, and Helle D. Ulrich. Ubc13–Mms2 cooperates with a family of RING E3 proteins in budding yeast membrane protein sorting. *Journal of Cell Science* **133** (2020).